Year 2024

Università di Torino

Doctoral school in Pharmaceutical and Biomolecular sciences
XXXVI cycle

PhD tesis

Analytical Strategies For The Characterization of Botanicals

Giulia Mastellone

Supervisor: Dr. Cecilia Cagliero

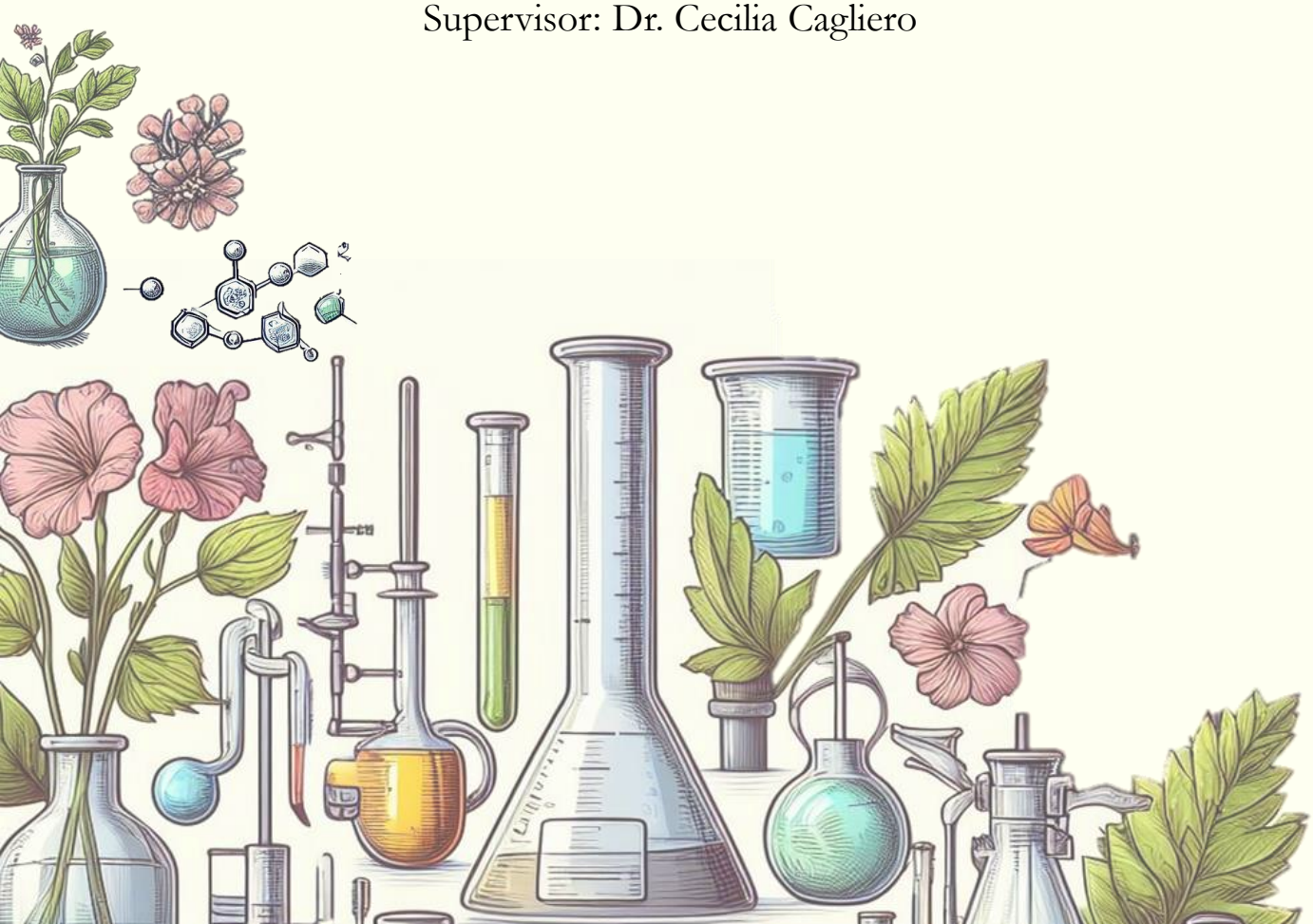

Introduction

ABSTRACT

Plants and their derived products have always played a crucial role in human well-being, ranging from food, cosmetic and medical applications. Since ancient times, the study of natural extracts has attracted mankind, revealing that plants are rich in phytochemicals with proven antioxidant, anti-inflammatory, antimicrobial, antitumor and prebiotic properties, among others. If plants can be considered a sustainable source of valuable primary and specialized metabolites, most studies on plant phytocomplex still principally adopt traditional extraction techniques, thus requiring the use of disposable materials, energy-consuming equipment and instrumentation, and extraction methods that employ harmful solvents.

Since the introduction of the principles of Green Analytical Chemistry, within the frameworks of Green Chemistry, the analytical chemistry community has devoted a great deal of effort toward the reduction (and possible elimination) of organic and toxic solvents and reagents in the analysis procedure, the miniaturization and automation of methods, the minimization of energy consumption, the reduction of wastes, and the reuse of solvents and materials. More recently, attention was focused even more on the sample preparation step of the analytical process and the ten principles of green sample preparation were introduced. Thus, great efforts have been made to develop functional methods aimed at improving the greenness of the extraction processes.

The development of appropriate sample preparation methods in the plant field faces challenges as the complexity of plant systems can affect the reliable determination of target analytes. The choice of the appropriate extraction phase is of utmost importance and is one of the most critical parameters to be considered. In metabolomics studies, the extraction phase should cover the widest possible array of metabolites. On the other hand, a high selectivity and the enrichment of target analytes is required in studies dealing with the determination of specific compounds.

The main goal of this Doctoral Thesis was to develop simple, greener and reliable methodologies for future applications in the routine analysis of botanicals. A particular attention was paid to the choice of the extraction phase, exploring different solvents and materials to highlights their potential and limits, depending on the application. Among the new materials, ionic liquids (ILs), eutectic solvents (ESs) and metal organic frameworks (MOFs) were incorporated in different analytical applications in this Thesis. All these methods were properly

optimized using experimental design to maximize the amount of information obtained with the minimum number of experiments.

To test the applicability of these methods on plant matrices, three different samples were used as case-studies: *Vitis vinifera* L., *Corylus avellana* L., *Cannabis sativa* L.. These plants are largely exploited in the agro-food chain of our territory, producing agricultural wastes source of high-value phytochemicals. Thus, the studies described here were focused on the valorization of these by-products, to develop truly sustainable strategies.

This Thesis is divided in four Chapters: I) Introduction, II) Experimental, III) Results and Discussion, and IV) Conclusions.

The concept of Plant-based Chemistry and the evolution from Green Chemistry principles to Green Sample Preparation is briefly presented in the first part of the Introduction. A general overview of the new extraction phases developed and adopted for the study of plant endogenous and exogenous metabolites is then described.

Chapter II concerns the experimental section, including the analytes, materials, and instrumentation used, together with a description of the optimum procedures and the samples analyzed.

In Chapter III, the results obtained are presented and discussed; Section III.1 includes the studies on *Vitis vinifera* L., Section III.2 includes the studies on *Corylus avellana* L. and Section III.3 includes the studies on *Cannabis sativa* L.. For every plant, the following aspect have been addressed: an accurate phytochemical characterization of the non-volatile fraction (using LC-PDA-MS/MS), the development and optimization of the extraction method and preliminary *in-vitro* screenings of the biological activity to explore potential application of the obtained extracts.

Chapter IV includes the summary of the most relevant conclusions derived from Chapter III.

Table of contents

Chapter I
INTRODUCTION

GRAPHICAL ABSTRACT

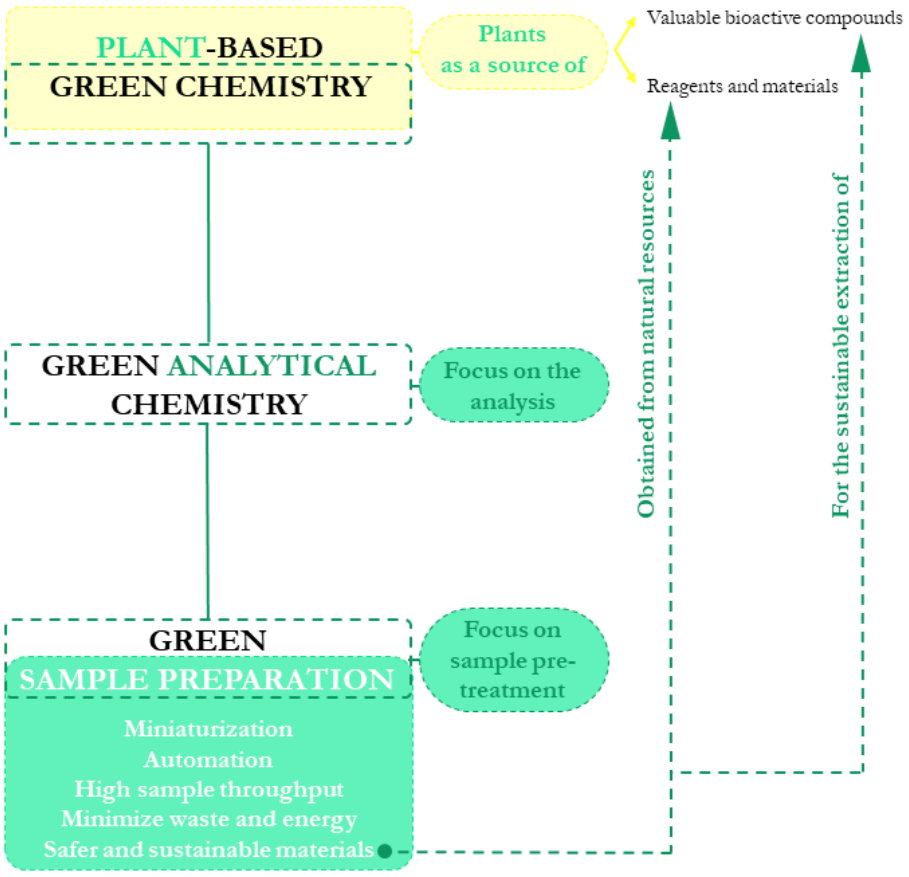

HIGHLIGHTS

Plant-based Chemistry as a solution from the past to face today's environmental challenges

Green chemistry concept has given rules for modern chemistry

Innovative **extraction phases** were developed in recent years for sample preparation but few applications were explored in plant field

Part of this chapter is a compilation of the following published review articles and book chapter:

Mastellone *et al.*, Trends in Analytical Chemistry 125 (2020) 115839

Mastellone *et al.*, Trends in Analytical Chemistry 141 (2021) 116288

Mastellone *et al.*, Ionic liquids in green sample preparation, RSC (2023) 179-211

I.1 Plant-based Green Chemistry

Before the development of petroleum-based materials, plants were the main source of products and reagents for food and non-food applications and have been largely exploited by different cultures around the world. Indeed, plants had a fundamental role for human health because incredible sources of primary and specialized metabolites, such as fats, dietary fibers, sugars, antioxidants, aromas, and pigments. Despite these properties, petroleum derivatives supplanted the use of plants in many applications, giving the way to the petroleum era. At the beginning of 1900, the employ of fossil resources developed quickly, thanks to the progress of extraction techniques which made them inexpensive and abundant. Moreover, petroleum presents a quite simple and constant composition, easy to manage in chemical processes. On the contrary, the complexity of plant matrices made challenging to isolate pure molecules[1,2]. However, the depletion of fossil resources and environmental concerns led to re-consider natural products as better resources of chemicals. In this regard, regulatory institutions are developing strategies and designing road maps to promote the efficient use of resources, the recovery of biodiversity, and the reduction of waste and pollution, encouraging a Circular Economy approach[3]. Plant-based chemistry could be one of the solutions from the past to the future as an ecologic chemistry, with a more conscious approach.

We already know that plant and plant-based products are source of bioactive compounds that can be exploited for health purposes, however the exploitation of plant should be regulated to protect ecosystems and avoid plant extinction or uncontrolled harvesting. In this sense, the valorization of agrifood by-products can play a key role. These products, such as seeds, peels, roots, leaves, and stems, which are produced during cultivation and food processing, generate large volumes of waste and represent a disposal problem for the agriculture and food industries. At the same time, the unexploited plant materials are often rich in bioactive phytochemical compounds, such as terpenoids, phenolic compounds, and alkaloids, with proven bioactivity against several common diseases. These phytochemicals can be exploited as green and renewable sources of nutrients and bioactive compounds for feed, functional food, and food supplement industries[4–7]. Moreover, enhanced extraction processes and greener technologies are now available to reduce the environmental impact of industrial activity[8,9].

Plants can also be employed as building blocks to obtain new and enhanced substances and materials for applications in the chemical, food, biotechnology and other technical fields. Several examples of solvents of natural origin are reported in literature as alternative to conventional ones; among these, limonene (major component of the citrus fruit skins essential oils), vegetable oils (produced by cold pressing from plant seeds) and 2-methyltetrahydrofuran (obtained by hydrogenation of hemicellulose derivatives from corn cobs or sugarcane). The availability of different functional groups on natural terpenes (highly abundant in essential oils) makes them suitable to introduce new functionality and further be modified, to synthetize other molecules[1,2,10]. Another interesting example of renewable and biodegradable resource of materials are biopolymers, obtained from natural sources. This group includes polysaccharides, protein and lipids derived from plants, being the polysaccharides the most commonly used due to their water-solubility, gelling, and emulsifying properties[11].

The list of green chemicals, materials and technologies that can be obtained from plants is extraordinary long making "Plant Based" Green Chemistry a valuable response to the challenges launched by today's world. However, it should be taken in to account that natural products are not always necessarily better for the environment because of the chemical processes related to the transformation of plant material[2]. Thus, apart from the starting material low-impact processes should be preferred to develop truly green and sustainable strategies.

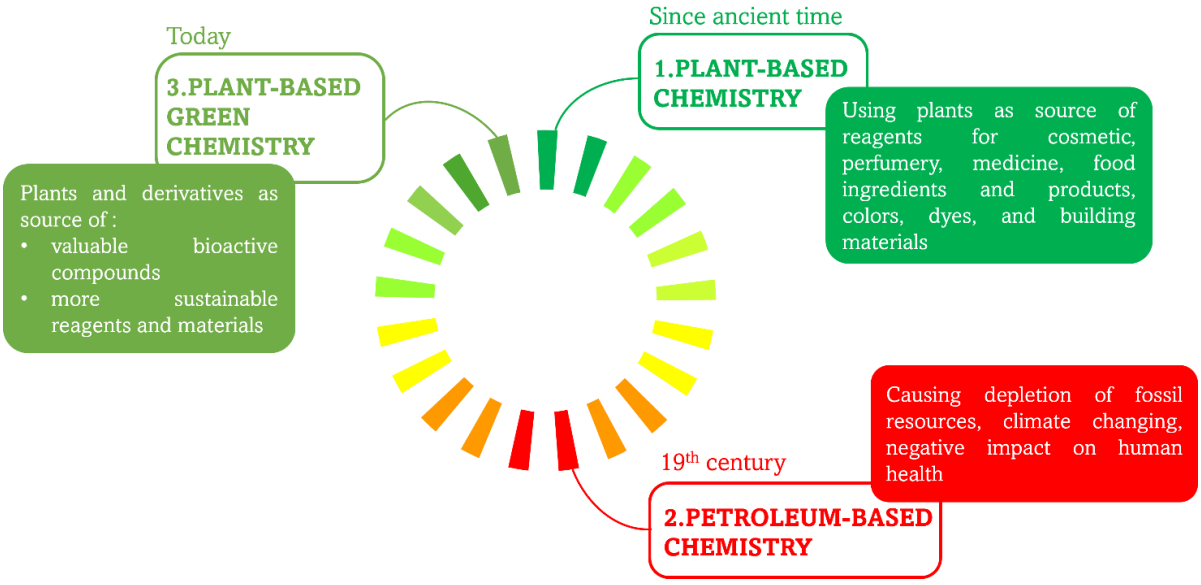

Figure .1. From Plant-based Chemistry to Plant-based Green Chemistry.

I.2 From Green Chemistry to Green Sample Preparation

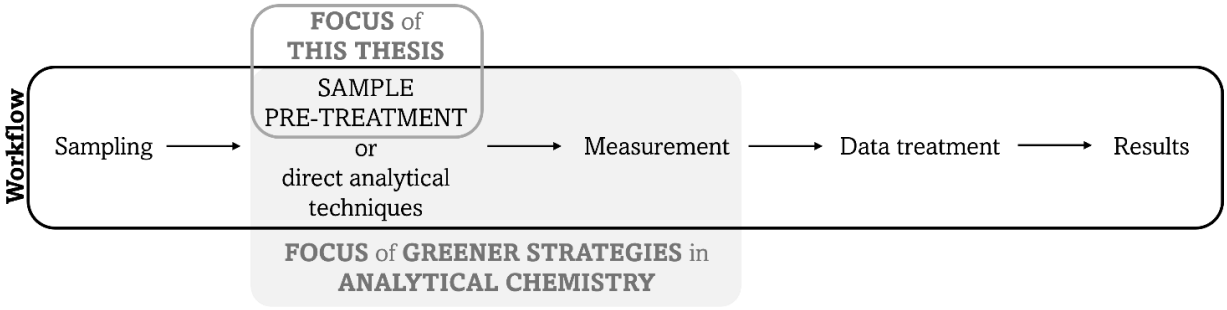

(a)

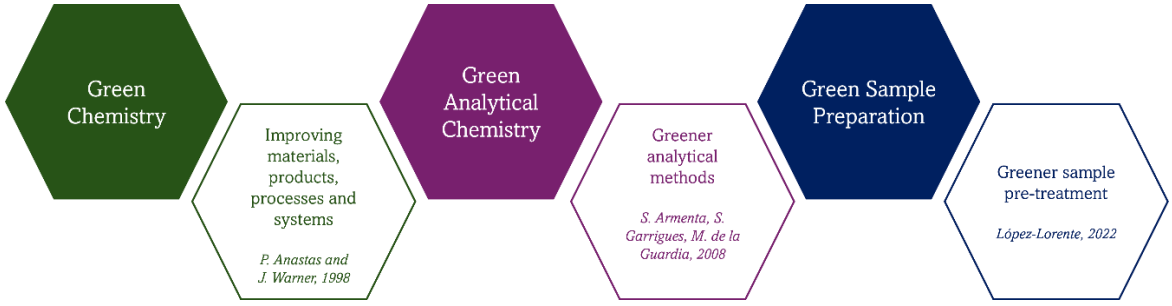

(b)

Figure 1. (a) General workflow of a measurement process in analytical chemistry and (b) main green approaches developed in the chemical field.

The concept of Plant-based Chemistry is closely related to the one of Green Chemistry (GC), which was one of the first efforts to reduce the use of hazardous reagents and introduce green practices within the chemical field. This perspective focuses on supporting safer strategies in the synthesis, production and application of chemicals; thus, on reducing or removing materials which represent a hazard towards human health and the environment. In order to achieve these goals, guidelines were provided for the first time by Anastas and Warner in their book "Green Chemistry: Theory and Practice", published in 1998[12]. Apart from the acute and chronic toxicity of chemicals for human health, particular attention was paid to direct and indirect ecological impacts such as plant and animal toxicity and persistence in the environment. The "core" of GC is contained in 12 principles that have been acknowledged as a reference code of best practices for chemists to develop clean and environmentally sustainable methodologies.

At first, GC was applied to the procedures of organic synthesis and then it also involved the analytical branch of chemistry. The incorporation of the GC principles in the analytical

process has emerged as one of the most important research lines within the analytical chemistry community, leading to the development of the Green Analytical Chemistry (GAC). GAC emerged in the 2000s for the purpose of implementing sustainable development criteria to analytical laboratories[13]. In order to apply GC principles to the different conditions and techniques of analytical chemistry, necessary adaptations were made. In particular, Galuska *et al.* proposed some improvements regarding sampling, disposal of analytical waste, safety of the operator and choice of methods and chemical reagents and solvents[14]. Indeed, they promoted the minimization, replacement, or elimination of harmful organic solvents in the analytical sample preparation procedure, the improvement of the methodologies by using on-line, automated and microextraction approaches (this way permitting a decrease of costs, number of steps and analysis time, while allowing the development of high-throughput methods)[11].

Despite the great efforts made by the scientific community to improve the extraction processes, forms of sample preparation are still necessary for the analysis of a large variety of complex matrices (e.g food, plant, biological and environmental samples). Sample preparation has a significant impact on the sustainability of the overall analysis process as it often requires the use of disposable materials, energy-consuming equipment and instrumentation, and extraction methods that employ harmful solvents. While GAC expects to "select direct analytical techniques" (principle 1) to avoid pre-treatment steps, Green Sample Preparation (GSP) principles aim to guide analytical chemists to minimize the impact of sample pre-treatment, when direct analysis is not possible. Proposed in 2022, GSP establish guidelines on issues pertaining to solvents, materials, waste, energy demand, miniaturization, procedure automation, and operator safety[15].

I.2.1 Green metrics

Since the introduction of GAC, a set of tools and metrics have been developed to "measure" objectively and globally the greenness of the analytical procedures. They can guide chemists toward more sustainable practices, although each tools adopts its own calculations and criteria. Indeed, every metrics consider different aspects of the analytical method and the choice of the most suitable to used is critical and need to be guided according to the analytical methodology employed and the information that the user want to obtain[16].

The first metrics introduced (e.g NEMI, GAPI) considered few criteria and parameters of the method, using a qualitative classification based on a color scale, or required tedious computing operation (e.g analytical eco-scale)[17–19]. In recent years, more user-friendly tools have been developed, based on simple open access software where the result is presented as a pictogram indicating qualitative and quantitative scores. Among these, one of the most popular is AGREE and its modified version AGREEprep[20,21]. While AGREE focuses on the entire methodology and is based on the twelve principles of GAC, AGREEprep was specifically designed to investigate the sample preparation steps by evaluating the choice of solvents, materials and reagents used, the sample size and throughput, the amount of waste generated, the energy consumption, and the operator safety. The environmental impact is analyzed by estimating the method compliance to the ten principles of GSP on a scale from 0 to 1. The criteria are not equal in terms of importance and they can be adjusted to the user's requirements by assigning them different weights. Since the improvement of sample preparation for the analysis of plant matrices is the main goal of this Doctoral Thesis, AGREEprep metric was mainly employed to critically evaluate the greenness of the developed methodologies.

Another interesting approach proposed by Nowak *et al.* aims to consider not only the greenness of the methods but also its analytical efficiency and productivity. The "White Analytical Chemistry" (WAC) concept can be considered an extension of the 12 principles of GAC[22]. It evaluates the quality of methods in terms of analytical efficiency, greenness and safety, and practical and economic aspects. For each aspect, four parameters are proposed, to each of which a score is assigned, and a global score is calculated to measure the overall compliance of the method to all principles. A "white" method is a balanced analysis method that fully satisfies all parameters. Representative output obtained with the metrics described above are schematically shown in Figure 2.

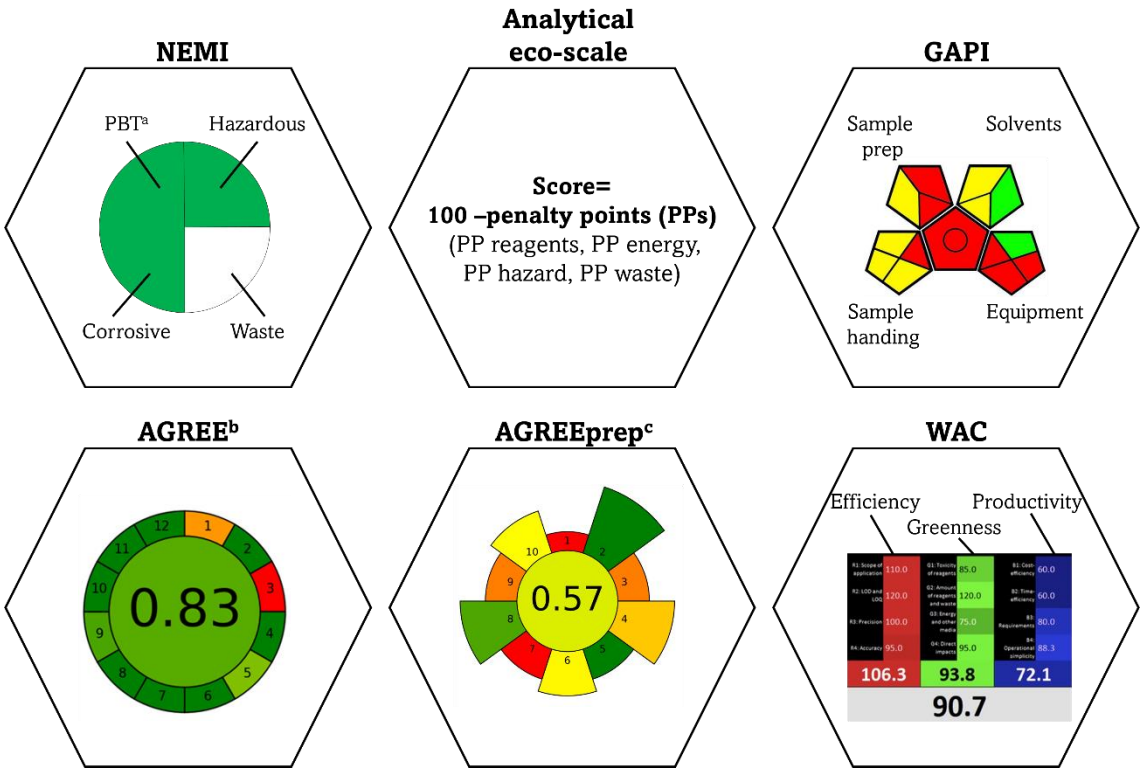

Figure 2. Representative output of the main metrics developed to critically evaluate analytical procedure in the chemical field.

[a] Persistent, bioaccumulative, toxic

[b] Criterion considered by the metric: 1. Direct analytical techniques should be applied to avoid sample treatment, 2. Minimal sample size and minimal number of samples are goals, 3. Measurements should be performed *in situ*, 4. Integration of analytical processes and operations saves energy and reduces the use of reagents, 5. Automated and miniaturized methods should be selected, 6. Derivatization should be avoided, 7. Generation of a large volume of analytical waste should be avoided, and proper management of analytical waste should be provided, 8. Multi-analyte or multi-parameter methods are preferred versus methods using one analyte at a time, 9. The use of energy should be minimized, 10. Reagents obtained from renewable sources should be preferred, 11. Toxic reagents should be eliminated or replaced, 12. Operator's safety should be increased.

[c] Criterion considered by the metric: 1. Sample preparation placement, 2. Hazardous material, 3. Sustainability and renewability of materials, 4. Waste, 5. Size economy of the sample, 6. Sample throughput, 7. Integration and automation, 8. Energy consumption, 9. Post-sample preparation configuration for analysis, 10. Operator's safety.

I.3 Sample preparation of vegetal matrices: how big is the challenge in analytical chemistry?

Natural product analyses must cover a wide range of topics, starting from the study of plant metabolomes to the quality control and determination of endogenous and exogenous compounds. In both cases, sample preparation plays a fundamental role. In fact, as many plant metabolites as possible should be extracted in metabolomics studies. However, a universal extraction phase or technique is practically impossible to find due to the complexity of plant systems and the chemical diversity of metabolites[23]. On the other hand, the determination of individual or multiple metabolites, which are often present in traces in plant materials, is required in quality control analyses. The analytical challenge here is to develop methods that can detect target compound(s) at low limits, as often required by regulations, meaning that proper enrichment is required[8].

The development of appropriate sample preparation methods in the plant field poses a particular challenge, as the complexity of plant biological systems can affect the reliable determination of target analytes. In fact, the metabolome of a plant comprises a wide variety of compounds, ranging from different classes of primary metabolites (sugars, proteins, lipids and nucleic acids) to a very wide range of specialized metabolites (such as terpenoids, alkaloids, phenolic compounds and others). Another issue in plant analysis is the presence of chlorophylls and other pigments and/or interfering compounds. These molecules are present in large quantities in the photosynthetic parts of the plant, but they are poorly compatible with downstream analyses, and especially with HPLC systems, because of their strong interaction with the commonly used reverse stationary phases. At the same time, it is important to remember that plant cells are protected by thick and robust lignocellulosic walls that should be disrupted if efficient extraction of intracellular metabolites is to be achieved.

Several mechanical means, including ultrasound and microwaves, can be adopted to increase the efficiency of metabolite extraction. However, the choice of the appropriate extraction phase is of utmost importance and one of the most critical parameters. The extraction phase should either cover the broadest possible range of metabolites in metabolomics studies or increase the selectivity and the enrichment of target analytes in studies dealing with the determination of specific compounds.

In this sense, most studies on plants still mainly use adopt traditional extraction techniques, including liquid-liquid extraction and Soxhlet extraction, which are associated with a high consumption of toxic organic solvents. However, the use of miniaturized techniques and new classes of more sustainable extraction phases is gaining ground as they meet the criteria of Green Analytical Chemistry[14].

This chapter aims to provide an overview of the extraction phases that have been developed and adopted in recent years, for the study of endogenous and exogenous plant metabolites. A critical evaluation of the main features of each phase will be provided as well as some ideas for new applications in the plant field. The potential, limits and future trends of innovative extraction solvents and sorbents will be deeply discussed. Figure 1 shows a representative flow chart for the choice of the most suitable extraction phases, depending on the features of the plant sample to be analyzed and on the goal of the study. Table 1 reports several applications that are extensively discussed in the following sections.

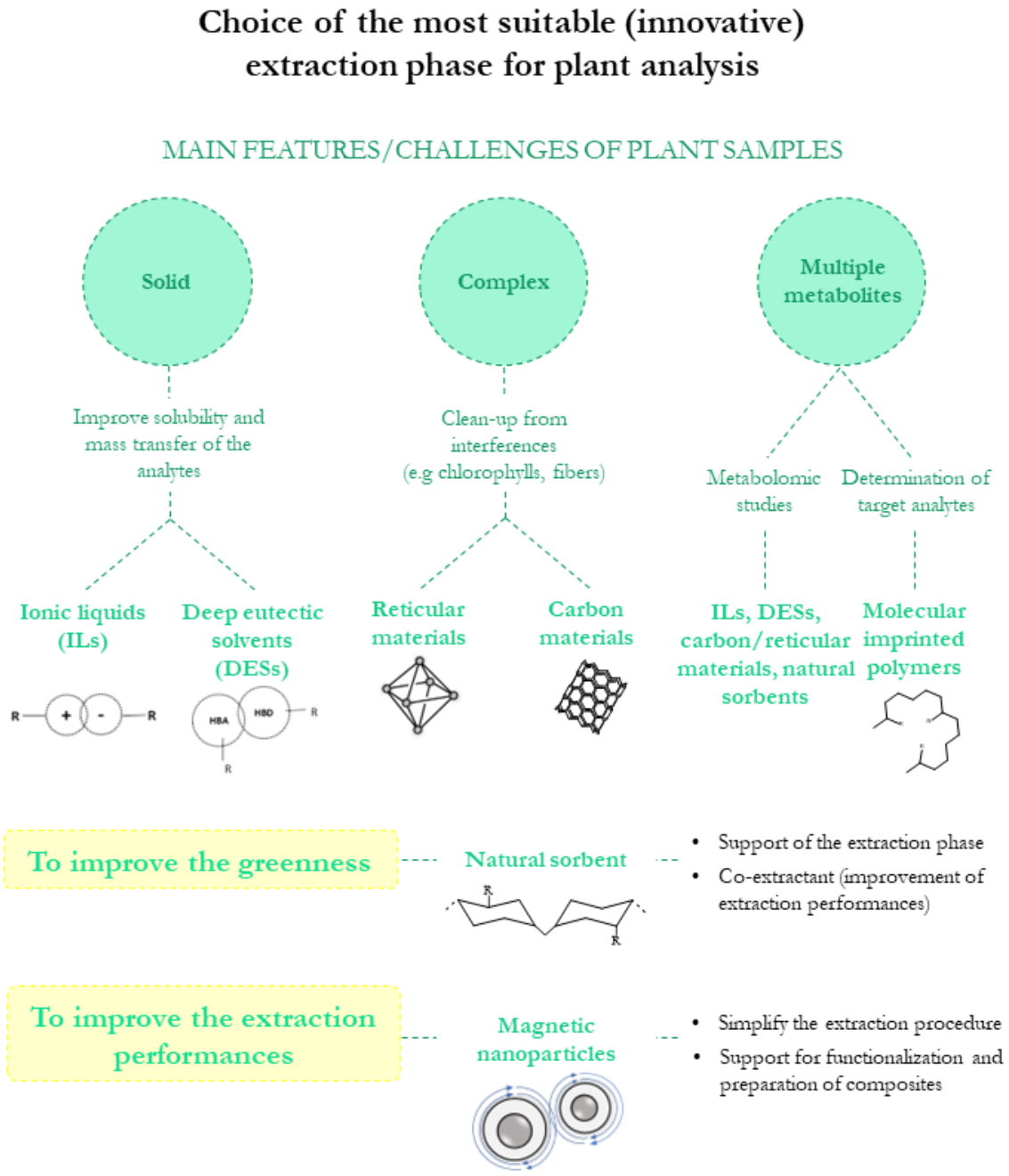

Figure 1. Flow chart to select the most suitable extraction phase for the analysis of plant samples

I.3.1 Liquid extraction phases

The search for new green solvents has become one of the most significant topics in the sample preparation field. In this regard, ionic liquids (ILs) and deep eutectic solvents (DESs) have received a great deal of attention as they may be able to replace organic solvents in the extraction of natural products.. In fact, these new solvents can be combined with a range of extraction techniques, such as ultrasound assisted extraction (UAE) and microwave-assisted extraction (MAE), as well as in microextraction.

3.1.1 Ionic liquids

Ionic liquids (ILs) are a class of molten salts whose physicochemical properties have inspired the rapid development of new applications in analytical chemistry and in sample-preparation. They are "molten salts" as they possess melting points at or below 100 °C. In most cases, they consist of an organic cation and an organic or inorganic anion, and are characterized by high thermal stability, low vapor pressure and varying viscosity, conductivity and miscibility in various solvents.

The chemical structure of ILs (type of functional groups and/or anion/cation combination) can be tailored to provide various solvation interactions (such as hydrogen bonding, electrostatic, hydrophobic and $\pi-\pi$ interactions) with both polar and apolar compounds, thus giving ILs with very different properties. In addition, as they present negligible vapor pressure at room temperature, they prevent solvent loss to the atmosphere and reduce the environmental footprint, thus making them a sustainable alternative to organic solvents[25].

Many studies have also demonstrated the ability of ionic liquids to dissolve cellulose and other cell-wall components (such as hemicellulose and lignin), via their decrystallization [24]. In fact, the anions of ionic liquids can form strong hydrogen bonds with the hydroxyl groups of cellulose, and thus eliminate their intramolecular hydrogen bonds and disrupt cell walls, causing cell lysis. This ability can be exploited for the pre-treatment of plant material even before its extraction, for instance before or during hydrodistillation to increase essential oil yield[26].

The above-mentioned properties have allowed ILs to find many applications as solvents in extraction and separation processes for bioactive compounds, either in solid-liquid extractions (SLE) or in microwave-assisted (MA) and ultrasound-assisted (UA) extractions[1].

Because of their versatility, ILs can be adopted in liquid-phase extractions of natural products using different extraction methods. They can be used as surfactants above their critical micellar concentration, as reported in the study presented in Section III.1.2, where 1-hexadecyl-3-butyl imidazolium bromide was employed as IL-based surfactant for the extraction of phenolic compounds from *Vitis vinifera* L. leaves[27]. In another work, Moučková *et al.* also evaluated a set of structurally different IL-based surfactants for the flavonoid determination of *Mangifera* spp. and *Passiflora* spp. leaves[28]. They can also form aqueous biphasic systems (ABS) when the aqueous IL solution is mixed with inorganic salts that promote phase separation and increase analyte(s) enrichment. This approach has been adopted for the HPLC-UV analysis of *Panax ginseng* C. A. Mey. In this study, the extraction of the analytes has been carried out by aqueous IL-based UAE and it has been followed by the separation of the IL phase with an ABS, using NaH_2PO_4[29]. Finally, dispersive liquid-liquid microextraction (DLLME) can be used when dealing with liquid samples, such as herbal teas. In this case, hydrophobic ILs are dispersed in the water solution with the aid of a dispersive solvent and the IL-phase can be recovered and directly analyzed. In addition, the solubility of target analytes in ILs can be optimized by changing the temperature. An ultrasonic-assisted temperature-controlled IL-DLLME approach has recently been applied for the determination of pyrethroid residues in herbal teas[30].

ILs can also incorporate a paramagnetic element into their structure, either in the cation or in the anion, leading to magnetic ionic liquids (MILs), a sub-class of ILs whose application in sample preparation is rapidly increasing[31]. MILs have found some applications in the plant field, in particular in the extraction of sinomenine from *Sinomenium acutum* (Thunb.) Rehder & E. H. Wilson[32] and of berberine from the rhizome of *Coptis* spp[33]. They also have been used for the isolation of DNA from *Arabidopsis thaliana* (L.) Heynh. and other plants[34]. These compounds have great potential for the extraction of endogenous and exogenous metabolites from vegetable matrices because they combine all the features of ILs with the ability to exploit their paramagnetic characteristics that enabled them to be easily separated using an external magnetic field, in a very rapid process that avoids centrifugation and filtration steps.

ILs can also be incorporated into solid phase platforms, either alone (as polymeric ionic liquids, PILs) or in combination with other sorbents to form composites[35]. PILs are polyelectrolytes obtained through the polymerization of IL monomers. PILs not only retain the

main features of ILs, but also present the inherent properties of polymers with enhanced mechanical stability and conductivity properties. They can be used in solid phase microextraction (SPME) as sorbent coatings and can be applied in both direct immersion (DI) and headspace (HS) extraction modes and can be coupled to both HPLC and GC analysis. For instance, PIL coatings have found use in the profiling of the volatile compounds from *Echinacea* spp. flowers by HS-SPME[36], coupled to GC-MS analysis.

ILs as sorbents have also been widely employed in combination with natural sorbents, molecular imprinted polymers (MIPs) and carbon-based materials. These composites will be better described in the next paragraphs.

Thanks to the tunability of their structure and, consequently, of their properties, ILs can be applied to both metabolomics studies and the selective extraction of specific endogenous and exogenous compounds. When dealing with metabolomics studies, ILs can be exploited for the simultaneous determination of volatile and non-volatile components[37,38]. In the first case, ILs were used as additives in hydrodistillation coupled with liquid-liquid extraction (ILMHDE) for the distillation of essential oil and the simultaneous extraction of a set of non-volatile flavonoids from the inflorescences of *Helichrysum arenarium* (L.) Moench. [37]. ILs can also be used in combination with enzyme digestion, as clearly shown in a study in which a solution of 1-butyl-3-methylimidazolium bromide and a mixture of cellulase and pectinase have been used as pretreatment before hydrodistillation of volatile components and Soxhlet extraction of procyanidins from pinecones of *Pinus koraiensis* Siebold & Zucc.[39] The ability to extract hydrophilic and hydrophobic non-volatile compounds at the same time is also another interesting application. For instance, an ionic-liquid-based ultrasonic-assisted extraction has been used to simultaneously extract gingerols and polysaccharides from ginger (*Zingiber officinale* Roscoe) with high yields and reduced extraction times for both classes of compound[40]. The use of temperature-responsive hydrophobic ionic liquids (TRILs) is another alternative. In fact, TRILs are soluble in water above a certain temperature (the upper critical solution temperature, UCST) and immiscible below the UCST. The extraction process is carried out at high temperature, exploiting the different polarities of the two solvents, and then the *in-situ* separation and pre-concentration of the target compounds is achieved by reducing the temperature below the UCST, meaning that the extraction solvent will switch from being single-phase to two-phase. This approach has been

developed specifically for the extraction of bioactive compounds from medicinal plants, and has been applied to *Chrysanthemum* spp., as a case study[41].

On the other hand, the structure of ILs can be tuned for the selective recovery of plant metabolites belonging to specific chemical classes. Numerous examples can be found in literature, as reported in a recent review by Xiao *et al*[42]. Furthermore, ILs can be exploited for the selective extraction and pre-concentration of toxic exogenous compounds. An IL-based SPME and an IL-based *in-situ* DLLME method have been developed for the extraction of acrylamide from coffee[43] and an IL-based DLLME approach has been adopted for the selective extraction and determination of pyrethroid residues in herbal teas[30].

Despite the undoubted advantages of IL-based extractions, these molecules also have some limitations. One drawback is the difficulty of recovering the extracted compounds because of the negligible vapor pressure of ILs. This limit mainly affects their use in the isolation of natural compounds rather than their analytical application. However, the poor volatility of ILs also means that they are not directly compatible with LC-MS analyses or the direct injection into a GC system; as a result, a back-extraction of the analytes from the IL phase is required before their analysis.

In addition, although they were originally considered to be green chemicals, some concerns about the toxicity and potential environmental impact of ILs have started to arise in recent years. In fact, most of them are obtained from fossil sources and show poor degradability. In this respect, the current trend is to design ILs to be more degradable and less toxic. ILs with fluorine-free anions and with more biodegradable cations (e.g. pyridinium or guanidinium) have been developed, thanks to the fact that shorter IL side chains in any of the moieties reduce their toxicity. More eco-friendly guanidinium-based ILs have been applied in the above-mentioned extraction of flavonoids from *Mangifera* spp. and *Passiflora* spp. leaves[28]. These derivatives, although more environmentally sustainable, still require a large amount of non-renewable solvents in their synthesis, meaning that the use of anionic or cationic counterparts that are fully or partly derived from natural compounds would be preferred for the development of a new generation of bio-renewable ILs (Bio-ILs)[44]. For instance, matrinium-based ionic liquids, derived from the alkaloid matrine, isolated from *Sophora flavescens* Aiton, showed good physicochemical properties and low cytotoxicity[45]. Unfortunately, these Bio-ILs have rarely been applied in sample

preparation and there are no applications in the plant field. Future advancements in the development of bio-renewable ionic liquids are therefore expected and their application in the extraction of plant matrices should be explored.

3.1.2 Deep eutectic solvents

Deep eutectic solvents are systems formed by a hydrogen-bond acceptor (HBA) and a hydrogen-bond donor (HBD) and they are characterized by a lower melting point than the one of the individual components. They are usually associated with ILs because they have similar physicochemical properties, including low vapor pressure, low flammability and thermal stability. However, DES can be prepared by incorporating ionic or neutral species. Moreover, DESs overcome some of the limits of ILs due to their easy preparation, low cost of raw materials, as well as their lower toxicity and higher biodegradability (when composed by natural compounds) [46–49].

In this sense, DESs have been widely explored as valid alternatives to organic solvents for the extraction of bioactive compounds from different plant materials, with a focus on non-volatile endogenous compounds[49]. Of the various components that can be used to obtain a DES, HBAs and HBDs of natural origin, such as amines, sugars, carboxylic acids and polyalcohols, are an attractive source for the preparation of DESs. These natural deep eutectic solvents (NADES) have found promising applications in the plant field[47,49–51]. The solubility of most natural compounds in NADES, can be explained by a hypothesis developed by Choi *et al.*[52] who proposed that NADES are naturally present in plant cells and act as a third liquid phase in living organisms. In fact, they observed that some primary metabolites (sugars, organic acids and bases, amino acids) naturally occur in similarly high molar ratios in the plant cells, thus probably explaining the multistep biosynthesis of non-water-soluble compounds. In addition, several studies have demonstrated the ability of DESs to cleave lignin-carbohydrate complexes by disrupting covalent and hydrogen bonds, thus affecting the structure of the cell wall and accelerating the release of the compounds[46].

The heating and stirring method is the most common procedures employed to prepare DES. . It requires the mixing of two or three components under magnetic stirring, keeping the temperature at 40-90°C until a homogeneous liquid is formed[47,48,50,51,53,54]. A range of different

physicochemical properties were observed according to the HBA and HBD chosen, and the ratio used. For example, the widely used HBA choline chloride [Ch^+][Cl^-] can be combined with polyols (e.g. ethylene glycol, glycerol…), carboxylic acids, amides, alcohols, sugars and amino acids to give mixtures with different polarities and viscosities[47,48,50,51]. Viscosity is a key point when dealing with DES because it can affect the mass transfer of analytes during extraction. The main ways of reducing viscosity include higher extraction temperatures, which may result in the degradation of the target compounds if not properly controlled, and also of some HBDs and HBAs[46], and the addition of water[51]. The presence of water clearly affects the polarity of the solvent and the careful optimization of this parameter is fundamental to achieve good performance, also considering that the presence of water may also interfere with the formation of the hydrogen bonding network[46,53].

Ultrasounds[49,51,54–56] is often employed during the extraction to enhance the transfer of analytes from the vegetal matrix to the eutectic solvent, resulting in a greener approach due to the decrease of extraction time and energy consumption[1].

A further aspect in the use of DES is the absence of harmful organic solvents, both in the preparation of DESs and during the extraction process. As previously mentioned, the complex composition of vegetal materials, including the presence of pigments (e.g. chlorophyll), usually means that a pre-treatment process is needed to eliminate these interferences, and large quantities of harmful volatile organic solvents are consumed. The percentage of water added to the eutectic mixture prevent the transfer of chlorophyll and other apolar interferences from the plant material to the extract[47,51]. However, it is important to highlight that a certain volume of solvent is normally used to dilute the sample before the analysis, this step is necessary to decrease the viscosity of the final extract in order to prevent damage to the chromatographic system[54,56]. Nevertheless, as discussed for ILs, the direct injection of the DESs in the chromatographic system when LC is coupled to MS is not possible because of their low volatility and high amount in the sample. The recovery of the target analytes from the eutectic mixture is therefore mandatory for LC-MS analyses. This latter involves the use of macroporous resins[51,53,57] or antisolvents that disrupt the hydrogen bonding between the two components of the DES[49]. In this sense, Fu *et al.*[50] performed a purification step by SPE using a DES-modified adsorbent and a [Ch^+][Cl^-]-based DES for the elution of polyphenols from palm bark samples (*Trachycarpus*

fortunei (Hook.) H. Wendl), obtaining an enrichment of the analytes without using organic solvents and expensive SPE phases.

As mentioned above, DESs have found many applications in the plant field, mainly due of their ability to extract a very wide range of compounds. In particular, they have been extensively applied for the extraction of phenolic compounds that have been shown to dissolve better in DESs than in lipids or water[58]. Aside from phenolic compounds, other plant specialized metabolites have been extracted with DESs. In particular, Duan *et al.*[48] have thoroughly investigated the behavior of several DESs in the extraction of various bioactive compounds, including alkaloids, saponins and anthraquinones. For the alkaloids, carboxylic acid-based DES (e.g. betaine-levulinic acid) resulted to be a more efficient solvent, than MeOH, which is less suitable for the extraction of partially ionized compounds. On the other hand, acid-based DESs are not suitable for the extraction of saponins, and better results were obtained when using dimethylurea or methylurea as HBD. Finally, anthraquinones were poorly extracted by most hydrophilic DES as a result of the low polarity of these compounds. In this respect, hydrophobic DESs can be used to extend the application of these solvents to the analysis of poorly polar compounds. For instance, a HBA consisting of methyltrioctylammonium chloride combined with 1-propanol in a 1:4 ratio has been successfully applied for the extraction of artemisin, which is an apolar terpenoid used in malaria treatment, from *Artemisia annua* L.[59]. A new generation of hydrophobic NADES has also been developed by mixing menthol with different HBDs. The combination of menthol and 1-propanol has been used for the isolation of taxanes from *Taxus wallichiana* var. *chinensis* (Pilg.) Florin (syn. *Taxus chinensis* (Pilg.) Rehder) needles and was found to be more efficient than conventional solvents, such as MeOH or EtOH[54]. The same HBA has been combined with different carboxylic acids in an efficient extraction of four cannabinoids from *Cannabis sativa* L. inflorescences[55]. It is interesting to emphasize that the extraction yield was not only influenced by the viscosity of the mixture, but also by the different alkyl chain lengths of the HBD used, which may have enhanced the interactions with more lipophilic compounds. NADESs (together with ILs) have also been investigated in the extraction of ecdysteroids and 20-hydroxyecdysone, from spinach (*Spinacia oleracea* L.). Several advantages were found, including higher selectivity, simplicity, efficiency, and rapidity, as well as the recovery and much lower consumption of organic solvents, compared with conventional methods[60]. In addition, it has been shown that DESs are also able to enrich volatile compounds. In fact, the headspace SPME

of the DES extracts of peppermint leaves and tobacco powder shows a richer volatile profile than that other extracts[61,62].

Very interestingly, DESs are also able to preserve the bioactivity of the compounds. Several studies have demonstrated the ability of DESs to increase the antioxidant capacity of natural products. For instance, the choline chloride-based extract of phenolic compounds from *Rosmarinus officinalis* L., provided higher antioxidant capacity and lower degradation kinetics than the corresponding ethanolic extract[63]. NADESs composed by HBAs and HBDs that are commonly introduced in our daily diet (such as sugars, amino acids or citric acids) can likely be directly used for food and pharmaceutical purposes[53]. However, current studies rarely investigate the bioactivity, biotoxicity and metabolism of these derivatives.

The psychochemical characteristics and environmentally friendly profile of DESs (and in particular NADESs) perfectly match the principles of GAC, including the replacement of harmful organic solvents. At the same time, there is a need to overcome some drawbacks in their use related to their viscosity, which can negatively affect extraction time (up to 2 hours), extraction capacity and compatibility with the main analytical platforms, if not properly controlled.

3.2 Sorbents

A wide range of new sorbents has recently been applied in the plant field, in particular for the clean-up and pre-concentration of specific analytes from water and organic extracts. It should be noted that plant matrices are commonly solids, as are the sorbents, meaning that previous sample extraction has to be carried out to allow a solid phase extraction with the sorbents. In most cases, it is performed with organic solvents, and this decreases the sustainability of the whole process. However, greener alternatives are available in the form of matrix solid-phase dispersion extraction (MSPD), and via pre-extraction with the green solvents described above.

In this section, the potential of the main classes of solid sorbents that have been exploited in the extraction of natural products will be discussed, together with their main limits and future trends.

3.2.1 Natural sorbents

Natural sorbents are certainly the greenest alternative to conventional materials in extraction procedures, and respond to the growing concern for environmental sustainability and safety. Apart from their low ecological impact, these sorbents are cheaper than with other extraction phases, and readily available from natural sources. They include sorbents with a range of characteristics, but the common principle is the exploitation of natural products as raw materials for the preparation of sustainable and efficient extraction phases. Over the years, many natural sorbents have been demonstrated to possess good extraction capacities as well as suitable characteristics for extraction, such as mechanical strength, gelling properties and tunability[11,64].

According to literature, two main classes have been explored as sorbent phases in plant extraction: i) biopolymers; and ii) food by-products. The first are isolated from living organisms and consist of monomeric units (e.g. nucleotides, monosaccharides, amino acids) that are covalently bonded to form a polymeric chain. Polysaccharides have undergone the most widespread explorations in the extraction of endogenous and exogenous compounds from plants. Chitosan and cellulose have been used in different formats, including as dispersants[65], SPE cartridges[66], nanoparticles[67], and fibers[68], thanks to their versatility. Unlike cellulose, which is abundant in the walls of vegetal cells, chitosan (deacylated form of chitin) is mainly derived from the skeletons of marine animals. Both materials present surfaces that are rich in hydrophilic groups, which can easily form hydrogen bonding and electrostatic interactions with target analytes[64]. Sporopollenin, a major component of the external walls of pollen grains, is another interesting biopolymer. It has gained attention as a sorbent material for its impressive resistance to high temperatures and chemical treatments and, it has found application in combination with other sorbents, such as carbon-based materials and magnetic nanoparticles[69].

The use of food by-products as sorbent phases in the extraction of vegetable matrices has been documented in the literature, and some interesting applications have been proposed[70–72]. For example, Jiang *et al.* have used crab shells from a local restaurant as the starting materials for a chitosan-rich powder that has been used for the isolation of anthraquinones from *Senna* spp. (syn. Cassia)[70]. Food by-products can also be used to obtain carbon-based materials, and thus avoid the use of fossil fuel-based precursors. Hierarchical porous carbon from banana peel presented a large surface, rich in graphitized pores, and these pores have been exploited for their

selective interactions with the aromatic groups of carbamate pesticides[71]. Magnetic nanoparticles with a carbon structure have been also prepared from the hydrothermal carbonization of pomelo peel[72].

The reusability of a sorbent is also an important factor that reduces analysis costs and waste production. In general, many of these natural sorbents can be re-used several times[68,72].

The use of natural sorbent as such should be preferable in order to develop green methods. In many examples, natural materials exhibit excellent extraction capacities thanks to their specific functional groups and porous structures, which allow proper interactions with the target analytes without further functionalization[65,71]. On the other hand, the functionalization and/or combination of different sorption mechanisms can enhance extraction performance, and several works have developed hybrid phases starting from natural sorbents. For example, the incorporation of magnetic particles into a sorbent material is a well-known method to simplify extraction procedures[67,72,73].

Various extraction techniques have been developed for the isolation of compounds from plant samples, and the versatility of these natural materials can grant significant benefits. Several SPE cartridges have been prepared with chitosan[66], cotton[68] and treated food by-products[71], with these being simply packed into a cartridge and the compounds of interest eluted with a suitable organic solvent. Matrix solid-phase dispersion (MSPD) is an extraction method in which a sample is directly ground and mixed with a solid-phase sorbent and the analytes are subsequently isolated, via adsorption, and eluted with a certain volume of solvent. Cellulose and chitosan can act as optimal dispersants and sorbents in MSPD, and have been successfully employed for the extraction of anthraquinones[70] and caffeoylquinic acid derivatives[65] from various vegetal samples. Er *et al.*[73] have coupled natural sorbents with a miniaturized version of magnetic dispersive SPE (m-μ-dSPE) to develop a truly sustainable procedure. The method only required a small amount of chitosan nanoparticles, which were dispersed into the liquid sample, and a few microliters of organic solvent to elute the compounds from the sorbent.

These natural materials have been designed to improve the environmental friendliness of extraction approaches, but also to enhance the efficiency of analytical procedures. Comparisons with common approaches have shown similar or better results in terms of sample and solvent

volume, extraction time, LOD and RSD in many examples[70,72]. However, there is still a need to deeply investigate the reproducibility of these materials, in terms of composition and analytical performances, considering their natural origins.

3.2.2 Molecular imprinted polymers

Molecular imprinted polymers (MIPs) are a peculiar group of extraction materials with unique "mimic molecular recognition" properties. An interaction site with high affinity for a chosen template is formed during the synthesis of this polymeric matrix. The high selectivity of MIPs is therefore based on the geometry of this cavity and on the presence of specific functional groups that are complementary to the target analyte.

Regarding extraction in the plant field, MIPs are arising as a valid approach when the goal is to isolate target compounds from the rich phytocomplex typical of plants. Indeed, most extraction phases lack high selectivity for a specific analyte or class of compounds, meaning that pretreatment and/or purification steps for analyte enrichment are usually necessary before extraction. MIPs have been used for the extraction of endogenous bioactive compounds, including molecules with widely differing chemical structures, thanks to the possibility of obtaining tailor-made MIPs.

The synthetic protocol of MIPs involves several reagents and steps. A monomer interacts with the template (i.e. molecule with the same or similar chemical features as the target analytes) to form the specific cavity that characterizes every MIP. An initiator induces the polymerase chain reaction, while the porogen assures the formation of pores that facilitate interaction with the target analyte during extraction. Finally, a cross-linker ensures the formation of a rigid structure, which must be preserved after the removal of the template, at the end of the polymerization process. The choice of the reagents to use (especially the monomer) clearly depends on the the target compound to be isolated. Also, the correct selection of the porogen solvent seems to play a key role in the recognition ability of MIPs and can directly influence their morphology. Ionic liquids can be used as porogenic solvents when preparing MIPs as they form discrete polar and non-polar microenvironments that lead to enhanced interaction between the template and functional monomer and limit non-specific binding. In addition, ILs have been shown to accelerate polymerization and improve the effect of imprinting. This strategy has been

applied for the isolation of corilagin, a bioactive ellagitannin, from a *Phyllanthus urinaria* L. water extract[74]. Ionic liquids can also be used in combination with MIPs to form hybrid materials that combine the selectivity of MIPs with the ion-exchanging and electrostatic-attraction ability of ionic liquids. An IL−hybrid molecularly imprinted material (IL-HIM) has, in fact, been used as a sorbent for the solid-phase extraction of two plant-growth regulators from bean sprouts, coupled to HPLC analysis. The hybrid material is suitable for the simultaneous determination of the two target analytes in bean sprouts, but accurate selectivity and competitive experiments showed that the adsorption of 6-BA onto IL−HIM is based on selective imprinted recognition, whereas the adsorption of 4-CPA is mainly dependent on ion-exchange interactions[75].

While MIPs have mostly been associated with SPE, the primary goal in their use is currently the incorporation of miniaturized extraction techniques to improve the accuracy and precision of the method and, at the same time, decrease sample and sorbent consumption[76]. However, the combination of MIPs and microextraction methods in the plant field has yet to be thoroughly investigated. Some SPME coatings have recently been developed and successfully used for the enrichment of low concentration bioactive compounds, such as auxins[77] and for the rapid detection of the potentially toxic pyrrolizidine alkaloids[78].

Apart from selectivity, versatility is one of the main advantages of MIPs. Their characteristics, including durability over a wide range of pH values and temperatures, make them suitable for innovative applications as extraction phases. A recent review by Arabi *et al.* gives a comprehensive overview of the new trends in MIP-based SPE, including nano-scale MIPs, composite MIPs, hollow porous MIPs and many others[79]. Again, the application of these novelties in plant field have been less frequently explored compared to other application fields but an interesting example is the preparation of surface-imprinting MIPs that are based on boron nitride and DESs, adopted for the isolation of flavonoids[80].

Although MIPs show outstanding features, there are still some critical points. The synthesis of MIPs requires many steps and reagents, including high amounts of toxic solvents to remove the template. The incorporation of green materials/solvents should be considered to avoid the large-scale consumption of hazardous substances. The synthesis of water-compatible MIPs is another hot topic, because the presence of water can negatively affect non-covalent binding with the analyte, decreasing interactions. However, some water-compatible MIPs, that

can be directly used in aqueous media, have been developed. . Moreover, compounds from the same chemical class can present quite different functional groups in their structure, and molecules with low similarity to the template may have some difficulties interacting with MIP cavities. To solve these problems, Sun *et al.* have developed an off-line two-dimensional MIP-SPE for the extraction of ellagitannins from pomegranate[81]. Ellagic acid and punicalagin MIP SPE columns were prepared and used as the first and second dimensions, respectively.

3.2.3 Magnetic nanoparticles

Metallic materials have also found applications in microextraction approaches in the plant field. They have been used because of their high thermal, mechanical and chemical stability, and easy functionalization. The nanoparticles made from transition metals (Fe, Co and Ni), and from their oxides, such as Fe_3O_4, are the most commonly used[82]. Given their superparamagnetic properties, which permit their easy and quick isolation when applying an external magnetic field, they have emerged as useful tools for the development of magnetic solid-phase extraction (m-SPE) protocols that avoid centrifugation and separation steps.

Moreover, these magnetic nanoparticles (MNPs) are often modified to give composite materials with a magnetic core and a functional shell that can provide more active sites for adsorption, while protecting the magnetic core. These composite materials have been also employed for the extraction of plant samples. For instance, cellulose MNPs have been developed for the extraction and determination of polychlorobiphenyls (PCB) in juice samples[83] and magnetic β-cyclodextrin (CD) modified graphene oxide nanoparticles (Fe_3O_4@SiO_2/GO/β-CD) have been applied as a sorbent for m-SPE of plant growth regulators from vegetable methanolic extracts[84]. MNPs that were functionalized with tetraethyl orthosilicate, 3-(trimethoxysilyl)propyl methacrylate, polymethacrylate have been successfully adopted for the determination of contaminants in red fruit samples (strawberries, blueberries, and raspberries) using GC-MS and QuEChERS extraction.

MNPs that were coated with an amino-terminated supramolecular cucurbit-[6]-uril pseudorotaxane motif have been developed for the extraction of four salvianolic acids from *Salvia miltiorrhiza* Bunge root water extracts.[85]. The investigated MNPs, which provided good

recyclability and stability, showed improved adsorption capacity towards the target analytes, compared to the non-functionalized NPs, while the combination of electrostatic interactions, van der Waals interactions, hydrophilic interactions and hydrogen bonding was thought to be the driving force behind the interaction between the analytes and sorbent. . .

Most of the magnetic composite nanoparticles applied in the plant field are composed of magnetic nanoparticles coated with metal organic frameworks (MOFs) because of their large surface areas, high porosity, uniform pore sizes and structural diversity. These composite sorbents will be thoroughly described in the following section.

3.2.4 Reticular materials

Reticular materials are another important group of novel solid sorbents. They are large crystalline frameworks made up of building blocks linked by either covalent or coordination bonds, depending on the type of reticular material. These materials are characterized by impressive porosity, good chemical and thermal stability, and by the possibility of post-synthetic modification, which makes them suitable sorbents for microextractions.. The most common types of reticular materials are metal-organic frameworks (MOFs) and covalent-organic frameworks (COFs), which are mainly differentiated by the organic or inorganic nature of their building blocks. COFs are formed by organic molecules with non-metallic light elements (C, H, O, N, B and Si), which are then linked by covalent bonds that are ordered in two- or three-dimensional networks, while MOFs are made up of metal ions or metallic clusters and organic linkers as building blocks, linked by strong coordination bonds[86]. Of the two classes of reticular materials, MOFs have been more widely applied in the plant field.

Mainly used for the extraction of contaminants from plant extracts, MOFs have also shown great potential as sorbents in combination with microextraction techniques to extract active compounds from plants and plant products. A copper-based MOF has been adopted for the selective isolation of chamazulene from a chamomile hexane extract. The driving force behind this selectivity is probably the chemical structure of the target compound, which is different from the other components in the extract, as chamazulene is the only aromatic compound[87]. Azeolitic imidazolate framework has also been investigated for the selective extraction of an antioxidant flavonoid derivative from an *Caragana jubata* (Pall.) Poir ethanolic extract. In this case, an adsorption mechanism study has shown that the target compound is adsorbed onto the MOF

surface, and that the *o*-phenolic hydroxyl group plays a significant role in the selective adsorption of the investigated flavonoid[88]. As a possible limitation in the use of MOFs as extraction material, it should again be noted that the raw plant material has to be submitted to analyte pre-extraction. In addition, attention must be paid to the fact that analytes are strongly adsorbed by MOFs, meaning that their desorption must be carefully optimized. However, MOFs can also be used in MSPD extractions. For instance, a zirconium-based MOF (MOF-808) has been applied for the MSPD extraction of ginsenosides from *Panax ginseng* C.A. Meyer. Only two hundred microliters of methanol were used for the elution and the collected filtrate was analyzed using UHPLC-ToF-MS[89]. As previously mentioned, MOFs are very commonly combined with magnetic nanoparticles to increase the magnetic susceptibility. The combination of magnetic Fe_2O_4 nanoparticles with a zinc-based metal organic framework (MOF-5) has been successfully applied for the extraction of colchicine, a bioactive alkaloid, from autumn and spring *Colchicum* spp. root ethanolic extracts.. Colchicine sorption occurs by combination of various mechanisms such as ion exchange, hydrogen bonding, electrostatic, π-π, and dipole-ion interaction[90]. SiO_2@Fe_3O_4 magnetic nanoparticles have been anchored onto an aluminum-based MOF (MIL53) and used for the extraction of aflatoxin B1 from several herbal teas via magnetic SPE coupled with spectrofluorimetric determination[91]. Furthermore, SiO_2@Fe_3O_4 magnetic nanoparticles have also been grafted onto a titanium-based MOF for the extraction of caffeic acid from methanolic/water extracts and coupled to HPLC-UV analysis[92]. Magnetic MOF nanoparticles can also be adopted to speed-up the mechanochemical extraction (MCE)of analytes from plant samples. MCE is a room-temperature process that disrupts the lipid membrane layers and cell walls using a multi-directional, mechanical liquid collision between the sample and specialized ceramic beads. This approach is adopted to achieve the complete release of target compounds, while preserving their chemical integrity. It can be combined with m-SPE with Fe_3O_4@MOF, meaning that the extraction of the analytes and their enrichment can be performed in one single step with a very fast removal of the extraction phase through a simple magnet. This approach has been successfully applied in the determination of organochlorine pesticides in tea leaves[93]. The combination of MOF with silica nanoparticles is another interesting possibility[94]. In addition, MOFs can be coated onto different materials. For instance, a zirconium-based MOF has been coated onto cotton fibers. The sorbent, packed into a pipette tip, has been successfully used for the extraction of phenoxy herbicides from cucumber-water extracts[95]. MOFs have also been

coated onto polymeric monolithic columns and adopted for the determination of ursolic acid from several ethanolic plant extracts[96,97] and of aristolochic acid from methanolic plant extracts[98]. MOFs have also been grafted onto SPME fiber[99] but their use in the plant field has not yet been widely explored. As for the other sorbents, it is important to remark that further improvements are desirable in terms of sustainability of the whole extraction process, such as the elimination of the pre-extraction step.

3.2.5 Carbon-based materials

Carbon-based materials also present exceptional physical and chemical properties, such as versatility, large surface areas with delocalized π-electrons, and easily modifiable surfaces. They constitute a group of different hexagonal structures of sp^2 hybridized carbon atoms. A single layer of these materials is called graphene. Together with graphene oxide (GO), and reduced graphene oxide (rGO), they are the most used forms of carbon-based materials in analytical chemistry. The difference between them lies in the presence of oxygen functional groups on their surface and their water solubility; graphene and rGO are non-polar and hydrophobic, while GO is hydrophilic. The three-dimensional forms of graphene are single or multiple wall carbon nanotubes (CNTs). CNTs share the same exceptional properties as graphene and its derivatives, but with a few differences as the inner walls of these materials are blocked by steric hindrance[100].

Both two and three-dimensional carbon-based materials have been applied in the plant field although graphene and GO are rarely used alone because they are prone to form aggregates. Ionic liquids can be adopted to prevent the aggregation of graphene, increasing, at the same time, the ability of π-π interactions, ionic exchange, electrostatic interactions and hydrogen bonding between the sorbent and the analytes. An IL-functionalized graphene adsorbent has, in fact, been developed for the pipette-tip solid-phase extraction of auxins from soybean sprouts[101].

However, graphene and, even more, GO are mainly applied to modify other sorbent to form composites[69,102]. For instance, GO has been added to a composite made of sporopollenin and Fe_3O_4 MNPs to increase the adsorption capacity and selectivity towards polar compound of the sorbent material. The composite has been then adopted to the determination of polar organophosphorus pesticides in several vegetables that had been pre-treated with water and methanol[69].

Due to their high hydrophobicity, MWCNTs can be successfully applied for the clean-up of plant extract. In fact, they can provide very high chlorophyll removal and a decrease in the matrix effect[103]. For instance, MWCNTs have been successfully applied to remove interferences from vegetables submitted to the QuEChERS procedure. MWCNTs provided up to a 94% reduction in chlorophyll and lower matrix effects compared to the commonly used primary-secondary amine (PSA) sorbent thus making the extracts fully compatible with HPLC–MS/MS analyses[104].

MWCNTs can also be combined with other materials to form MWCNT composites that have been used in SPEFe_3O_4/MWCNT composites have been used as SPE sorbents for simultaneous determination of zearalenone and other mycotoxins in the extracts of *Salvia miltiorrhiza* Bunge roots and ryzhome[105] and for the extraction of a set of chiral pesticides from several plant extracts[106]. MWCNTs can also be grafted with β-cyclodextrins to increase the absorption capacity of the composite thanks to their ability to form inclusion complexes with the target compounds. For instance, multiwalled carbon nanotube-β-cyclodextrin composites have been incorporated into a poly(butyl methacrylate-ethylene dimethacrylate) monolith for the online extraction of psoralen and isopsoralen from a methanolic *Cullen corylifolium* (L.) Medik. (syn. *Psoralea corylifolia* L.) fruit extract[107].

MWCNTs composites incorporated in SPME fibers show a great potential also for i*n vivo* analyses. A very interesting application has been reported where MWCNTs/polyaniline-polypyrrole@polydimethylsiloxane (PANI-PPy@PDMS) fiber has been prepared by electrodeposition followed by polymer surface modification for the *in vivo* extraction of pesticides from garlic by direct contact SPME[108].

Carbon-based materials are usually used in the form of composites. The incorporation of different materials can enhance their extraction capacity for complex samples such as those in the plant field. However, as many other sorbents, their synthesis can be long and complex and may require the consumption of materials and reagents, being a limitation for their use in routine analysis.

Table 1. Representative applications of innovative extraction phases in plant field.

Sample	Analytes	Phase	Additional materials	Extraction method[a]	Analytical platform	Ref.
IL-based extraction						
Elaeagnus rhamnoides (L.) A.Nelson .	essential oil, non-volatile compounds	$[C_4mim]^+[Br]^-$[c]	/	UA/MA distillation extraction	HPLC-UV/GC-MS	38
Coptidis spp.	berberine hydrochloride	MIL two phase system $[N_{1\,1\,5\,2}OH]^+[Br]^-$ and $[TEMPO\text{-}OSO_3]^-[Na]^+$[d]	/	magnetic ABS	HPLC-UV	33
Chrysanthemum spp.	lipophilic and hydrophilic endogenous compounds	Temperature-responsive $[HMIM]^+[BF_4]^-$[e]	/	*in-situ* solid-liquid extraction	UHPLC-UV-QTOF-MS	41
DES-based extraction						
Trachycarpus fortunei (Hook.) H.Wendl.	polyphenols	ChCl/Ph[f] sorbent ChCl DES eluent	/	SPE	HPLC-MS	50
Mentha×piperita L.	volatile monoterpenes, phenols	ChCl/D(+)-glucose	/	solid-liquid UAE	UHPLC-QTOF-MS/GC-MS	62
Taxus wallichiana var. *chinensis* (Pilg.) Florin	taxanes	menthol/1-propanol	/	solid-liquid UAE	HPLC-UV	109
Natural sorbent-based extraction						
Fruits	triazole fungicides	carbon (from pomelo peel) NPs	Fe_3O_4	m-SPE	GC-MS	72
Azolla imbricate (Roxb. ex Griff.) Nakai	caffeoylquinic acid derivatives	chitosan	/	MSPD	HPLC-UV	65
MIP-based extraction						
Phyllanthus urinaria L.	corilagin	Corilagin-MIP	$[BMIM]^+[BF_4]^-$[h]	SPE	HPLC-UV	74
Tussilago farfara L.	pyrrolizidine alkaloids	PA[i]-MIP	/	SPME	UHPLC	78
MNP-based extraction						
Salvia miltiorrhiza Bunge	salvianolic acids	magnetite@silica NPs	curcubit pseudorotaxane complex	m-d-SPE	HPLC-MS	85
Reticular material-based extraction						
Panax ginseng C.A.Mey	saponins	MOF-808	/	μ-MSPD	UHPLC-QTOF-MS	89
Camellia sinensis (L.) Kuntze	organochlorine pesticides	MIL-100	Fe_3O_4	m-SPE	UHPLC-UV/GC-MS	93
Carbon material-based extraction						
Vegetables	parabens	MWCNTs	/	QuEChERS (SPE)	HPLC-MS/MS	104
Allium sativum L.	pesticides	MWCNTs	PANI-PPy@PDMS[m]	DI/*in vivo*/*in vitro* SPME	GC-MS	108

[a] for the acronyms of the techniques, see abbreviation list; [b] silica particles with polyvinyl alcohol chains modified by *N*-methyl imidazole proline salt; [c] 1-butyl-3-methyl imidazole bromine salt; [d] alkyl(2-hydroxyethyl)-dimethylammonium bromides, sodium 4-sulfonatooxy-2,2,6,6-tetramethyl piperidine-1-yloxyl; [e] 1-hexyl-3-methylimidazolium tetrafluoroborate; [f] phenol; [g] microcrystalline cellulose; [h] 1-butyl-3-methylimidazolium tetrafluoroborate; [i] pyrrolizidine alkaloid; [l] gallic acid; [m] polyaniline-polypyrrole@polydimethylsiloxane

Chapter II
EXPERIMENTAL

II.1 Samples

The samples object of study of this Doctoral Thesis were selected based on their availability (local plants) and potential application in the nutraceutical and health field.

Regarding the studies on ***Vitis vinifera* L.,** the following samples were employed:

(i) A mixture of green pruning residues (GPRs) and leaves of red and white grapevine Italian cultivars harvested in an experimental vineyard located in Piedmont (North West Italy)[110]. This pool was used for the optimization of the ILs-based microwave-assisted method developed in Section III.1.2.

(ii) Grapevine leaves from six Canarian cultivars, kindly provided by the Canary Agronomic Research Institute (ICIA, Tenerife, Spain), were used for the quantification studies in Section III.1.2. They included three white grapevine varieties (Malvasía Lanzarote (ML), Moscatel Alejandría (MA), and Listán Blanco (LB)), and three red grapevine varieties (Tintilla (T), Negra Moll (NM), and Listán Negro (LN)).

(iii) Four pools of GRPs harvested in Piedmont kindly provided by the Institute of Sciences of Food Production, National Research Council (Grugliasco, Italy) were employed for the digestion experiment in Section III.1.3: Chardonnay and Müller Thurgau as white grapevine and Nebbiolo and Aglianico as red grapevine.

All the samples were freeze-dried, grounded in a mortar, to obtain a fine powder, and stored in a dryer, to prevent degradation.

Regarding the studies on ***Corylus avellana* L.**, the following sample was employed:

(i) Hazelnut skin as industrial by-product, kindly provided by the group of Organic Chemistry at the department of Drug Science and Technology, University of Turin (Section III.2).

Regarding the studies on ***Cannabis sativa* L.,** the following samples were employed:

(i) Twenty-four samples of fiber-type *Cannabis sativa* L. were kindly provided by the Institute of Sciences of Food Production, National Research Council (Grugliasco, Italy). The plants were grown in the Western Po Valley (Italy) and the aerial parts

(mainly stems and leaves) were collected at four progressive morphological stages, from mid-vegetative to early flower stage, on three different land plots (A, B, and C). The harvested samples were immediately subjected to oven-drying (in a forced-draft oven at 65 °C to constant weight) and freeze-drying (using a lyophilizer), and subsequently ground into a fine powder to pass a 1 mm screen with a Cyclotec mill (Tecator, Herndon, VA, USA). A mix of all 24 samples was prepared for the optimization of the extraction methods developed in Section III.3.

(ii) Seedless dried inflorescences of fiber-type *Cannabis sativa* L. purchased from a local Cannabis "light" shop (Cbweed). The inflorescences were labelled as coming from organic farming with Δ^9-THC content <0.5% (Section III.3.5).

(iii) Hemp extract in medium chain triglycerides (MCT) from coconut oil, labelled as "CBD oil" (7% CBD). It was purchased from a local Cannabis "light" and stored at -18 ◦C to prevent degradation (Section III.3.5).

Table 1 lists the main characteristics of the plant matrices used in this Thesis.

Table 1. Main characteristics of the samples employed in this Thesis.

Plant	N° of samples	Characteristics	Application in this Thesis	Reference section
Vitis vinifera L.	1 (mix)	GPRs[a] and leaves	Optimization of extraction method	III.1
Vitis vinifera L.	6	leaves	Application of the method and quantification	III.1
Vitis vinifera L.	4	GPRs	*In vitro* digestion	III.1
Corylus avellana L.	1	skin	Optimization of extraction method, *in vitro* screening of antioxidant activity	III.2
Cannabis sativa L.	24	Aerial parts	Optimization of extraction method, quantification, *in vitro* screening of biological activity	III.3
Cannabis sativa L.	1	Inflorescences	Optimization of extraction method, quantification	III.3
Cannabis sativa L.	1	Oil	Optimization of extraction method, quantification	III.3

[a] Green pruning residues

II.2 Solvents and reagents

De-ionized water (18.2 MΩ cm) was obtained from a Milli-Q purification system (Millipore, Bedford, MA, USA). HPLC and LCMS-grade acetonitrile, methanol (>99.9% purity), acetone (>99.0% purity), formic acid (>98.0% purity), diethyl ether (>99.0% purity), ethyl acetate (>99.5% purity), hexane (>98.5% purity), diethyl ether (>99.0% purity), ethyl acetate (>99.5% purity), isopropanol (>99.5% purity), hydrochloric acid and potassium bromide (KBr) (>99.5% purity) were supplied by Merck Life Science S.r.l. (Milan, Italy). Ethanol absolute was supplied by VWR International Srl (Milan, Italy). For ^{1}H NMR analysis and ^{13}C NMR, dimethyl sulfoxide-d_6 (DMSO-d_6) and chloroform-d ($CDCl_3$) was procured from Cambridge Isotope Laboratories (Andover, MA, USA). For GC-MS analysis, pyridine and *N,O*-bis(trimetilsilil)trifluoroacetamide (BSTFA) from Merck Life Science S.r.l. were used for the derivatization of *Cannabis sativa* L. acetone extracts in Section III.3.2.

The synthesis of the IL-based surfactants (Section III.1.2) required 1H-pyrazole-1-carboxamidine-hydrochloride (99%), decylamine (99%), 1-butylimidazole (98%), and 1-bromohexadecane (97%), which were supplied by Merck Life Science S.r.l

The reagents tripropylamine, trihexylamine, trioctylamine, dimethylaminoethanol, 2-bromoethanol, 1-bromohexane, 1-bromodecane, 1-bromododecane, 1-bromotetradecane, and 1-bromohexadecane, obtained from Merck Life Science S.r.l, were used in the synthesis of $[Ch^+][Br^-]$-modified salts. Tetrabutylammoniumbromide and tetraoctylammoniumbromide were selected as reference commercial salts and were provided by Merck Life Science S.r.l.

For the preparation of natural eutectic solvents, (-)-menthol (CAS 2216-51-5), ±linalool (CAS 78-70-6), thymol (CAS 89-83-8), carvacrol (CAS 499-75-2), (-)-terpinen-4-ol (CAS 20126-76-5), eugenol (CAS 97-53-0), choline chloride (CAS 67-48-1), lactic acid (CAS 79-33-4), betaine (CAS 107-43-7), levulinic acid (CAS 123-76-2), glycerol (CAS 56-81-5) were purchased from Merck Life Science S.r.l., while glucose and fructose were from the laboratory collection.

For the synthesis of CIM-80(*Al*) MOF, aluminum nitrate nonahydrate (>98% purity), mesaconic acid (>99% purity) and urea (>99% purity), were purchased from Merck Life Science S.r.l.

For the *in vitro* colorimetric assays, $DPPH^{\bullet}$ (1,1-diphenyl-2-picrylhydrazyl) and $ABTS^{+\bullet}$ (2,2'-azinobis (3-ethylbenzothiazoline-6-sulfonic acid) diammonium salt) radicals, kojic acid,

sodium phosphate monobasic monohydrate, sodium phosphate dibasic anhydrous, L-tyrosine, mushroom tyrosinase (8503 U/mg), dimethyl sulfoxide (DMSO), trizma base, and *N*-Succinyl-Ala-Ala-Ala-p-nitroanilide elastase from porcine pancreas (5 U/mg) were purchased from Merck Life Science S.r.l.

Depending on the matrices under study, several phytochemicals were identified and selected as marker analytes to monitor:

Seven compounds were used as markers in *Vitis vinifera* L. samples: caftaric acid (CAS 67879-58-7) quercetin (CAS 117-39-5), quercetin-3-*O*-glucoside (CAS 482-35-9), quercetin 3-*O*-glucuronide (CAS 22688-79-5), rutin (CAS 153-18-4), kaempferol 3-*O*-glucoside (CAS 480-10-4) were acquired from Phytolab (Vestenbergsgreuth,Germany) and kaempferol 3-*O*-glucuronide (CAS 22688-78-4) from Merck Life Science S.r.l. Individual standard solutions were prepared by dissolving them in methanol at 500 mg L^{-1}, except for caftaric acid, which was prepared at 650 mg L^{-1}. Working standard solutions containing all the analytes were prepared at different concentrations in acetonitrile, to obtain the calibrations curves.

Five compounds were used as markers in *Corylus avellana* L. samples: gallic acid (CAS 149-91-7), protocatechuic acid (CAS 99-50-3), catechin (CAS 7295-85-4), procyanidin B1 (CAS 20315-25-7), quercetin 3-*O*-rhamnoside (CAS 522-12-3) supplied by Merck Life Science S.r.l. Individual standard solutions were prepared by dissolving each standard in ACN 5%, methanol 20%, methanol 100%, deionized water, and methanol 100%, respectively, at 1 mg mL^{-1} and then diluted at different concentrations to obtain the calibration curves with an external calibration method.

Ten compounds were used as markers in *Cannabis sativa* L. samples: cannabidiol, CAS 13956-29-1, (CBD), cannabidiolic acid, CAS 1244-58, (CBDA), cannabichromenic acid, CAS 185505-15-1, (CBCA), cannflavin A (CAS 76735-57-4) apigenin 7-*O*-glucuronide (CAS 29741-09-1), and luteolin 7-*O*-glucuronide (CAS 29741-10-4) were supplied by Merck Life Science S.r.l. Acacetin (CAS 480-44-4), apigenin (CAS 520-36-5), diosmetin (CAS 520-34-3), and coumaric acid (CAS 501-98-4) were supplied by Extrasynthese (Genay Cedex, France). Individual standard solutions were prepared by dissolving them in MeOH at 1 mg mL^{-1} and MeOH 85% for luteolin 7-*O*-glucuronide and then diluted at different concentrations to obtain the calibration curves.
All these solutions were kept protected from light and refrigerated at -18 °C.

II.3 Instrumentation and equipment

A Radwag analytical balance (Radom, Poland) was used to weight reagents, standards, and samples. An ultrasonic bath (Soltec, Sonica S3 EP 2400), a centrifuge (Remi group, Mumbai, India), a vortex (Thermo Fisher Scientific, Rodano, Italy), a rotavapor (Phoenix instruments, Garbsen, Germany), and a Visiprep™ SPE vacuum manifold (Merck Life Science S.r.l) were employed for the extraction procedures. C18 solid-phase extraction (SPE) cartridges bed mass (500 mg, volume 1 mL) (Agilent Technologies, Wilmington, DE, USA) were used for the purification of the extracts from chlorophylls. Before SPE, the extracts were filtered with filter paper (12 cm in diameter). Polyvinylidene fluoride (PVDF) syringe filters from CPS Analitica (Milan, Italy) were used to filtrate all the extracts before LC/GC analysis. To ensure the absence of any residual solvents in the hemp extract obtained with organic solvents (Section III.3.2), the head space of the extracts was sampled through solid-phase microextraction (HS-SPME) using a Divinylbenzene/Carboxen/Polydimethylsyloxane (DVB/CAR/PDMS) 50/30 μm film thickness and 2 cm length fiber from Merck (Milan, Italy), and analyzed by GC-MS. Sampling was conducted at room temperature for 15 min

A Shimadzu Nexera ×2 UHPLC system was used for qualitative analysis. It was equipped with an SPD-M20A photodiode array detector in series with a Shimadzu LCMS triple quadrupole system with an electrospray ionization (ESI) source (Shimadzu, Dusseldorf Germany). Mass spectrometer operative conditions were as follows: heat block temperature, 200 °C; desolvation line (DL) temperature, 230 °C; nebulizer gas (N_2) flow rate, 3 L min^{-1}; and drying gas (N_2) flow rate, 15 L min^{-1}. Full scan mass spectra were acquired from 50 to 2000 m z^{-1}, both in positive and in negative scan modes, with an event time of 0.5 s. When protonated/deprotonated ions $[M + H]^+$ in ESI^+ or $[M - H]^-$ in ESI^- were identified, they were subjected to collision (collision energy, −35.0 V for ESI^+ and 35.0 V for ESI^-) in product ion scan mode with an event time of 0.2 s. Quantitative analyses were carried out with a Shimadzu UHPLC XR chromatograph equipped with a photodiode array detector SPD-M20A (Shimadzu, Dusseldorf, Germany). Mobile phase A was water/formic acid (99.9:0.1, v/v) and mobile phase B was acetonitrile/formic acid (99.9:0.1 v/v) in all the analysis. The flow rate was 0.4 mL min^{-1} and the column temperature was set at 30 °C. For the analysis of *V. vinifera* L., the best separation was obtained using an initial composition of 5% of B, which was increased to 100% in 52 min. For *C. avellana* L., the gradient was as follows: 0 to 5 min 5% phase B, 5 to 30 min 5%-15% B, 30 to

50 min 15%-35% B, 50 to 57 min 35%-100% B. For the analysis of *C. sativa* L. aerial parts, the gradient program was as follows: 0 to 2 min 15% B, 2 to 52 min 15%- 86% B, and 52 to 55 min 86% B, while for hemp inflorescences and oil the gradient program was 0 to 2 min 30% B, 2 to 42 min 30–86% B, 42 to 44 min 86% B.

GC-MS analyses were also carried out for identification purposes using a TRACE GC Ultra gas-chromatograph platform from Thermo equipped with a Thermo 3000 Series Automatic Sampling System (AI 3000) and hyphenated to a Thermo DSQ mass spectrometer with an electron impact source (EI mode). GC conditions: injector temperature: 280 °C, injection mode: split, ratio: 20:1; carrier gas: helium, and flow rate: 1 mL min^{-1}. Temperature program: from 50 °C to 250 °C at 3 °C min^{-1}, and from 250 °C to 300 °C at 10 °C/min. The MS transfer line temperature was set at 270 °C. The single quadrupole mass spectrometer was used in full scan mode (mass range: 50–700 m z^{-1}) for the analysis of the derivatized extract of *C. sativa* aerial parts. The same GC-MS conditions reported above were used except for the mass range, which was set to 30–300 m z^{-1}, for the analysis of residual solvents.

An Ascentis Express RP-C18 column (15 cm × 2.1 mm, 2.7 μm, Supelco, Bellefonte, USA) was employed for the analysis of hemp extracts and an InfinityLab poroshell 120 C18 poroshell column (10 cm × 4.6 mm, 4 μm, Agilent, Santa Clara, USA) was used to analyze hemp extract obtained with MOF. An Ascentis Express RP Amide column (10 cm × 2.1 mm, 2.7 μm, Supelco, Bellefonte, PA, USA) were used for the analysis of grapevin, hazelnut extracts and hemp extracts obtained with natural ESs as well as for the $ABTS^{+\bullet}$ offline analysis. GC-MS analyses were carried out on a capillary MEGA-5 MS column (5% phenyl- and 95% methyl-substituted polysiloxane) with the following characteristics: l: 30 m, d_c: 0.25 mm, and d_f: 0.25 μm (MEGA, Legnano, Italy).

To measure the hydrophobicity of the ESs, water content was analyzed by a Metrohm 831 Karl Fischer coulometric titration system (Herisau, Switzerland) before and after mixing the solvent with water at neutral pH and 25 °C. The titration cell was filled with a Hydranal-Coulomat AG reagent, and the contents of the chamber were stirred at 300 rpm.

For the characterization of the eutectic solvents in Section III.3. a FTIR-ATR spectrometer (PerkinElmer, Waltham, Massachusetts, USA) and a Bruker (Massachusetts, USA) 600 MHz NMR spectrometer were used.

Bruker (Massachusetts, USA) 600MHz and JEOL ECZR (Massachusetts, USA) 600 MHz NMR spectrometers were used to characterize the purity of the salts and choline bromide-based HESs (Section III.3.4).

Differential scanning calorimetry (DSC) was performed on HESs to investigate their thermal properties using a NETZSCH DSC 214 Polyma instrument (Selb, Germany), and all thermograms were analyzed using NETZSCH Proteus software. The solvatochromic response of fluorescent dyes was studied using a Synergy H1 microplate reader (Biotek, Winooski, Vermont).

HES viscosity was measured using an AMETEK Brookfield DV1 cone and a plate viscometer (Middleborough, MA, USA) equipped with a CPA-51Z cone spindle, at 21.6 °C.

All ESs were analyzed using Fourier transform infrared (ATR−FTIR) spectroscopy and scanned between 4000 and 500 cm^{-1}. All IR measurements were performed on a Bruker VERTEX 80 FTIR spectrometer (Billerica, MA, USA).

Solvation characteristics of $[Ch^+][Br^-]$-based HESs were studied using inverse gas chromatography by employing them as GC stationary phases. An Agilent 7890B gas chromatograph (Santa Clara, USA) equipped with a flame ionization detector was employed for IGC experiments. A deactivated fused silica capillary was procured from MEGA (Legnano, Milano, Italy). Inlet/detector temperatures were kept constant at 150 °C, while a 20:1 inlet split ratio was employed (1 mL min^{-1} constant f low).

CIM-80(*Al*) MOF was characterized by powder X-ray diffraction using a PANalytical Empyrean diffractometer (Eindhoven, The Netherlands) with Cu Kα radiation (λ = 1.5418 Å) and operating with Bragg–Brentano geometry. Phase identification of the synthetized MOFs was carried out by X-ray powder diffraction on a X'Pert Diffractometer (Panalytical, Netherlands) operating with Bragg–Brentano geometry. Data collection was carried out using Cu Kα radiation (λ¼ 1.5418 Å) over the angular range from 5.01° to 80.00° with a total exposure time of 30 min. The microscopic morphology of the material was examined by a JSM6300 scanning electron microscope (JEOL, Tokyo, Japan). Figure 1 reports the comparison of X-ray between simulated and synthesized CIM-80(*Al*) MOF and the SEM images for the synthetized MOF.

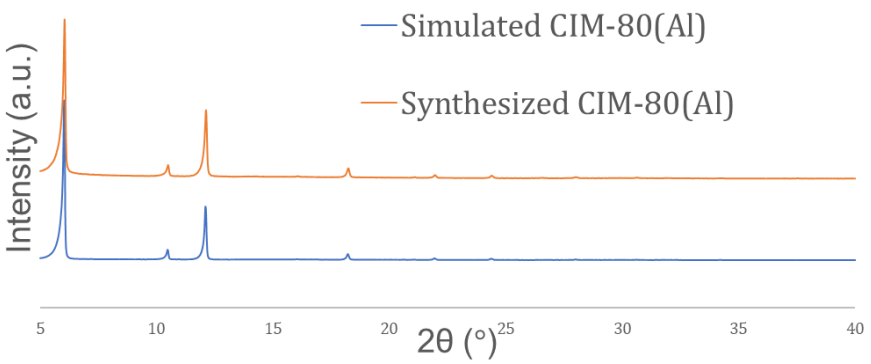

(a)

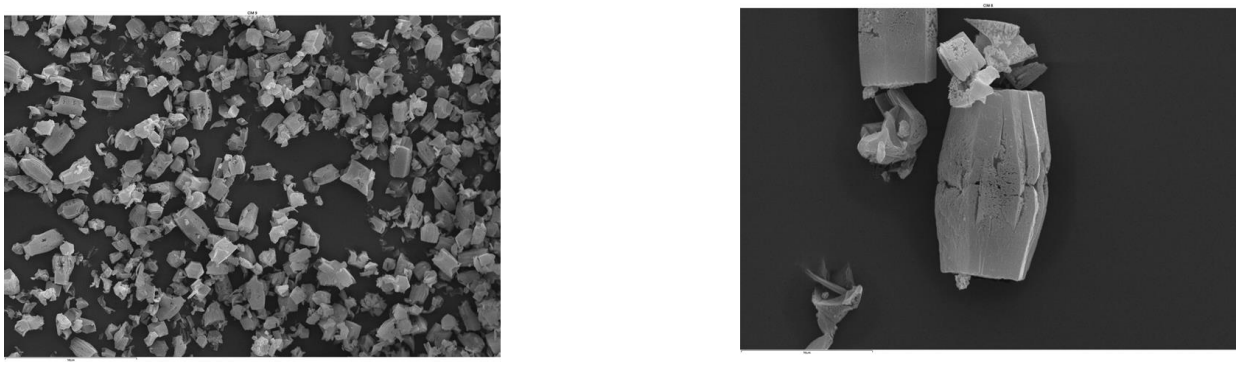

(b)

Figure 1. (a) X-ray of simulated and synthetized CIM-80(*Al*) and (b) SEM images.

II.4 Procedures

4.1 Synthesis of IL-based surfactants (Section III.1.2)

Decylguanidinium chloride (C_{10}Gu-Cl) used as extraction solvent in Section III.1.2, was synthetized by following a previously reported procedure[111]. Briefly, 1.70 mL of decylamine and 1.24 g of 1H-pyrazole-1-carboxamidine hydrochloride were dissolved in 2.5 mL of ethanol. This solution was left under magnetic stirring at 35 °C for 48 h. Then, the IL was washed 3 times with 2.5 mL of ethanol, which was evaporated under vacuum (50 °C 150 mbar) until the viscous IL was obtained. The IL-based surfactant 1-hexadecyl-3-butyl imidazolium bromide ($C_{16}C_4$Im-Br) was synthetized as was previously described in the literature[112]. Briefly, 12.4 g of 1-butylimidazole and 33.6 g of 1-bromohexadecane were refluxed in 20 mL of isopropanol at 70 °C for 24 h under stirring. The solvent was removed under vacuum (60 °C, 140 mbar), and the product was dissolved in 25 mL of water. It was washed 5 times with 15 mL of ethyl acetate, and, finally, water was evaporated under vacuum (80 °C, 70 mbar), and the product was dried in a vacuum oven, to obtain the solid IL-based surfactant.

4.2 Synthesis of choline bromide-modified salts (Section III.3.4)

Six [Ch$^+$][Br$^-$]-modified salts were synthesized to obtain hydrogen bond acceptors (HBAs) with hydrophobic features. Two main classes of ammonium salts were obtained: (A) [$N_{xxx(2OH)}^+$][Br$^-$] and (B) [$N_{11y(2OH)}^+$][Br$^-$],where x=3 or 6 and y=10, 12, 14, or 16. Moreover, two commercial ammonium salts, tetrabutylammonium bromide and tetraoctylammonium bromide, were used for comparison purposes. Table 2 summarizes the reaction conditions for every salt. For the first group (A), the synthesis protocol was modeled based on that reported by Dupont *et al.,*[113] with some modifications, and the purity was confirmed by ^{1}H and ^{13}C NMR. Briefly, amine and bromoethanol were dissolved in toluene and allowed to react under reflux for 48h at 110 °C. After cooling, the solvent was removed under rotary evaporation, and the product was purified to form a white powder. For the second group (B), the synthesis protocol was based on that reported by Costa *et al.*[114] after some modification and purity confirmed by ^{1}H and ^{13}C NMR. In this case, the alkyl halide and 2-(dimethylamino)ethanol were mixed in hexane and heated to 80 °C under reflux for 8−10h. The white solid precipitate was then filtered and washed with hexane. All products were dried under reduced pressure and stored in a vacuum oven.

Table 2. Reaction conditions of the [Ch$^+$][Br$^-$]-modified salts synthesized in the study.

[Ch$^+$][Br$^-$]-modified salts	Reagent 1	Reagent 2	Solvent	Molar ratio	Purification	Yield (%)	Characterization	Ref.
[$N_{1\ 1\ 10\ (2OH)}^+$][Br$^-$]	Dimethylamminoethanol	1-Bromodecane	Hexane	1 : 1.1	Wash with hexane	50%	^{1}H and ^{13}C NMR	114
[$N_{1\ 1\ 12\ (2OH)}^+$][Br$^-$]	Dimethylamminoethanol	1-Bromododecane	Hexane	1 : 1.1	Wash with hexane	70%	^{1}H and ^{13}C NMR	114
[$N_{1\ 1\ 14\ (2OH)}^+$][Br$^-$]	Dimethylamminoethanol	1-Bromotetradecane	Hexane	1 : 1.1	Wash with hexane	70%	^{1}H and ^{13}C NMR	114
[$N_{1\ 1\ 16\ (2OH)}^+$][Br$^-$]	Dimethylamminoethanol	1-Bromohexadecane	Hexane	1 : 1.1	Wash with hexane	70%	^{1}H and ^{13}C NMR	114
[$N_{3\ 3\ 3\ (2OH)}^+$][Br$^-$]	Tripropylamine	Bromoethanol	Toluene	1 : 1	Rotary evaporation + wash with diethyl ether	30%	^{1}H and ^{13}C NMR	113
[$N_{6\ 6\ 6\ (2OH)}^+$][Br$^-$]	Trihexylamine	Bromoethanol	Toluene	1.2 : 1	Rotary evaporation, wash with diethyl ether + crystallization in ethyl acetate	30%	^{1}H and ^{13}C NMR	113

4.3 Synthesis of CIM-80(*Al*) metal organic framework (Section III.3.6)

According to the optimized procedure, 750 mg of $Al(NO_3)_3$*$9H_2O$, 260 mg of mesaconic acid and 180 mg of urea were weighted in a Teflon lined hydrothermal autoclave, together with 30 mL of water. This mixture was left to react in an oven at 150 °C, for 24 hours. Once the reaction was completed, the solid was quantitatively transferred in a falcon tube and washed three times with water and three times with EtOH, to remove any unreacted residues. Before to use the sorbent, it was activated at 100 °C for 24 hours.

4.4 Preparation of eutectic solvents (Section III.2 and III.3)

Several eutectic solvents of different nature were used as extraction solvents in the extraction methods developed in this Thesis. All the ESs were prepared following the heat and stirring method[46]. Briefly, the HBA and HBD were mixed at the selected molar ratio under magnetic stirring for 30 min at 40 °C/60 °C depending on the components. After obtaining a homogeneous solvent, they were dried and store in a desiccator to prevent moisture absorption from the atmosphere. All the ESs prepared are reported in Table 3.

Table 3. Eutectic solvents prepared in this Thesis.

Component 1	Component 2	Molar ratio	Reference section
Hydrophilic			
Choline chloride	Lactic acid	1 : 1	III.2
Choline chloride	Lactic acid	1 : 2	III.2
Choline chloride	Levulinic acid	1 : 3	III.2
Choline chloride	Levulinic acid	1 : 5	III.2
Betaine	Glycerol	1 : 5	III.2
Betaine	Lactic acid	1 : 2	III.2
Betaine	Lactic acid	1 : 3	III.2
Betaine	Lactic acid	1 : 5	III.2
Betaine	Levulinic acid	1 : 2	III.2
Betaine	Levulinic acid	1 : 3	III.2
Betaine	Levulinic acid	1 : 5	III.2
Hydrophobic			
Menthol	Linalool	1 : 1	III.3
Menthol	Terpinen-4-ol	1 : 1	III.3
Menthol	Thymol	1 : 1	III.3
Menthol	Carvacrol	1 : 1	III.3
Linalool	Terpinen-4-ol	1 : 1	III.3
Linalool	Thymol	1 : 1	III.3
Linalool	Carvacrol	1 : 1	III.3
Linalool	Eugenol	1 : 1	III.3
Terpinen-4-ol	Thymol	1 : 1	III.3
Terpinen-4-ol	Carvacrol	1 : 1	III.3
Choline bromide-based			
$[N_{3\,3\,3\,(2OH)}^{+}][Br^{-}]$	Thymol	1 : 2	III.3
$[N_{6\,6\,6\,(2OH)}^{+}][Br^{-}]$	Thymol	1 : 2	III.3

$[N_{1\,1\,10\,(2OH)}^{+}][Br^{-}]$	Thymol	1 : 2	III.3
$[N_{1\,1\,12\,(2OH)}^{+}][Br^{-}]$	Thymol	1 : 2	III.3
$[N_{1\,1\,14\,(2OH)}^{+}][Br^{-}]$	Thymol	1 : 2	III.3
$[N_{1\,1\,16\,(2OH)}^{+}][Br^{-}]$	Thymol	1 : 2	III.3

4.5 Derivatization for GC-MS analysis (Section III.3.2)

To confirm the identification of cannabinoid compounds, the extracts were further analyzed by GC-MS. To prevent the decarboxylation of cannabinoid acids in the injector of the GC, the derivatization of the acetone extract was performed before chromatographic analysis, according to Acquadro *et al.* [115]. Briefly, 80 µL of pyridine and 120 µL of BSTFA were added to 2 mg of the extract and allowed to react for 30 min at 60 °C in a water bath.

4.6 Measurement of ESs hydrophobicity by Karl Fischer titration (Section III.3)

The same amount (500 mg) of HES and water was gently mixed for 30s with a spatula to avoid the formation of bubbles and then subjected to centrifugation to facilitate rapid separation of the two phases. Finally, the HES phase was sampled using a 3 mL Luer lock tip sterile plastic syringe, and its water content was measured. The same measurement was carried out before mixing the ES with water.

4.7 Measurement of ESs thermal properties by DSC (Section III.3.4)

The thermal properties of select HESs were characterized using the following protocol: the samples were cooled from 40 to −120 °C at a rate of 10 °C min^{-1} and subsequently heated to 80°C at the same rate using differential scanning calorimetry (DSC). DSC thermograms were analyzed to obtain the melting peak and/or glass transition temperatures for DESs.

4.8 Measurement of ESs polarity by solvatochromic dye method (Section III.3.4)

To investigate the polarity of hydrophobic $[Ch^{+}][Br^{-}]$-based HESs using the solvatochromic dye method, the dyes 4-nitroaniline (4-NA), Nile red (NR), and *N,N*-diethyl-4-nitroaniline (*N,N*-DENA) were employed. Each dye was dissolved in methanol at a 0.01 M concentration and refrigerated under 4 °C before transferring 100 µL into an Eppendorf tube. A steady stream of nitrogen was passed through the Eppendorf tube to evaporate methanol, leaving behind the solvatochromic dye as a thin film on the walls of the tube. A 100 µL volume of each HES was transferred into the Eppendorf tube and mixed thoroughly with the dye until a homogeneous mixture was obtained. A 20 µL volume of the resulting mixture was transferred

into a 96-well plate to measure its solvatochromic behavior using a microplate reader. UV−Vis molecular absorbance data was acquired through spectral scanning of HES/dye mixtures between wave lengths of 350 and 700 nm in 1 nm increments, and the maximum absorption wavelength (λ 19 max) was recorded. Spectroscopic measurements were conducted in triplicate, and the average of all values was calculated.

4.9 Inverse gas chromatography (Section III.3.4)

To prepare ES chromatographic columns using the static method of column preparation, 32 mg of each ES was transferred into a clean 20 mL glass vial and solubilized in 10 mL of dichloromethane. The ES solutions were injected into 5 m segments of a deactivated fused silica capillary, which were then sealed at one end, while the other end was connected to a vacuum, before placing the resulting setup in a water bath maintained at 40 °C. Dichloromethane was gradually and steadily evaporated, leaving behind a uniform thin film of ES coated on the inner walls of the fused silica capillary having an approximate thickness of 0.20 μm prior to performing GC measurements, all columns were placed inside a gas chromatograph and thoroughly conditioned by flowing helium (1 mL min $^{-1}$ constant flow) at 60 °C for 30 min. Additionally, inverse GC measurements were conducted at 40, 50, and 60 °C by systematically varying the GC oven temperature. Column efficiencies were measured by chromatographically separating naphthalene (1 g L^{-1}) at 60 °C and were determined to range from 1500 to 2900 plates/meter. Probe molecules comprising volatile organic compounds such as branched and straight-chained alcohols, nitroalkanes, and haloalkanes were dissolved in dichloromethane at the same concentration (1 g L^{-1}) and injected onto the ES columns to study their chromatographic retention.

4.10 Scavenging effect on DPPH• radicals (Section III.2 and III.3)

The capacity of the obtained extracts to scavenge the free radical DPPH• was investigated using the method reported by Król[116], with some modifications. A methanolic solution containing the DPPH• radical (25 μg mL^{-1}) was prepared to have an absorbance value between 0.65 and 0.72 at 515 nm and 2 mL of this solution was mixed with the extract. The mixture was shaken vigorously and left to stand for 30 min at room temperature in the dark (until absorbance values were stable). Reduction of the DPPH• radical was measured by monitoring the absorption decrease at 515 nm. Different concentrations of the extract were prepared in order to obtain a

dose-response curve. For each concentration, the DPPH scavenging effect was calculated with the following equation:

$$\% \text{ scavenging effect} = [(A_{DPPH} - A_S) / A_{DPPH}] \times 100$$

where A_{DPPH} is the absorbance of the DPPH$^{\bullet}$ solution and A_S is the absorbance of the DPPH$^{\bullet}$ solution after addition of the sample extract. The amount of matrix used to prepare an extract providing 50% inhibition (EC_{50}) was calculated by the equation of the dose-response curve. The same procedure was used to obtain the EC_{50} of Trolox, a phenolic compound with a well-known antioxidant capacity, which was used as a positive control to validate the procedure.

4.11 Scavenging effect on ABTS$^{+\bullet}$ radicals (Section III.2 and III.3)

The ABTS method was applied according to Król *et al.*[116] with some modifications. The ABTS$^{+\bullet}$ radical solution was prepared by adding 5 mL of $K_2S_2O_8$ solution (0.66 mg mL^{-1}) to 5 mL of ABTS (3.84 mg mL^{-1}) and the obtained solution was kept in the dark for 16h at −20 °C. This solution was diluted in EtOH/water (50:50 v/v) to obtain the working reagent with an absorbance of 0.70 ± 0.02 at λ = 734 nm. 2 mL of ABTS$^{+\bullet}$ radical solution was added to 100 μL of the extract, and the absorbance was measured after 6 min, at λ = 734 nm. The ABTS$^{+\bullet}$ scavenging effect was calculated as g equivalent of Trolox per kg of matrix. The Trolox calibration curve was built up by analyzing the standard compound at concentrations ranging from 25 to 100 mg L^{-1}.

4.12 Offline combination of antioxidant assays and HPLC-PDA analysis (Section III.3.7)

To investigate which compounds of the hemp extract prepared had a higher affinity with DPPH$^{\bullet}$ and ABTS$^{+\bullet}$, an HPLC-PDA analysis was carried out before and after the reaction with the two radicals. For DPPH$^{\bullet}$, 30 μL of the hemp extract (diluted in MeOH at the concentration providing the EC_{50}) was mixed with 2 mL of DPPH$^{\bullet}$ reagent (25 μg mL^{-1}), shaken vigorously, and left to stand for 30 min at room temperature in the dark. After the reaction, the solvent was evaporated with a gentle nitrogen steam and the dried extract was diluted with 150 μL of MeOH before injection into the LC system. The chromatographic profile of the extract after reaction with the DPPH$^{\bullet}$ radical solution was compared with that of the same extract before reaction, diluted 1:5. With regard to ABTS$^{+\bullet}$, 100 μL of the hemp extract at 2 g L^{-1}, diluted in EtOH, was mixed with 2 mL of ABTS working solution, shaken vigorously, and left to stand for 6 min at

room temperature in the dark. After the reaction, the solvent was evaporated with a gentle nitrogen steam and the dried extract was diluted with 2 mL of MeOH before injection into the LC system. The chromatographic profile of the extract after reaction with the $ABTS^{+\bullet}$ radical solution was compared with that of the same extract before reaction.

4.13 Tyrosinase inhibition activity assay (Section III.3)

The tyrosinase inhibition activity of the hemp extracts was tested with a colorimetric assay optimized by Zengh *et al.*[117], with slight modifications. The formation of dopachrome from L-tyrosine was monitored by measuring the absorbance at 475 nm. The dried extracts were previously dissolved in DMSO to obtain the concentration of 50 mg mL^{-1}. Subsequently, 10 μL of this solution was added to 600 μL of phosphate buffer 0.02 M (pH = 6.8) and 400 μL of mushroom tyrosinase 250 U mL^{-1}, previously dissolved in a phosphate buffer. The mixture was pre-incubated for 6 min at 30 °C. After the pre-incubation, 500 μL of tyrosine solution in a phosphate buffer (0.1 mg mL^{-1}) was added and the absorbance of the mixture was measured. In particular, the absorbance was registered from time "0" to 6 min every minute to obtain a kinetic response curve. A blank solution (without the enzyme) was used to calibrate the instrument. The reaction progress curves were performed for the methanolic and acetone extracts, as well as for the control (10 μL of DMSO instead of the extract) and for a positive control (kojic acid at 0.2 mg mL^{-1}). The initial velocity (v_o) of each curve, which is equivalent to the slope of the line, was measured and the % of tyrosinase inhibition was determined as follows:

$$\% \text{ tyrosinase inhibition} = [(\text{slope control} - \text{slope sample}) / \text{slope control}] \times 100$$

4.14 Elastase inhibition activity assay (Section III.3)

The elastase inhibition activity of the hemp extracts prepared was tested with a colorimetric assay optimized as reported by Bieth *et al.*[118], with slight modifications. The elastase inhibition assay is based on the spectrophotometric evaluation of the release of *p*-nitroaniline from *N*-succinyl-Ala-Ala-Ala-*p*-nitroanilide, stimulated by elastase. The formation of *p*-nitroaniline was determined at 410 nm. The dried extracts were dissolved in DMSO to obtain the concentration of 50 mg mL^{-1}. Then, 5 μL of this solution were added to 1345 μL of Trizma buffer (pH= 8) and 50 μL of elastase solution 0.6 U mL^{-1} (ratio 1:99 in Trizma buffer). During the measurements, the temperature of the elastase solution was kept around 0–4 °C, while the other reagents were at room temperature. The obtained mixture was pre-incubated for 6 min at

30 °C and subsequently 100 μL of substrate 1 mg mL^{-1} solution in Trizma buffer was added. The absorbance was registered from time "0" to 30 min every three minutes and a blank solution (without the enzyme) was used to calibrate the instrument. The reaction progress curves were performed for the methanolic and acetone extracts, as well as for the control (5 μL of DMSO instead of the extract) and positive control (ursolic acid, at EC_{50} 5 mg mL^{-1}). The initial velocity (v_o) of each curve, which is equivalent to the slope of the line, was measured and the % of elastase inhibition was determined with the same equation reported for tyrosinase.

II.5 Extraction methods

Different extraction methods were developed in this Thesis depending on the material used as extraction phase, the target analytes, and the samples analyzed. This section includes the optimized conditions for each of those analytical methods, while the different conditions evaluated during the optimization studies are detailed in the corresponding section of Chapter.

5.1 Microwave-assisted solid liquid extraction method using an IL-Based Surfactant (Section III.1)

0.100 g of grapevine sample was placed in a centrifuge tube, together with the stir bar, and 2.25 mL of 0.1 mM of an aqueous solution of the IL-based surfactant $C_{16}C_4$Im-Br IL was added. The mixture was introduced in the focused microwave system and programmed at 70 °C and 50 W for 30 minutes, while applying magnetic stirring. Once the extraction was completed, the mixture was left to cool to room temperature and centrifuged for 5 min at 2504 × g. The supernatant was collected by using a Pasteur Pipette and filtrated (using PVDF syringe filters) before injection in the LC system.

5.2 Ultrasound-assisted solid liquid extraction method using hydrophilic ESs (Section III.2 and III.3)

100 mg of hazelnut skins were transferred in a tube together with 1 mL of ES. The mixture was then submitted to US for 30 minutes. After 10 seconds of vortex the sample was centrifuged for 15 minutes at 4000 rpm and filtrated (using PVDF syringe filters) before injection in the LC system.

5.3 Ultrasound-assisted solid liquid extraction method using organic solvents (Section III.1, III.3)

10 mL of solvent of MeOH were added to 100 mg of dried grapevine (pre and digested samples) and a US-assisted extraction was performed for 15 min at 40 KHz at room temperature. The liquid phase was then subjected to centrifugation at 2200×g for 10 min while the US extraction procedure was repeated twice on the same plant matrix to obtain an exhaustive extraction of the target analytes. After the centrifugation, the supernatant was collected and filtered with filter paper and the solvent was completely evaporated at 40 °C in a rotary evaporator, under vacuum. At this point, the dried extract was subjected to an SPE procedure to eliminate the chlorophylls which can damage the chromatographic column. For this purpose, the extract was reconstituted with 1.5 mL of MeOH/water (40:60, v/v) and eluted with 8 mL of MeOH/water (85:15, v/v) through a C18 cartridge (previously activated with 4 mL of MeOH and 4 mL of water). The obtained extract was dried with a gentle nitrogen stream, diluted to a final concentration of 2 mL with ultrapure water and finally filtered (0.20 μm, PVDF) before the injection in the LC system.

5 mL of solvent (MeOH or acetone) were added to 100 mg of dried hemp sample and a US-assisted extraction was performed for 10 min at 40 KHz at room temperature. The liquid phase was then subjected to centrifugation at 2200×g for 10 min while the US extraction procedure was repeated twice on the same plant matrix to obtain an exhaustive extraction of the target analytes. After the centrifugation, the supernatant was collected and filtered with filter paper and the solvent was completely evaporated at 40 °C in a rotary evaporator, under vacuum. At this point, the dried extract was subjected to an SPE procedure to eliminate the chlorophylls which can damage the chromatographic column. For this purpose, the extract was reconstituted with 1.5 mL of MeOH/water (40:60, v/v) and eluted with 8 mL of MeOH/water (85:15, v/v) through a C18 cartridge (previously activated with 4 mL of MeOH and 4 mL of water). The obtained extract was dried with a gentle nitrogen stream, diluted to 5 mg mL^{-1} with MeOH/water (85:15, v/v), and finally filtered (0.20 μm, PVDF) before the injection in the LC system.

5.4 Dispersive solid-liquid microextraction method using natural ESs and $[Ch^+][Br^-]$-based HESs (Section III.3.4)

100 mg of hemp were transferred in a centrifuge tube with 2 mL of water (KBr 30% aqueous solution for $[Ch^+][Br^-]$-based HESs) and 100 μL of the ES. After 30 s of vortex, the

mixture was transferred in the bath sonicator (40 KHz at 25 ◦C) for 10 min. Once the extraction was completed, it was submitted to other 30 s of vortex and centrifuged for 5 min at 2200×g. Three different phases formed, starting from the bottom: (1) the plant, (2) water, and (3) the ES-rich phase. To allow an easy isolation of this latter, it was re-suspended in water (2) and the mixture (without the plant) was transferred in another tube and centrifuged again for 5 min at 2200×g. At this point, the aqueous phase was removed with a Pasteur pipette and the remaining upper phase (ES-rich phase) was diluted in 500 µL of MeOH/H_2O (70:30, v/v). Before the injection in the LC system, the extract was filtered with 0.20 µm, PVDF filter. The same method was used to simulate the extraction of the reference standard compounds (luteolin-7-*O*-glucuronide, apigenin-7-*O*-glucuronide and CBDA), without the plant.

The same procedure was followed for hemp inflorescences with few modifications. In this case, 20 mg of plant was used and moisten with 40 µL of EtOH before adding KBr aqueous solution and 100 µL of ES. The mixture was then placed in a sonic bath (40 KHz at 25 ◦ C) for 10 min after 30 s of vortexing. Once the extraction was complete, it was subjected to another 30 s of vortexing and centrifuged for 5 min at 2200×g. Three different phases were formed, starting from the bottom: plant, water, and the ES-rich phase. This latter was re-suspended in the water layer, and the mixture (without the plant) was transferred in another tube and centrifuged again for 5 min at 2200×g. Finally, the aqueous phase was removed with a Pasteur pipette, and the remaining upper phase (ES-rich phase) was diluted with 4 mL of EtOH 100% and filtered before the analysis.

For CBD oil sample, 100 mg were transferred to a centrifuge tube with 1 mL of KBr 30% w/w aqueous solution and 100 µL of ES (N16). The mixture was then placed in a sonic bath (40 KHz at 25 °C) for 10 min after 30 s of vortexing. Once the extraction was complete, it was subjected to another 30 s of vortexing and centrifuged for 5 min at 2200×g. The oil and aqueous phase were removed with a Pasteur pipette, and the remaining phase (ES-rich phase) was diluted in 200 µL of EtOH. The extract was filtered with a 0.20 µm PVDF filter prior to analysis.

5.5 Matrix solid-phase dispersion with MOFs (Section III.3.6)

Under optimum conditions, 20 mg of hemp sample were placed in a mortar with 40 mg of CIM-80(*Al*) MOF and this mixture was grounded with a pestle for 2 minutes. The powder obtained was carefully transferred into a glass tube and 0.5 mL of MeOH water (85:15 v/v), was

added. After 4 minutes of vortexing, the suspension was centrifuged at a high speed (2200×g) for 2 minutes. The supernatant was then collected using a Pasteur pipette and filtered with 0.2 μm pore size PVDF filter, before injection in the HPLC-PDA system

5.6 Reference extraction methods

For every matrix, conventional extractions were used as reference methods for the phytochemical characterization of the samples and for comparison purposes with the new methodologies.

For the study on *Vitis vinifera* L., a method previously developed for the analysis of grapevine leaves and GPRs[110], was employed with slight modification. In this method, 0.100 g of sample was weighed in a beaker, and 10 mL of MeOH water (70:30, v/v) was added. The mixture was placed in the ultrasonic bath at room temperature for 15 min, and then the mixture was transferred to a centrifuge tube and centrifuged for 10 min at 2515×g. The supernatant was then placed in a separatory funnel, and 5 mL of hexane was added, in order to remove the chlorophylls contained in the leaves. Two phases were obtained: the top phase, containing the green pigments, and the hydroalcoholic phase in the bottom, containing the extracted phenolic compounds. The latter phase was collected and evaporated in the rotary evaporator, at 50 °C, until a volume of 1 mL was obtained. Finally, the solution was poured into a graduate cylinder, and methanol was added to reach a final volume of 2 mL. Before the injection in the LC system, the extract was filtered using PVDF syringe filter.

For the study on *Corylus avellana* L., a EtOH-based extraction method was employed. 100 mg of hazelnut skin was weighted into a flask and 5 mL of solvent (EtOH water 80:20 v/v with 0.1% of formic acid) was added with a graduated pipette. Afterwards, the flask was submitted to US extraction for 5 minutes. Once the extraction was completed, the solvent was transferred into a centrifuge tube. This step was repeated two times more to obtain an exhaustive extraction. The three tubes were then submitted to centrifugation for 5 minutes at 2200×g in order to separate the supernatant from the not-extracted material. After centrifugation, the solvent was eliminated by rotary evaporation, at 40 45°C. After a partial evaporation of the solvent the extract was transferred in a vial. The remaining solvent was then evaporated under nitrogen flow. 10 mg of the dried extract were solubilized in 1 mL of MeOH water (20/80 v/v) and 40 μL of this solution

were diluted 5-fold with EtOH water (50/50 v/v) before the injection in the analytical instrument.

For the study on *Cannabis sativa* L., the MeOH-based solid–liquid extraction developed in section III.3.2 was used as reference method.

III.6 Software

Experimental designs and the elaboration of the violin plots were carried out by using Statgraphics® 18–X64 software. Statistical analysis and chemometrics were obtained with XLSTAT statistical and data analysis solution (Addinsoft 2020, New York, NY, USA). while the heatmap was created by using Morpheus software (https://software.broadinstitute.org/morpheus). Excel software (Microsoft Office, v.2016) was employed for the remaining calculations. For inverse gas chromatography experiments, statistical calculations and multiple linear regression analysis were performed using Analyze-it (Microsoft, USA). BioRender.com was employed to create several figures of this Thesis.

Chapter III
RESULTS AND DISCUSSION

GRAPHICAL ABSTRACT

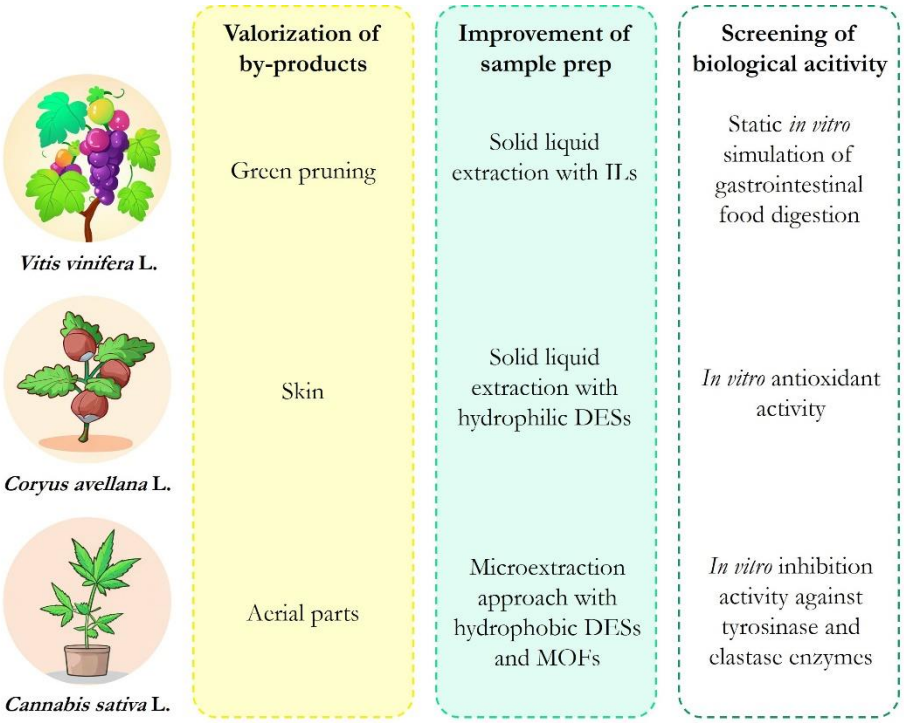

HIGHLIGHTS

***Vitis vinifera* L.:** a IL-based solid liquid extraction was developed. Preliminary *in vitro* tests revealed the stability of the marker compounds after gastrointestinal digestion.

***Corylus avellana* L.:** hydrophilic ESs was tested in the extraction of phenolic compounds in hazelnut skin. The contribution of ESs on the total antioxidant activity of the extracts was studied.

***Cannabis sativa* L.:** hydrophobic ESs and MOFs were employed in a microextraction approach. The bio-activity of the plant was screened by spectrophotometric assays to evaluate potential dermo-cosmetic applications.

Section III.1

Vitis vinifera L.

1.1 Introduction

1.2 Sustainable micro-scale extraction of bioactive phenolic compounds from *Vitis vinifera* L. leaves with ionic liquid-based surfactants

- 1.2.1 Preliminary extraction screening using different IL-based surfactants
- 1.2.2 Optimization of the MA-SLE method using the $C_{16}C_4$Im-Br IL
- 1.2.3 Influence of chlorophyll content on the method performance
- 1.2.4 Quantification of phenolic compounds by HPLC-PDA
- 1.2.5 Comparison between UA-SLE and MA-SLE method using Italian cultivars
- 1.2.6 Analysis of Canarian leaves varieties by MA-SLE HPLC-PDA

1.3 Evaluating the effect of *in vitro* digestion on the total polyphenol content of *Vitis vinifera* L. by-products

- 1.3.1 Phytochemical characterization of *Vitis vinifera* L. pruning
- 1.3.2 Digestion protocol
- 1.3.3 Optimization of the extraction procedure
- 1.3.4 Quantitative analysis of polyphenols in raw and digested samples

1.1 Introduction

Of the over 60 species belonging to *Vitis* genus, *Vitis vinifera* L. is the most known for its economic importance in the agri-food industry. Wine production and viticulture presents several areas of environmental concern, typical of agricultural field. This includes a large use of water, the production of solid waste, energy and chemical use, exploitation of the land and the consequent impact on ecosystems[119]. Even though these issues do not concern only viniculture, it is one of the main agro-activities in the world, making necessary to improve environmental strategies. One of the main approaches developed in recent years is the better usage of organic waste material. For instance, many grapevine by-products, such as grape pomace, seeds, and stems, have been investigated for their interest content in bioactive phytochemicals, mainly polyphenols. Because of their properties, these compounds could be used as natural antioxidants and functional food ingredients for different purposes[120]. To study the composition of grapevine by-products, sample treatment is needed to isolate the bioactive compounds of interest before the analysis. Studies have focused on conventional solid-liquid extraction methods that normally require numerous pretreatment steps (e.g drying, filtration, purification) and the consumption of large amounts of organic solvents resulting in tedious and environmentally unfriendly procedures[110].

Taking into account the above considerations, this section aimed to develop a more innovative approach for the valorization of *Vitis vinifera* L. by products. The first part of the study focused on the improvement of the extraction method performances, using a sustainable approach in the choice of the solvent of extraction, and in the optimization of the method to find the best conditions with the fewest number of experiments. On the other side, if the final aim is to exploit by-products as food supplements or for producing functional foods, it is crucial to support chemical data with studies on the bio-accessibility of phytochemicals during digestion. Thus, a protocol of simulated static *in vitro* digestion was used to verify the stability of the bioactive compounds, after the extraction process.

Sustainable micro-scale extraction of bioactive phenolic compounds from *Vitis vinifera* L. leaves with ionic liquid-based surfactants

This paragraph is reproduced from a published article
(Mastellone *et al.*, Molecules 25, 2020, 3072)

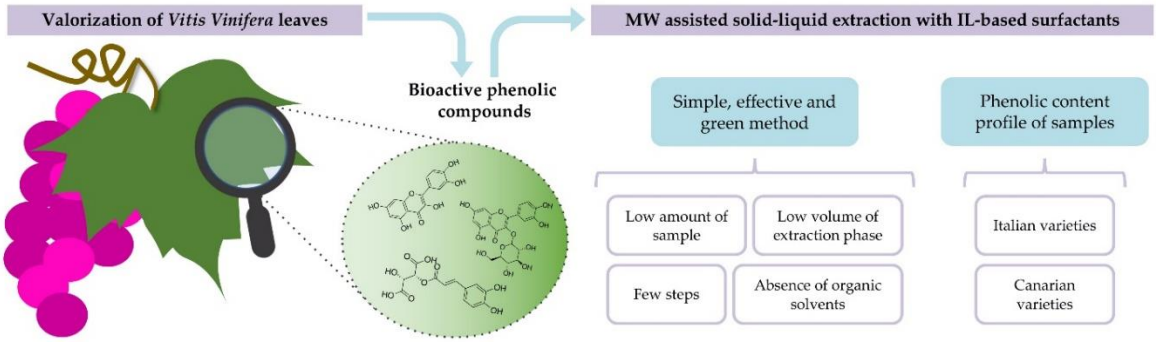

1.2 Sustainable micro-scale extraction of bioactive phenolic compounds from *Vitis vinifera* L. leaves with ionic liquid-based surfactants

The aims of this study were the development of a truly green, fast, and reliable method for the micro-scale extraction of bioactive phenolic compounds from grapevine leaves for analytical purpose and the evaluation of the phytochemical pattern of the leaves of a set of varieties of *Vitis vinifera* L. (harvested in the Canary Islands), in view of their possible exploitation as a source of antioxidant compounds. The proposed method consisted of a focused-microwave-assisted solid-liquid extraction approach (MA-SLE), using micellar aqueous solutions of an ionic liquid-based surfactant, followed by HPLC-PDA analysis. Different ILs were evaluated, while the experimental conditions were optimized by using an experimental design to obtain the maximum extraction efficiency. Furthermore, the proposed method was compared in terms of extraction capacity and greenness with an ultrasound-assisted (UA-SLE) approach and other methods reported in the literature for the grapevine leaves analysis.

1.2.1 Preliminary extraction screening using different IL-based surfactants

One of the most important variables to consider when developing a new method is the nature of the material to be used as extraction phase of the target compounds. Due to the complexity of the samples under study, a liquid extraction approach was employed. Figure 1 shows the chemical structure of the two IL-based surfactants evaluated in this study, which were selected considering their critical micelle concentration (CMC) values and their performance under cytotoxicity studies. Furthermore, both ILs were compatible with HPLC analysis due to their solubility in the mobile phase, thus not requiring a back-extraction of the IL extract before the injection in the instrument. The C_{10}Gu-Cl IL-based surfactant characterizes for its low cytotoxicity in comparison with conventional surfactants and more common IL-based surfactants containing imidazolium moieties, which has been demonstrated by cell viability assays[111,121]. The length of the apolar tail of this IL confers surface active properties with CMC values ranging from 18.6 mM[111] to 22 mM[122], depending on the technique used for its determination. In the case of $C_{16}C_4$Im-Br IL-based surfactant, the long alkyl chain in its structure leads to a really low CMC, with a value of 0.1 mM[112].

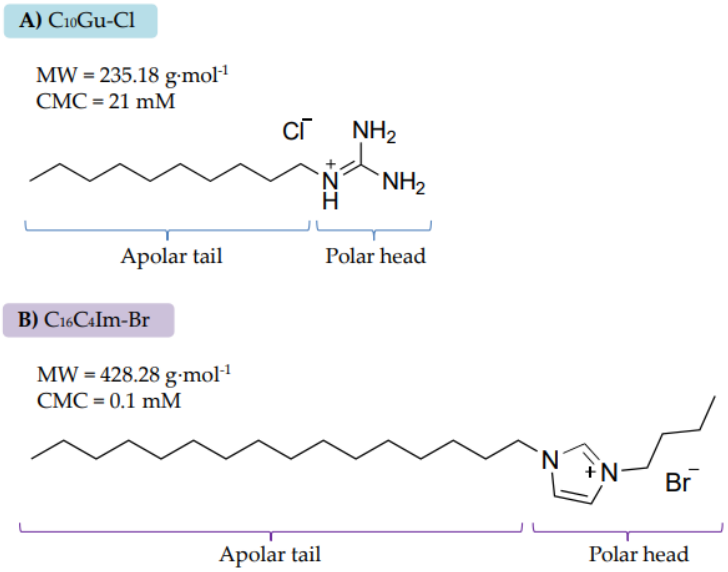

Figure 1. Chemical structure and main characteristics of the IL-based surfactants used in this study.

In order to evaluate the extraction capacity and behavior of the IL-based surfactants for this specific application, both ILs were used in a microwave-assisted solid-liquid extraction (MA-SLE) method using a mix of the leaves from Italian cultivars, and following the experimental conditions previously reported for a similar MA-SLE procedure with food samples, but with slight modifications[123]. With comparison purposes, the ultrasound-assisted solid-liquid extraction (UA-SLE) method that has been applied in a previous study for this batch of Italian cultivars was also performed[110].

Figure 2 includes the peak areas obtained for the target phenolic compounds using the conventional UA-SLE method and the MA-SLE with both IL-based surfactants. It can be observed that the results obtained with the $C_{16}C_4$Im-Br IL-based surfactant and MA-SLE method are similar to those obtained with the UA-SLE method for all the compounds, except for quercetin (QU), for which the conventional method provided higher peak area. It is important to point out that the conditions used for the UA-SLE method are those previously optimized for this specific application[110], while the MA-SLE method was performed under random preliminary conditions (which can be clearly improved if optimized). Furthermore, QU is present in very low amount and a lower extraction will not significantly influence the bioactivity of the extracts. Regarding C_{10}Gu-Cl IL-based surfactant, it revealed a limited ability of extraction for the majority of compounds in comparison with the imidazolium IL and the UA-SLE method, in particular for the CA, while similar results were observed for QUGlucur.

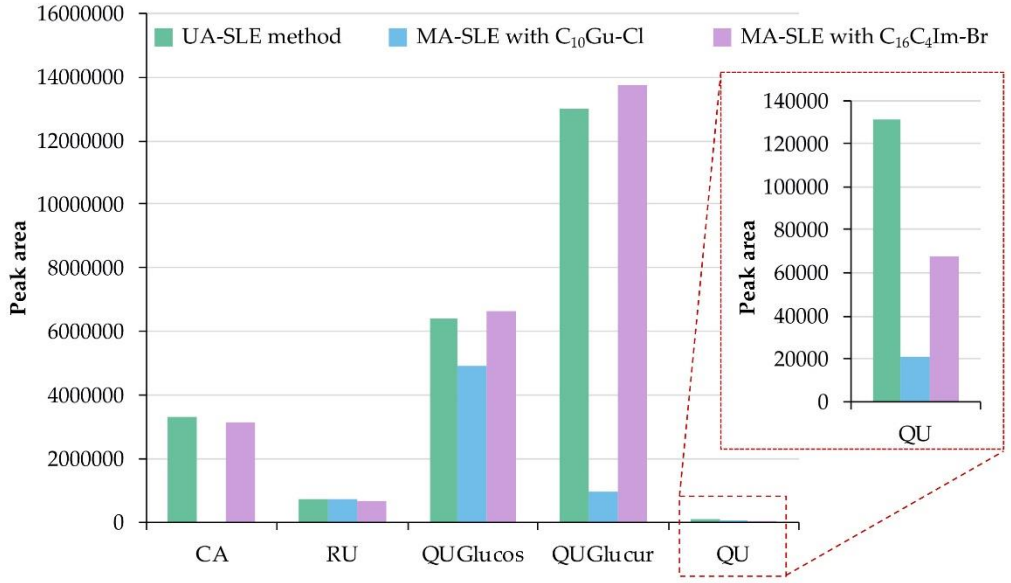

Figure 2. Preliminary screening of the extraction performance (evaluated as peak area) of the proposed MA-SLE method, using C_{10}Gu-Cl and $C_{16}C_4$Im-Br IL-based surfactants in comparison with the UA-SLE method used as reference method. The preliminary experimental conditions for the MA-SLE method were 100 mg of leaves, 2.25 mL of IL-based surfactant aqueous solution at 2.5 mM for $C_{16}C_4$Im-Br and 300 mM for C_{10}Gu-Cl, MW treatment at 70 °C, and 50 W for 30 min. Legend: CA, caftaric acid; QU, quercetin; QUGlucos, quercetin 3-*O*-glucoside; QUGlucur, querceting 3-*O*-glucuronide; RU, rutin.

Therefore, taking into account the results of this screening study, $C_{16}C_4$Im-Br IL-based surfactant was selected for the development of the MA-SLE method. Despite C_{10}Gu-Cl presents lower cytotoxicity in comparison with $C_{16}C_4$Im-Br (but that of $C_{16}C_4$Im-Br still acceptable if compared with conventional surfactants[121]), the CMC of the imidazolium IL-based surfactant is significantly lower (0.1 mM). This characteristic allows the use of small amounts of the IL-based surfactant to exploit its surface-active properties. This may benefit the extraction procedure and goes in accordance with GAC guidelines due to the reduced amounts of reagents involved in the procedure.

1.2.2 Optimization of the MA-SLE method using the $C_{16}C_4$Im-Br IL

The optimization of the MA-SLE method using aqueous solutions of the $C_{16}C_4$Im-Br IL-based surfactant as extraction medium was performed with an experimental design to reduce the number of experiments and to determine the interactions between the variables that affect the extraction efficiency towards the target analytes. Several experimental parameters in the method were fixed with the aim of avoiding time and energy-consuming steps, guaranteeing the use of low amounts of sample and reagents in the procedure while considering other operational limitations. Therefore, 0.100 g of leaves sample and 2.25 mL of the IL aqueous solution were used, while the centrifugation step to separate the sample from the extraction solution was set to 5 min at 2504 × g. Taking into account previous studies dealing with MA-SLE methods, the MW power was fixed at 50 W, since higher power values do not lead to better extraction efficiencies[123]. Thus, the variables considered for the optimization of the process were the IL-based surfactant concentration (mM), and the extraction temperature (°C) and time (min) during the MW treatment. Figure 3 reports the results obtained in the screening of the main variables and in the Doehlert experimental design, during the optimization of the MA-SLE method.

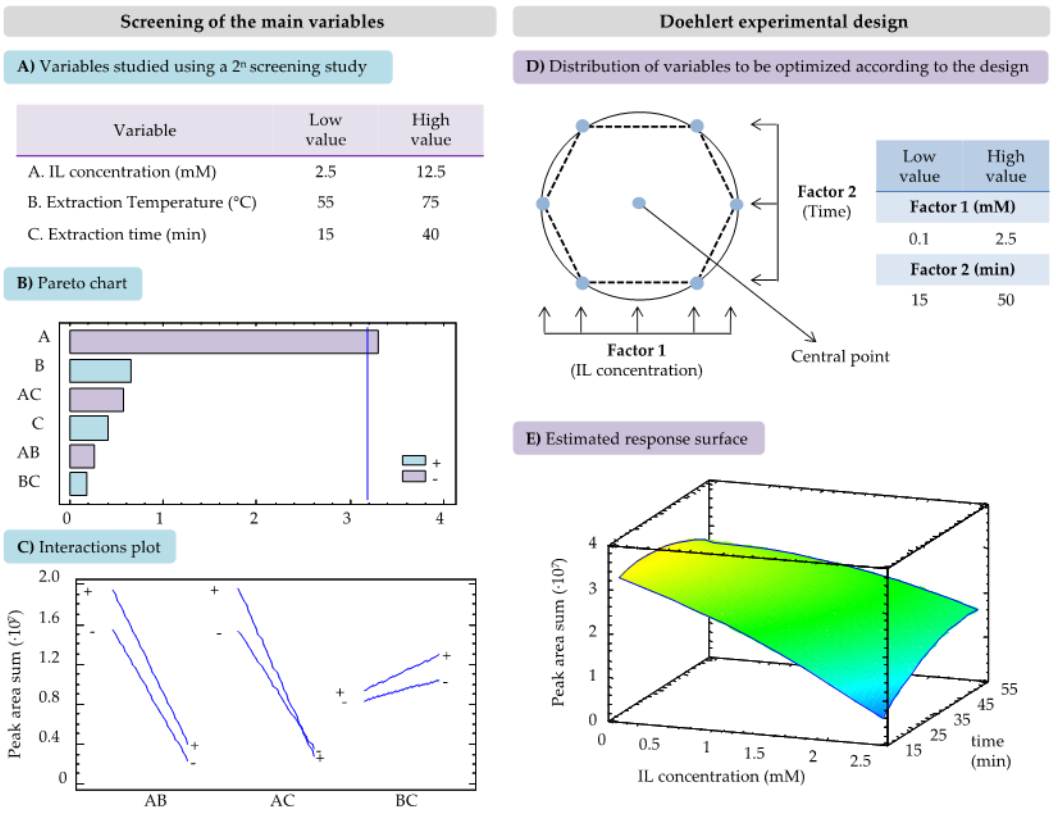

Figure 3. Results obtained in the screening of the main variables and in the Doehlert experimental design, during the optimization of the MA-SLE method. A) Variables considered in the screening process. B) Effects of the main factors in the resulting peak area sum for all the compounds. C) Interaction among factors for all the compounds. D) Spatial distribution of the experimental points in the Doehlert design. E) Estimated response surface for peak areas sum for all the compounds, considering IL concentration and time of extraction factors.

A screening test was initially carried out to determine which of those parameters significantly affect the extraction, with the purpose of reducing the number of variables to optimize in the experimental design. A full two-level factorial design (2^n, with n = 3 variables) was used for this preliminary study, which comprises 8 experiments combining the minimum and maximum values considered for each factor. Moreover, 3 replicates of the central point (intermediate value for each variable) were carried out to monitor the reproducibility of the method. The IL-based surfactant concentration was evaluated in a range high above the CMC of the IL (CMC = 0.1 mM), and therefore the low and high limits were set at 2.5 and 12.5 mM, respectively. Regarding the extraction temperature, a minimum value of 55 ℃ was required for the MW treatment, while the maximum value was set in accordance with literature data that show the possible degradation of phenolic compounds above 75 °C[124]. The limits for the extraction time were selected for being common times reported in the literature in MA methods. Figure 3 A) shows the ranges in which the three variables were studied, while Table 1 includes the design matrix for the screening study. Once the 11 experiments were performed, the extraction efficiency was evaluated in terms of the sum of the peak areas obtained for all the target compounds at their corresponding wavelength.

Table 1. Design matrix for the screening analysis, a 23 factorial design and 3 central points, in the optimization of the MA-SLE method.

Experiment	IL-based surfactant concentration (mM)	MW temperature (ºC)	MW time (min)
1	2.5	55	15
2	2.5	55	40
3	2.5	75	15
4	2.5	75	40
5	12.5	55	15
6	12.5	55	40
7	12.5	75	15
8	12.5	75	40
9	7.5	65	27.5
10	7.5	65	27.5
11	7.5	65	27.5

The Pareto chart included in Figure 3 B) shows that the IL-based surfactant concentration is the most influential variable on the method and, interestingly, it is inversely proportional to the peak area value. This means that lower concentrations of $C_{16}C_4$Im-Br (always above the CMC) allowed to extract higher amounts of the analytes. This behavior may be associated to the increased viscosity of the extraction solution that has been observed when high concentrations of long alkyl chain ILs are used, which may limit the transfer of the analytes from the sample to the extraction phase[125,126]. Both the extraction temperature and time during the MW treatment had a positive effect on the peaks area, but in a lesser extent than the IL-based surfactant concentration. However, in the interactions plot shown in Figure 3 C), it is observed the intersection between extraction time and IL concentration, demonstrating the interaction between these two factors when they are varied within the range studied. Based on these results, the extraction temperature was set at 70 ºC, while the IL concentration and the extraction time were the factors considered for further optimization using a Doehlert experimental design.

Table 2. Matrix of the experiments of the Doehlert design used in the optimization of the MA-SLE method, including the coded values and the operating values.

Experimental	IL-based surfactant concentration (mM)		MW time (min)	
	C_1[a]	X_1	C_2[a]	X_2
1	0	1.3	0	32.5
2	1	2.5	0	32.5
3	0.5	1.9	0.866	50
4	-1	0.1	0	32.5
5	-0.5	0.7	-0.866	15
6	0.5	1.9	-0.866	15
7	-0.5	0.7	0.866	50
8	0	1.3	0	32.5
9	0	1.3	0	32.5

[a] C_1 and C_2 are the coded values for the levels of IL-based surfactant concentration (mM) and time of MW treatment (min), respectively. The relationship between coded and real values is given by: $C_i = \frac{X_i - X_i^o}{\Delta X_i}\alpha$, where C_i is the coded value for the level of factor i, X_i is its real value in an experiment, X_i^0 is the real value at the center of the experimental domain, ΔX_i is the step of variation of the real value, and α is the coded value limit for each factor. The number of experiments required (N) is given by $N = k^2 + k + C_0$, where k is the number of variables and C_o is the number of center points.

Figure 3 D) shows a scheme of the spatial distribution of the different experimental points according to the Doehlert design for 2 variables selected in this study. Table 2 includes the matrix of the experiments carried out, which consist in 9 experiments considering the hexagonal geometry of the design plus 3 replicates of the central point. This sophisticated experimental design requires fewer experiments because they are more efficient and uniformly distributed within the experimental domain, in comparison with other response surface designs commonly used in optimization studies[127]. As it was demonstrated in the screening study, the IL-based surfactant concentration had the strongest influence and it was studied at 5 levels in a lower concentration range, from 0.1 mM (its CMC value) to 2.5 mM. The extraction time was assessed at 3 levels in the same range, from 15 to 50 min. The response surface included in Figure 3 E) was obtained considering the sum of the peak area for all the compounds in each experiment and fitting the values to the polynomial equation using the Lagrange's criterion[127]. It can be observed that the maximum enhancement of the signal is obtained when the IL-based surfactant concentration was the lowest (0.1 mM) with the extraction time between 25 and 35 min. Taking into account these results, the optimum conditions for the MA-SLE method for the extraction

of the target phenolic compounds were the following: 0.100 g of leaves sample, 2.25 mL of an aqueous solution containing the $C_{16}C_4$Im-Br IL-based surfactant at 0.1 mM, extraction temperature of 70 ℃ at 50 W, and extraction time of 30 min. Figure 4 reports the comparison between the schemes of the extraction procedures with the proposed MA-SLE method (A) and the reference UA-SLE method (B).

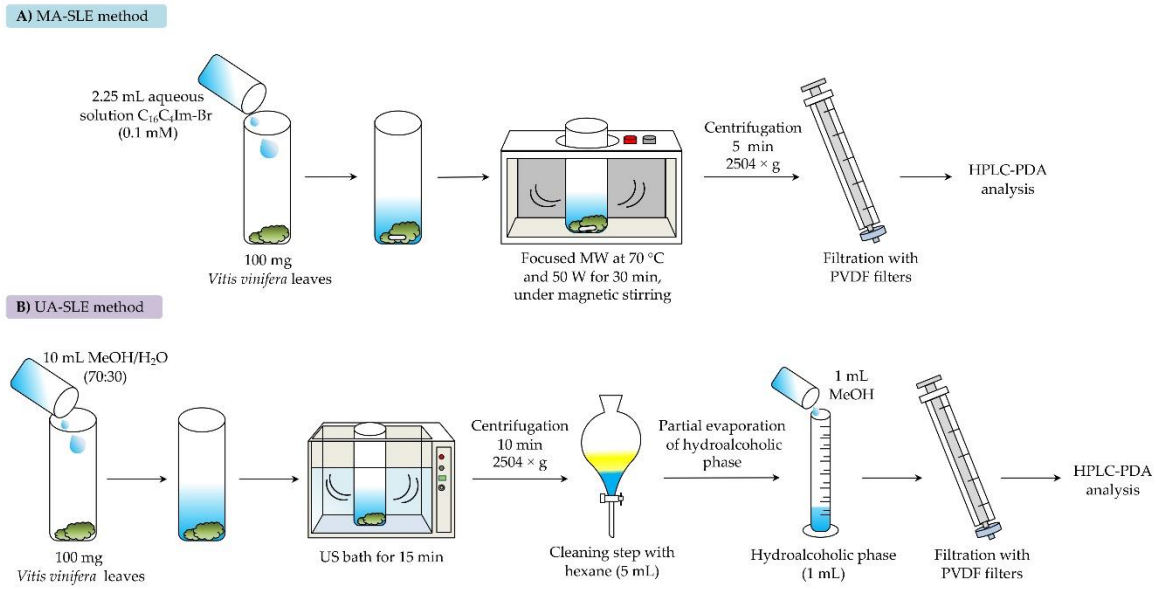

Figure 4. Scheme of the extraction procedures from *Vitis vinifera* leaves: A) Proposed MA-SLE method and B) UA-SLE method used with comparison purposes, which was previously reported for this specific application[110].

1.2.3 Influence of chlorophyll content on the method performance

One of the most important issues regarding the analysis of plant samples is the content of strongly binding molecules, such as pigments, which eventually could compromise the analytical performance of the chromatographic column[128]. For this reason, these pigments, mainly chlorophylls, are usually removed before the analysis in the HPLC by using solvents or an additional clean-up step based on solid-phase extraction methods. Indeed, in the UA-SLE method previously reported for the same application developed in this study, a liquid-liquid extraction (LLE) step using an apolar solvent is accomplished right after the UA extraction for the elimination of chlorophylls, as shown in Figure 4 B). Petroleum-based solvents, which are commonly used for the removal of these interfering substances, present many drawbacks, such as high volatility and flammability, and high toxicity with an important impact in both the environment and human health[1]. Moreover, these toxic solvents are not entirely effective for the extraction of these pigments, and part of them still remains in the aqueous or alcoholic phase.

Therefore, the incorporation of this tedious additional step not only increases the analysis time but also compromises the sustainability of the entire process. In this sense, one of the goals of the present study was the elimination of this step to ensure the development of a greener method in terms of both energy-consumption and elimination of toxic solvents.

The presence of chlorophylls is easy to evaluate since they provide a bright green color to the final extracts. In the case of the C_{10}Gu-Cl IL-based surfactant used in the screening study, the extract after the MA-SLE method (under random preliminary conditions) exhibited a strong green color, revealing the presence of the pigments. Interestingly, the extract obtained with the optimum MA-SLE method using the $C_{16}C_4$Im-Br IL-based surfactant (which uses low concentrations of the IL) presented a similar yellowish color to that of the UA-SLE method after the cleaning LLE step, thus supporting the scarce presence of chlorophylls in the extract. It is important to highlight that the extraction was carried out in an almost pure aqueous medium, with a small amount of IL (0.1 mM). This medium is not favorable for the extraction of non-polar interferences, besides chlorophylls, such as lipids or other non-polar compounds, which may lead to the presence of important interferences further affecting the quantification results.

1.2.4 Quantification of phenolic compounds by HPLC-PDA

After the optimization of the method and correct identification of the target compounds in the chromatogram, their quantification was required in order to determine the concentration of the analytes in the different samples. The external standard calibration method was used for the quantification of the analytes in the samples.

Table 3 includes several quality analytical figures of merit of the method, including the linearity range, the calibration sensitivity (evaluated as the calibration slope), determination coefficients (R^2), limits of detection (LODs), and limits of quantification (LOQs), for each compound. The LODs were experimentally determined by decreasing the concentration of the analytes until a signal to noise ratio (S/N) of 3 was obtained. The LOQs were estimated as 10/3 times the LODs and experimentally verified by injecting the standards at the predicted concentrations. Thus, the LODs ranged from 0.5 $mg \cdot L^{-1}$ for QU to 3.0 $mg \cdot L^{-1}$ for CA, while the LOQs were between 1.7 and 5.0 $mg \cdot L^{-1}$ for the group of analytes. Considering the LOQ values obtained, the calibration curves were obtained using 7 calibration levels in the range of 5 to 500

mg·L^{-1} for all the phenolic compounds, except for CA, for which the calibration range reaches 650 mg·L^{-1}. The R^2 values were higher than 0.992 in all cases, which demonstrates the good linearity obtained in the studied calibration range. Regarding the sensitivity, QU exhibited the highest calibration slope, which agrees with the low LOD obtained compared with the rest of the analytes.

Table 3. Several quality analytical parameters of the HPLC-PDA method.

Compound	Λ max[a] (nm)	Linear range ($mg \cdot L^{-1}$)	Slope ± SD[b]	$S_{y/x}$[c]	R^2[d]	LOD[e] ($mg \cdot L^{-1}$)	LOD[f] ($mg \cdot L^{-1}$)
CA	320	5 – 650	11154 ± 664	272	0.997	3.0	5.0
RU	360	5 – 500	19604 ± 2422	872	0.992	1.0	3.3
QUGlucos	360	5 – 500	13460 ± 513	199	0.999	1.0	3.3
QUGlucur	360	5 – 500	5560 ± 283	110	0.998	1.0	3.3
QU	360	5 – 500	20014 ± 937	338	0.999	0.5	1.7

[a] wavelength used for quantification; [b]standard deviation within the calibration range for n = 7 calibration levels; [c] standard deviation of the residuals or error of the estimate; [d] determination coefficient; [e] limit of detection, determined by decreasing the concentration of the standards until a S/N ratio of 3 was obtained; [f] limit of quantification, estimated as 10/3 times the LOD, and experimentally verified using standards at the predicted concentrations

1.2.5 Comparison between UA-SLE and MA-SLE method using Italian cultivars

Once the calibration curves were obtained, the analysis of the samples was carried out by injecting the extracts after applying the proposed MA-SLE or the UA-SLE method to the Italian leaves samples. Each extraction was performed in triplicate to express the results as the mean concentration together with the standard deviation (SD), which is used as a measure for the precision of the method. Furthermore, given the high concentration of some analytes in the samples, their quantification required the dilution of the extracts with ultrapure water (1:20) to obtain signals included within the calibration range.

Table 4 includes the concentrations of the target phenolic compounds found in the Piedmont leaves (Italian cultivar) after their analysis by the UA-SLE HPLC-PDA and the proposed MA-SLE HPLC-PDA method[119,129]. The results were expressed as mean values ± SD in mg g^{-1}. A similar absolute composition was obtained using both methods, in which the most abundant compound in the Piedmont variety was QUGlucur, followed by CA and QUGlucos. Indeed, these results agree with those obtained in the previous study in the literature that determined the phenolic content of the same sample[110]. However, it is important to highlight that the concentrations obtained after the analysis by the MA-SLE method are higher compared with those obtained with the UA-SLE approach, especially for QUGlucur and QUGlucos. For

these two phenolic compounds, the difference is more significant, obtaining concentrations of 32.1 ± 0.4 mg·g^{-1} and 10.3 ± 0.4 mg·g^{-1} with the MA-SLE method, and values of 17 ± 2 mg·g^{-1} and 5 ± 1 mg·g^{-1} using the UA-SLE approach, respectively. These values demonstrate that the proposed MA-SLE method with the IL-based surfactant provides better extraction efficiency.

Furthermore, as shown in the quantification results, lower SD values were obtained with the MA-SLE procedure. The precision of the proposed method was also evaluated with the relative standard deviation values (%RSD, n=3) by performing three extractions of the Italian cultivars in the same day (intra-day) and in three non-consecutive days within a week (inter-day). The intra-day RSD values ranged between 4.6 and 11%, while the inter-day RSD values varied from 6.8 to 15% for QUGlucos and RU, respectively.

Apart from the differences in the extraction performance of both methods, it is important to highlight other advantages of the proposed MA-SLE method over the already reported UA-SLE for the same application. As shown in Figure 4, the proposed MA-SLE method comprises fewer steps, making the process less tedious and faster due to the elimination of the clean-up stage, in which the chlorophylls are removed, and the solvent is partially evaporated. Moreover, the proposed procedure is more sustainable since the extraction phase consists of an aqueous solution of an IL-based surfactant at a quite low concentration level (less than 10 mg of IL are required in each extraction). Besides, the absence of organic solvents in the entire procedure in comparison with other common MA-SLE methods reported in the literature for plant analysis [130–138], makes it comply with one of the most important requirements set by the GAC. Despite other MA-SLE methods using ILs have been previously proposed in the literature for the extraction of bioactive compounds from plant material, those methods usually incorporate a clean-up step prior the injection in the analytical system[139–141], or require the dilution of the extract with organic solvents[142–145]. Moreover, most of these applications do not fit with the miniaturization recommendations set by GAC[146], with the amount of plant sample and IL solution around 0.5–1 g and 10 mL, respectively[139,142–144].

1.2.6 Analysis of Canarian leaves varieties by MA-SLE HPLC-PDA

Once the adequate performance of the extraction method was demonstrated, it was used for the determination of the phenolic composition profile of different varieties of *Vitis vinifera* leaves.

Some reports in the literature indicate a variation in the phenolic composition of the by-products of *Vitis vinifera* depending on the variety, the characteristics of the soil, water availability, cultural practices and climatic conditions, including temperature and luminosity[147–149]. Therefore, six different Canarian varieties were selected as samples (see Table 5). Three of them produce red wine (LN, MN and T), while the other three yield white wine (LB, ML, MA). Moreover, with the aim of investigating the influence of geographic position of the cultivars, the phenolic composition profile obtained was also compared with the Italian mix cultivar previously analyzed in this study.

Each pool of leaves was analyzed with the proposed MA-SLE HPLC-PDA method in triplicate to express the concentration results with their corresponding SD. The data obtained from these analyses are reported in Table 4.

Table 4. Phenolic content in the different *Vitis vinifera* varieties analyzed in this study expressed as mg·g^{-1} ± SD (for 3 replicates) and using the MA-SLE method and the US-SLE method for comparison purposes, together with the amounts reported in the literature for other varieties and using different methods.

Vitis vinifera variety (method)	CA	RU	QUGlucos	QUGlucur	QU
This study					
Piedmont, Italian (US-SLE-HPLC-PDA)	7.2 ± 0.9	0.6 ± 0.1	5 ±1	17 ± 2	0.27 ± 0.01
Piedmont, Italian (MA-SLE-HPLC-PDA)	9.8 ± 0.5	0.9 ± 0.1	10.3 ± 0.4	32.1 ± 0.4	0.19 ± 0.01
ML, Canarian (MA-SLE-HPLC-PDA)	7.7 ± 0.3	4.8 ± 0.2	8.1 ± 0.6	34 ± 2	0.25 ± 0.01
MA, Canarian (MA-SLE-HPLC-PDA)	11 ± 2	1.4 ± 0.1	10 ± 1	65 ± 9	0.20 ± 0.01
LB, Canarian (MA-SLE-HPLC-PDA)	9.7 ± 0.9	1.05 ± 0.07	7 ± 1	38± 3	0.26 ± 0.07
T, Canarian (MA-SLE-HPLC-PDA)	13.1 ± 0.7	3.3 ± 0.1	5.5 ± 0.2	62 ± 9	0.25 ± 0.02
NM, Canarian (MA-SLE-HPLC-PDA)	12.4 ± 0.7	1.9 ± 0.3	9 ± 1	39 ± 3	0.26 ± 0.01
LN, Canarian (MA-SLE-HPLC-PDA)	10.0 ± 0.5	1.57 ± 0.05	3.4 ± 0.4	21 ± 1	0.23 ± 0.01
Values reported in the literature					
Serbian (SLE-HPLC-MS/MS)[a]	–	0.83 ± 0.02	5.8 ± 0.2	–	0.13 ± 0.03
Calabrian, Italian (US-SLE-HPLC-PDA)[b]	–	0.10 ± 0.01	–	–	0.15 ± 0.01
Brazilian (SLE-HPLC-MS/MS)[c]	–	0.03	0.82	3.78	–

[a] Mean values for nine different Serbian cultivars[4];[b] mean values for six different Calabrian cultivars[129]; [c] mean values for four different Brazilian cultivars[119].

The MA sample had the highest phenolic content among all the varieties, while LN presented the lowest amount of total target phenolic compounds. The most significant differences were observed for the content of QUGlucur, since an average value around 33 mg g^{-1} was obtained, but the T and MA varieties exhibited concentrations of 62 ± 9 mg g^{-1} and 65 ± 9 mg g^{-1}, respectively. In the case of RU, the highest content was found in ML variety, with a concentration of 4.8 ± 0.2 mg g $^{-1}$. The concentration of QUGlucos was around 8.5 mg g^{-1}, except for the lower content found in LN and T varieties, with values of 3.4 ± 0.4 mg g^{-1} and 5.5 ± 0.2 mg g^{-1}, respectively. The amount of the remaining phenolic compounds CA and QU was similar in all the samples, being QU the least abundant among all the analytes considered.

Table 5. Vitis vinifera leaves varieties from Canary Islands, employed for the determination and quantification of phenolic markers.

Variety name (abbreviation)	Classification	Leaf anatomy[a]
Malvasía Lanzarote (ML)	White variety	
Moscatel Alejandría (MA)	White variety	
Listán Blanco (LB)	White variety	
Tintilla (T)	Red variety	
Negro Moll (NM)	Red variety	
Listán Negro (LN)	Red variety	

[a] photos of the samples used in the study

The extracts of several of the analyzed Canarian cultivars presented additional peaks apart from those of the target phenolic compounds. In particular, a peak was found in the NM variety with a similar peak area as RU (see Figure 5). Considering the UV-Vis spectrum of that peak and the data of the analysis of *Vitis vinifera* leaves in the literature[110], this new peak can be tentatively identified as vitilagin or isovitilagin.

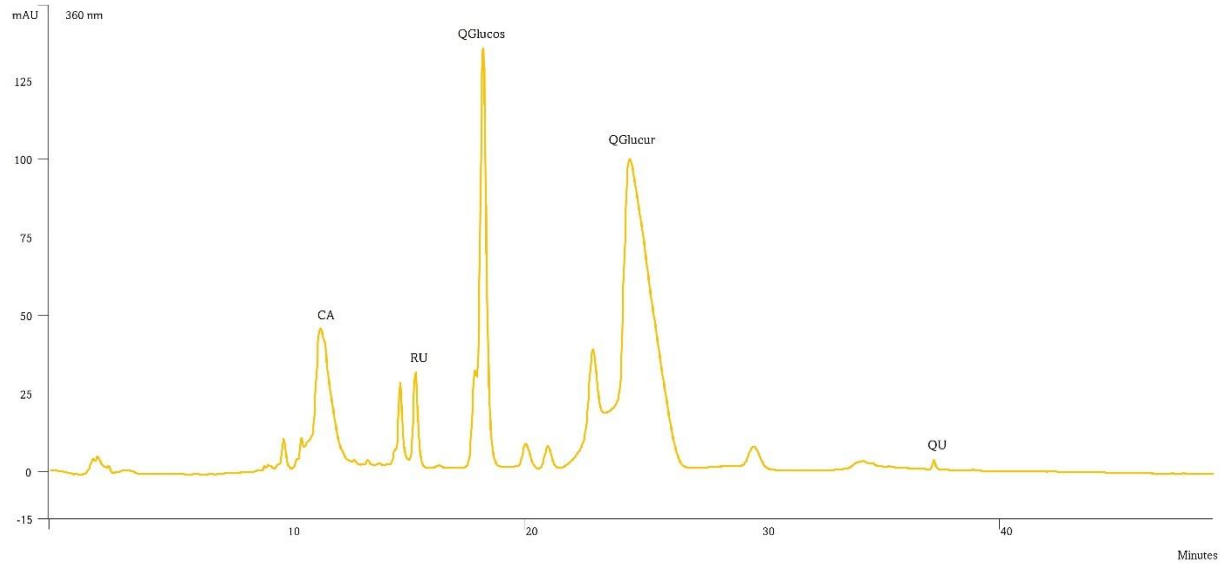

Figure 5. Chromatographic profile of Negro Moll variety at 360 nm.

A peak before CA was also observed with a high peak area in the LN variety, but also in the profiles of ML and NM. Two more peaks were detected in all the samples close to QUGlucur.

The results obtained from the analysis of the Canarian leaves were compared with the phenolic composition profile of the Italian leaves mix used for the development of the proposed MA-SLE method. As it is shown in Figure 6, a similar distribution of the target compounds was observed, in which QUGlucur was the most abundant compound, followed by CA and QUGlucos. The content of RU was low in all the samples, while QU represented a very small part of the total phenolic composition. The specific levels found for each compound in the Italian cultivars, together with the concentrations reported in the literature for other varieties of *Vitis vinifera* leaves from Serbia[4], Italy[129] and Brazil[119], are included in Table 4. The QU concentration values obtained for the Canarian samples and the Italian mix analyzed in the present study are similar to those reported for other varieties, with values around 0.20 $mg \cdot g^{-1}$. However, it is important to highlight that all the Canarian leaves presented a notable higher content of RU in comparison with the other varieties, for which concentrations lower than 1 $mg\ g^{-1}$ were obtained, while amounts up to 4.8 $mg\ g^{-1}$ were found in the samples from the Canary Islands. It is also interesting to point out that, despite the total phenolic content of the Brazilian samples is considerably lower, the most abundant compound in these leaves is QUGlucur, as it was observed for the samples analyzed in the present study. Recently, it was also demonstrated that all the compounds considered in the phenolic content profile present a similar antioxidant effect[110]. Therefore, the antioxidant activity of the product is mainly related to the total

concentration of phenolic compounds in the sample. Given these results, it is possible to assume that the geographic distribution slightly influences the composition of the phenolic profile, and the Canarian varieties that presented the highest phenolic content, may have some significant outcomes with respect to the valorization of these by-products.

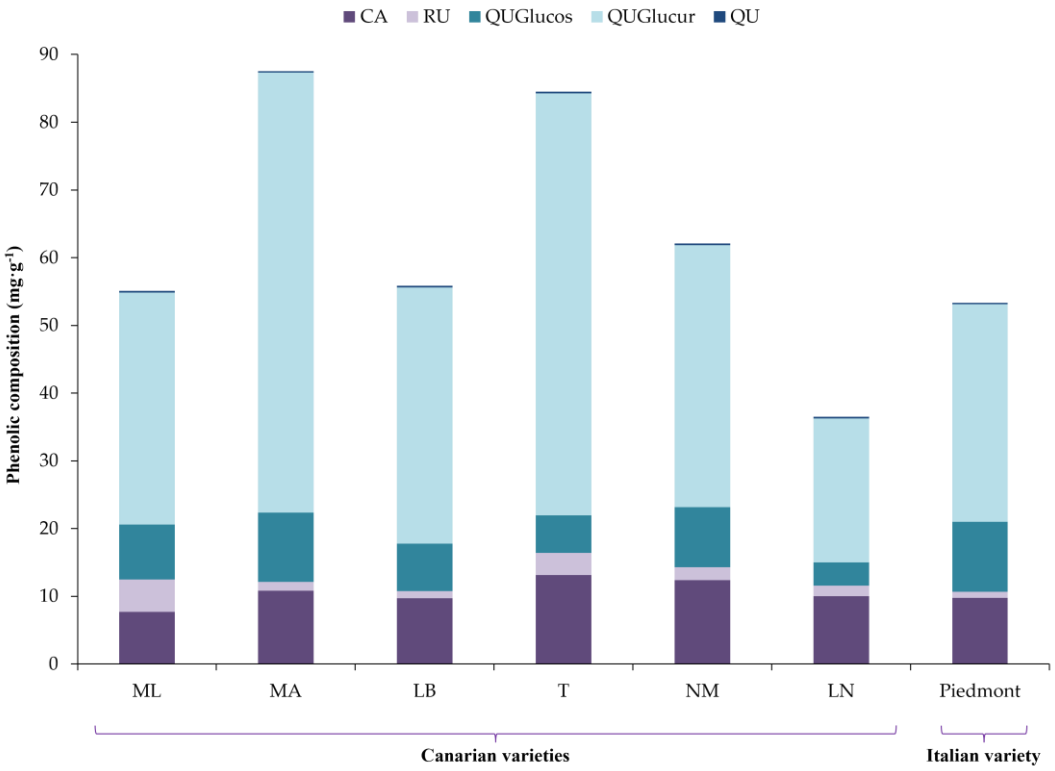

Figure 6. Phenolic composition of the different *Vitis vinifera* varieties analyzed in this study with the proposed MA-SLE method using the $C_{16}C_4$Im-Br IL-based surfactant.

.

Evaluating the effect of *in vitro* digestion on the total polyphenol content of *Vitis vinifera* L. by-products

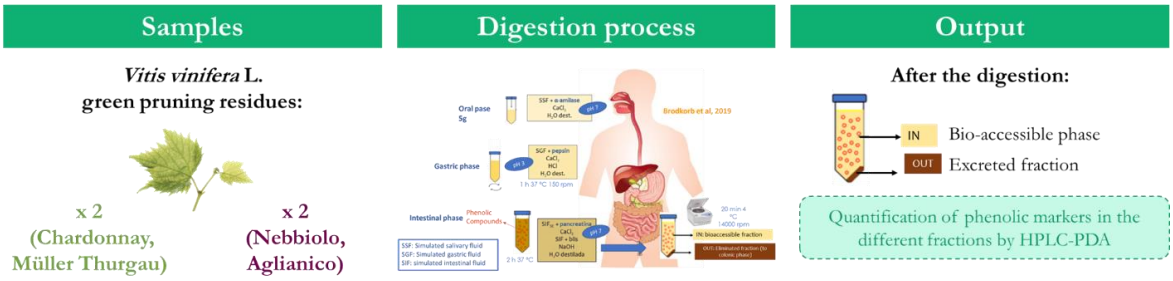

1.3 Evaluating the effect of *in vitro* digestion on the total polyphenol content of *Vitis vinifera* L. by-products

Natural compounds present in plants are considered sustainable ingredients employed in pharmaceutical and food industries for their multiple biological activities. Polyphenols are a class of secondary metabolites almost ubiquitous in plants and their beneficial properties are mainly correlated to the antioxidant activity. Many studies have demonstrated the presence of polyphenols in grape and grape by-products but fewer data are available regarding the effects of digestive enzymes and pH conditions on the stability of these metabolites, which may affect their bioavailability and potential activity *in vivo*. In this study, an *in vitro* gastrointestinal digestion process was simulated on grape by-products and the digestion products were analyzed by liquid chromatography to evaluate the release and bioaccessibility (amount available for absorption in the human gastrointestinal tract) of polyphenols from this matrix[150].

1.3.1 Phytochemical characterization of *Vitis vinifera* L. pruning

Representative cultivars of *Vitis vinifera* L., harvested in Piedmont (Italy), were selected for this study: (i) Chardonnay and Müller Thurgau as white grape and (ii) Nebbiolo and Aglianico as red grape. The samples were composed by green pruning residues of grape, GRPs, (mainly fruitless young twists and leaves), considered a by-product of viticulture[110]. To investigate the effect of *in vitro* gastrointestinal digestion on the total polyphenol content of the samples, the phytochemical characterization was firstly performed on the raw matrices (before the digestion) by UHPLC-UV-ESI-MS/MS analysis. Methanol was employed as extraction solvent to have comparable data to the one obtained after the digestion, where a methanolic extraction were performed on the digested GRPs. The non-volatile fraction of *V. vinifera L.* by-products was extensively studied in the previous work (see Section III.1.2) and a similar chromatographic profile was obtained (Figure 1).

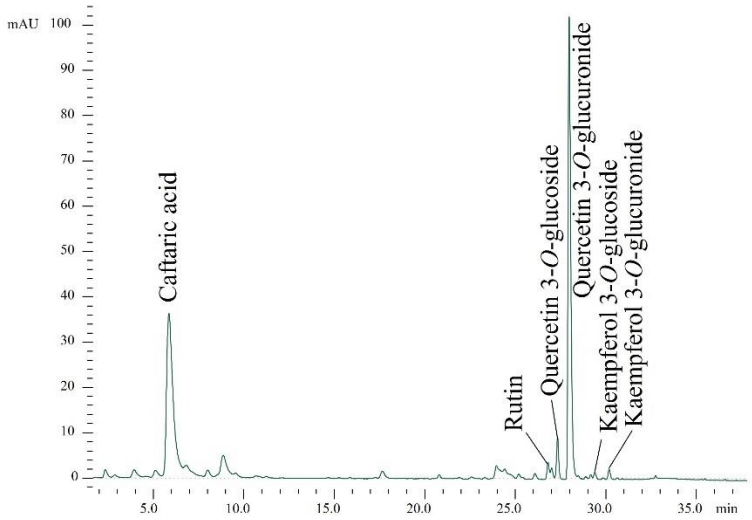

Figure 1. Representative chromatographic profile at 330 nm of the methanolic extract of Nebbiolo cultivar

The UV spectra for each peak provided a preliminary indication of the group of compounds. The molecular weight of each peak was also defined by its mass spectral pattern, through the complementary correspondence between positive and negative protonated/deprotonated ions in ESI^+ and ESI^- modes. The product ion scan analysis of these ions provided diagnostic fragments for each compound. The identity of 6 compounds in the extract was confirmed by co-injection of authentic commercial standards. The identification information of the analytes are reported in Table 1. In agreement with previous data reported for polyphenols of *V. vinifera*[5,110,151], flavonoids were the most representative group of compounds, in the form of *O*-glycosides of quercetin and kaempferol. Caftaric acid, a phenolic acid derivative, was also found. These molecules have been used as target compounds in subsequent evaluations. Literature data shows that, contrary to tannins and more complex compounds, smaller polyphenols and phenolic acids seems to be more easily absorbed by intestinal mucosa and be bioaccessible to reach the target tissues[152].

Table 1. List of identified (target) compounds in *V. vinifera* GPRs extracts. For each analyte, identified compound names, UV maximum/a, protonated/deprotonated ions, and fragment ions obtained by product ion scan mode (PIS) are given.

Compound	λ max (nm)	Mol. Weight (g mol $^{-1}$)	$[M - H]^+$ *m/z*	$[M + H]^-$ *m/z*
Caftaric acid	326/244	312	313	311
Rutin	354	610	611	606
Quercetin 3-*O*-glucoside	254/351	464	465	463
Quercetin 3-*O*-glucuronide	254/351	478	479	477
Kaempferol 3-*O*-glucoside	266/346	448	449	447
Kaempferol 3-*O*-glucuronide	265/344	462	463	461

Once the identification was performed, the chromatographic method was switched to a UHPLC-PDA equipment for quantification and further analysis. The quantitative data obtained by an external calibration method were used to estimate the amount of polyphenols before and after the digestion. As shown in Table 2, the four samples presented a similar composition in polyphenols before the digestion, with no major differences between the cultivars.

Table 2. Quantification data of the target compounds in *V. vinifera* green pruning residues (mg g^{-1} of matrix).

Sample	Caftaric acid	Rutin	Quercetin 3-*O*-glucoside	Quercetin 3-*O*-glucuronide	Kaempferol 3-*O*-glucoside	Kaempferol 3-*O*-glucuronide
Chardonnay (white berry)	3.9 ± 0.3	0.4 ± 0.1	1.0 ± 0.1	8.0 ± 0.9	0.2 ± 0.1	0.2 ± 0.1
Müller Thurgau (white berry)	3.9 ± 0.1	0.7 ± 0.1	0.5 ± 0.1	11.4 ± 0.1	0.1 ± 0.1	0.3 ± 0.1
Nebbiolo (red berry)	2.0 ± 0.1	0.2 ± 0.1	0.2 ± 0.1	3.7 ± 0.8	0.1 ± 0.1	0.1 ± 0.1
Aglianico (red berry)	3.1 ± 0.1	0.4 ± 0.1	0.6 ± 0.1	11.6 ± 0.1	0.1 ± 0.1	0.2 ± 0.1

1.3.2 Digestion process

The digestion process was performed by the Universitat Politècnica de València, following the "INFOGEST static *in vitro* simulation of gastrointestinal food digestion" standardized protocol[152]. Every sample of GRPs was subjected to sequential *in vitro* oral, gastric and small intestine digestion and parameters such as electrolytes, enzymes, bile, dilution, pH and time of digestion were adjusted according to available physiological data. At the end of the process, two phases were obtained for every digested sample: the bioaccessible ("IN") and the excreted ("OUT") fractions. This latter contains the unavailable phytochemicals that precipitate or are in complexed form. After the digestion, all the fractions were lyophilized and received as dried extracts. In the same digestion process, two batches of the same sample and a blank were carried out and three separate replicates of the digestion was performed for every sample. In Figure 2 a scheme of the digestion method is illustrated while Table 2 reported the samples analyzed and the digested fractions obtained.

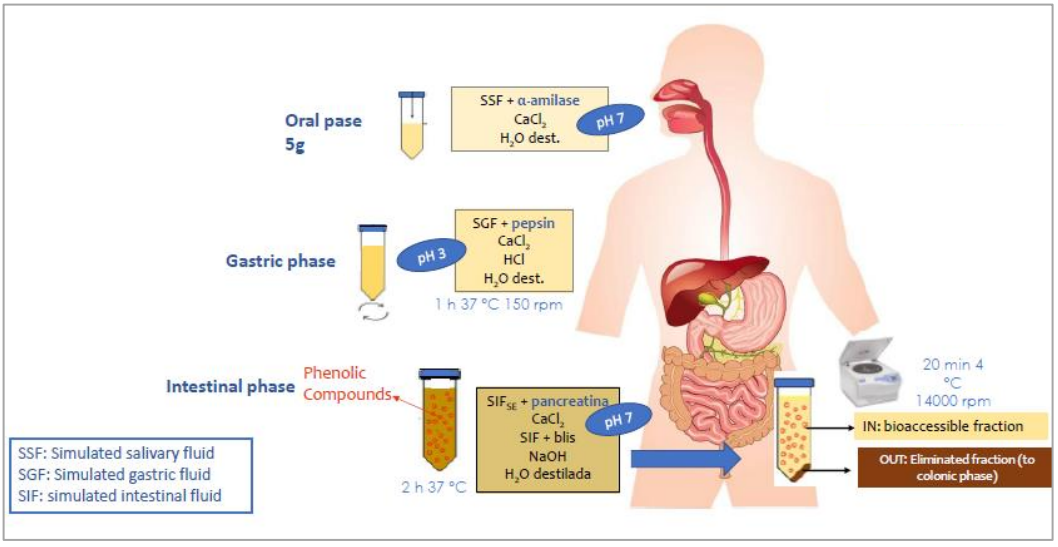

Figure 2. Scheme of the INFOGEST static *in vitro* gastrointestinal food digestion method employed in the study.

Table 2. Samples submitted to the digestion process and digested fractions obtained.

Sample	Digestion replicate 1			Digestion replicate 2			Digestion replicate 3		
Chardonnay (white berry)	Replicate 1 (IN, OUT)	Replicate 2 (IN, OUT)	Blank	Replicate 1 (IN, OUT)	Replicate 2 (IN, OUT)	Blank	Replicate 1 (IN, OUT)	Replicate 2 (IN, OUT)	Blank
Müller Thurgau (white berry)	Replicate 1 (IN, OUT)	Replicate 2 (IN, OUT)	Blank	Replicate 1 (IN, OUT)	Replicate 2 (IN, OUT)	Blank	Replicate 1 (IN, OUT)	Replicate 2 (IN, OUT)	Blank
Nebbiolo (red berry)	Replicate 1 (IN, OUT)	Replicate 2 (IN, OUT)	Blank	Replicate 1 (IN, OUT)	Replicate 2 (IN, OUT)	Blank	Replicate 1 (IN, OUT)	Replicate 2 (IN, OUT)	Blank
Aglianico (red berry)	Replicate 1 (IN, OUT)	Replicate 2 (IN, OUT)	Blank	Replicate 1 (IN, OUT)	Replicate 2 (IN, OUT)	Blank	Replicate 1 (IN, OUT)	Replicate 2 (IN, OUT)	Blank

1.3.4 Extraction procedure

The raw samples and digested fractions (IN, OUT) were submitted to extraction with methanol before the analysis by UHPLC-PDA. Before selecting methanol, other organic solvents were screened for the extraction (data no shown) with the aim to selectively isolate the target compounds without extracting interfering substances deriving from the digestion process (e.g salts or enzymes). The same extraction method was used to process all the sample under study. The GRPs and the OUT fractions presented a green color (marker of the presence of chlorophylls) contrary to the IN fractions. Probably, most of the pigments presented in the samples passed in the extracted fractions, thus not be absorbed. In preliminary tests, a solid phase extraction with C18 cartridges was optimized on the raw samples and OUT fractions to purify the samples from chlorophylls. In the final method, also IN fractions were purified by SPE to submit all the samples to the same conditions. The entire extraction procedure was adjusted following the method previously developed for similar matrices. Briefly, 100 mg of each sample was extracted with 10 mL of methanol in an ultrasonic bath for 15 min. The procedure was then repeated with fresh solvent on the same matrix and the supernatant collected and centrifuged at 4500 rpm for 10 min. Afterwards, the extract was completely evaporated at 40 °C in a rotary evaporator, under vacuum. The dried extract was reconstituted with 1.5 mL of MeOH/water (40:60, v/v) and eluted with 8 mL of MeOH/water (85:15, v/v) through a C18 cartridge (previously activated with 4 mL of MeOH and 4 mL of water). The obtained extract was dried

with a gentle nitrogen stream, diluted with 2 mL of water, and finally filtered before the injection in the LC system.

1.3.5 Quantitative analysis of polyphenols in raw and digested samples

The chromatographic profile of the pre-digested samples was compared with the one obtained for the corresponding digested fractions (IN and OUT). By a qualitative point of view, the polyphenol composition did not seem to be affected by the digestion process. As shows in Figure 3, the chromatogram before and after the digestion presented the same profile.

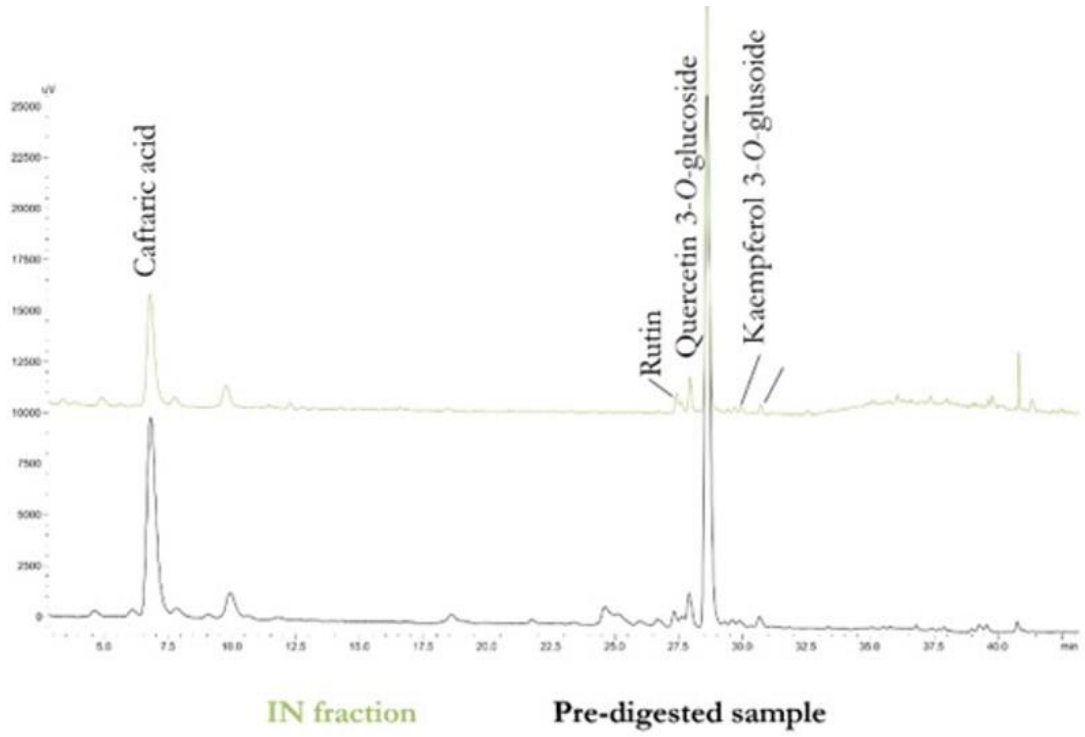

Figure 3. Representative chromatographic profile at 330 nm of pre-digested and IN sample.

Oxidation is considered one of the major deterioration mechanisms for polyphenols chemical instability, in fact dissolved oxygen levels negatively affect the bioaccesibility of phenols[153,154]. The digestion process was conducted under nitrogen and the contribution of oxygen was not taken into account. Another factor that was not considered is the metabolism of colonic microflora that can convert polyphenols into low molecular weight compounds, that are better absorbed through the colonic barrier than their original compounds. More interesting information were obtained from the quantitative data. Figure 4 clearly shows that for all the samples, the majority (>60%) of the target polyphenols passed in the bioaccesible fraction (IN) and only a smaller portion precipitated in the excreted fraction (OUT). It could be noticed that

in some case (e.g kaempferol 3-*O*-glucoside in Müller Thurgau, Nebbiolo and Aglianico or caftaric acid in Aglianico) the total amount of analyte after digestion, considering IN and OUT fraction, is higher than the amount found in the raw samples. This could be ascribed to the fact that the samples were subjected to a multi-step treatment, including a digestion process and an extraction with solvent. This may have caused a loss of sample/analyte, explaining variability of the results. However, the quantitative results are in agreement between the different cultivars and an acceptable repeatability was obtained for both digestion (11-17% RSD) and extraction process (8-12% RSD).

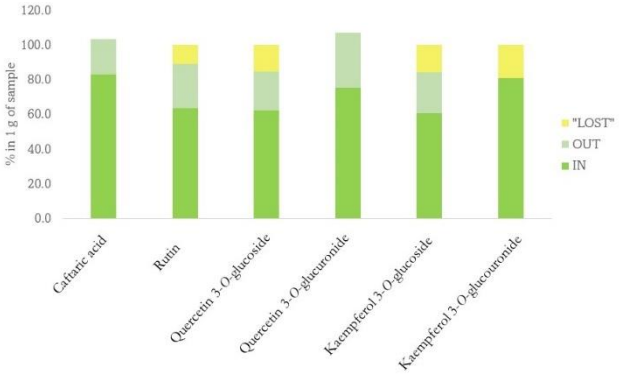

(a)

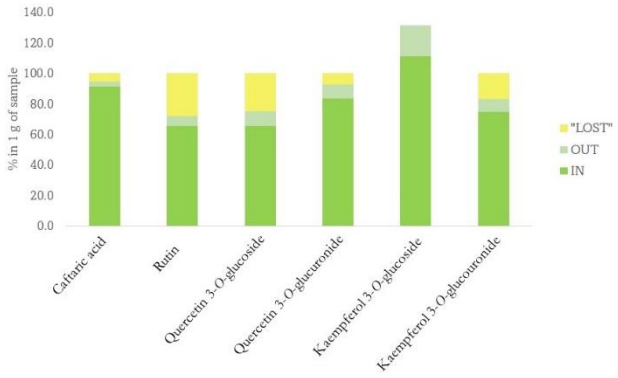

(b)

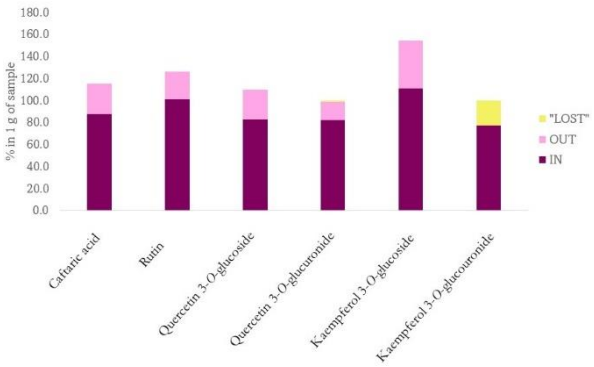

(c)

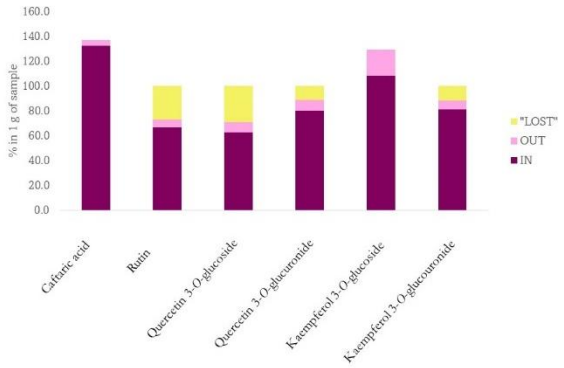

(d)

Figure 4. Quantitative data of (a) Chardonnay, (b) Müller Thurgau, (c) Nebbiolo and (d) Aglianico GPRs samples before and after *in vitro* gastrointestinal digestion process.

Section III.2

Corylus avellana L.

2.1 Introduction

European hazelnut plant is a member of the family of Betulaceae, genus *Corylus*, species *avellana*, whose name derives from the Italian city of Avella. Hazelnut is widely cultivated in several countries and it holds considerable agricultural, food and economic value. Turkey represents the most important world hazelnut producer, followed by Italy and China. Hazelnuts are a good source of nutrients: they contain proteins, lipids (monounsaturated and polyunsaturated fatty acids), carbohydrates, fiber, minerals (magnesium, zinc, selenium), vitamins (vitamin E, vitamin B complex), phytosterols, and also phenolic antioxidants. For this reason, hazelnut consumption can have a positive effect on human health and its benefit in reducing cardiometabolic disease risk has been demonstrated by different studies. In the hazelnut supply chain, a large amount of by-products as shells, skins, husks and leaves, is produced during harvesting and processing, while kernels, which represent less than 50% of the total nut weight, are the only portion of the plant to be used in food products. Therefore, in order to arrange a proper and greener management of this waste, different options were explored. Specifically, hazelnut shells and husks can have a use as raw materials for biofuels productions because of their high lignin and cellulose content. Another potential application of hazelnut shell, skin and husk is also suggested by their chemical composition: they are a source of phenolic compounds which possess a certain value to be used for pharmaceutical, cosmetic, and nutraceutical purposes because of their antioxidant and radical scavenging activities[155–157].

The aim of the studies included in this section is to investigate the secondary metabolites present in hazelnut skin by-products, using a more sustainable and less time-consuming approach. Several hydrophilic natural deep eutectic solvents (NADESs) were tested for the extraction of phenolic compounds and the antioxidant activity of the NADES-based extracts was evaluated by spectrophotometric assays.

Exploring the behavior of hydrophilic deep eutectic solvents for the extraction of polyphenols in *Corylus avellana* L. skin

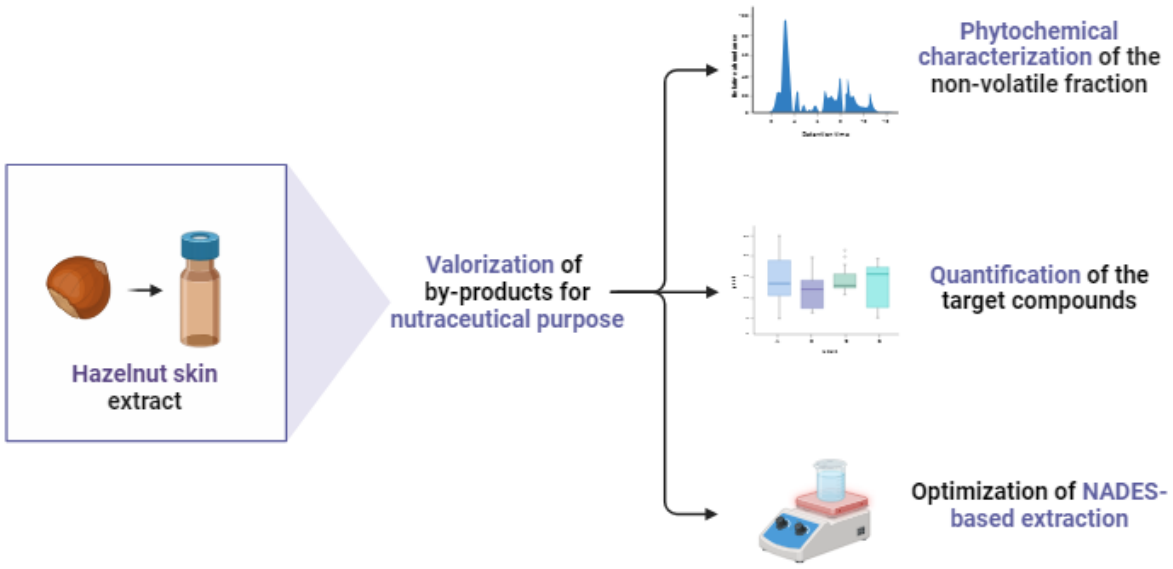

2.1 Exploring the behavior of hydrophilic deep eutectic solvents for the extraction of polyphenols in *Corylus avellana* L. skin

2.1.1 Fingerprinting of hazelnut skin and identification of the target compounds

The qualitative characterization of *Corylus avellana* skin L. was carried out through HPLC-PDA-ESI-MS/MS analysis. Several studies focused on the phytochemical characterization of the hazelnut or its kernel[156,158–160] and fewer data are available on the chemical composition of the skin. For this reason, the first part of this study was directed to the identification of the non-volatile secondary metabolites in the hazelnut skin samples under study. For this purpose, the hydroalcoholic extract was analyzed and the UV spectra for each peak provided a preliminary indication of the chemical classes of the compounds. The hydroalcoholic extraction was employed for the fingerprinting of the samples because of the low compatibility of eutectic solvents (used in this study as alternative solvents) with the ESI source of the mass spectrometer. In fact, the ESs employed are non-volatile and abundant and could interfere with the MS signal. The chromatographic profile at 280 nm is shown in Figure 1.

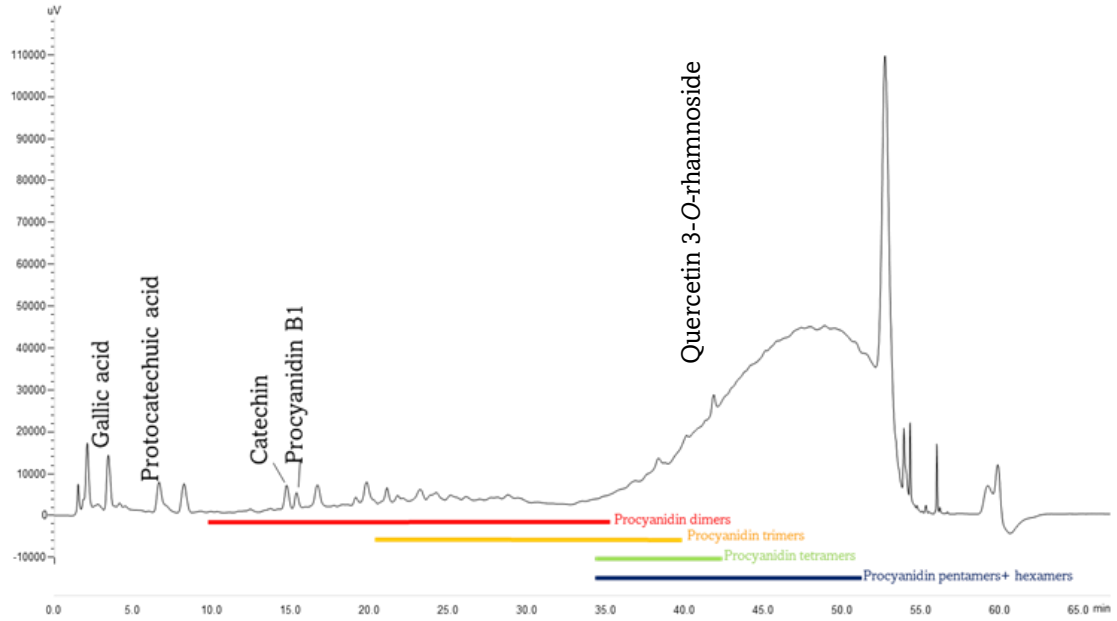

Figure 1. Chromatographic profile at 280 nm of the hydroalcoholic extract of hazelnut skin by HPLC-PDA.

Information about the molecular weight of the single compounds were obtained by mass spectrometric data in SCAN mode through the complementary correspondence between positive and negative protonated/deprotonated ions in the ESI^+ and ESI^- modes. Based on UV and MS data, five main informative peaks were identified or tentatively identified and selected as target compounds for further studies. The identity was confirmed by the co-injection of the

corresponding commercial standards. The information about the analytes under study are reported in Table 1. The identification data were in agreement with other studies reported in literature[156,157,161], where gallic acid, protocatechuic acid, catechin, procyanidin B1 and quercetin 3-*O*-rhamnoside are identified among the main secondary metabolites in hazelnut skin.

Table 1. List of identified compounds in hazelnut skin. For each analyte, retention time, UV maximum, protonated/deprotonated ions are reported.

Compound	λ max (nm)	Mol. Weight (g mol $^{-1}$)	[M – H] $^{-}$ *m/z*	[M + H] $^{+}$ *m/z*
Gallic acid	270	170	169	171
Protocatechuic acid	260	154	153	155
Catechin	280	290	289	291
Procyanidin B1 dimer	280	578	577	579
Quercetin 3-*O*-rhamnoside	350	448	447	449

Several studies[157,162,163] have reported the presence of compounds belonging to the family of condensed tannins, in hazelnut samples. To investigate the presence of tannin compounds in the extracts under study, the protonated/deprotonated ions obtain by UV-ESI-MS/MS analysis were fragmented by product ion scan mode (scan range from a 100 m z^{-1} to 2000 m z^{-1}). Comparing the molecular weight of the fragments with literature data, different condensed tannins were identified, as shown in Table 2. The main compounds found included procyanidin dimers with molecular weight of 594 and 730 g mol^{-1}, corresponding to the molecular formula $C_{30}H_{26}O_{13}$ and $C_{37}H_{30}O_{16}$ respectively; procyanidin trimers with molecular weight of 866 and 1303 g mol^{-1}, corresponding to the molecular formula of $C_{45}H_{38}O_{18}$ and $C_{47}H_{54}O_{28}$. Pentamers and hexamers of procyanidins were also found: the first with molecular formula of $C_{75}H_{62}O_{30}$ and $C_{75}H_{62}O_{31}$, and the second with molecular formula of $C_{90}H_{74}O_{36}$. For tannin compounds, it was not possible to confirm their identity with the co-injection of commercial standard compounds, because not available.

Table 2. List of identified procyanidins in hazelnut skin hydroalcoholic extract.

Compound	λ max (nm)	Retention time (min)	Mol. Weight (g mol $^{-1}$)	[M – H] $^{-}$ *m/z*	[M + H] $^{+}$ *m/z*	M^{2-} *m/z*	M^{2+} *m/z*	Molecular formula
Procyanidin dimer	277	10.92	594	593	595	/	/	$C_{30}H_{26}O_{13}$
Procyanidin dimer	278	25.95	730	723	731	/	/	$C_{37}H_{30}O_{16}$
Procyanidin trimer	279	18.38	866	865	867	/	/	$C_{45}H_{38}O_{18}$
Procyanidin trimer	279	33.45	1303	1302	1304	/	/	$C_{47}H_{54}O_{28}$
Procyanidin pentamer	278	34.18	1441	1440	1442	717	721	$C_{75}H_{62}O_{30}$
Procyanidin pentamer	278	34.2	1456	1455	1457	725	729	$C_{75}H_{62}O_{31}$
Procyanidin hexamer	279	33.18	1763	1762	1764	877	881	$C_{90}H_{74}O_{36}$

2.1.2 Quantification of the target compounds

Once the marker analytes were identified, the chromatographic method was adapted on a HPLC-PDA equipment to allow the analysis of NADES-based extracts without affecting the ESI source. The external calibration method was employed for the quantification of the compounds; Table 3 reports the quality analytical parameters of the HPLC-PDA.

Table 3. Quality analytical parameters of the HPLC-UV method

Analyte	Calibration curve	R^2	Linearity range (mg L^{-1})
Gallic acid	y = 22870x + 9891,6	0.9982	1 - 40
Protocatechuic acid	y = 28462x + 2707	0.9999	1 - 40
Catechin	y = 3960x - 49,015	0.9998	1 - 40
Procyanidin B1	y = 3108x + 399,42	0.9995	1 - 40
Quercetin rhamnoside	y = 16564x + 7845	0.9999	1 - 40

A stock solution of each standard (gallic acid, protocatechuic acid, catechin, procyanidin B1 and quercetin 3 *O*-rhamnoside) was prepared at a concentration of 1 mg mL^{-1}. Two mix solution were obtained: gallic acid and procyanidin B1 in the mix A and protocatechuic acid, catechin and quercetin 3 *O*-rhamnoside in mix B. To build the calibration curve, the following working solutions of the two mix were prepared: 40, 20, 10, 5, 2.5 and 1 mg L^{-1}. The obtained calibration curve was employed for the quantification of the marker analytes in the hydroalcoholic and NADES-based extracts of hazelnut skin. The quantitative data of the hydroalcoholic extract (Table 4) were used as reference to study the performance of extraction of the natural solvents.

Table 4. Quantification (μg g^{-1} of extract) of the target compounds in the conventional extract of hazelnut skin and using NADESs with 10% and 20% of water (n=3).

Sample	Gallic acid	Protocatechuic acid	Catechin	Procyanidin B1	Quercetin-3-*O*-rhamnoside
Hydroalcoholic extract					
Hydroalcoholic extract	208 ± 11	226 ± 10	418 ± 5	456 ± 10	109 ± 10
NADES with 10% of water					
$[Ch^+][Cl^-]$:LA 1:2	191 ± 14	242 ± 3	644 ± 3	796 ± 35	98 ± 6
Bet:LA 1:5	196 ± 19	259 ± 12	598 ± 30	768 ± 31	106 ± 7
Bet:Lev 1:3	182 ± 10	262 ± 0.1	499 ± 35	556 ± 2	110 ± 5
NADES with 20% of water					
$[Ch^+][Cl^-]$:LA 1:2	110 ± 9	163± 15	426 ± 42	296 ± 15	65 ± 5
Bet:LA 1:5	147 ± 35	178 ± 34	419 ± 52	287 ± 5	74 ± 18
Bet:Lev 1:3	124 ± 17	117 ± 0.2	261 ± 2	170 ± 12	44 ± 0.4

2.1.3 Optimization of the NADES-based extractions

As already mentioned, eutectic solvents have found several applications for the extraction of natural compounds in plants. Some studies have successfully employed $[Ch^+][Cl^-]$-based NADES to extract polyphenols from hazelnut skin[164–166]. Given these promising results, different combination of hydrophilic HBAs and HBDs were tested in this study. Betaine was also included as component of the NADESs because, contrary to $[Ch^+][Cl^-]$, it is included in the list of accepted novel foods by EU[167]. In this way, NADESs completely food grade were prepared with no need to eliminate the solvent after the extraction of the phenolic fraction. Table 5 reports the combination and molar ratio prepared.

Table 5. NADES prepared in this study. In green the mixture that form a liquid solvent at RT and in red the combination that did not form a homogeneous liquid at RT.

HBA-HBD[a]	Molar ratio	Preparation outcome
[Ch^+][Cl^-] : LA	1 : 1	
	1 : 2	
[Ch^+][Cl^-]: Lev	1 : 1	
	1 : 3	
	1 : 5	
Bet : Gly	1 : 1	
	1 : 2	
	1 : 5	
Bet : LA	1 : 2	
	1 : 3	
	1 : 5	
Bet : Lev	1 : 2	
	1 : 3	
	1 : 5	

[a] Ch: choline chloride, LA: lactic acid, Lev: levulinic acid, Bet: betaine, Gly: glycerol

The NADESs liquid at RT were tested for the determination of the target analytes in hazelnut skin, using an ultrasound-assisted solid liquid extraction (UA-SLE). The NADES-based extracts were analyzed by HPLC-PDA, using the same chromatographic parameters employed during the identification studies. The chromatographic profile was compared with the one obtained from the hydroalcoholic extract and no qualitative differences were observed (data not showed).

Figure 2 reported the comparison between the hydroalcoholic and the NADES-based extraction methods. Apart from the lower amount of solvent used, the new method resulted to be faster to perform, not requiring the evaporation of the solvent.

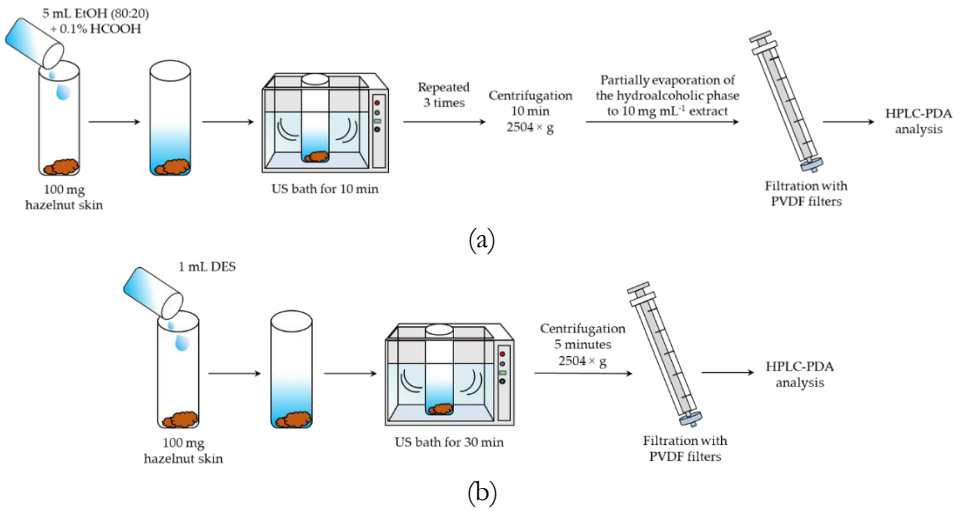

Figure 2. Comparison of the hydroalcoholic (a) and NADES-based extraction method (b).

Several green metrics have been developed in recent years to "measure" objectively the greenness of analytical procedures. Among these, AGREEprep metric is the most suitable to evaluate the impact of sample preparation. Figure 3 shows the comparison of the pictograms obtained for the hydroalcoholic and NADES-based methods. The NADES-based extraction method required a more straightforward approach and a lower quantity of solvent compared to the conventional one, resulting in a higher score.

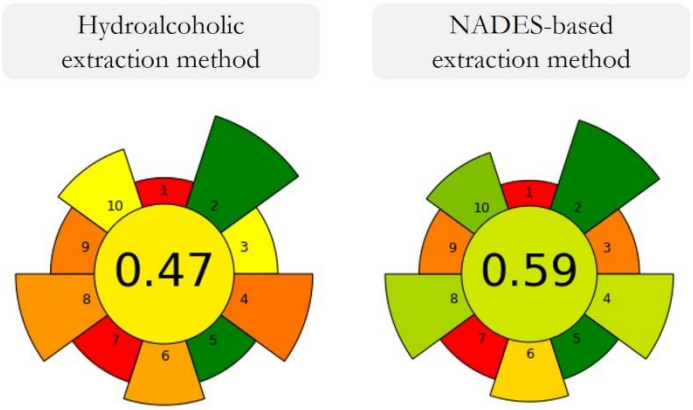

Figure 3. Pictograms obtained with AGREEprep metric[21], for the hydroalcoholic and NADES-based methods

To reduce the viscosity of the solvent (fundamental parameter to favor the mass transfer from the matrix to the solvent), different amounts of water were added after the preparation of the NADESs. The addition of higher amount of water (> 50%) significantly decreased the viscosity; however, it is reported in literature that content of water higher than

50% could destroyed the hydrogen bond network between the HBA and HBD[168]. For this reason, NADES with 10 and 20% of water content were prepared and used for the UA-SLE. After these preliminary experiments, the NADESs with the best extraction performances resulted to be [Ch^+][Cl^-]:LA 1:2, Bet:LA 1:5 and Bet:Lev 1:3. The quantitative results are reported in Table 4. The quantitative results showed that the amount of analytes found in the extracts was slightly affected by the type of HBA and HBD used. Contrary, the content of water had a higher impact on the extraction efficiency, showing better performances with 10% of water. These results can suggest that the addition of higher volume of water could affect the hydrogen bonding network of the DES, thus reducing the interaction with the target analytes.

Fast *in vitro* screening of the antioxidant activity of *Corylus avellana* L. skin using DPPH$^{\bullet}$ and ABTS$^{+\bullet}$ colorimetric assays

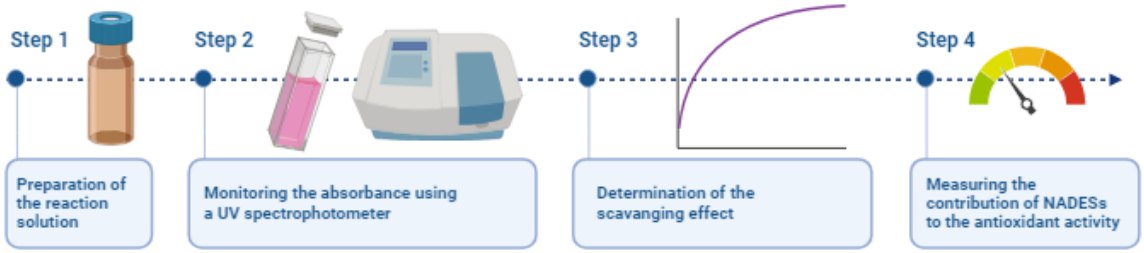

2.2 Fast *in vitro* screening of the antioxidant activity of *Corylus avellana* L. skin using DPPH• and ABTS+• colorimetric assays

Colorimetric assays are cheap and user-friendly tools to study the biological activity of plant matrices. The combination of chromatographic and spectrophotometric data was employed to obtain an overview of the antioxidant capacity, due to the content of phenolic compounds found in the first part of the study. DPPH• and ABTS+• *in vitro* colorimetric assays were performed on the six NADES-based extracts (both 10% and 20% water content were considered). The tests were made in triplicate and repeated in different days to assure the repeatability and the stability of the results obtained over time.

2.2.1 DPPH• assay

Each extract was prepared at seven different concentrations in order to build a dose-response curve of the scavenging activity against DPPH• radical. For all the extracts, a logarithmic curve was obtained: further increasing the concentration of the extract did not cause an increasing of the response, reaching a plateau of the activity. A representative example is showed in Figure 1. For each extract the mg of extract able to scavenge 50% of DPPH• solution at 25 μg mL^{-1} (EC_{50}) was calculated using the individual formula of the calibration curve.

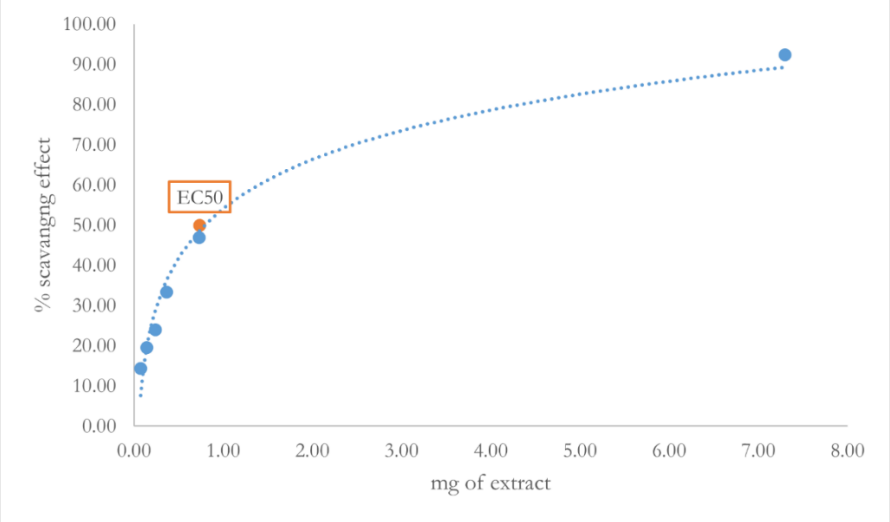

Figure 1. Representative dose-response curve and EC_{50} of Bet:Lev 1:3 (20% of water) extract.

The values of EC_{50} calculated for the different extracts are reported in Table 1 together with the calibration curve equation obtained from the dose-response curve.

Table 1. Calibration curves and EC_{50} of the NADES-based extracts for the scavenging effect on DPPH•.

NADES-based extract	% of water	Calibration curve	EC_{50} (mg of extract)
$[Ch^+][Cl^-]$:LA 1:2	10	y = 17.984ln(x) + 71,607	0.301
Bet:LA 1:5	10	y = 17.589ln(x) + 69,596	0.328
Bet:Lev 1:3	10	y=19.755ln(x)+63,091	0.516
$[Ch^+][Cl^-]$:LA 1:2	20	y=18.373ln(x)+77,4	0.225
Bet:LA 1:5	20	y=23.698ln(x)+82,677	0.252
Bet:Lev 1:3	20	y=18.324ln(x)+55,616	0.736

The antioxidant activity of the NADES-based extracts was compared with Trolox, a reference compound with well-known antioxidant properties. As for the extracts, different concentration of Trolox (100, 75, 50 and 25 μg mL^{-1}) were prepared to obtain a calibration curve and calculate its EC_{50}. Figure 2 reports the comparison between the EC_{50} obtained for the NADES-based extracts and Trolox. In this case, the different percentage of water did not affect the antioxidant activity, while the presence of lactic acid as component of the solvents seemed to positively affect the EC_{50}. It is important to underline that in the extracts, the bioactive metabolites were not tested as pure compounds, contrary to Trolox. The ability to scavenge DPPH• radical was also tested for the neat NADES, to study their possible contribution to the overall activity of the extract. However, no activity was found for any of the NADESs used for the extraction.

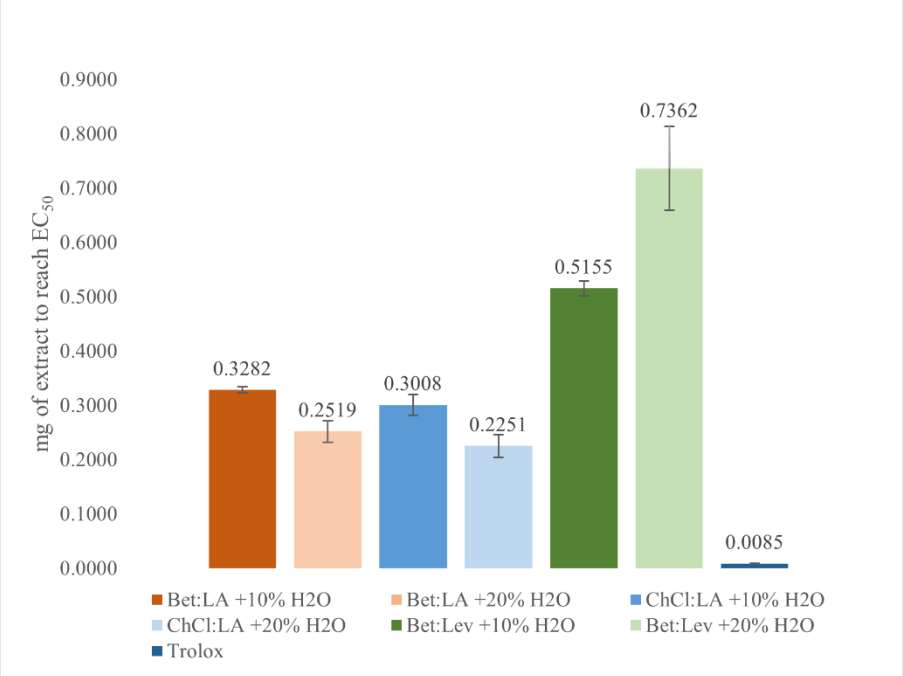

Figure 2. Amount of NADES-based extracts and Trolox necessary to obtain a scavenging effect of 50% of the DPPH• radical.

2.2.2 ABTS$^{\bullet+}$ assay

A similar approach was used for ABTS$^{\bullet+}$ assay. In this case, the scavenging effect of the NADES-based extracts was tested against ABTS$^{+\bullet}$ radical and the antioxidant capacity was expressed in mg equivalent of Trolox. The calibration curve of Trolox was prepared (100, 75, 50 and 25 µg mL^{-1}) and the corresponding absorbance measured at 515 nm. The test was carried out on the same extracts tested for DPPH$^{\bullet}$ assay. Their scavenging effect against ABTS$^{+\bullet}$ was related to the mg of Trolox that have an equivalent response to a gram of pure hazelnut skin extract. As shown in Figure 3, the antioxidant capacity of the NADES-based extract tested was similar (around 0.4 mg of Trolox corresponds to 1 g of extract) and did not seem to be affected by the composition of the NADES.

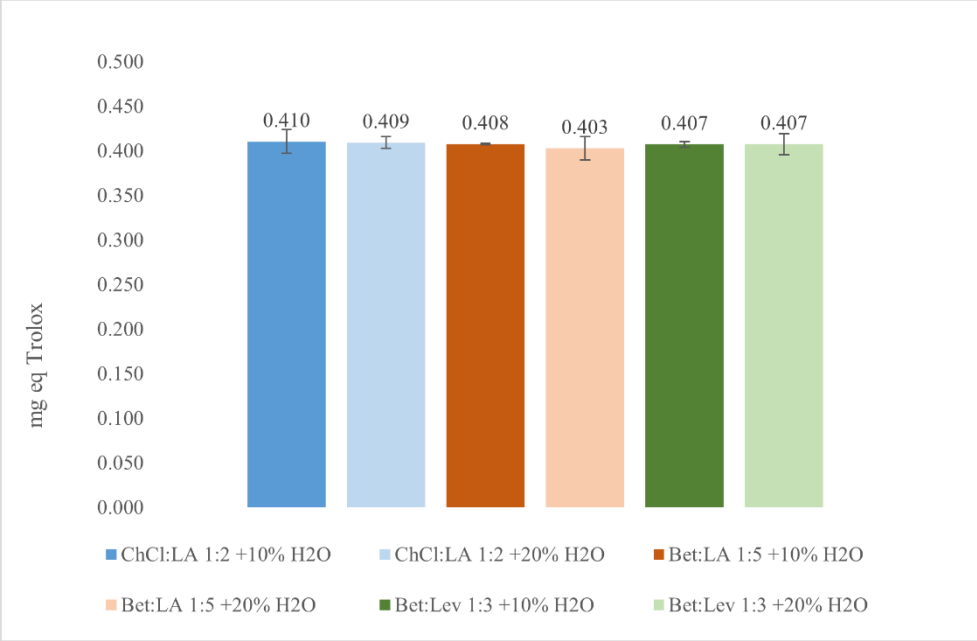

Figure 3. Equivalent (mg) of Trolox corresponding to 1 g of NADES-based extracts.

Also in this case, the neat NADESs were subjected to the assay. Contrarily to the results obtained with DPPH$^{\bullet}$, the solvents seemed to contribute to the overall scavenging effect, as shown in Figure 4. These results suggest that, apart from their interesting solvation properties, NADESs can increase the antioxidant power (thus the value) of the final extract, supporting their application in the extraction of natural compounds.

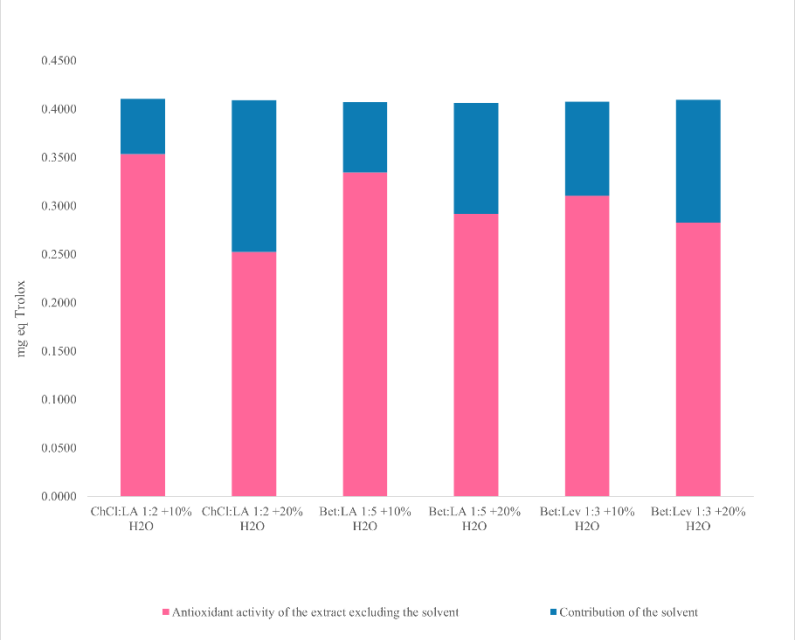

Figure 4. Contribution of NADES-based extracts of hazelnut skin and neat NADESs to the scavenging activity against $ABTS^{+\bullet}$ radical.

Section III.3

Cannabis sativa L.

3.1 Introduction
3.2 Characterization and biological activity of fiber-type *Cannabis sativa* L. aerial parts at different growth stages
  3.2.1 Fingerprinting and identification of target compounds
  3.2.2 Optimization of the ultrasound-assisted solid-liquid extraction method
  3.2.3 Analysis and quantification of the phenolic compounds and cannabinoids
  3.2.4 Statistical analysis and comparison of the phytochemical profile of the samples under study
3.3 Development of a dispersive solid-liquid microextraction method using natural eutectic solvents for a greener extraction of phytochemicals from fiber-type *Cannabis* sp.
  3.3.1 Preparation of the eutectic solvents
  3.3.2 Optimization of the dispersive solid liquid microextraction method
  3.3.3 Preliminary screening using different natural eutectic solvent and comparison with the conventional SLE method
  3.3.4 Characterization of the eutectic mixture
  3.3.5 Validation of the proposed method
3.4 New class of tunable choline bromide-based hydrophobic deep eutectic solvents for the extraction of bioactive compounds of varying polarity from a plant matrix
  3.4.1 Synthesis of $[Ch^+][Br^-]$-modified salts
  3.4.2 Choice of the most suitable HBD for the preparation of $[Ch^+][Br^-]$ based HES
  3.4.3 Evaluation of the hydrophobicity of $[Ch^+][Br^-]$-based HES
  3.4.4 Characterization of selected $[Ch^+][Br^-]$-based HESs in terms of viscosity and melting point

3.1 Introduction

Cannabis sativa L. is a dioecious (rarely monoecious) herbaceous annual plant, native of Central Asia but easily adaptable to different geographical conditions. Historically recognized for its textile, fiber, and chemical features, in the 1990s its cultivation was characterized by a slow decline because of the psychotropic effects of one of its major compounds, delta^9-tetrahydrocannabinol (Δ^9-THC)[169]. Currently, a renewed interest for this species is opening the way for its exploitation in different fields[170]. Although there is no consensus on its classification the most common refers to a single species (*C. sativa*) with different chemotypes based on the "total cannabidiol (CBD)"/"total THC" ratio. The drug type, richer in Δ^9-THC, and the fiber type, richer in CBD or related compounds (commonly known as hemp or industrial hemp), are the most important from the economic point of view. The first chemotype is normally subjected to restrictions according to the legislations of individual countries, while the second is the main source for the market, which includes food and personal care products but also medical formulations. Even though most attention has been on Δ^9-THC and CBD, hemp has a complex chemistry with many different chemicals found in different part of the plants (inflorescences, leaves, stems, and seeds). These include terpenes, carbohydrates, fatty acids, and their esters, amides, amines, phytosterols, phenolic compounds, and non-psychotomimetic cannabinoids that have been associated with health-promoting properties, e.g., neuroprotective, antioxidant, and anti-inflammatory effects[171–173]. Most studies have focused on the inflorescences and their biomarker compounds, and little information are available on leaves and stalks and on other specialized metabolites, such as polyphenols and derivatives that are characterized by several biomedical and pharmacological properties[174–176]. Due to the complex phytochemistry of *C. sativa* and the variability of its composition, it is important to have reliable and fast techniques of analysis to characterize the plant, differentiate strains and ensure safety of use. The common approach for the extraction and analysis of cannabinoids is a solid–liquid extraction with medium or low polarity organic solvents, such as ethanol, methanol or hexane[177,178]. Apart from the consumption of relatively high volume of solvents, these methodologies have a significant impact on the sustainability of the overall analysis process as they often require the use of disposable materials, energy-consuming equipment and instrumentation. More innovative approaches have been developed in recent years, with the aim of simplifying the extraction procedure and reducing the toxicity and amount of extraction materials.

Taking into account the above considerations, the aim of the studies included in this section are:

(i) The characterization of the non-volatile fraction of *Cannabis sativa* L. aerial parts, collected before flowering, using an ultrasound-assisted solid-liquid extraction method, coupled with liquid chromatography.

(ii) The development of a more innovative and user-friendly method to extract different phytochemicals from fiber-type hemp aerial parts, using hydrophobic eutectic solvents.

(iii) The enhancement of the eutectic solvents physicochemical properties to improve the extraction of the more polar compounds in the hemp samples under study.

(iv) The application of the optimized eutectic solvent-based extraction method for the determination of cannabinoids in different hemp products available on the market.

(v) Exploring the possibility to use a solid sorbent (MOFs) for the extraction of phytochemical from hemp samples.

(vi) The evaluation of the biological activity (i. e antioxidant activity and enzymatic inhibition) of hemp aerial parts by-products through colorimetric *in vitro* assays, for possible applications in the cosmetic field.

Characterization and biological activity of fiber-type *Cannabis sativa* L. aerial parts at different growth stages

This paragraph is reproduced from a published article
(Mastellone *et al.*, Plants 11, 2022, 419)

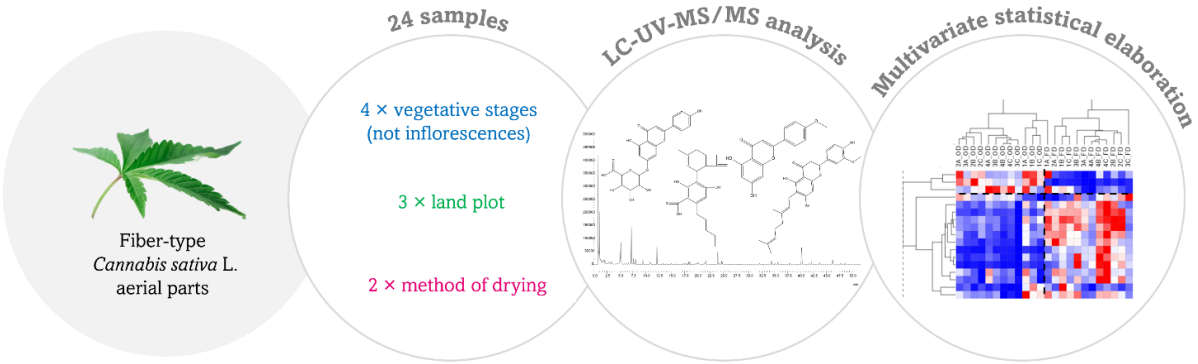

3.2 Characterization and biological activity of fiber-type *Cannabis sativa* L. aerial parts at different growth stages

3.2.1 Fingerprinting and identification of target compounds

A fundamental step in this study was the qualitative characterization of the plant sample. According to the existing literature[174,179–184], most of the studies on *Cannabis sativa* L. focused on the phytocomplex of the inflorescences and on cannabinoids which are synthetized in large amount in these plant parts. Our samples were collected at different growth stages (before flowering) and mainly composed by stems and leaves. The extractions, following the optimized method, were performed both in MeOH and acetone and followed by HPLC-PDA-ESI-MS/MS untargeted metabolite analysis. The chromatographic profile obtained at 254 nm is illustrated in Figure 1. The UV spectra for each peak provided a preliminary indication of the classes of compounds. The molecular weight was also defined by mass spectrometric data in SCAN mode, through the complementary correspondence between positive and negative protonated/deprotonated ions in ESI^+ and ESI^- modes. The product ion scan analysis of these ions provided diagnostic fragments for each compound. Based on UV and MS data, 27 informative peaks were identified or tentatively identified and selected as target compounds for the statistical analysis. All the information about the analytes under study are reported in Table 1.

Table 1. List of identified and putatively identified compounds in fiber-type *Cannabis sativa* L. aerial parts. For each analyte, retention time, UV maximum, protonated/deprotonated ions, fragment ions obtained by product ion scan mode (PIS) and identified or tentatively identified compound names are given. Identification confidence values and references are also included. In bold, the compounds confirmed with the injection of authentic commercial reference standards.

N°	λ max (nm)	$[M + H]^+$ *m/z*	$[M - H]^-$ *m/z*	Mol. Weight (g/mol)	M^{2+} *m/z*	M^{2-} *m/z*	Aglycon (g/mol)	Compound name	Identification levels§	Ref.
1	346/252	463	461	462	287	285	286	**Luteolin 7-*O*-glucuronide**	1	175,180,185
2	336/266	447	445	446	271	269	270	**Apigenin 7-*O*-glucuronide**	1	175,180,185
3	345/250	477	475	476	301	299	300	Diosmetin glucuronide derivative A	2	175,180,185
4	345/250	477	475	476	301	299	300	Diosmetin glucuronide derivative A	2	175,180,185
5	335/267	623	621	622	285	283	284	Acacetin glycoside A	2	175,180,185
6	332/267	593	591	592	285	283	284	Acacetin glycoside B	2	175,180,185
7	328/267	607	605	606	285	283	284	Acacetin glycoside C	2	175,180,185
8	334/267	461	459	460	285	283	284	Acacetin glucuronide derivative	2	175,180,185
9	336/266	271	269	270	/	/	/	**Apigenin**	1	175,180,185
10	343/252	301	299	300	/	/	/	**Diosmetin**	1	175,180,185
11	268/279	/	/	/	/	/	/	Not identified	/	/
12	268/279	/	/	/	/	/	/	Not identified	/	/
13	268/279	/	/	/	/	/	/	Not identified	/	/
14	267/334	285	283	284	/	/	/	**Acacetin**	1	175,180,185
15	310	/	667	/	/	163	/	Coumaric acid derivative	2	185
16	341/274	437	435	436	313	/	/	**Cannflavin A**	1	174,183
17	220/269/306	359	357	358	/	/	/	**Cannabidiolic acid (CBDA)**	1	174,183
18	220/268/305	361	359	360	219	/	/	Cannabigerolic acid (CBGA)	2	174,183
19	263/328	327	325	326	191	/	/	Cannabinoid	3	174,183
20	220/271/305	331	329	330	191,313,257,233	/	/	Varinic derivative A	2	174,183

21	220/272/304	331	329	330	191,257,233	/	/	Varinic derivative B	2	[174,183]
22	220/271/305	331	329	330	191,257,233	/	/	Varinic derivative C	2	[174,183]
23	268/306	347	345	346	205,175	/		Cannabinoid	3	[174,183]
24	/	355	353	354	337,281	/	/	Cannabinolic acid (CBNA)	2	[174,183]
25	220/271/304	359	357	358	219,243	/	/	Δ^9-Tetrahydrocannabinolic acid (Δ^9-THCA)	2	[174,183]
26	/	359	357	358	219,341,261	/	/	**Cannabichromenic acid (CBCA)**	1	[174,183]
27	266/305	375	373	374	233	/	/	Cannabinoid	3	[174,183]

§ Identification confidence according to the request of the Chemical Analysis Working Group (CAWG, 2007)[186]: Level 1, identified compound (a minimum of two independent and orthogonal data, such as retention time and mass spectrum) compared directly relative to an authentic commercial reference standard; Level 2, putatively annotated compound (compound identified by analysis of spectral data and/or similarity to data in a public database); and Level 3, putatively characterized compound class level.

Two main groups of compounds were identified: the more polar flavonoids and non-psychotomimetic cannabinoids which are reported to be among the main class of phytochemicals produced by hemp[185,187,188]. The flavonoids were mainly in form of glycosides and the most abundant (confirmed by co-injection with authentic commercial standards) were luteolin and apigenin as *O*-glucuronide derivatives. Other flavonoids glycosides detected in lower amount, including acacetin and diosmetin derivatives, were tentatively identified through their tandem mass spectrometry fragmentation pattern. The MS/MS fragmentation gave a potential aglycon of 300 g mol^{-1} for peak 3,4 which corresponds to diosmetin molecular weight, while for peak 5, 6, 7, 8 the fragment was 284 g/mol^{-1}, corresponding to acacetin. While apigenin and luteolin are normally reported in *Cannabis sativa* L. phytocomplex[175,185], to the best of authors' knowledge, no data are available on the presence of acacetin and diosmetin glycosides in hemp samples. However, their corresponding aglycones were found in traces in the samples and confirmed with reference standards, supporting the identification data. Interestingly, Pollastro *et al.*[185] reported two flavones (canniflavone 1 and 2), isolated in 1980 and only found in *Cannabis*, with close structural similarity to diosmetin.

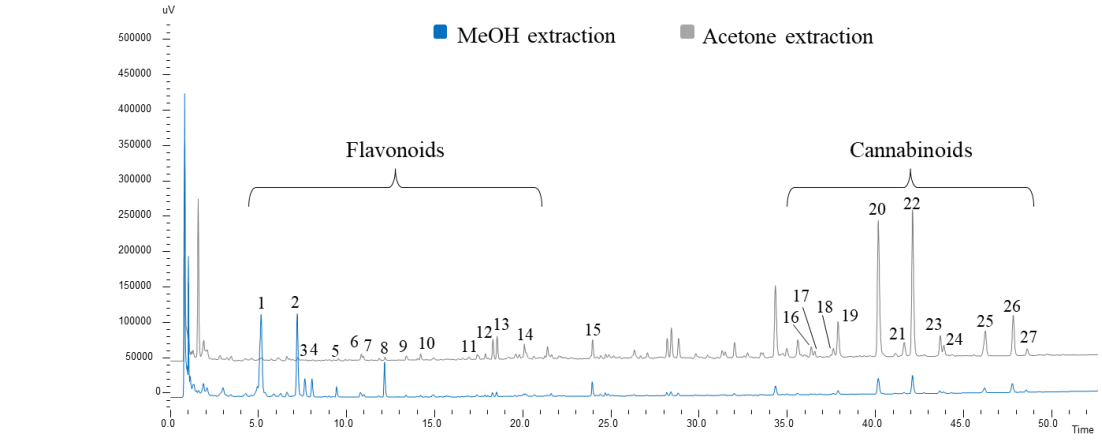

(a)

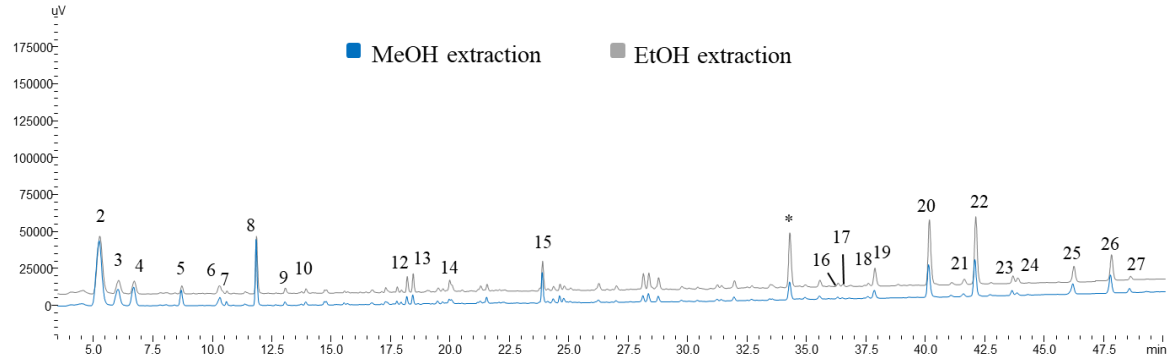

(b)

Figure 1. (a) Chromatographic profile at 254 nm of methanolic and acetone extraction of fiber-type *Cannabis sativa* L. aerial parts at 5 mg mL^{-1}. For peaks identification, see Table 1 and (b) Chromatographic profile at 254 nm of methanolic and ethanolic extraction of fiber-type *Cannabis sativa* L. aerial parts at 5 mg mL^{-1}. For peaks identification, see Table 1.

In accordance with the phenotype of the plant (fiber-type), only non-psychotomimetic cannabinoids were found. In this case, few of these terpenophenolic compounds are easily available as commercial standards[189] and only cannabidiolic acid (CBDA), cannflavin A and cannabichromenic acid (CBCA) were confirmed. The other analytes, which presented a similar retentions times and maximum UV adsorption typical of cannabinoids in the acid form (around 220, 270 and 300 nm, see Table 1), were tentatively identified through their tandem mass spectrometry fragmentation patterns which were compared with literature data[174,182,183]. As an example, the main cannabinoids (peak 20, 21 and 22) in the extracts were putatively identified as varinic acid derivatives (propyl cannabinoids) which presented protonated/deprotonated ions 331 *m/z* and 329 *m/z*, in ESI$^+$ and ESI$^-$ ionization modes, respectively, and fragmented to give diagnostic ions at *m/z* 313 (water loss), 257, 233, and 191 in ESI$^+$ (see Figure 2). Among the main

propyl cannabinoids, tetrahydrocannabiva-rinic acid (Δ^9-THCVA) and cannabivarinic acid (CBDVA) had similar fragments losses with some differences in ion intensity that are in agreement with our results[183].

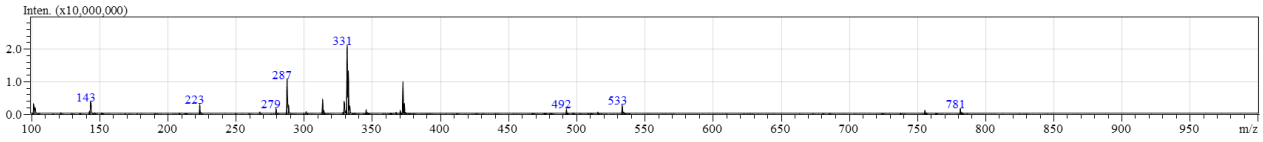

(a)

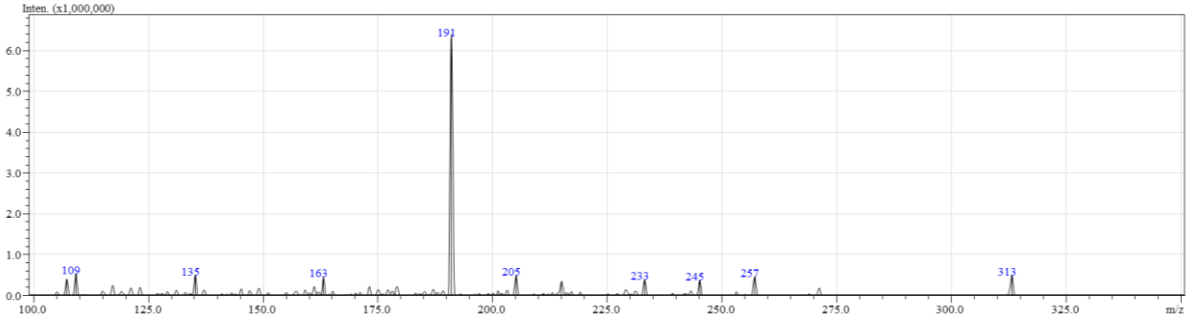

(b)

Figure 2. Representative MS spectrum of peak 21 in ESI^+ (a) and PIS fragmentation (b) of protonated ion 331m z^{-1} (putatively identified as varinic acid derivative according to [32]).

To support these results, a GC-MS analysis of the acetone extract, which presented higher content of cannabinoids, was carried out. In particular, the extract was derivatized with *N,O*-Bis(trimethylsilyl)trifluoroacetamide (BSTFA) before the injection, to avoid the decarboxylation of the cannabinoid acid, which easily form the neutral species in presence of high temperature[188,190]. The GC analysis confirmed the presence of propyl cannabinoids, CBDA, CBCA and Δ^9-THCA, from the comparison with commercially available mass spectral libraries and the injection of CBDA and CBCA authentic commercial standard (see Figure 3 for GC-MS profile and spectra). As mentioned before, leaves and stem (which are the main components of the sample under investigation) had a lower content in cannabinoids[171,175] compared to inflorescences and few data were available for comparison purpose. Besides CBDA, Δ^9-THCA, CBNA, CBGA and CBCA were other predominant chemicals of the class, depending also on the chemotype[175,188].

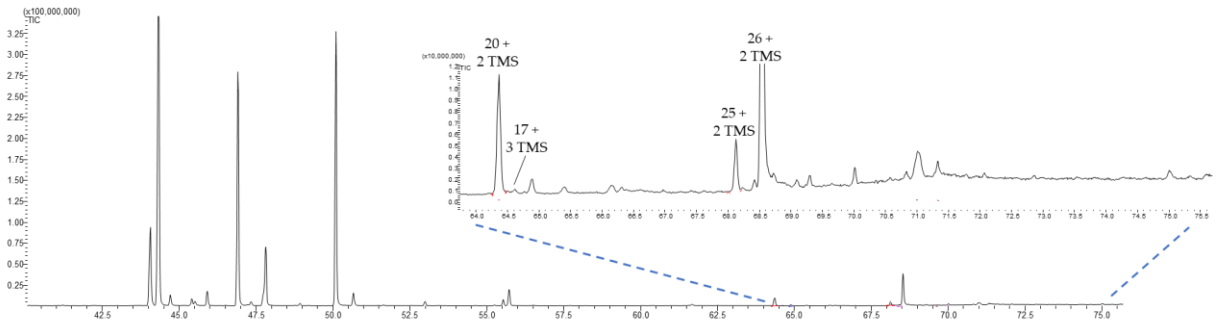

(a)

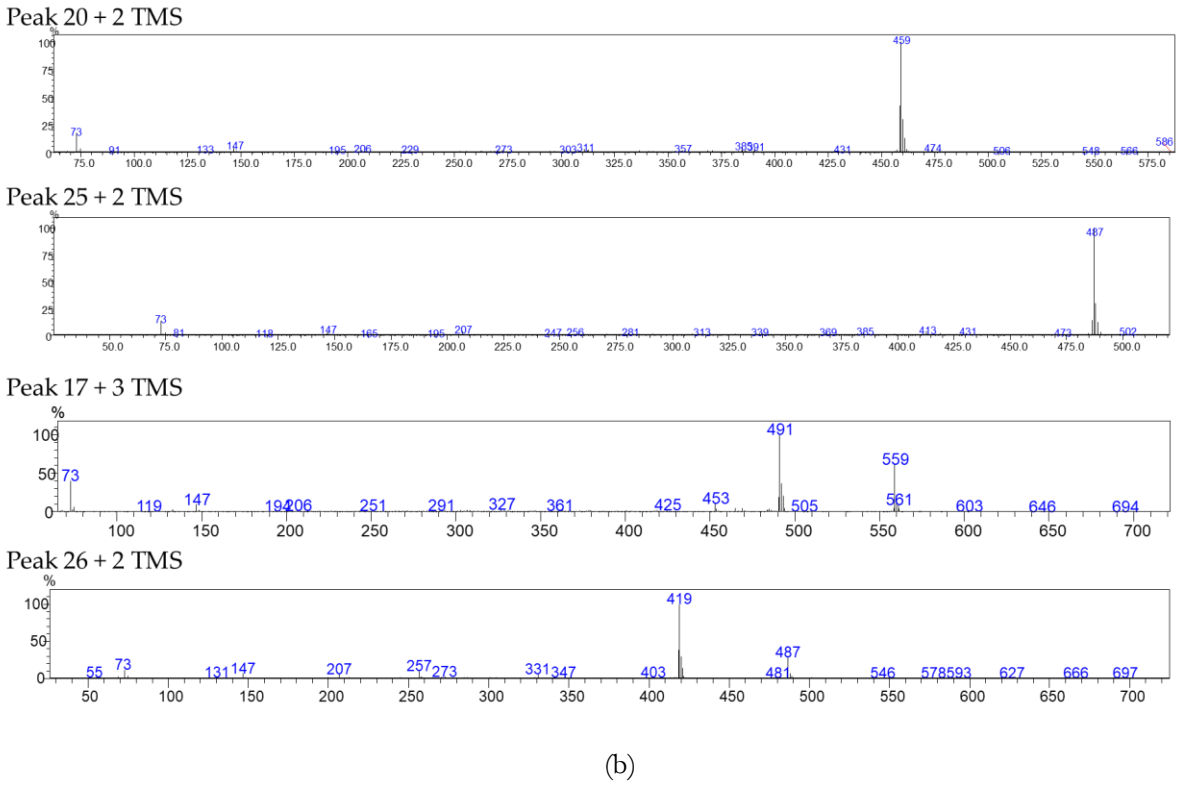

(b)

Figure 3. (a) GC-MS profile of the FD acetone hemp extract, after derivatization with BSTFA and (b) MS spectra of selected peak in the hemp extract. TMS, trimethylsilyl. See Table 1 for peak numbers.

3.2.2 Optimization of the ultrasound-assisted solid-liquid extraction method

The optimization of sample treatment before chromatographic downstream analysis is a fundamental step to reach a better extraction efficiency. This is particularly true for complex matrix, such as plant samples, which normally need several pre-treatments before the injection, especially when a liquid chromatography (LC) system is employed. In this case, different variables were taken into account for the extraction of fiber-type *Cannabis sativa* L. samples. In order to simplify the optimization study, a representative mix of all the 24 samples were prepared, taking

an equal amount from each sample. According to previous works which deal with plant analysis[10,110,191,192], an ultrasound-assisted solid liquid extraction (UA-SLE) method was selected, being efficient and easy to perform. Two solvents were tested for the solid-liquid extraction: methanol (MeOH) which presents a good affinity for different classes of compounds while acetone was reported to have a good solubility for cannabinoids[193,194]. This was confirmed by our results, where the methanolic extraction allowed to extract a higher number of compounds, belonging mainly to the classes of flavonoids and non-psychotomimetic cannabinoids, while the acetone extraction was more effective in selectively isolating cannabinoids (see Figure 1a). Some works report the use of ethanol for the selective extraction of cannabinoids, however our results showed that ethanol extraction capacity was similar to that exerted from MeOH and not superior to that of acetone (Figure 1b).

An experimental design was employed for the optimization of the other variables considered, which include the sample amount (mg), the volume of solvent (mL), the percentage of water in the solvent (%) (considered only for MeOH extraction) and the time of extraction (min) with US. A full two-level factorial design (2^n, with n = 4/3 variables) was used for the screening study, which comprises sixteen (MeOH) or eight (acetone) experiments combining the minimum and maximum values considered for each factor. Moreover, three replicates of the central point (intermediate value for each variable) were carried out, to monitor the reproducibility of the method. For the sample amount the low and high limits were set at 100 and 500 mg, the volume of solvent ranged between 5 and 50 mL, while the time of extraction with US was evaluated between 10 and 30 minutes. Regarding the percentage of water, a maximum value of 50% was set for the extraction in MeOH, to evaluate the influence of water in the extraction of the target analytes. For all the factors under study, the values were set with the aim of reducing the time of analysis and consumption of materials (see Table 2).

Table 2. Variables considered in the experimental design (2^n screening study).

Variable	Low value	High value
Sample amount (mg)	100	500
Volume of solvent (mL)	5	50
Water in the solvent (%)	0	50
Extraction time with US (min)	10	30

Once the experiments were performed, the extraction efficiency was evaluated in terms of the peak areas obtained for all the target compounds. The results are shown in the Pareto

charts, Figure 4. For both the solvents, the increasing of the sample amount led to a higher extraction efficiency. However, the ratio between the peak area and the amount of sample showed a linear trend without an exponential increasing of the performance of extraction. Considering the good sensibility of the extraction method, already obtained with 100 mg of the sample, the employed amount was set to the low value, also to reduce the consumption of raw material. Regarding the methanolic extraction, the other variable which truly affect the peak area was the content of water. While the amount of water was not significant for the flavonoids compounds, the extraction of cannabinoids was negatively influenced by higher amount of this polar solvent and therefore the percentage of water was set at its lower value (zero). For the extraction in acetone, the most influential variable was the time of extraction, which again, have a negative effect on the extraction efficiency of the cannabinoids. This may be caused by the slight increasing of temperature during longer extraction times with US, being cannabinoid acids sensitive to high temperatures[190]. Based on these results, for both the solvents, the minimum value for all the factor was selected as the optimum conditions. Moreover, the elimination of water in the solvent of extraction allowed to reduce the time of solvent evaporation needed to obtain the dried extract. Therefore, the optimized method required 100 mg of sample, 5 mL of solvent and 10 min of extraction with US. Once the method was optimized, the exhaustivity of the extraction was evaluated for both solvents, considering the decrease of peak area for each compound, after five cycles of extraction on the same matrix. Three consecutive extractions allowed to recover the 88% and 96% of the total amount of the components for MeOH and acetone, respectively, and were therefore selected for subsequent analyses. The optimized method was then applied for the extraction of the 24 samples of *Cannabis sativa* L.

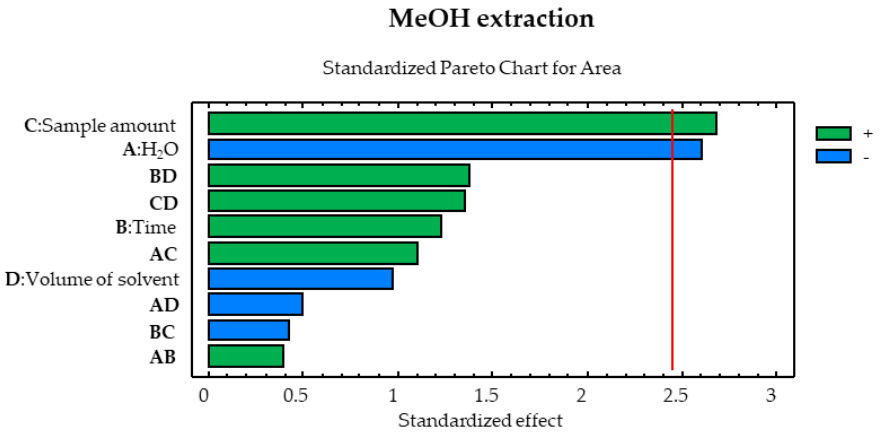

(a)

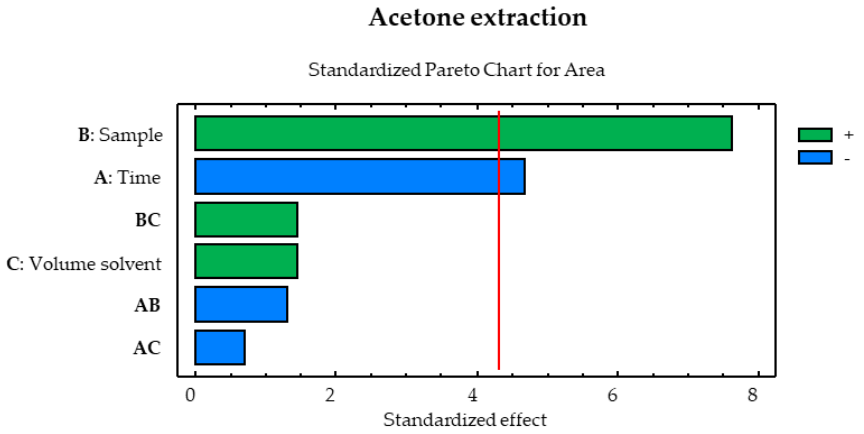

(b)

Figure 4. Pareto charts obtained in the screening of the main variables for the methanolic (a) and acetone extraction (b).

3.2.3 Analysis and quantification of the phenolic compounds and cannabinoids

The most abundant phenolics and cannabinoids were quantified by LC-PDA analysis, using the external calibration method. Several quality analytical parameters of the chromatographic method are reported in Table 3.

Table 3. Quality analytical parameters of the HPLC-UV method.

Compound	λ (nm)	Linear range (mg/L)	R^2	Calibration curve equation	Peak quantified
Luteolin 7-*O*-glucuronide	346/252	25-150	0.9989	y = 14487x - 24394	1
Apigenin 7-*O*-glucuronide	336/266	10-350	0.9986	y = 20488x + 47085	2
Apigenin	336/266	0.1-25	0.9989	y = 35166x – 2365.2	9
Diosmetin	343/252	0.1-25	0.9970	y = 37180x - 1940.9	3, 4, 10
Acacetin	267/334	1-25	0.9990	y = 32388x + 9461.5	5, 8
Coumaric acid	310	1-10	0.9950	y = 50388x + 22980	15
CBDA	220/270/310	5-50	0.9999	y = 13839x - 21.947	20, 21, 22, 23, 24, 25, 26, 27

The quantification of the 24 samples was performed on the methanolic extracts which had a more comprehensive phytochemical profile. When available, the corresponding authentic commercial standard was used to build the calibration curve (luteolin 7-*O*-glucuronide, apigenin 7-*O*-glucuronide, apigenin, diosmetin, coumaric acid and acacetin). CBDA was employed as reference standard for the quantification of cannabinoids since its UV maximum adsorption was consistent with that of this class of compounds[171]. The results were illustrated in Figure 5 and expressed as sum of compounds belonging to the same chemical class in terms of μg of compound in 100 mg of matrix.

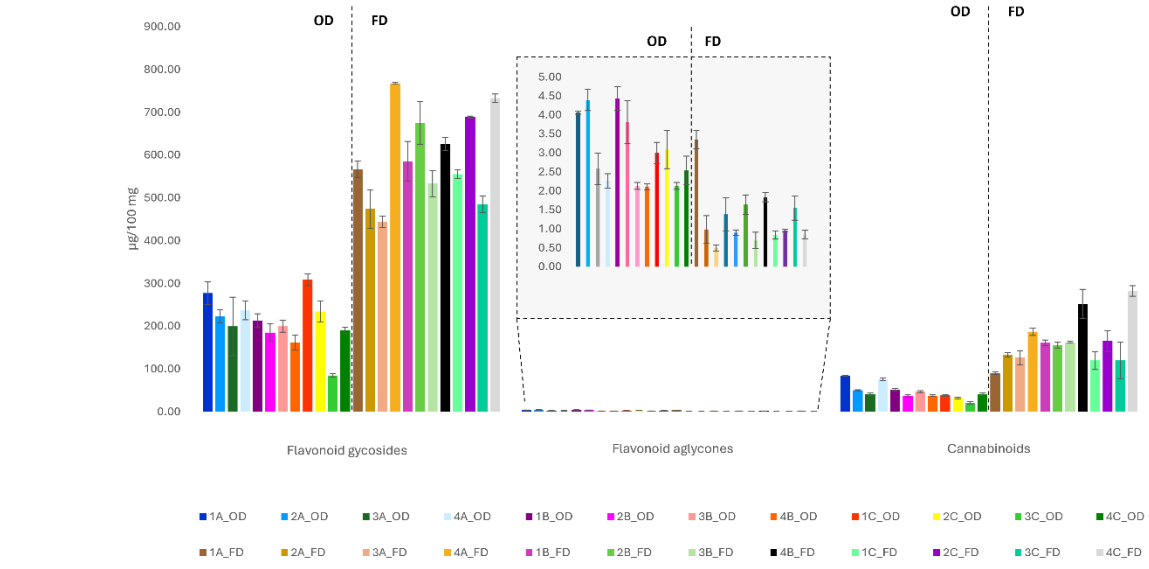

(a)

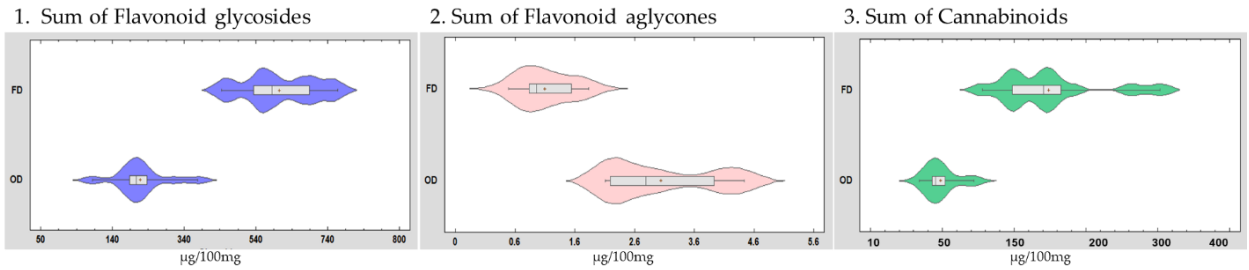

(b)

Figure 5. Representation of the quantification data of hemp methanolic extracts, expressed as µg of compound in 100 mg of sample: (a) Distribution of the target analytes in the samples (sample code: 1-4 growth stage; A-C land plot); (b) Violin plot of quantification results for flavonoid glycosides, aglycones and cannabinoids in the freeze-drying (FD) and oven-drying (OD) samples.

The graphs showed that the cannabinoids amount is lower compared to flavonoids content and only traces (around 2 µg in 100 mg) of flavonoid aglycones could be detected. Moreover, there was a clear difference between the samples lyophilized and dried in the oven. In particular, the cannabinoids in freeze-dried samples were around 0.2% of the total content, in agreement with data reported on hemp stem and leaves[175] (ranging from 0.1 to 2%), while for the oven-dried ones, the percentage decreased to 0.05%. Regarding the flavonoids, the difference was less marked and ranged between 0.2% and 0.6% for oven and freeze-drying, respectively, in accordance with literature[175]. The Violin representation (Figure 5(b)) shows a cluster of freeze-dried samples with a higher content of cannabinoids, which differs from the trend of the other lyophilized matrices. Compared to the previous stages, the samples at the 4th growth stage

presented a higher amount of cannabinoids, being near to the flowering where the synthesis of these phytochemicals increase[195].

3.2.4 Statistical analysis and comparison of the phytochemical profile of the samples under study

The 24 hemp samples under study, were characterized by different growth stages, location of growth land plot and method of drying (4 growth stages × 3 land plots × 2 methods of drying). A multivariate statistical analysis was carried out on quantification data (17 target analytes) to investigate the role of these factors as possible discriminants between the samples. First, unsupervised analyses (hierarchical clustering HC and principal component analysis PCA) were performed to investigate natural groupings existing between the samples. As already mentioned, a clear separation between lyophilized and oven dried samples is reported in the HC with heatmap visualization (Figure 6(a)).

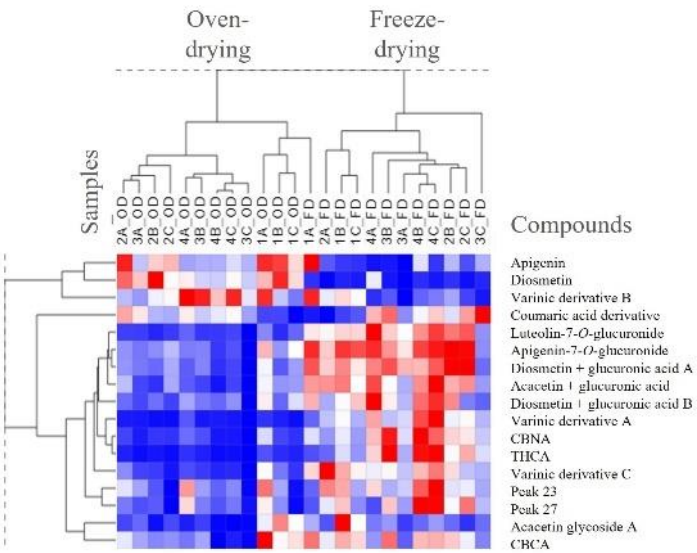

(a)

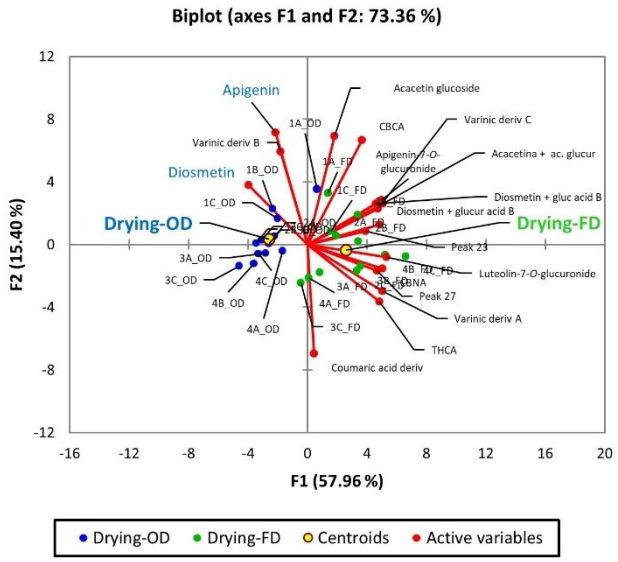

(b)

Figure 6. Main results from multivariate statistical analysis on quantification data: (a) HC based on Pearson distances and heat-map visualization (24 samples × 17 compounds); (b) biplot of the principal component analysis relative to the distribution of the *Cannabis* samples and target compounds according to the method of drying, growth stages and landplot (OD and FD samples are highlighted in blue and green, respectively).

The FD samples were characterized by a higher amount of flavonoid glycosides and cannabinoids which are mainly in the acid form, while the oven dried samples had a major relative content of the corresponding flavonoids aglycones. As demonstrated by Jimenez-Garcia *et al.*[196], freeze-drying seems to be a better drying method to preserve flavonoids compounds, especially in form of glycosides, considering that they may lose the sugar and degrade to the corresponding aglycone if exposed at high temperature (65 °C), for prolonged time. The same susceptibility is reported for cannabinoids in the acid form although the degradation normally occurs at higher

temperature than 65 °C. However, the prolonged time of heating in the oven could have affected their content. Moreover, for some cannabinoids, the degradation reaction is more complex, and it is associated with undetermined side reactions[190]. These data are in agreement with PCA results (Figure 6(b)), represented in the figure as biplot. The observations (samples) are rationally distributed over the Cartesian plane according to the method of drying (visible along the first principal component F1 from right to left). The biplot show the correlation between the distribution of the samples and the compound content, with a higher amount of flavonoids glycosides and cannabinoids in the freeze-dried samples (green color). To eliminate the strong influence of the drying method on the sample clustering, two different PCA analysis were conducted to study the influence of the growth stage and growth land plot on the phytocomplex of the plant, considering as data matrix the oven-dried and freeze-dried samples, separately (data not shown). Interestingly, the growth stage seems to have a lower impact on the contents of the target analytes, for both methods of drying. A recent study[195], reported a variation in the content of cannabinoids and flavonoids before and after flowering, being the inflorescences rich of glandular trichomes which are devoted to the production of specialized metabolites. As mentioned before, this was confirmed for cannabinoids by the slight increase of their content at the 4th growth stages, while for flavonoids not significant differences were highlighted. As expected, the sample clustering was not affected by the location of the plot, being in the same geographical area and characterized by similar growing conditions (data not shown).

Development of a dispersive solid-liquid microextraction method using natural eutectic solvents for a greener extraction of phytochemicals from fiber-type *Cannabis* sp.

This paragraph is reproduced from a published article
(Mastellone *et al.*, Industrial Crops & Products 187, 2022, 115476)

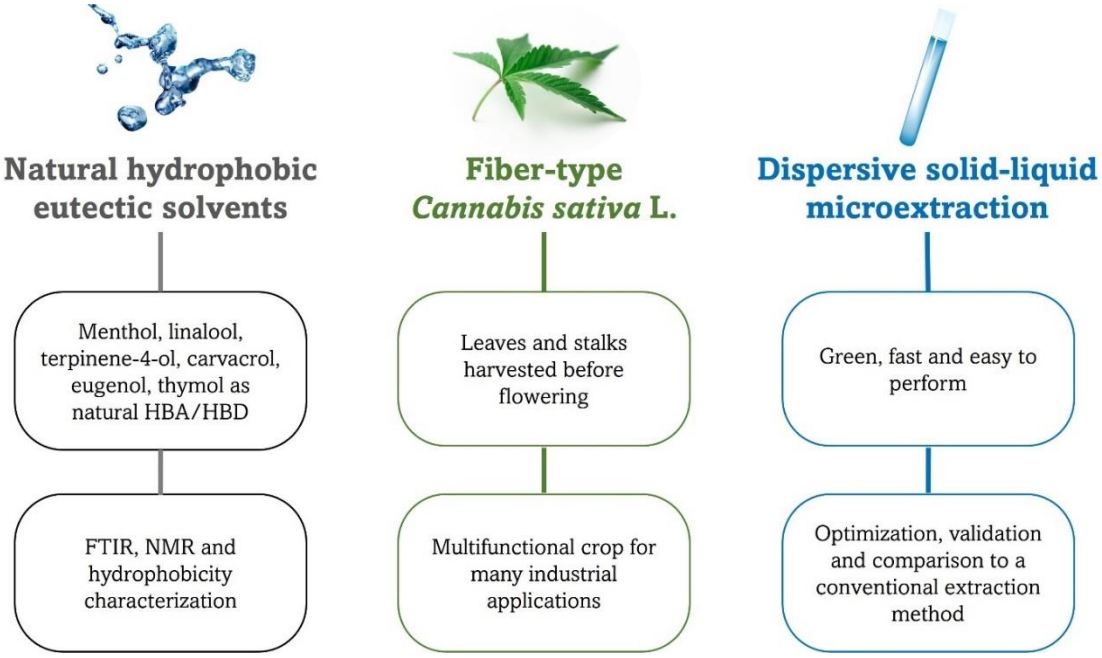

3.3 Development of a dispersive solid-liquid microextraction method using natural eutectic solvents for a greener extraction of phytochemicals from fiber-type *Cannabis* sp.

3.3.1 Preparation of the eutectic solvents

A set of different natural HBA and HBD were tested for the preparation of the ESs and after some preliminary tests, the combination menthol : linalool (1:1) resulted to be the most promising. For this reason, similar compounds were selected as acceptor and donor and the resulting combinations are reported in Table 1. The heat and stirring method was selected because easy and fast to perform.

In order to minimize possible degradations caused by the exposure of the compounds at high temperatures for prolonged time[46], 10 minutes and 40 °C were selected as optimum conditions to obtain homogeneous and stable solvents. After their preparation, the ESs were followed up at frequent intervals to monitor the formation of crystals, signal of instability. All the solvents showed to be stable even up to a month. To prevent evaporation of the components or moisture absorption they were sealed with parafilm and store in a desiccator.

Table 1. List of the ESs prepared in this study.

ID	Component 1	Component 2	Molar ratio	Method of preparation
ML	Menthol	Linalool	1:1	Heat and stirring
MTe	Menthol	Terpinen-4-ol	1:1	Heat and stirring
MTh	Menthol	Thymol	1:1	Heat and stirring
MC	Menthol	Carvacrol	1:1	Heat and stirring
LTe	Linalool	Terpinen-4-ol	1:1	Heat and stirring
LTh	Linalool	Thymol	1:1	Heat and stirring
LC	Linalool	Carvacrol	1:1	Heat and stirring
LE	Linalool	Eugenol	1:1	Heat and stirring
TeTh	Terpinen-4-ol	Thymol	1:1	Heat and stirring
TeC	Terpinen-4-ol	Carvacrol	1:1	Heat and stirring

3.3.2 Optimization of the dispersive solid liquid microextraction method

The combination menthol : linalool (1:1) was selected for preliminary tests and optimization of the extraction method for the analysis of the aerial parts of fiber-type *Cannabis sativa* L. dispersive solid-liquid microextraction (DSLME) method was developed with the aim of avoiding any pre-treatment of the solid sample. In fact, plant matrices, when dispersive liquid-liquid microextraction (DLLME) is applied, usually are previously subjected to liquid-liquid extraction (LLE) with solvent[197]. In this case, water was simply used as co-solvent to promote the dispersion of the ES in the hemp sample. The volume and the pH of water, the sample amount and US time were the parameters considered in the optimization of the extraction method. A screening test was carried out to determine which of these factors significantly affected the extraction performances. A full two-level factorial design (2^n, with n = 4 variables) was used for this preliminary study, which comprises sixteen experiments combining the minimum and maximum values considered for each factor. Moreover, three replicates of the central point (intermediate value for each variable) were carried out, in order to monitor the reproducibility of the method. The volume of water was evaluated in a range to have enough solvent to completely cover the sample and to not exceed the volume of the test tube and therefore the low and high limits were set at 1 and 4 mL, respectively. Regarding the sample amount, a minimum value of 50 mg and a maximum value of 100 mg were set. The limits for the extraction time were selected as 5 and 20 minutes, being common times reported in the literature for plant extraction based on US. Also, the pH of water was taken into account, considering the presence of acid cannabinoids in the hemp sample, as reported in the previous study (Section III.3.2).

With the aim of decreasing the ionization and solubility of these compounds in the water phase, an acid environment (pH = 3) was compared to the neutral condition (pH = 7). Once the experiments were performed, the extraction efficiency was evaluated in term of the sum of the peaks area of the target analytes. The Pareto chart and interactions plot reported in Figure 1a-b showed that none of the variables considered had a significant influence on the extraction of the target analytes.

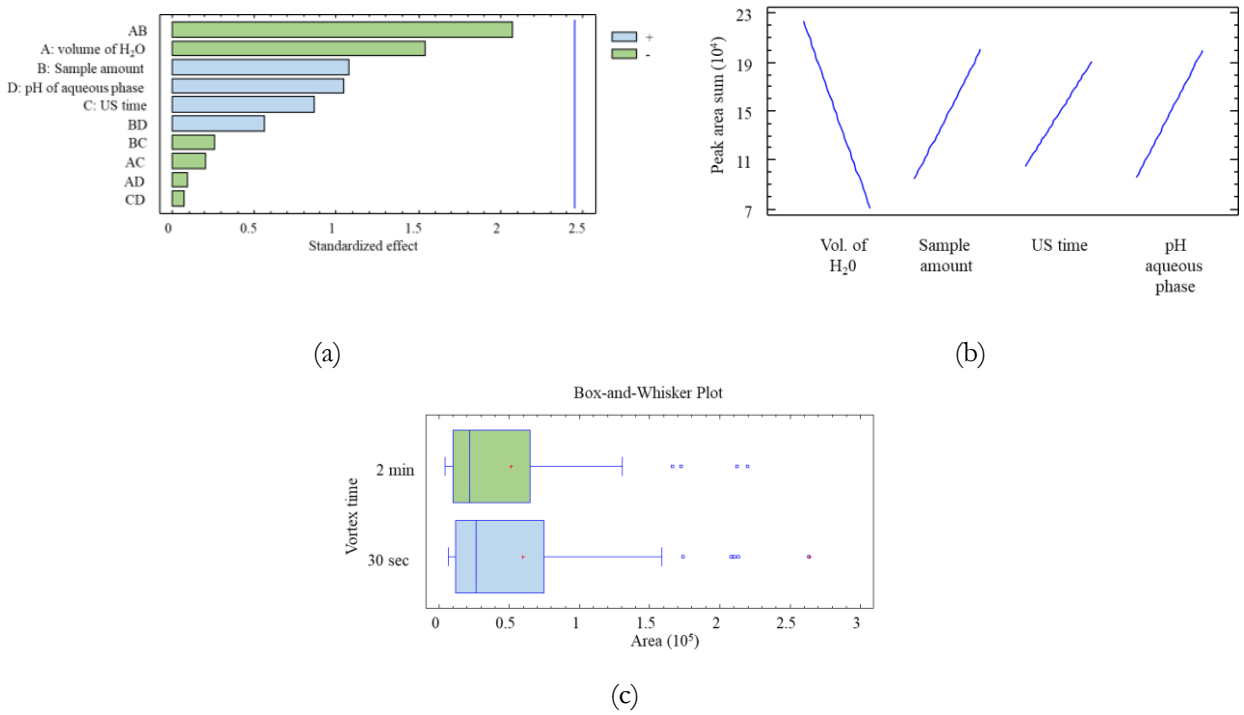

Figure 1. (a) Pareto chart of the 2^n screening study, (b) interactions plot of the 2^n screening study and (c) box-and-Whisker Plot.

For this reason, the optimum conditions were chosen in order to simplify as much as possible the procedure. The volume of water (at a neutral pH) was set at 2 mL to completely cover the sample powder and allow an easy dispersion and separation of the ES. To easily compare the proposed DSLME method with a conventional SLE (Section III.3.2) already reported for the same hemp sample, the same amount of plant (100 mg) was used. Eventually, the US time was set at 10 minutes to reduce the time of analysis but also allow the cell disruption and the release of the target analytes.

In addition, the effect of vortex time was considered in the optimization study, being the fundamental step to disperse the ES in the sample. A minimum time of 30 seconds and a maximum of 2 minutes were tested, taking into account for the higher value, the operator's health. In this case, an analysis of variance (ANOVA) test was carried out and no significance difference (F-ratio 0.28, P-value 0.60) in term of the sum of the peaks area of the target analytes was found between the two conditions and therefore 30 seconds was chosen as optimum time. In Figure 1c, the results are shown graphically in the Box-and-Whisker plot.

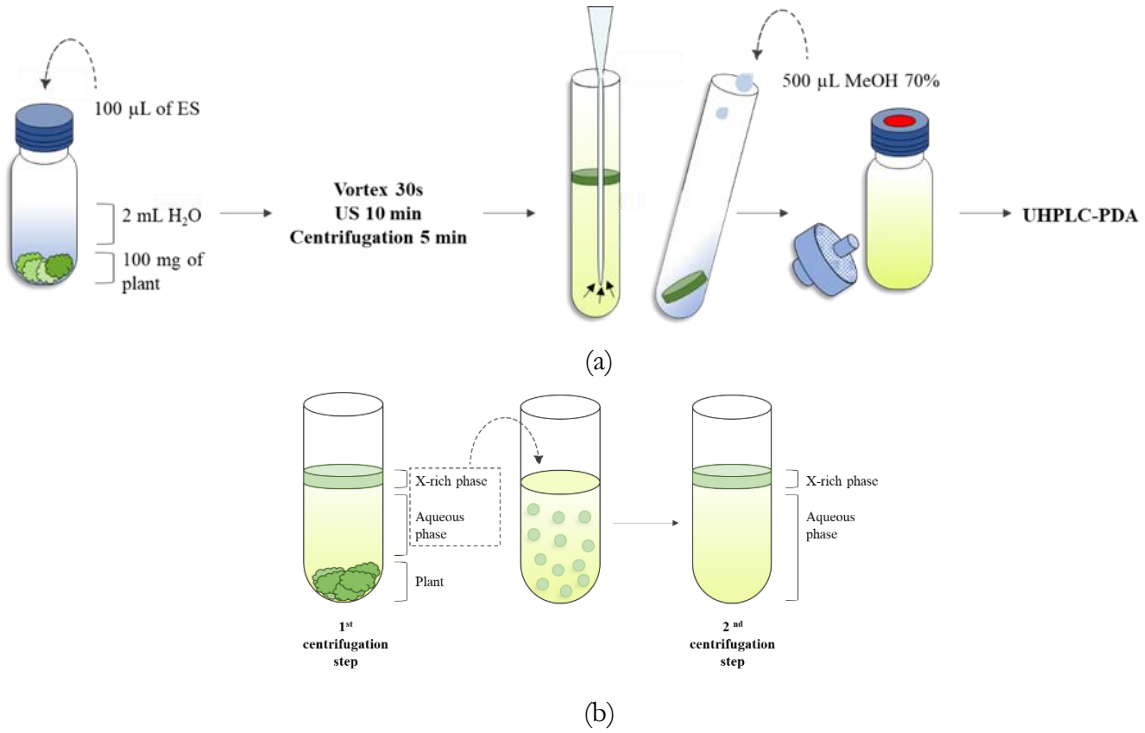

Figure 2. (a) Optimized DSLME method and (b) focus on centrifugation step.

The optimum conditions (Figure 2a) were compared versus the same procedure without the US and the vortex steps to investigate the contribution of each step of the method to the extraction of the compounds of interest. Moreover, one extraction was performed by adding the ES after the US step. As reported in Figure 3, the best results were obtained with the optimized method, for all the compounds. This suggested that (1) as already reported for solid plant sample, US was fundamental to break the cell walls with the consequent release of the target analytes[198]; (2) the vortex step helped to form a fine droplet of the ES in the sample, thus increasing the area of contact between the analytes and the extraction solvent; (3) the ES did not only pre-concentrate the analytes but also helped their extraction during the US step. In fact, as reported for ionic liquids[199,200], also DESs seem to be able to interact with the hydroxylic groups of cellulose, one of the main components of the plant cell wall. This interaction helps the disruption of the hydrogen bonding between the polymers thus favoring the releasing of the metabolites from the cells[201].

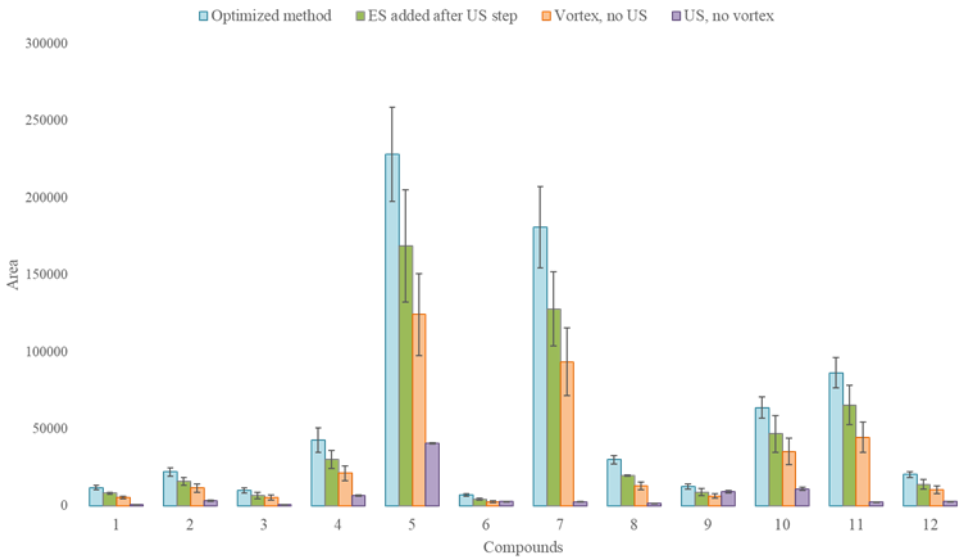

Figure 3. Comparison of the extraction performances (in term of peaks area) between the optimized DSLME method (blue), the addition of the ES after US step (green), the extraction without the US step (red) and without the vortex step (violet). For peaks identification, see Figure 5.

Before the injection in the LC system, the analytes in the ES-rich phase were diluted in a small amount (500 μL) of MeOH H_2O (70/30, v/v). Also, the percentage of water in the hydroalcoholic diluting solution was optimized to make the final solution compatible with the chromatographic initial solvent composition and to avoid the interference of chlorophylls in the final extract.

3.3.3 Preliminary screening using different natural eutectic solvent and comparison with the conventional SLE method

Once the DSLME method was optimized, all the prepared solvents (Table 1) were tested as extraction media to analyse the phytocomplex of the aerial parts of fiber-type *Cannabis sativa* L. Each extraction was performed in triplicate and the results expressed as the mean area together with the standard deviation (SD). The results are reported in Figure 4.

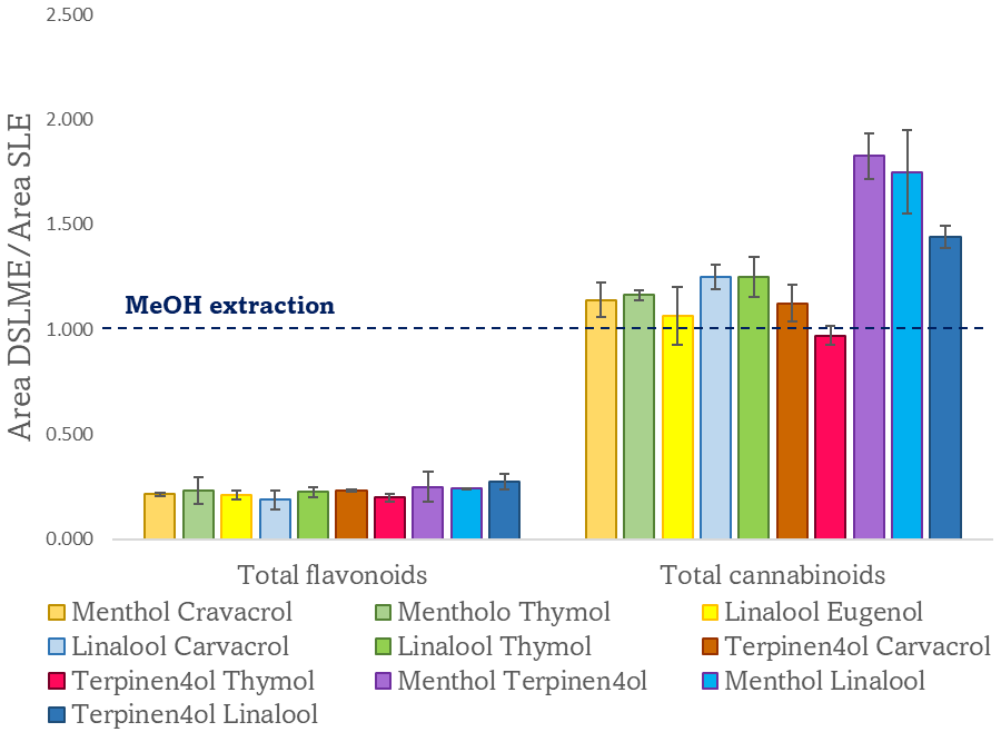

Figure 4. Comparison of the extraction performances (in term of peaks area) between the conventional SLE and the proposed DSLME, for flavonoids and acid cannabinoids. The blue line represents the results obtained with the MeOH-based SLE method.

The chromatogram in Figure 5 showed that the main class of compounds present in the sample were flavonoids glycosides and the more apolar acid cannabinoids. The profile of ML as pure solvent presented some peaks at the wavelength of interest, however they did not interfere with the target analytes.

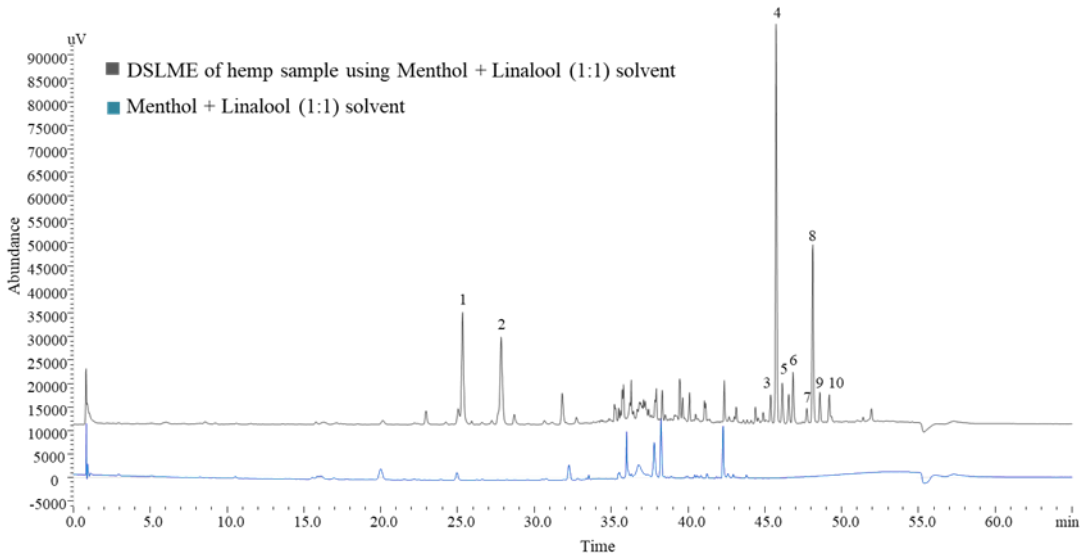

Figure 5. Chromatographic profile at 270 nm of the hemp extract after DSLME with ML and of the ML as pure solvent. Peaks identification: (1) luteolin-7-*O*-glucuronide, (2) apigenin-7-*O*-glucuronide, (3) cannabinoid A, (4)

varinic acid derivative A, (5) varinic acid derivative B, (6) varinic acid derivative C, (7) cannabinolic acid, (8) Δ9-tetrahydrocannabinolic acid, (9) cannabinoid B (10) cannabichromenic acid. For more details on identification data see Section III.3.2.

The SLE with MeOH as extraction solvent was more effective, compared to the ES, in the extraction of flavonoids which are more polar, while an opposite behavior could be observed for the acid cannabinoids. This can be explained by the hydrophobic characteristics of the ES which resulted in a higher interaction with the less polar cannabinoids. This is particularly true for three combinations: ML, MTe and LTe. In general, the presence of aromatic groups in the structure of one of the components (thymol, carvacrol, eugenol) did not seem to help the extraction. In fact, as reported in Table 3, the compounds forming the three ESs (ML, MTe and LTe) with the best extraction performances, do not present aromatic rings in their structure.

Table 3. Molecular weight and chemical structure of the compounds used to prepare the ESs.

Compound	Molecular weight (g mol^{-1})	Chemical structure
Carvacrol	150.22	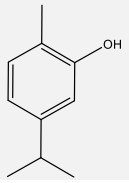
Eugenol	164.20	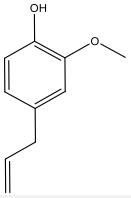
(±)-Linalool	154.25	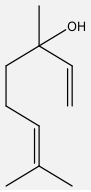
(-)-Menthol	156.27	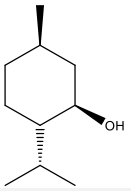
(-)-Terpinen-4-ol	154.25	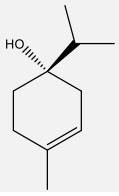
Thymol	150.22	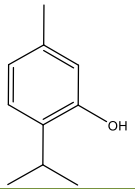

Apart from the differences in the extraction efficiency of both methods, it is important to also consider the sustainability of the two approaches. The SLE required the use of a larger volume of methanol (15 mL), long evaporation time to concentrate the final extract and a purification step with SPE to eliminate chlorophylls prior to injection in the HPLC. The proposed DSLME is faster, comprises fewer steps and the use of a small volume (100 µL) of a greener solvent, thus being less tedious and easy to perform. Eventually, it could be a greener alternative for a selective and good enrichment of acid cannabinoids, without the need of evaporating the solvent by using nitrogen or energy.

3.3.4 Characterization of the eutectic mixture

The three solvents that showed the best extraction performances were subjected to a deeper characterization through FTIR, NMR and hydrophobicity measurement.

FTIR analysis

ML, MTe and LTe were characterized by FTIR spectroscopy to monitor the correct formation of hydrogen bonding between the two components. In particular, the IR spectra of the single components were compared with that of the solvent, to monitor the shift of the band corresponding to the hydroxylic group.

Figure 6 shows the representative FTIR spectra of the three solvents and their components. Regarding the single compounds, the menthol spectra showed the representative band of the hydroxyl group at 3248 cm^{-1}, linalool at 3381 cm^{-1} and terpinen-4-ol at 3463 cm^{-1}. For ML, when the solvent is formed, the band of the hydroxyl group of menthol shifts to a higher wavenumber than that of pure menthol and is slightly different from that of linalool. In the fingerprinting region (between 1500 and 600 cm^{-1}) a difference between the spectra of linalool and the solvent (e.g. 1000 cm^{-1}) can also be observed, suggesting the formation of new interactions. A similar behavior was observed with MTe, where menthol represents the acceptor of the hydrogen bonding, while a smaller shift of the hydroxylic band is reported for LTe.

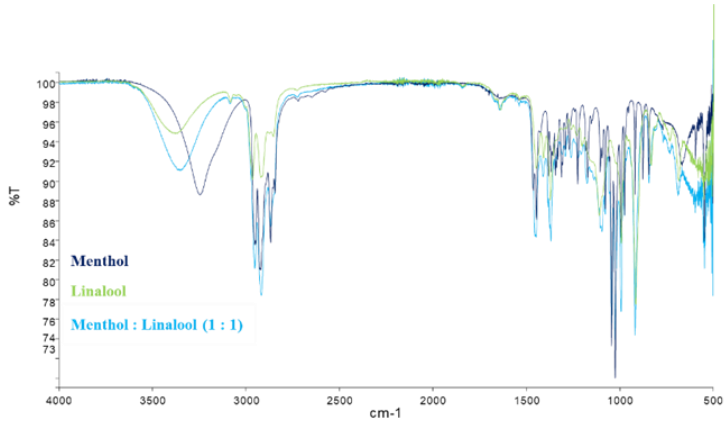

(a)

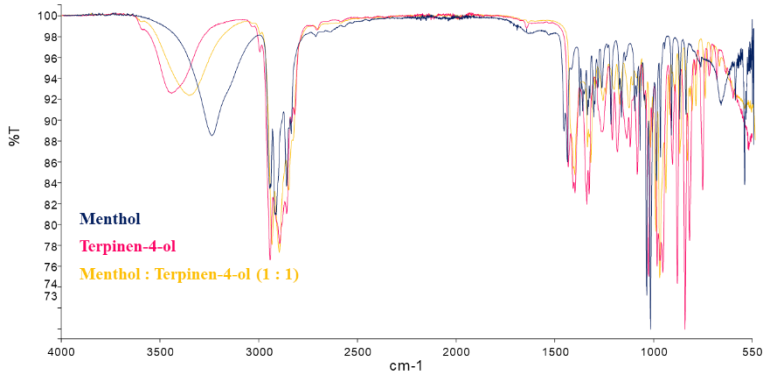

(b)

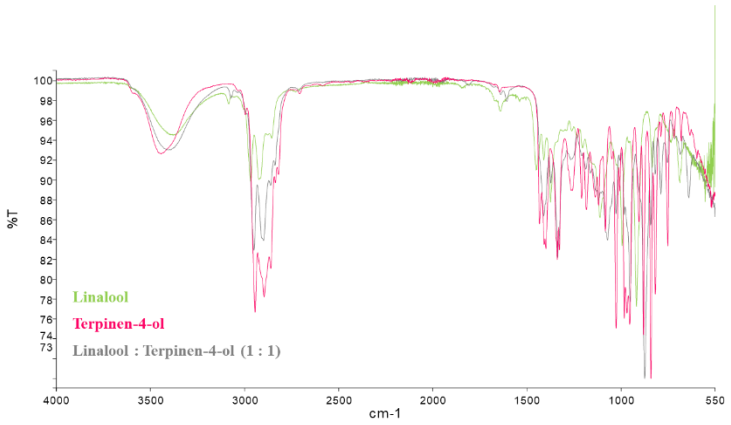

(c)

Figure 6. FTIR spectra of (a) menthol, linalool and ML, (b) menthol, terpinene-4-ol and MTe and (c) linalool, terpinene-4-ol and LTe.

The stability of the ES during the extraction process was then investigated by comparing the FTIR spectra before and after performing the DSLME. This investigation was fundamental to understand whether the ES was responsible of the extraction and not only one of the components since, as reported by Cao *et al.*[202], the presence of water could break the hydrogen bonding of ESs, compromising their structure. Adopting the optimized method, the extraction was simulated without the plant and the ES-rich phase isolated and submitted to FTIR analysis. As reported in Figure 7, the profile of ML (used as reference during the optimization) before and after the extraction were comparable, confirming that the interaction and enrichment of the target analytes was due to the ES.

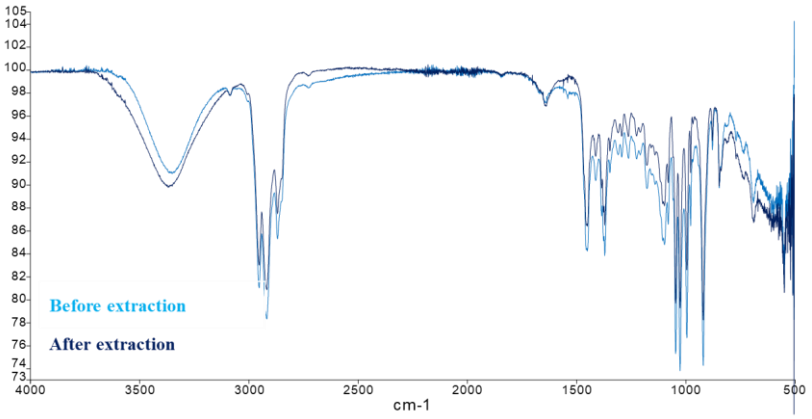

Figure 7. FTIR spectra of ML as pure solvent and after the DSLME process.

NMR analysis

The formation of the ES and the molar ratio between the HBA and HBD was also verified by ^{1}H NMR. A mixture of the ES and water (in the same amount) was prepared, and the water layer was also analyzed by ^{1}H NMR. All spectra are reported in the Figure 8. Recently, some concerns about the hydrophobicity of hydrophobic deep eutectic solvents (HES) arose in the scientific community[202]. In fact, it was demonstrated that in some cases, only one of the components of the solvent is hydrophobic and the other partly solubilizes when the ES is put in contact with water. The NMR spectra of the water layer clearly showed that both the components of the ES tested are characterized by a low solubility in water. These results were also supported by the water content percentage, measured by Karl Fischer Titration (see the following paragraph).

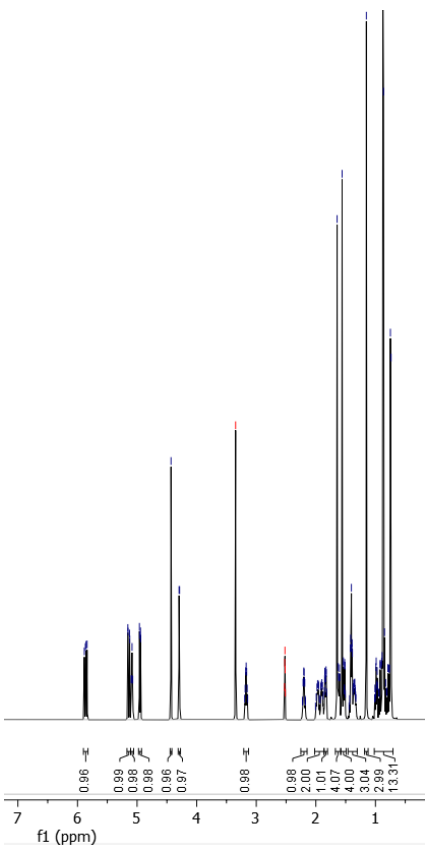
0.96
0.99
0.98
0.98
0.96
0.97
0.98
0.98
2.00
1.01
4.07
4.00
3.04
2.99
13.31
7 6 5 4 3 2 1
f1 (ppm)

1(a)

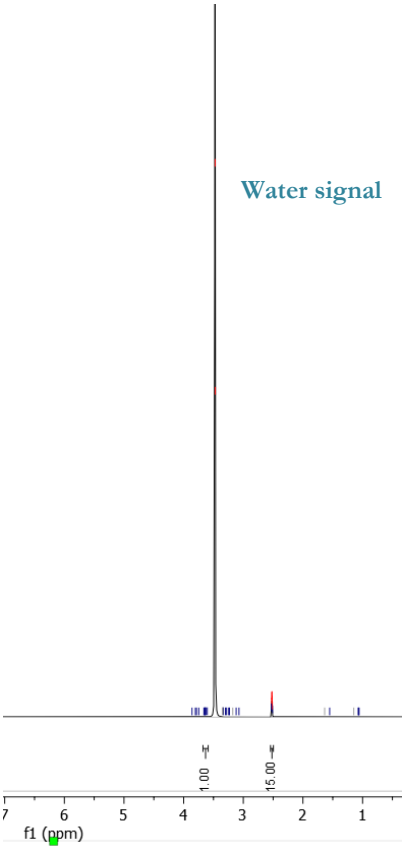
Water signal
1.00
15.00
7 6 5 4 3 2 1
f1 (ppm)

1(b)

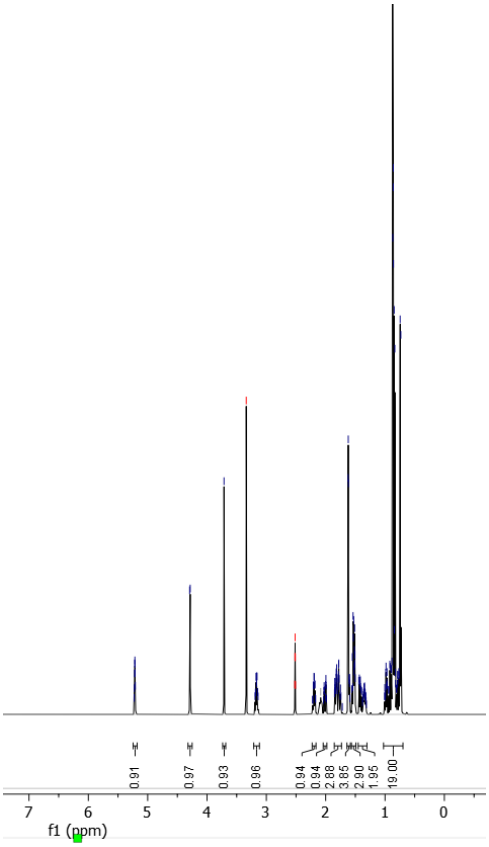
0.91
0.97
0.93
0.96
0.94
0.94
2.88
3.85
2.90
1.95
19.00
7 6 5 4 3 2 1 0
f1 (ppm)

2(a)

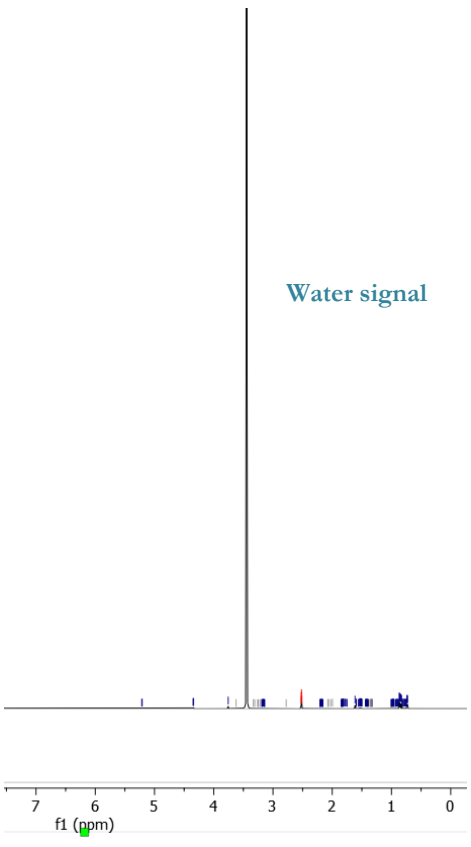
Water signal
7 6 5 4 3 2 1 0
f1 (ppm)

2(b)

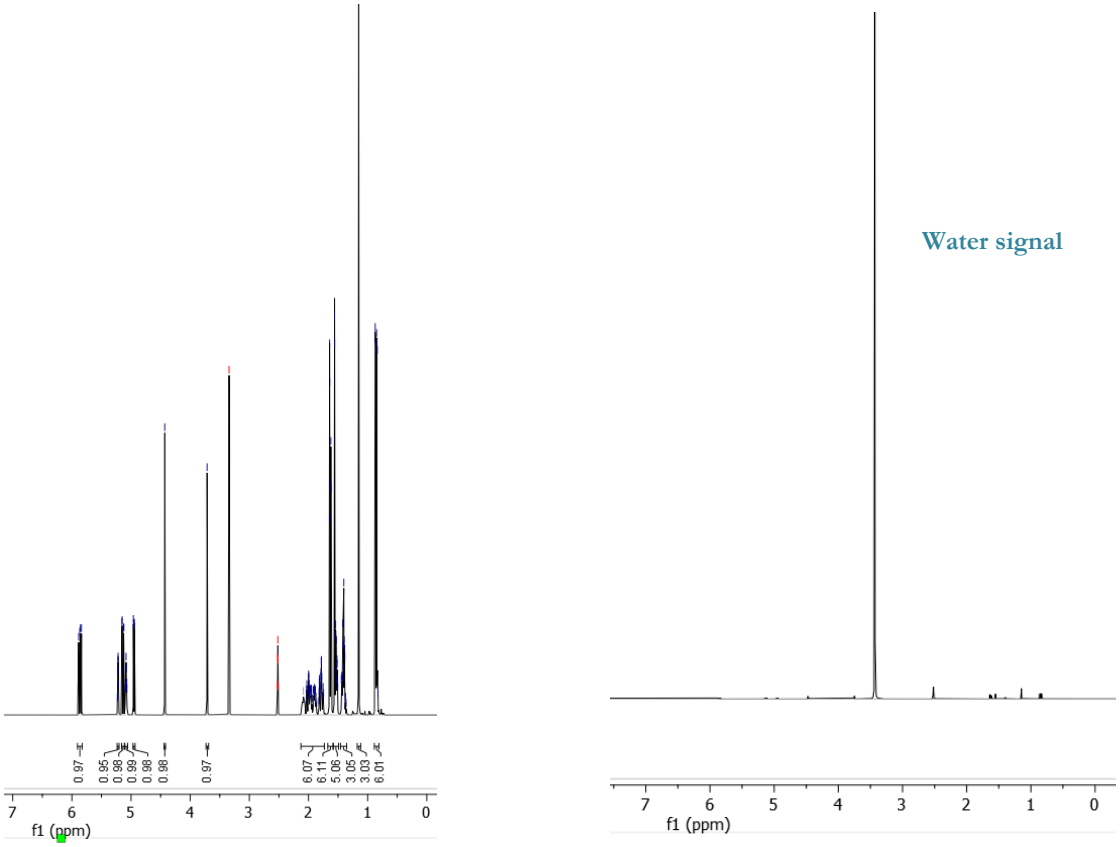

3(a) 3(b)

Figure 8. ^{1}H NMR spectra of 1(a) ML and 1(b) its water layer, 2(a) MTe and 2(b) its water layer and 3(a) LTe and 3(b) its water layer.
ML: 1H NMR (600 MHz, DMSO) δ 5.86 (dd, J = 17.3, 10.7 Hz, 1H), 5.14 (dd, J = 17.4, 2.0 Hz, 1H), 5.08 (t, J = 6.7 Hz, 1H), 4.95 (dd, J = 10.8, 2.0 Hz, 1H), 4.43 (s, 1H), 4.29 (d, J = 5.6 Hz, 1H), 3.17 (tt, J = 10.2, 4.9 Hz, 1H), 2.20 (pd, J = 7.0, 2.6 Hz, 1H), 2.02 – 1.80 (m, 3H), 1.68 – 1.59 (m, 4H), 1.59 – 1.48 (m, 4H), 1.46 – 1.31 (m, 3H), 1.15 (s, 3H), 1.02 – 0.72 (m, 13H).
MTe: 1H NMR (600 MHz, DMSO) δ 5.21 (ddt, J = 4.4, 3.0, 1.6 Hz, 1H), 4.29 (d, J = 5.6 Hz, 1H), 3.71 (s, 1H), 3.16 (tdd, J = 10.1, 5.6, 4.2 Hz, 1H), 2.19 (hd, J = 7.0, 2.7 Hz, 1H), 2.01 (dp, J = 17.6, 2.6 Hz, 1H), 1.87 – 1.70 (m, 3H), 1.65 – 1.59 (m, 4H), 1.59 – 1.49 (m, 3H), 1.46 – 1.37 (m, 1H), 1.37 – 1.29 (m, 1H), 0.99 – 0.71 (m, 20H).
LTe: 1H NMR (600 MHz, DMSO) δ 5.86 (dd, J = 17.3, 10.7 Hz, 1H), 5.22 (tp, J = 3.1, 1.4 Hz, 1H), 5.14 (dd, J = 17.3, 2.0 Hz, 1H), 5.08 (tp, J = 7.2, 1.4 Hz, 1H), 4.95 (dd, J = 10.7, 2.0 Hz, 1H), 4.43 (s, 1H), 3.71 (s, 1H), 2.13 – 1.73 (m, 6H), 1.67 – 1.59 (m, 6H), 1.58 – 1.48 (m, 5H), 1.46 – 1.34 (m, 3H), 1.15 (s, 3H), 0.85 (dd, J = 14.0, 6.9 Hz, 6H).

Karl Fischer titration

As report by Florindo and colleagues[203], the hydrophobicity of the ES can be evaluated by measuring their solubility in water. Karl Fischer titration is a well-established method to determine trace amounts of water in samples. In literature, the initial water contents of HESs after preparation are in the range between 0.004 and 0.8 weight (wt) %, while, when mixed with water, they vary from 0.523 to 6.938 wt% in HESs. In order to test the hydrophobicity of our solvents, the water content was measured before and after mixing the ES with the same amount

of water. As reported in Table 4, all the ES tested in this study were within the accepted values for conventional HESs.

Table 4. % of water in selected ES, measured by Karl Fischer titration.

ES component 1	ES component 2	H_2O content before partitioning	H_2O content after partitioning
Menthol	Linalool	0.044%±0.005	0.671%±0.005
Menthol	Terpinen-4-ol	0.079%±0.002	0.270%±0.013
Linalool	Terpinen-4-ol	0.105%±0.008	0.674%±0.027

3.3.5 Validation of the proposed method

The combination menthol : linalool (1:1) was selected as reference extraction solvent for the validation of the proposed DSLME method for the extraction of the non-volatile compounds from hemp aerial parts. The presence of a solid matrix adds more challenges in the validation and quantification of the target analytes, compared to a liquid sample. In fact, the analytes are subjected to different partitions: plant-aqueous phase and aqueous phase-ES. To study the behavior of the analytes in a simpler system, some preliminary tests were carried out with the commercial standard of luteolin 7-*O*-glucuronide, apigenin 7-*O*-glucuronide and CBDA, by performing the extraction without the plant. This latter was used as the reference standard for all the acid cannabinoids due to the similar physicochemical features. In agreement with the previous results, CBDA was successfully extracted in the ES-rich phase, while the two flavonoids were poorly recovered (Figure 9). The selectivity of the method for this class of compounds was therefore confirmed and the validation study was focused on the acid cannabinoids.

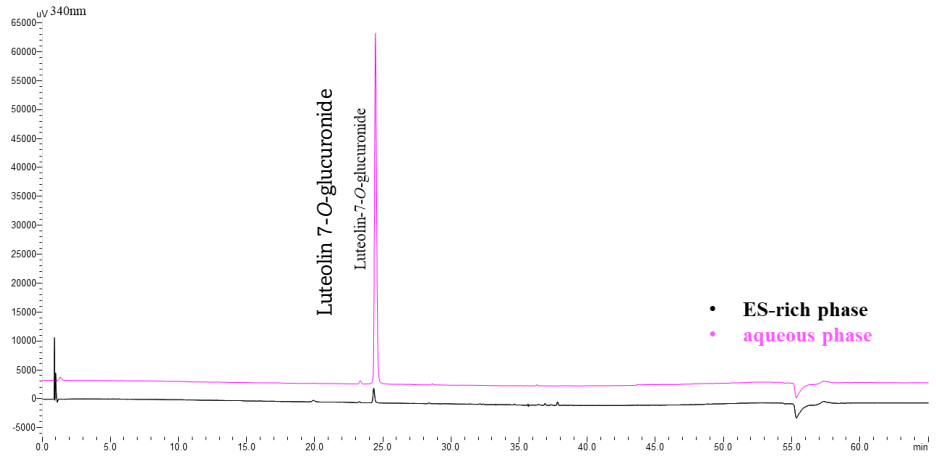

(a)

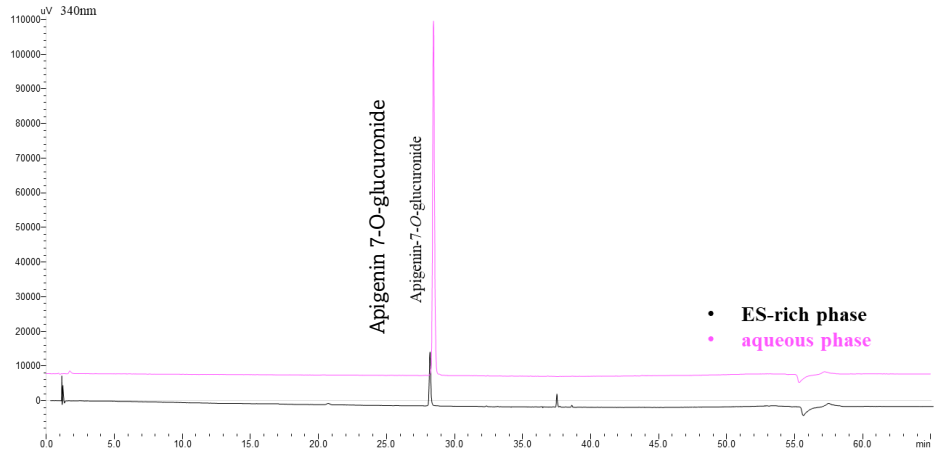

(b)

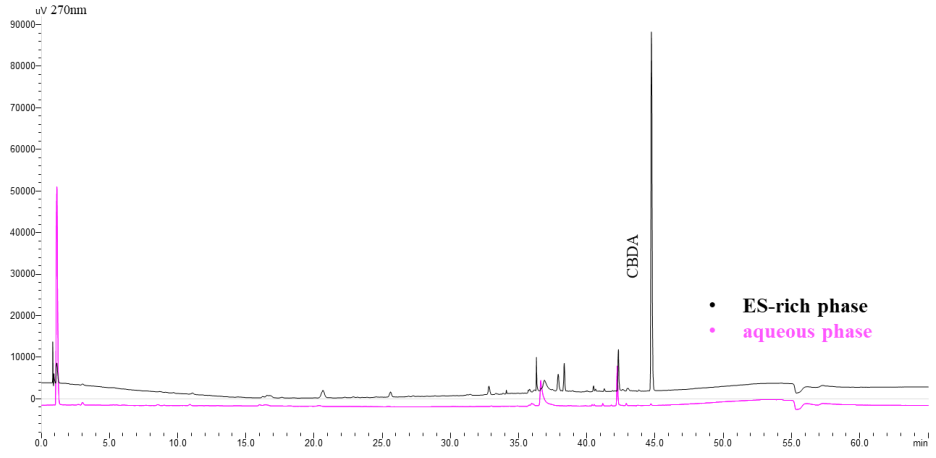

(c)

Figure 9. Comparison of the chromatographic profile of (a) luteolin 7-*O*-glucuronide, (b) apigenin 7-*O*-glucuronide and (c) CBDA in the ES-rich phase versus the aqueous layer, after performing the DSLME.

Table 5 reports several quality analytical figures of merit of the method, including the λ selected for quantification, the linearity range, the calibration sensitivity (evaluated as the calibration slope), determination coefficient (R^2), limit of detection (LOD) and limit of

quantification (LOD) of CBDA. In order to evaluate a possible carry over effect for the analytes between consecutive analysis, a blank sample (MeOH 70%) was injected occasionally and randomly, confirming the absence of residual peaks for all the analytes of interests. The LODs were experimentally determined by decreasing the concentration of the analyte in the extraction phase until a signal-to-noise ratio (S/N) of 3 was obtained. The LOQs were estimated as S/N of 10 and experimentally verified by injecting the standard compound at the predicted concentration. The LOD and LOQ values were 0.20 mg L^{-1} and 0.25 mg L^{-1}, respectively.

Table 5. Figure of merits of the UHPLC-UV method for CBDA.

Compound	Λ max nm)	Linearity range (mg L^{-1})	Slope ± SD	$S_{y/x}$	R^2	LOD (mg L^{-1})	LOQ (mg L^{-1})
CBDA	270	0.5 - 50	13592 ± 44	0.89	0.999	0.20	0.25

Studies on intra-day repeatability, intermediate precision and enrichment factor were carried out to prove the improvement and applicability of the proposed method in the analysis of acid cannabinoids in real hemp samples. The quantification data obtained from the previous study (after assuring an exhaustive extraction of the compounds from the sample) (see Section III.3.2) were used as a reference value to calculate the enrichment of the analytes from the plant. As reported in Table 6, the RSD values (intra and inter-day) for all the compounds are lower than 15%, showing a good reproducibility of the method. The enrichment factor (EF) of the proposed method was compared to the one obtained by performing the MeOH extraction, followed by evaporation of the solvent to concentrate the extract. The proposed DSLME with ES allowed to obtain comparable EF to the ones of SLE with MeOH. It is however important to highlight that in the conventional approach the extraction was repeated three times on the same matrix and the pre-concentration of the extract required the evaporation of the solvent with consumption of toxic organic solvents, nitrogen and energy for the rotary evaporator.

Table 6. Quantification data for cannabinoids, expressed as μg g-1 of hemp (±SD), precision data and enrichment factor for DSLME and the reference SLE.

Compound	μg g^{-1} of plant found with DSLME	Precision (*n*=3)		EF	
		Intra-day RSD %	Inter-day RSD %	DSLME	SLE[a]
Cannabinoid A	27.5 ± 3.0	9.2	4.9	5	7
Varinic acid A	245.8 ± 35.2	12.0	4.1	4	6
Varinic acid B	21.3 ± 2.1	8.1	1.2	8	7
Varinic acid C	43.3 ± 5.0	10.2	4.2	5	7
CBNA	18.5 ± 1.7	8.0	3.4	6	6
THCA	119.4 ± 17.0	11.7	2.8	4	5
Cannabinoid B	25.5 ± 2.6	10.4	3.9	6	6
CBCA	27.0 ± 3.4	12.0	1.9	5	5

[a]quantitation data obtained with an exhaustive SLE[204]

The main features of the proposed extraction method were compared to similar applications for the extraction of non-volatile phytochemicals from *Cannabis sativa* L. plant, reported in literature in recent years. Most of the studies focused on similar approaches, using US-assisted extraction or maceration in organic solvents, such as methanol, ethanol and acetone[175,179,205]. More innovative methodologies are employed for the analysis of cannabinoids in non-plant origin samples, for forensic and clinical applications[206–209] (e.g blood, hair, oral fluid, urine). As reported in Table 7, the DSLME developed in the present study, demonstrates to meet the requirements in terms of novelty, sustainability, and reliability of the results.

Table 7. Main features of representative extraction methods from *Cannabis sativa* L. samples, for the analysis of phytochemicals by liquid chromatography.

Sample	Target analytes	Pre-treatment of the sample	Type of solvent	Volume of solvent	Extraction time	Analytical platform	LOQ	Ref.
Reference studies								
Leaves, stem	Flavonoids, cannabinoids	SLE[a]	MeOH and acetone	15 mL	30 min, US[b]	UHPLC-PDA/MS	nr[c]	204
Inflorescences	Flavonoids, cannabinoids, terpenoids	SLE	EtOH 70%	5 mL	30 min, US	UPLC-MS	nr	205
Inflorescences, leaves, stem bark, and roots	Flavonoids (1) cannabinoids (2)	SLE	EtOH, water, HCl 25:10:4, MeOH (1) MeOH (2)	5 mL, 50 mL (1) 20 mL (2)	135 min, water bath (2),20 min, US (2)	HPLC-PDA/MS	nr	210
Inflorescences	Flavonoids (1), cannabinoids (2)	SLE	*n*-Hexane, acetone (1) EtOH (2)	25 mL, 25 mL (1) 25 mL (2)	45 min (1) 45 min (2)	HPLC-PDA/MS	1.3-2.5 mg L^{-1}	179
This work								
Leaves, stem	Flavonoids, cannabinoids	DSLME	Hydrophobic ES	100 µL	10 minutes, US	UHPLC-PDA	0.25 mg L^{-1}	This work

[a] Solid liquid extraction
[b] Ultrasound
[c] Not reported

New class of tunable choline bromide-based hydrophobic deep eutectic solvents for the extraction of bioactive compounds of varying polarity from a plant matrix

This paragraph is reproduced from a published article
(Mastellone *et al.*, ACS Sustainable Chem. Eng., 2023, 11, 6665−6675)

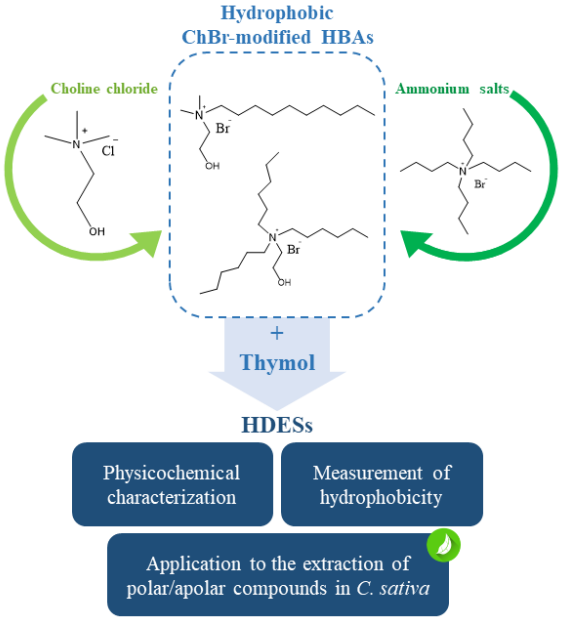

3.4 New class of tunable choline bromide-based hydrophobic deep eutectic solvents for the extraction of bioactive compounds of varying polarity from a plant matrix

Choline chloride([Ch^+][Cl^-])-based DESs were among the first eutectic mixtures reported by Abbott *et al.* in 2003[211].They are the most studied types of DESs due to their relative biodegradability and the low toxicity of [Ch^+][Cl^-]. Moreover, [Ch^+][Cl^-] can form DESs with a wider variety of HBDs, contrary to other tetraalkylammonium salts. The chemical structure of [Ch^+][Cl^-] features a hydroxyl group on one of the alkyl chain substituents, which is not present in the structure of other tetraalkylammonium salts. Migliorati *et al.*[212] compared through molecular dynamics simulations the arrangement of the hydrogen bonding network when [Ch^+][Cl^-] and butyltrimethylammonium chloride are mixed with urea at a 1:2 molar ratio. The unique three-dimensional structure of these DESs affects the melting point depression, which is larger for [Ch^+][Cl^-]-based DES due to more favorable interactions. However, the hydrophilic nature of [Ch^+][Cl^-] makes it a less favorable candidate for HDES preparation. A number of less hydrophilic salts are commercially available and have been used to prepare HDESs, such as tetrabutylammonium bromide / chloride, tetraoctyl ammoniumbromide / chloride, and ethyltrioctyl ammonium bromide/chloride. Contrary to [Ch^+][Cl^-], these alkylammonium salts do not feature the hydroxyl group on one of the alkyl chain substituents which, as mentioned above, is important for the formation of the hydrogen bonding network. The main goal of this study was to obtain a novel class of hydrophobic compounds to be used in the preparation of HESs. The chemical structure design of these new compounds was guided according to the following features: (i) low solubility in water and (ii) capacity to form a hydrogen bonding network. The structure of choline was employed as a model, and the length of alkyl chain substituents appended to the ammonium head group was increased to improve the hydrophobicity and broaden the range of application of the new compounds. Contrary to other commercial ammonium salts, the hydroxyl functional group feature of choline was maintained, thus improving the capacity of the new compounds to form hydrogen bonding.

3.4.1 Synthesis of [Ch$^+$][Br$^-$]-modified salts

The aim of the first part of this study was to synthesize hydrophobic HBAs featuring similar chemical structure to [Ch$^+$][Cl$^-$] through modification of its chemical structure. To obtain compounds with higher hydrophobicity, this study focused on the synthesis of choline derivatives with longer alkyl chain substituents, while also maintaining the hydroxyl functional group. During preliminary tests, [Ch$^+$][Br$^-$] derivatives were found to be faster to synthesize and with a higher yield than the corresponding chlorine salts. Moreover, the bromide salts exhibited lower solubility in water (data not shown). Figure 1 shows the chemical structures of the three groups of salts prepared in this study. For synthesis of groups A and B, two different approaches were employed. Route (A) involved reaction of 2-dimethylaminoethanol and alkyl bromide to form surfactant-like salts featuring a more polar head and long alkyl chain substituents (Figure 1A) or route (B) where the amine and bromoethanol were reacted to form "bulky salts", characterized by three carbon chain substituents of equal length as substituents of the ammonium group (Figure 1B). Tetrabutylammonium bromide and tetraoctylammonium bromide (Figure 1C) were chosen as representative commercial salts to compare their physicochemical properties with those of the synthesized [Ch$^+$][Br$^-$] derivative. The NMR spectra for all synthesized compounds are provided in the Appendix of this Thesis.

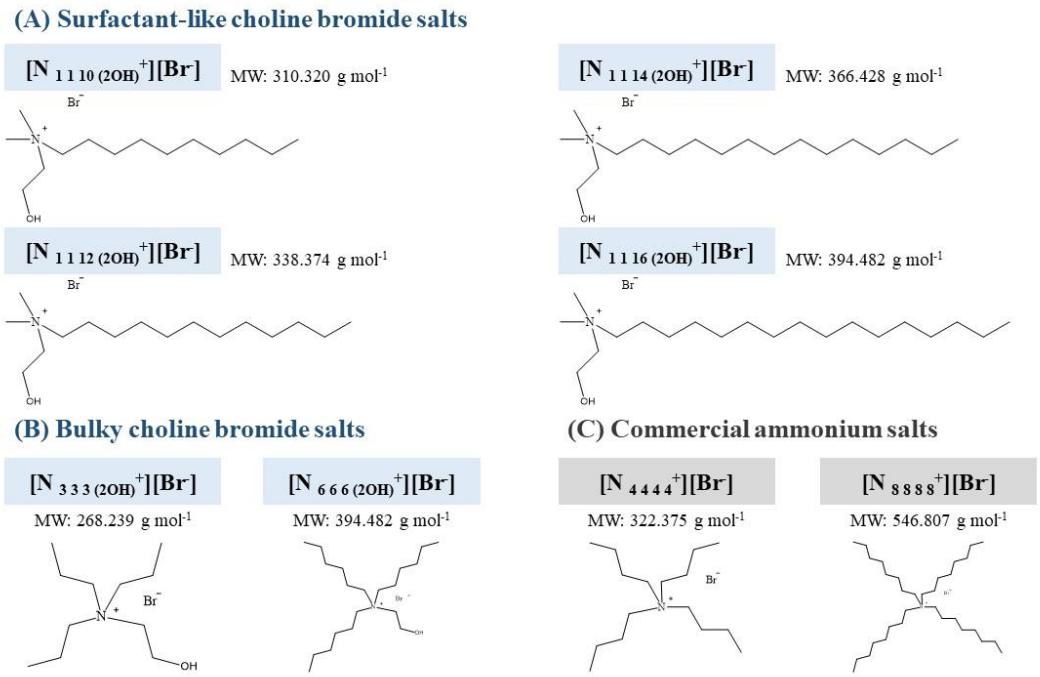

Figure 1. Chemical structures and molecular weight of the salts used in this study, where groups (A) and (B) were obtained by chemical synthesis and group (C) was used for comparison purposes.

3.4.2 Choice of the most suitable HBD for the preparation of [Ch$^+$][Br$^-$]-based HES

After synthesizing HBAs, they were used in the preparation of HESs. According to previous reports,[202,213,214] several examples of alcohols, carboxylic acids and natural phenolics and terpenoids have been employed as HBDs owing to their capability of interacting via hydrogen bonding. To reduce the number of candidates for testing, the main criteria used in choosing the HBD for combining with the synthesized [Ch$^+$][Br$^-$]-modified salts included the overall hydrophobicity, capability of forming a liquid HES at room temperature, and cost. Moreover, compounds of natural origin enhance the greenness of the solvent. Ten compounds were tested as HBDs with different HBA/HBD ratios (see Table 1). Thymol was able to easily form liquids with all six [Ch$^+$][Br$^-$]-modified salts at a molar ratio of 1:2 and was therefore selected for subsequent studies.

Table 1. Combinations and molar ratio of [Ch^+][Br^-]-modified salts and HBDs tested to form HESs. In green, ESs liquid at RT, in yellow the one liquid at 40-50 °C and in orange the one that did not form.

HBD / HBA	Octanoic acid	Decanoic acid	Dodecanoic acid	Eugenol	Linoleic acid	(±) Menthol	Phenylpropanoic acid	Phenylacetic acid	(-)-Terpinen-4-ol	Thymol
[$N_{3\,3\,3\,(2OH)}^+$][Br^-]	1:4			1:2	1:4					1:2
[$N_{6\,6\,6\,(2OH)}^+$][Br^-]	1:4	1:2	1:2	1:2	1:2		1:3		1:2	1:2
[$N_{1\,1\,10\,(2OH)}^+$][Br^-]	1:3			1:3	1:2		1:2	1:2	1:2	1:2
[$N_{1\,1\,12\,(2OH)}^+$][Br^-]	1:3			1:3	1:3		1:2	1:2	1:4	1:2
[$N_{1\,1\,14\,(2OH)}^+$][Br^-]	1:3			1:3			1:3	1:3	1:4	1:2
[$N_{1\,1\,16\,(2OH)}^+$][Br^-]	1:4			1:4			1:3	1:3	1:4	1:2

3.4.3 Evaluation of the hydrophobicity of [Ch^+][Br^-]-based HES

Hydrophobicity of the proposed ESs is a fundamental parameter of this work to identify new hydrophobic solvents that can easily separate from water. Florindo and co-workers[203] have reported that the hydrophobicity of DESs can be evaluated by measuring their miscibility in water. The initial water content of all six synthesized salts was measured by Karl Fischer analysis after their preparation and storage in a vacuum oven prior to measurements. The ESs were then placed in contact with water (see experimental section for details) and the measurement repeated. According to the literature,[202] the initial water content of HESs after preparation is reported to be in the range between 0.01 and 0.80 wt%, while when mixed with water, it can vary from 0.52 to 6.94 wt%. For [Ch^+][Br^-]-based HDESs, the water content after preparation varied from 0.03 wt% to 0.62 % wt and increased to 0.98 wt% - 2.69 wt% after mixing with water, as shown in Figure 2. These results are in agreement with the reported values, proving the hydrophobic character of the solvents. Only the [$N_{3\,3\,3\,(2OH)}^+$][Br^-] : 2 Thymol ES yielded a water content higher than 10 wt% after mixing with water.

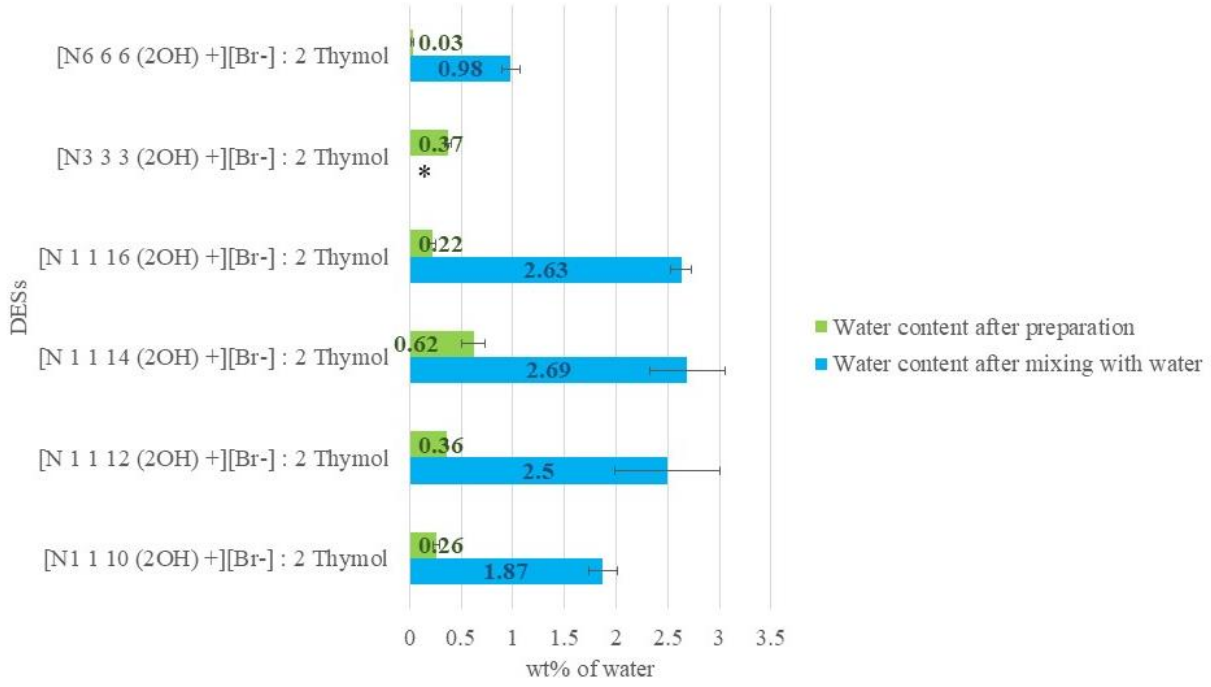

* not possible to measure with accuracy due to a value higher than 10%.

Figure 2. Water content (wt%) of [Ch$^+$][Br$^-$]-based HESs measured by Karl Fischer titration, before and after mixing in water, expressed as the mean for n=3 replicates.

Since the second part of this study involved the use of [Ch$^+$][Br$^-$]-based HESs as extraction solvents in aqueous solution, the stability of these eutectic mixtures in water was also monitored by ^{1}H NMR. As reported below, the [N $_{3\,3\,3\,(2OH)}$$^+$][Br$^-$] : 2 Thymol DES was found to be partially soluble in water, revealing a higher hydrophilicity compared to the other [Ch$^+$][Br$^-$]-based HESs. Despite the lower hydrophobicity of the [N $_{3\,3\,3\,(2OH)}$$^+$][Br$^-$] : 2 Thymol ES, it was used in subsequent studies to compare its extraction efficiency with the other [Ch$^+$][Br$^-$]-based HESs. The NMR spectra are provided in the Appendix of this Thesis.

3.4.4 Characterization of selected [Ch$^+$][Br$^-$]-based HESs in terms of viscosity and melting point

The following four representative [Ch$^+$][Br$^-$]-based HESs belonging to the three investigated groups of HESs were selected for measurement of viscosity, melting point and solvation properties: [N $_{1\,1\,10\,(2OH)}$$^+$][Br$^-$] : 2 Thymol and [N $_{1\,1\,16\,(2OH)}$$^+$][Br$^-$] : 2 Thymol for the surfactant-like salts, [N $_{3\,3\,3\,(2OH)}$$^+$][Br$^-$] : 2 Thymol from the bulky salts, and [N $_{4\,4\,4\,4}$$^+$][Br$^-$] : 2 Thymol for the commercial salts. With regard to thermal properties of the investigated HESs, it can be observed from Table 2 that HESs comprised of surfactant-like HBAs often exhibited a melt peak while no clear melting point could be identified for those comprised of bulky salts. The viscosity measurements, reported in Table 3, showed that HESs composed of bulky HBAs

possessed significantly higher viscosities of up to 2228.33 cP ($[N_{4\,4\,4\,4}^{+}][Br^{-}]$: 2 Thymol HES) compared to only 138.96 cP for the $[N_{1\,1\,10\,2(OH)}^{+}][Br^{-}]$: 2 Thymol HES that was comprised of a surfactant-like salt.

Table 2. Melting peak/glass transition temperatures of HESs as measured by a Thermal Advantage DSC Q2000 instrument.

HDES	T_g (°C)[a]	T_m (°C)[b]
$[N_{1\,1\,10\,2(OH)}^{+}][Br^{-}]$: 2 Thymol	-64.2	-
$[N_{1\,1\,16\,2(OH)}^{+}][Br^{-}]$: 2 Thymol	-84.0	6.9
$[N_{3\,3\,3\,2(OH)}^{+}][Br^{-}]$: 2 Thymol	-44.1	-
$[N_{4\,4\,4\,4}^{+}][Br^{-}]$: 2 Thymol	-43.2	-
$[N_{6\,6\,6\,2(OH)}^{+}][Br^{-}]$: 2 Thymol	-89.9	-

[a] glass transition temperature, [b] melting peak temperature
"-" no Tm/Tg peak was observed/reported

Table 3. Viscosity data obtained at 21.6 °C for all HESs.

HES	Viscosity (cP)
$[N_{1\,1\,10\,2(OH)}^{+}][Br^{-}]$: 2 Thymol	138.96
$[N_{1\,1\,16\,2(OH)}^{+}][Br^{-}]$: 2 Thymol	96.14
$[N_{3\,3\,3\,2(OH)}^{+}][Br^{-}]$: 2 Thymol	1856.33
$[N_{4\,4\,4\,4}^{+}][Br^{-}]$: 2 Thymol	2228.33
$[N_{1\,1\,1\,2(OH)}^{+}][Br^{-}]$: 2 Thymol	-[a]
$([Ch^{+}][Br^{-}])$: 2 Thymol	-

[a] HES resembled a chunky solid at 21.6 °C

3.4.5 Characterizing hydrophobic $[Ch^{+}][Br^{-}]$-based HESs using infrared spectroscopy

To investigate the extent of hydrogen bonding between the HBA and HBD, all HESs were studied using ATR-FTIR spectroscopy. Figure 3a demonstrates the FTIR spectrum obtained for the $[N_{3\,3\,3\,2(OH)}^{+}][Br^{-}]$ HBA. Vibrational band appearing at 3240 cm^{-1} corresponds to O-H stretching while those occurring at 2969-2880 cm^{-1} refer to a C-H stretching of a sp^3 hybridized functional group. In Figure 3b, the FTIR spectrum for the thymol HBD is being shown. While the O-H stretching band was observed at 3283 cm^{-1}, the C-H stretching of sp^2 and sp^3 alkyl substituents were obtained at 3067-3036 and 2958-2868 cm^{-1}, respectively. Additionally,

overtone bending was identified between 1875-1709 cm^{-1} and bands corresponding to C=C stretching is shown at 1621 cm^{-1}. Figure 3c demonstrates the IR imaging for the $[N_{3\,3\,3\,2(OH)}{}^{+}][Br^{-}]$: 2 Thymol ES and bands related to functional groups of both the HBA and HBD could be seen. It was observed that the O-H stretching band at 3263 cm^{-1} was significantly broader and much weaker compared to the corresponding band observed for the HBA and HBD in Figures 3a and 3b, indicating strong intermolecular hydrogen bonding interactions between the ES components in comparison to the starting materials. Similar phenomenon was noted for other HESs compared to their components, indicating that the hydroxyl functional groups of both the HBA and HBD engage in strong hydrogen bonding interactions with the bromide hydrogen bond base in order to form stable HESs.

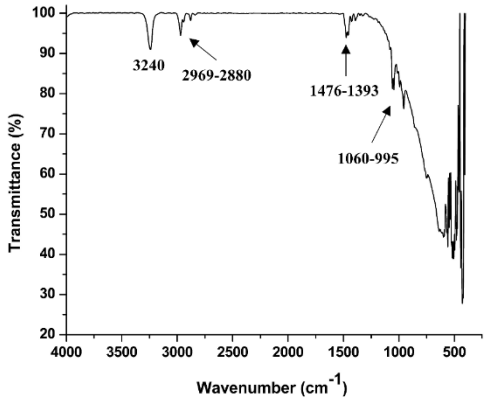

(a)

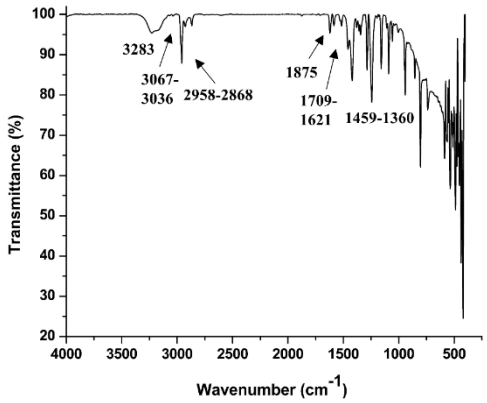

(b)

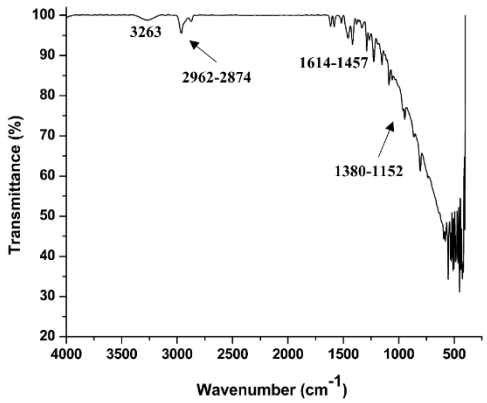

(c)

Figure 3. Representative ATR-FTIR spectrum for (a) $[N_{3\,3\,3\,2(OH)}^{+}][Br^{-}]$ HBA, (b) thymol HBD and (c) $[N_{3\,3\,3\,2(OH)}^{+}][Br^{-}]$: 2 Thymol ES, obtained under ambient conditions.

3.4.6 Influence of HBA on HES solvation properties

Three independent methods were used to evaluate the solvation properties of hydrophobic [Ch$^+$][Br$^-$]-based HESs. First, the most popular fluorescent dye polarity scales were employed. A detailed description of dyes, equations and methods used to examine raw data from the solvatochromic dye method are provided in the Appendix of this Thesis. Given that only thymol was employed as the HBD and the HBA/HBD ratio was kept constant at 1:2 for all HESs, only the effect of HBA was investigated. To estimate the polarity of bulky and surfactant-like HBAs, the nile red polarity scale (ENR) was employed. Table 4 provides the ENR values for 4 HESs examined in this study. The polarity values ranged from (50.21±0.06) to (51.33±0.05) and were generally very similar within the same class of HBA.

Table 4. E_{NR} polarity values and Kamlet-Taft solvent parameters for HESs composed of [$N_{1\,1\,10\,2(OH)}^+$][Br$^-$], [$N_{1\,1\,16\,2(OH)}^+$][Br$^-$], [$N_{3\,3\,3\,2(OH)}^+$][Br$^-$], and [$N_{4\,4\,4\,4}^+$][Br$^-$] HBAs and thymol as the HBD. The E_{NR} values and Kamlet-Taft solvent parameters are expressed as the mean for n=3 replicates and the standard deviation for each term is provided in parenthesis.

HES	E_{NR} (kcal/mol)	α[a]	β[b]	π*[c]
[$N_{1\,1\,10\,2(OH)}^+$][Br$^-$] : 2 Thymol	50.33 (0.05)	0.83 (0.02)	0.39 (0.02)	1.00 (0.03)
[$N_{1\,1\,16\,2(OH)}^+$][Br$^-$] : 2 Thymol	50.45 (0.06)	0.80 (0.03)	0.33 (0.03)	0.98 (0.04)
[$N_{3\,3\,3\,2(OH)}^+$][Br$^-$] : 2 Thymol	50.21 (0.06)	0.86 (0.03)	0.49 (0.01)	1.02 (0.02)
[$N_{4\,4\,4\,4}^+$][Br$^-$] : 2 Thymol	51.33 (0.05)	0.66 (0.03)	0.60 (0.02)	0.93 (0.01)

[a]hydrogen bond donating ability, [b] hydrogen bond accepting ability, [c] dipolarity/polarizability (π*)

To better understand the types of solvation interactions, the same HESs were further investigated using the Kamlet-Taft solvent parameters. Values for the hydrogen bond donating ability (α), hydrogen bond accepting ability (β), and dipolarity/polarizability (π*). The hydrogen bond donating ability varied from (0.66±0.03) to (0.86±0.03) and was observed to be significantly higher for HESs possessing a hydroxyl functional group in the HBA due to an additional acidic proton. Comparing the α-term values for the [$N_{1\,1\,10\,2(OH)}^+$][Br$^-$] : 2 Thymol (0.83±0.02), [$N_{1\,1\,16\,2(OH)}^+$][Br$^-$] : 2 Thymol (0.80±0.03), and [$N_{3\,3\,3\,2(OH)}^+$][Br$^-$] : 2 Thymol HESs (0.86±0.03) reveals no significant difference in hydrogen bond donating ability between the bulky and surfactant-like hydrophobic [Ch$^+$][Br$^-$]-based HBAs. In contrast, β-term values were found to be (0.39±0.02), (0.33±0.03), and (0.49±0.01) for the [$N_{1\,1\,10\,2(OH)}^+$][Br$^-$] : 2 Thymol, [$N_{1\,1\,16\,2(OH)}^+$][Br$^-$] : 2 Thymol, and [$N_{3\,3\,3\,2(OH)}^+$][Br$^-$] : 2 Thymol HESs, respectively, indicating that the hydrogen bond accepting ability varies significantly between bulky and surfactant-like HBAs as well as within the same

class. The $[N_{3\,3\,3\,2(OH)}^{+}][Br^{-}]$: 2 Thymol ES possessed a drastically lower hydrogen bond accepting ability compared to the $[N_{4\,4\,4\,4}^{+}][Br^{-}]$: 2 Thymol HES (0.60±0.02), which can be attributed to the presence of an additional acidic proton on the hydroxyl functional group that can interact with the bromide anion and reduce its hydrogen bond basicity. In addition, HESs comprised of bulky HBAs possessed higher hydrogen bond accepting ability compared to those comprised of surfactant-like salts, irrespective of the presence/absence of the hydroxyl functional group. Moreover, dipolar interactions were found to range from (0.93±0.01) to (1.02±0.02) but no specific trend could be determined for the two types of HBAs employed in this study.

HESs comprised of the $[N_{1\,1\,10\,2(OH)}^{+}][Br^{-}]$, $[N_{1\,1\,16\,2(OH)}^{+}][Br^{-}]$, $[N_{3\,3\,3\,2(OH)}^{+}][Br^{-}]$, $[N_{4\,4\,4\,4}^{+}][Br^{-}]$, and $[N_{6\,6\,6\,2(OH)}^{+}][Br^{-}]$ salts as the HBA were further examined using inverse gas chromatography between 40 and 60 °C. Given the volatile nature of thymol, triethylene glycol (TEG) was chosen as the HBD in the preparation of ESs for IGC studies. All salts formed a homogenous eutectic mixture with TEG at a molar ratio of 1:4; this molar ratio was kept constant in order to investigate the effect of HBA on ES solvation interactions. The unique solvation interactions were deconvoluted using the Abraham solvation parameter model and a detailed description of equations and methods used to generate system constants from the model are provided in the Appendix of this Thesis. Dipolar interactions were generally found to vary between (1.79±0.07) and (2.25±0.06) at 60 °C and were observed to be lower for ESs comprised of surfactant-like HBAs compared to those composed of bulky salts. The strength of dispersive-type interactions was generally dependent on the length of alkyl substituents on the cation with the lowest value of (0.52±0.01) obtained for the $[N_{3\,3\,3\,2(OH)}^{+}][Br^{-}]$: 4 TEG ES and the highest l-term value of (0.67±0.01) exhibited by the $[N_{1\,1\,16\,2(OH)}^{+}][Br^{-}]$: 4 TEG ES. ESs comprised of bulky salts generally offered lower dispersive-type interactions compared to those comprised of surfactant-like HBAs.

Like most classes of ESs, hydrogen bonding was among the strongest type of solvation interaction measured. The hydrogen bond basicity ranged from (3.76±0.11) to (4.28±0.14) at 60 °C and was often observed to be higher for ESs comprised of bulky salts compared to surfactant-like HBAs. Within the class of bulky HBAs, ESs that possessed longer alkyl substituents in the cation exhibited higher hydrogen bond basicity, which is consistent with the trend previously reported for both tetraalkylammonium and $[Ch^{+}][Cl^{-}]$-based ESs[215,216]. In contrast, longer alkyl

functional groups in surfactant-like HBAs resulted in lower hydrogen bond basicity, as observed in the b-term values for the $[N_{1\ 1\ 10\ 2(OH)}^{+}][Br^{-}]$: 4 TEG (4.10±0.09) and $[N_{1\ 1\ 16\ 2(OH)}^{+}][Br^{-}]$: 4 TEG ESs (3.76±0.11) at 60 °C. These trends are further supported by the chromatographic retention behavior of alcohols (provided in Table 5), which are acidic in nature and can strongly interact with the bromide anion. Additionally, the retention characteristics of basic probe molecules, such as *N,N*-DMAC, also provide insights into the relative strength of hydrogen bond acidity in these ESs. It was observed that *N,N*-DMAC produced retention factors as high as 48.04 on the $[N_{6\ 6\ 6\ 2}(OH)^{+}][Br^{-}]$: 4 TEG ES compared to only 37.04 on the $[N_{1\ 1\ 16\ 2}(OH)^{+}][Br^{-}]$: 4 TEG ES at 60 °C, indicating that bulky salts exhibit higher hydrogen bond acidity compared to surfactant-like HBAs.

Table 5. Retention factors of various probe molecules at 60 °C measured on deep eutectic solvents comprised of choline chloride and choline acetate hydrogen bond acceptors.

Probe	ESs				
	$[N_{1\,1\,10\,2(OH)}^+][Br^-]$: 4 TEG	$[N_{1\,1\,16\,2(OH)}^+][Br^-]$: 4 TEG	$[N_{3\,3\,3\,2(OH)}^+][Br^-]$: 4 TEG	$[N_{4\,4\,4\,4}^+][Br^-]$: 4 TEG	$[N_{6\,6\,6\,2(OH)}^+][Br^-]$: 4 TEG
Methanol	0.84	0.62	1.02	1.07	0.67
Ethanol	1.01	0.80	1.21	1.33	0.88
1-Propanol	2.13	1.80	2.26	2.56	1.042
1-Butanol	4.30	3.96	4.26	5.29	5.40
1-Pentanol	8.87	8.70	7.95	10.52	11.18
Cyclopentanol	12.67	11.80	12.30	14.50	15.17
1-Hexanol	18.41	19.03	13.99	20.84	29.58
Cyclohexanol	26.14	25.92	23.29	29.00	31.94
Napthalene	48.52	55.40	49.76	59.75	61.90
Nitrobenzene	55.35	50.97	55.07	69.72	75.04
Acetophenone	44.55	40.80	44.74	51.85	54.07
Benzonitrile	28.54	25.55	30.43	37.43	36.66
Benzaldehyde	18.91	16.89	20.05	22.44	22.76
N,N-Dimethylformamide (*N,N*-DMF)	18.72	16.07	21.19	19.77	21.72
N,N-Dimethylacetamide (*N,N*-DMAC)	37.04	35.80	42.45	40.84	48.04

Despite both being totally different approaches, it is vital that the results of the Kamlet-Taft solvent parameters and the Abraham solvation parameter model are in complete agreement with each other for solvation interactions that can be quantified using both methods, such as hydrogen bond basicity and dipolarity. The trend in relative strength for hydrogen bond accepting ability (β) was observed to be as follows: $[N_{1\,1\,16\,2(OH)}^+][Br^-] < [N_{1\,1\,10\,2(OH)}^+][Br^-] < [N_{3\,3\,3\,2(OH)}^+][Br^-] < [N_{4\,4\,4\,4}^+][Br^-]$. Comparing this with the a-term for the same ESs revealed a similar trend for the same set of ESs. Clearly, both methods indicate that surfactant-like HBAs offer lower hydrogen bond basicity compared to bulky salts. This is useful in explaining some trends observed in the extraction of flavonoids and cannabinoids. It was observed that flavonoids, such

as luteolin 7-*O*-glucuronide and apigenin 7-*O*-glucuronide, generally resulted in higher extraction with ESs that exhibit lower hydrogen bond basicity.

3.4.7 [Ch^+][Br^-]-based HES for the extraction of phytochemicals with different polarity from *Cannabis sativa* L. samples

After characterization of the [Ch^+][Br^-]-based HESs, their applicability in the extraction of natural compounds was explored. Apart from the extraction performance of the new solvents, their compatibility with liquid chromatography was also investigated since chromatographic techniques are fundamental for the analysis and study of plant metabolome to separate and identify the analytes of interest in complex samples. In this sense, it was important to verify that the signal of thymol (HBD in the HESs) in the chromatogram did not interfere with the signal of the target analytes. Moreover, blank injections of MeOH 100% were regularly repeated within the analysis of [Ch^+][Br^-]-based HES extracts to detect potential carry-over.

When dealing with plant matrices, solvents able to extract a wide range of phytochemicals are fundamental in obtaining extracts representative of the plant metabolome. The simultaneous presence of hydrophilic domains (hydroxyl group and charge of ammonium) and long alkyl chain substituents in the structure of [Ch^+][Br^-]-based HESs may promote the extraction of phytochemicals with different polarity. The aerial parts of fiber-type *Cannabis sativa* L. were chosen due to the rich phytocomplex comprised of several classes of non-volatile bioactive compounds. As reported in Section III.3.2, the main phytochemicals identified in this matrix were flavonoid glycosides and non-psychotomimetic cannabinoid acids. The previous study (Section III.3.3) on neutral HESs composed of terpenoids compounds of natural origin have highlighted that these solvents were capable of extracting cannabinoid compounds, but less effective in the enrichment of the flavonoid fraction.

3.4.8 Optimization of the dispersive solid-liquid microextraction (DSLME) method for the analysis of *Cannabis sativa* L. aerial parts

To evaluate the extraction performance of the proposed HESs for all target analytes identified in the hemp sample, a DSLME method was firstly applied to a mix of representative standard compounds (e.g., luteolin 7-*O*-glucuronide, apigenin 7-*O*-glucuronide and CBDA) in an effort to simulate their behavior in a less complex system. The DSLME approach was employed for simplicity and speed of the procedure while also reducing the amount of solvent to improve

the enrichment of analytes in the final HES extract. To reduce the number of experiments, the ([N $_{1\ 1\ 16\ (2OH)}^{+}$][Br^{-}] : 2 Thymol) HES was selected for use in the first part of the optimization. The extraction was performed on 10 µg of the three standards following the procedure reported in Figure 4.

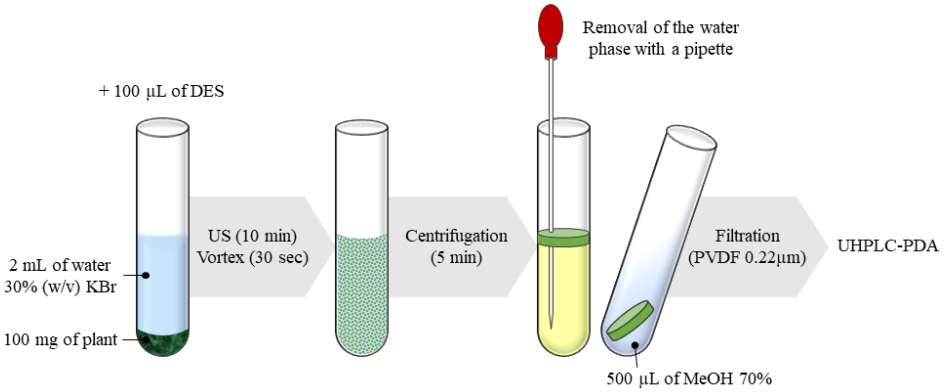

Figure 4. Dispersive solid-liquid microextraction (DSLME) method used for the extraction of phytochemicals from fiber-type *Cannabis sativa* L. aerial parts.

To improve transfer of analytes from the water layer to the HES, the addition of aqueous solutions of KBr (30% (w/w) and 50% (w/w)) of the saturation concentration) was also tested. Although NaCl is usually employed,[217] KBr was used to prevent an ion exchange reaction between the [Cl^{-}] anion of NaCl and [Br^{-}] anion of [Ch^{+}][Br^{-}]-bases HESs during the extraction step. Figure 5a shows the results obtained when 0% (w/w), 30% (w/w) and 50% (w/w) of KBr salt were examined. As expected, the addition of 30% KBr decreased the solubility in water of the three analytes, thus favoring their partitioning to the HES phase. A further increase of KBr in the water solution (50%) improved the enrichment of CBDA, while the extraction efficiency of flavonoid glycosides was lower compared to that observed at 30% KBr. These results are in agreement with previous studies in which a lower extraction efficiency at very high salt concentration was reported[218–220]. This behavior can be ascribed to the increase of viscosity of the aqueous solution, which results in a slower mass transfer. For this reason, an aqueous solution containing 30% of KBr was selected as optimal solvent for the following steps.

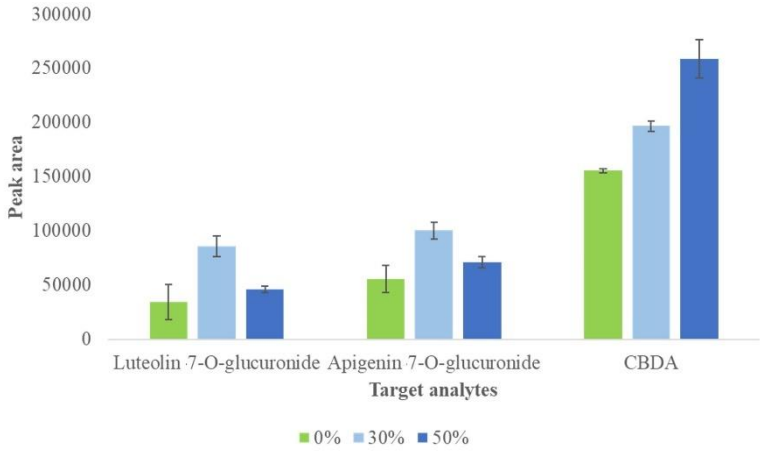

(a)

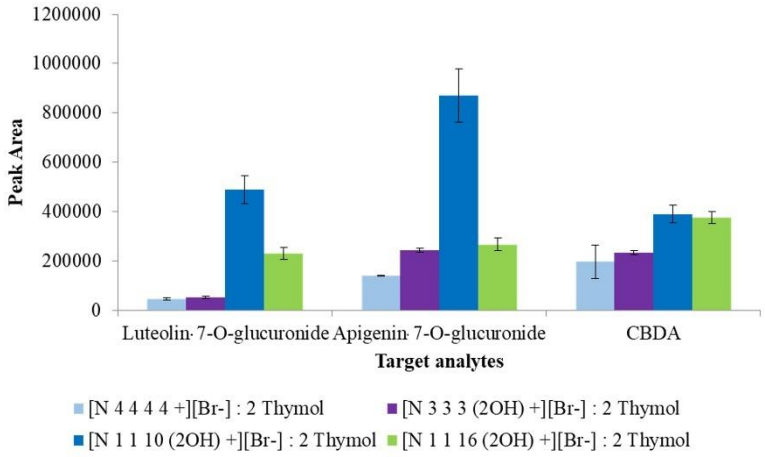

(b)

Figure 5. (a) Optimization of KBr content (% of saturation concentration) in the DSLME method using the $[N_{1\ 1\ 16\ (2OH)}^{+}][Br^{-}]$: 2 Thymol HES as solvent (n=3) and (b) evaluation of the extraction performance (evaluated as peak area) of the HESs under study for the three target analytes: luteolin 7-*O*-glucuronide, apigenin 7-*O*-glucuronide and CBDA. The results are expressed as the mean for n=3 replicates.

Once the method was optimized, it was applied to study the extraction performance of the $[Ch^{+}][Br^{-}]$-based HESs on pure standard compounds. Figure 5b shows the extraction efficiencies for the three analytes, expressed as chromatographic peak areas. In general, HDESs formed from surfactant-like salts exhibit higher extraction performance for all compounds, with a clear predominance of the $[N_{1\ 1\ 10\ (2OH)}^{+}][Br^{-}]$: 2 Thymol HES in the extraction of flavonoid glycosides, while this difference is less marked for CBDA. It is noteworthy that the lower peak area of flavonoid glycosides, observed in $[N_{1\ 1\ 16\ (2OH)}^{+}][Br^{-}]$: 2 Thymol extract, may be due to the breakage of bonds between the aglycone (luteolin or apigenin) and the sugar (glucuronic acid) during extraction. To support this, Figure 6 shows the presence of two additional peaks in the chromatographic profile of the extract, which were identified as luteolin and apigenin aglycone.

These peaks are not present in the other extracts, suggesting that the long alkyl chain substituents within the [N $_{1\,1\,16\,(2OH)}^{+}$][Br^{-}] salts may undergo interaction with the glycosidic bond present in the flavonoid glycosides.

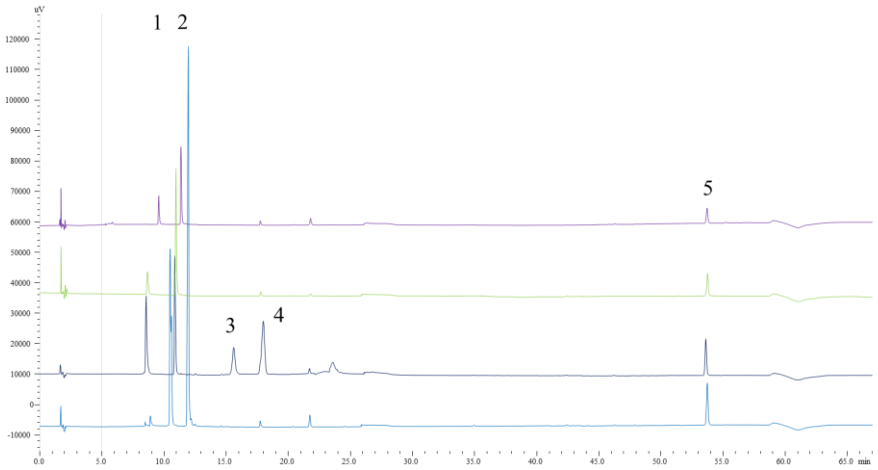

Figure 6. Chromatographic profiles at 340 nm of the DSLME of luteolin 7-*O*-glucuronide, apigenin 7-*O*-glucuronide and CBDA standard compounds, using [N $_{1\,1\,10\,(2OH)}^{+}$][Br^{-}] : 2 Thymol (light blue), [N $_{1\,1\,16\,(2OH)}^{+}$][Br^{-}] : 2 Thymol (blue), [N $_{3\,3\,3\,(2OH)}^{+}$][Br^{-}] : 2 Thymol (green) and [N $_{4\,4\,4\,4}^{+}$][Br^{-}] : 2 Thymol (purple) as solvents. Peaks identification: 1. luteolin 7-*O*-glucuronide, 2. apigenin 7-*O*-glucuronide, 3. luteolin, 4. apigenin, 5. CBDA. The shift of the peaks in the first part of the chromatogram is due to the interference given by the salts used as HBAs

Once the method was optimized for standard compounds, it was applied for the extraction of the non-volatile fraction of fiber-type *Cannabis sativa* L. aerial parts (see Figure 4). In this case, the extraction was carried out with all six [Ch^{+}][Br^{-}]-based HESs to investigate differences in the extraction performance between all solvents. For comparison purposes, the optimized DSLME method was also performed with the two HESs formed by the commercial ammonium salts and with a eutectic mixture composed of menthol and linalool. The menthol : linalool mixture was selected as reference because it was previously employed as an extraction solvent for the same hemp sample[221]. Figure 7 shows the extraction efficiencies obtained for the target compounds expressed as chromatographic peak areas. The behavior of the [Ch^{+}][Br^{-}]-based HES, when the method was applied on the plant, slightly differs from that observed in the aqueous solution (see previous paragraph).

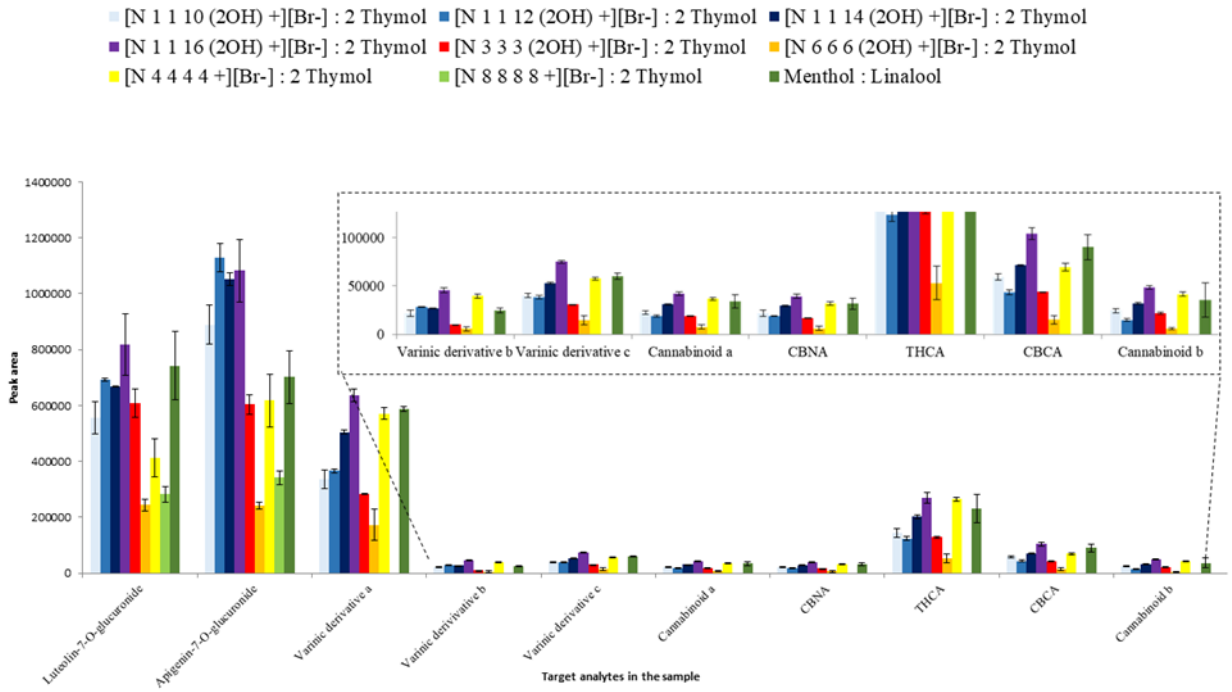

Figure 7. Extraction performance (evaluated as peak area, expressed as the mean for n=3 replicates) of the investigated HESs in the analysis of the non-volatile fraction of fiber-type *Cannabis sativa* L. aerial parts. The identification of the analytes follows the one reported in Section III.3.2: Cannabinolic acid (CBNA), tetrahydrocannabinolic acid (THCA), cannabichromenic acid (CBCA), varinic derivative A/B and cannabinoid A/B were putatively identified at class level through retentions times, maximum UV adsorption and tandem mass spectrometry fragmentation patterns.

With regard to the flavonoid fraction, the peak areas were observed to increase in accordance with an increase of the apolar tail length (from C10 to C16) of the surfactant-like salts. In this case, the aglycones are not detected, indicating that the plant matrix prevents degradation of the glycosidic bond. This may explain why, contrary to extraction from aqueous solution, the $[N_{1\,1\,16\,(2OH)}^{+}][Br^{-}]$: 2 Thymol HES was more effective than $[N_{1\,1\,10\,(2OH)}^{+}][Br^{-}]$: 2 Thymol HES in terms of extraction performance. As previously observed in the extraction of pure compounds, the two HESs based on $[Ch^{+}][Br^{-}]$-modified bulky salts provide lower efficiency, with higher peak areas obtained for the $[N_{3\,3\,3\,(2OH)}^{+}][Br^{-}]$: 2 Thymol HES. A similar trend is observed for the HESs based on commercial salts, where the shorter chains of the $[N_{4\,4\,4\,4}^{+}][Br^{-}]$: 2 Thymol HES appears to extract more analytes compared the $[N_{8\,8\,8\,8}^{+}][Br^{-}]$: 2 Thymol HES. The peculiar chemical structure of the surfactant-like salts characterized by a long alkyl chain substituent may assist in interaction of the solvent with the plant's cell wall, which is necessary for release of the target compounds. On the other hand, larger steric hindrance around the ammonium group in the other salts may negatively affect interaction with the analytes. Moreover, the viscosity data obtained for selected HESs (see Table 3) shows that bulky and

commercial salts provide higher viscosity compared to surfactant-like HESs. This suggests that the lower extraction efficiency of HESs based on bulky and commercial salts could also be a result of their higher viscosity, which may interfere with transfer of the analytes from the plant to the solvent[222]. This is confirmed by the extraction efficiency offered by the menthol : linalool eutectic mixture, which is higher or similar to the bulky/commercial salt-based HESs. Despite the higher hydrophobicity of the terpenoid mixture, the viscosity of neutral HESs is typically much lower compared to the ionic ones[223].

Regarding cannabinoid compounds, the extraction efficiency of the different HESs is similar to those observed for flavonoids, except for the $[N_{4444}^{+}][Br^{-}]$: 2Thymol HES, which follows a similar trend to that of the $[N_{1116(2OH)}^{+}][Br^{-}]$: 2 Thymol HES. This could be justified by the lower polarity of the $[N_{4444}^{+}][Br^{-}]$: 2Thymol HES, which provides more favorable interactions with cannabinoids compared to the more polar flavonoid glycosides. The high viscosity of the $[N_{8888}^{+}][Br^{-}]$: 2Thymol HES negatively affected extraction of the cannabinoid fraction, whose peaks were not detected in the chromatographic profile.

Based on these results, the $[N_{1116(2OH)}^{+}][Br^{-}]$: 2 Thymol HES appeared to be the best among all eutectic mixtures tested with regard to analysis of phytochemicals with different polarity in *Cannabis sativa* L. aerial parts. It exhibited higher enrichment of more polar compounds while maintaining a similar extraction efficiency of cannabinoids compared to reference menthol : linalool hydrophobic solvent. It is also interesting to highlight that $[N_{1116(2OH)}^{+}][Br^{-}]$ and surfactant-like salts, in general, consist of simpler and faster synthetic processes and higher yields compared to the bulky salts, thus enabling a more reliable application in analytical procedures.

3.4.9 Stability of HESs during the extraction

Due to its capacity in undergoing hydrogen bonding, water is supposed to undergo interaction with the hydrogen bonding network of DESs[224]. For this reason, it is important to verify their stability when performing applications involving aqueous solutions. In the DSLME method, an aqueous solution of 30% KBr is used as co-solvent to form a dispersion of the HES in the sample. To verify that the HES remains intact during extraction, its ^{1}H NMR profile was compared before and after extraction. To avoid interference of the plant and analytes in the NMR spectra, the extraction was carried out by substituting the plant material with 2 mL of KBr

aqueous solution. The extraction was then carried out as reported in Figure 4 and the recovered HESs diluted in deuterated solvent and subjected to NMR measurements. For all HESs, ^{1}H NMR spectra showed the presence of both the HBA and HBD after the extraction, confirming that hydrogen bonding is intact after dispersion in water and that the entire HES is responsible for the extraction. The molar ratio between the HBA and HBD was also monitored and showed to be stable after extraction. The only exception was the [$N_{3\,3\,3\,(2OH)}^{+}$] : 2 Thymol HES, where the molar ratio between [$N_{3\,3\,3\,(2OH)}^{+}$] and Thymol changed after the extraction process. In fact, part of [$N_{3\,3\,3\,(2OH)}^{+}$] dissolved in the water phase during the extraction and it was therefore found in lower relative amounts in the HES phase. This behavior appears to be linked to its higher hydrophilicity, already observed in the measurement of water content. The ^{1}H NMR spectra of [$N_{3\,3\,3\,(2OH)}^{+}$] : 2Thymol and [$N_{1\,1\,16\,(2OH)}^{+}$] : 2 Thymol before and after the extraction are shown in Figure 8.

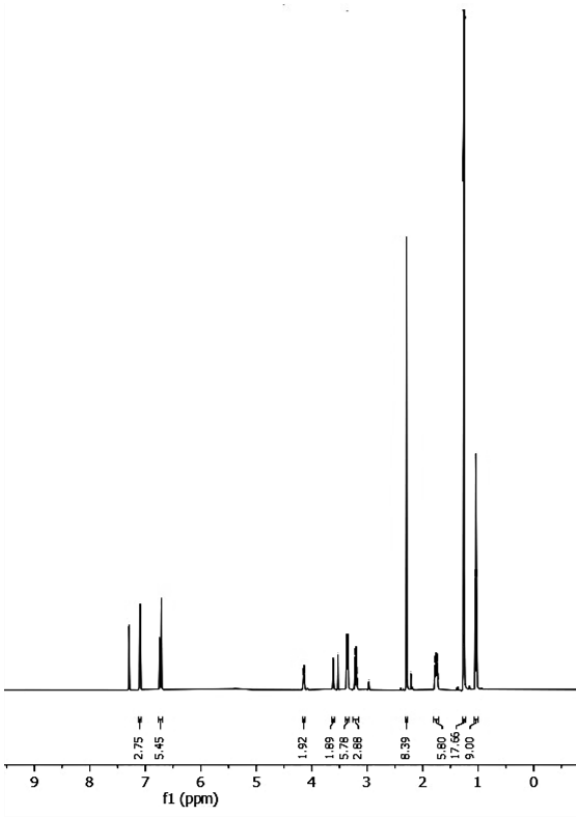

(a)

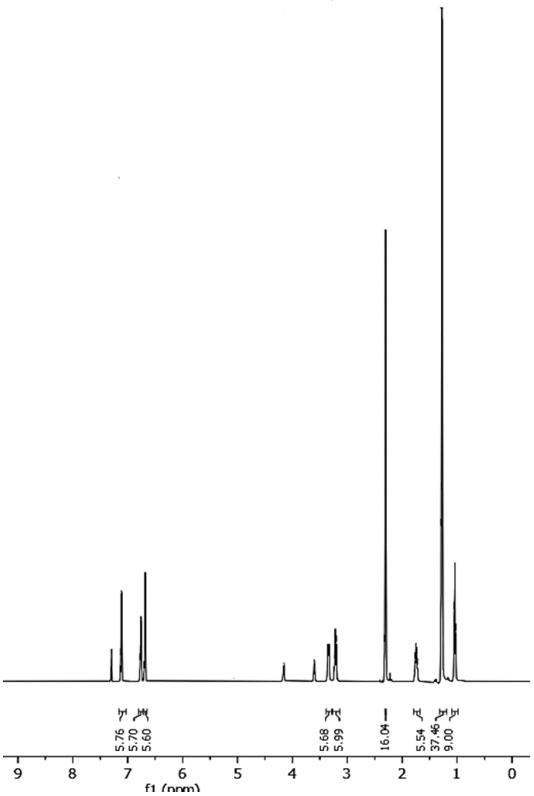

(b)

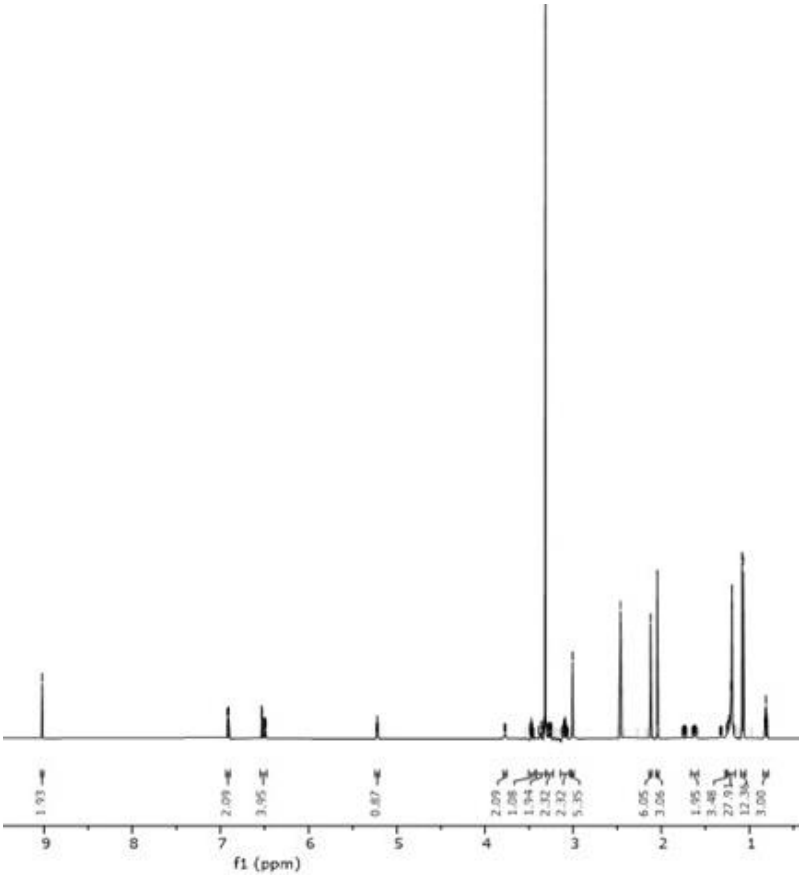
1.93
2.09
3.95
0.87
2.09
1.08
1.94
2.32
2.32
5.35
6.05
3.06
1.95
3.48
27.91
12.36
3.00
9
8
7
6
5
4
3
2
1
f1 (ppm)

(c)

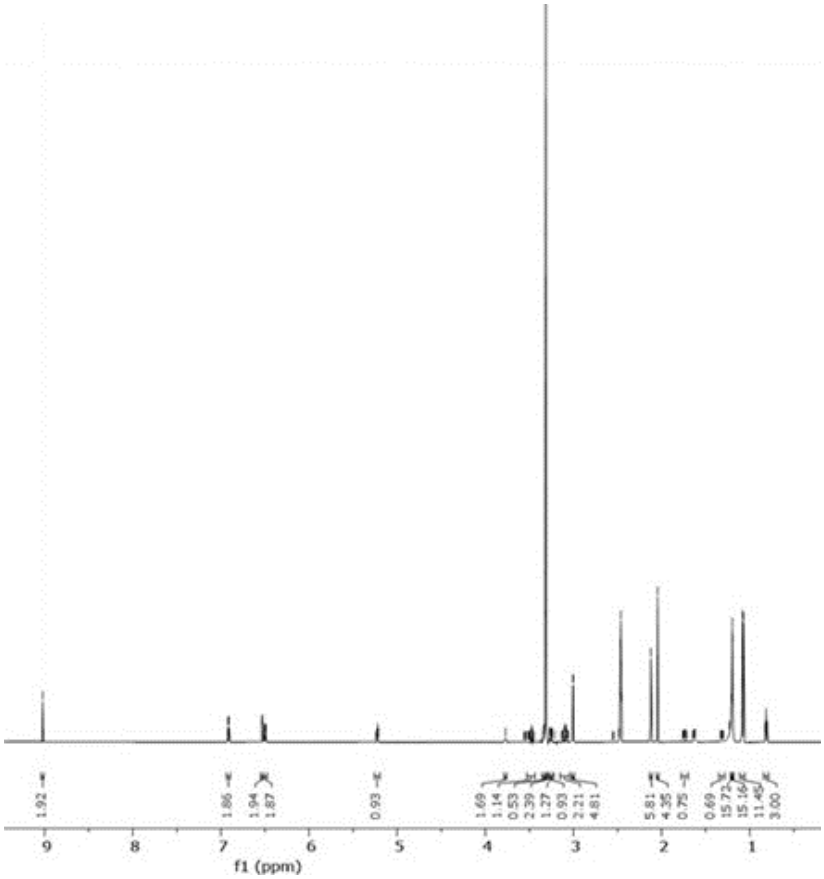

(d)

Figure 8. ^{1}H NMR of (a) $[N_{3\,3\,3\,(2OH)}^{+}][Br^{-}]$: 2 Thymol HES before extraction in KBr 30% aqueous solution, (b) $[N_{3\,3\,3\,(2OH)}^{+}][Br^{-}]$: 2 Thymol HES after extraction in KBr 30% aqueous solution, (c) $[N_{1\,1\,16\,(2OH)}^{+}][Br^{-}]$: 2 Thymol HES before extraction in KBr 30% aqueous solution and (d) $[N_{1\,1\,16\,(2OH)}^{+}][Br^{-}]$: 2 Thymol HES after extraction in KBr 30% aqueous solution.

Ultrasound-assisted dispersive solid-liquid-based microextraction method with eutectic solvents for the determination of cannabinoids in different hemp products

This paragraph is reproduced from a published article
(Mastellone *et al.*, Journal of chromatography B, 2024, 1232, 123967)

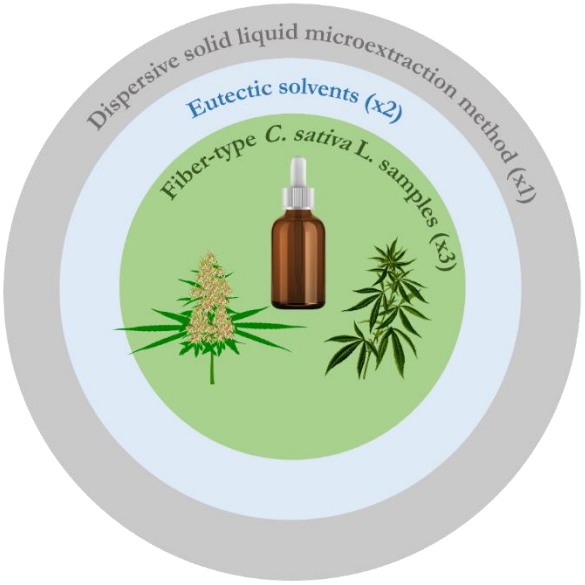

3.5 Ultrasound-assisted dispersive solid-liquid-based microextraction method with eutectic solvents for the determination of cannabinoids in different hemp products

This study aimed to develop a simple ultrasound-assisted dispersive solid-liquid microextraction method coupled to HPLC-PDA detection for the analysis of cannabinoids in different hemp products. ESs with different physicochemical features (chemical composition and hydrophobicity) were tested to find the optimal extraction solvent for the enrichment of cannabinoids from complex matrices. The method was optimized to be easy adaptable for the analysis of the aerial parts of *Cannabis sativa* L. collected before flowering, inflorescences, and a commercial sample called CBD oil.

3.5.1 Phytochemical characterization of the hemp samples

The qualitative characterization of the three samples was performed by UHPLC-PDA-ESI-MS/MS metabolite analysis, in order to identify the marker compounds to monitor in this study. The characterization focused on the specialized non-volatile metabolites. For this step, the reference methods (see Chapter II, Experimental) were used to extract all the compounds of interest from the matrices. For the aerial parts (collected before flowering), qualitative data were obtained from the previous study (Section III.3.2), in which flavonoids and non-psychotomimetic cannabinoids were identified. For the inflorescences and the CBD oil a similar chromatographic profile was obtained, and mainly cannabinoids (CBDA and CBD as the most abundant) were found. The identification of CBDA and CBD was confirmed by the injection of authentic commercial reference standards. As previously reported[195], the content of cannabinoids in *C. sativa* L. is lower before flowering, while it normally increases approaching the flowering period. On the contrary, the polyphenols are more abundant before flowering. According to the label, the CBD oil was composed of a hemp extract obtained with food grade solvent. Due to the high content of CBD in hemp inflorescences of the plant, this extract was probably obtained from the flowers, justifying the similar profile of the oil and inflorescences. The information regarding the identification of the marker analytes under study are reported in Table 1.

Table 1. List of identified and putatively identified compounds in fiber-type *Cannabis sativa* L. aerial parts, inflorescences and CBD oil.

Compound name	λ max[a] (nm)	$[M + H]^{+}$ [b] *m/z*	$[M - H]^{-}$ [c] *m/z*	Mol. Weight ($g\ mol^{-1}$)
Aerial parts[d]				
Luteolin 7-*O*-glucuronide	347/253	463	461	462
Apigenin 7-*O*-glucuronide	336/266	447	445	446
Varinic acid derivative A	222/270/305	331	329	330
Varinic acid derivative B	222/270/305	331	329	330
Varinic acid derivative C	222/270/305	331	329	330
Cannabinoid unknown	263/328	347	345	346
Cannabinolic acid (CBNA)	*n.v.*[e]	355	353	354
Tetrahydrocannabinolic acid (THCA)	222/270/305	359	357	358
Cannabichromenic acid (CBCA)	*n.v.*[e]	359	357	358
Cannabinoid unknown	270/305	375	373	374
Inflorescences and CBD oil				
CBDA	222/267/306	359	357	358
CBD	210/273	315	/	314

[a] UV maximum adsorption, [b] protonated ion, [c]deprotonated ion, [d] Identification data obtained from[204], [e] n.v. – not visible

The chromatographic profiles at 254 nm of the three samples after conventional extraction, are illustrated in Figure 1.

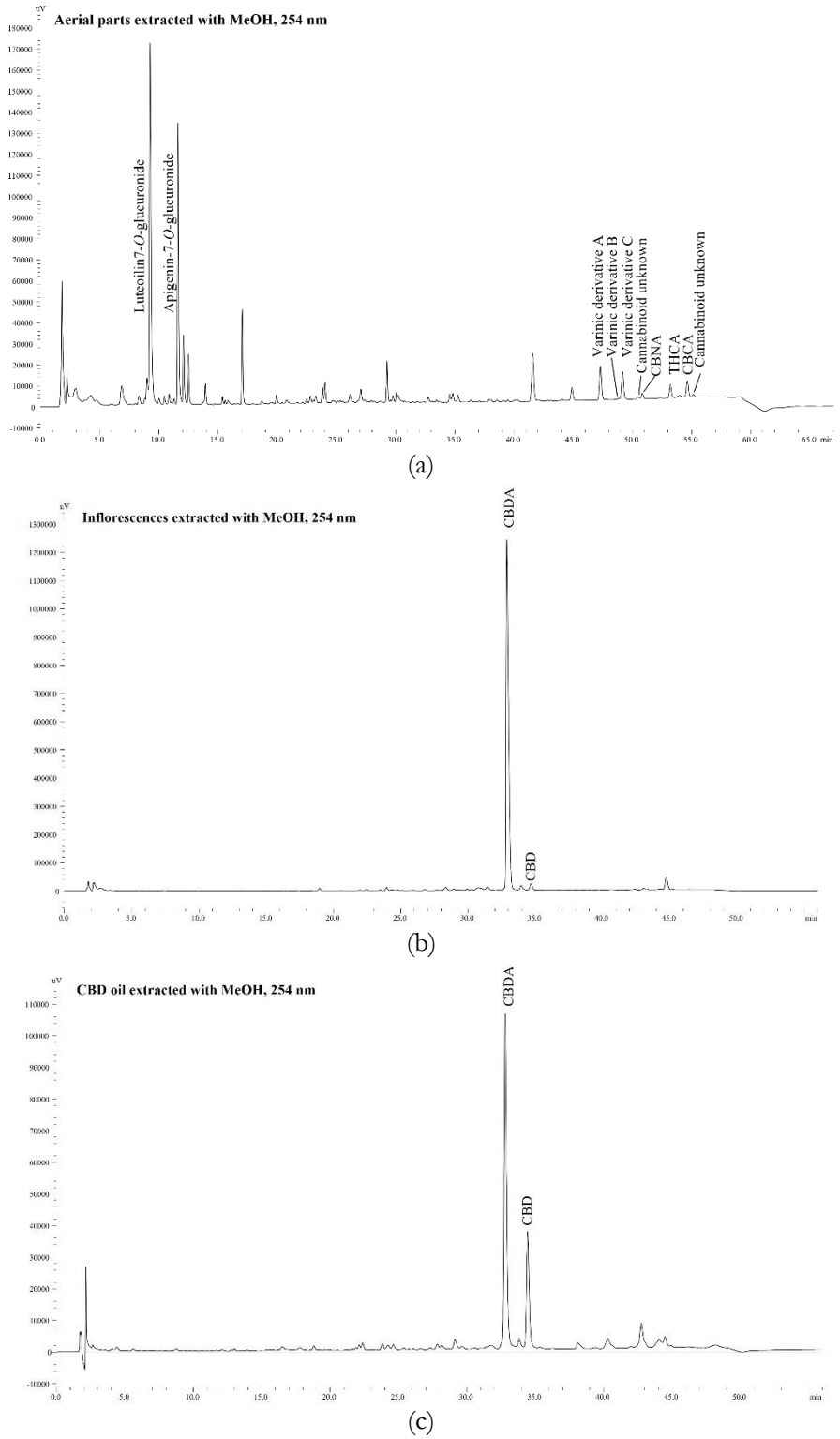

Figure 1. Chromatographic profile at 254 nm of the (a) aerial parts, (b) inflorescences and (c) CBD oil, after performing a solid-liquid MeOH extraction coupled to HPLC-PDA detection.

3.5.2 Chromatographic method

Two chromatographic methods were used to achieve the optimal analytical separation of the marker analytes in the three complex samples. The presence of both more polar (flavonoids) and less polar (cannabinoids) compounds in the extract of the aerial parts required the optimization of a longer chromatographic method, starting with a higher percentage of water (85% instead of 70%) as mobile phase. Moreover, 5 μL of aerial parts and CBD oil extract samples were injected in the UHPLC system, while the injection volume for the inflorescences was decreased to 3 μL of sample because of the high signal of CBDA which saturated the detector, even after dilution of the extract. The same injection volume was used in the validation of the method.

Mix solutions of the target compounds (CBD and CBDA) were injected at increasing concentration, using the two adopted injection volumes, for the calibration curves preparation. Calibration curves were linear with determination coefficients(R^2) higher than 0.992. The LODs were experimentally determined by decreasing the concentration of the analyte until a signal-to-noise ratio (S/N) of 3 was obtained. The LOQs were estimated as S/N of 10 and experimentally verified by injecting the standard compound at the predicted concentration. The LOD ranged between 0.03 μg mL^{-1} and 1 μg mL^{-1}, and the LOQ between 0.1 μg mL^{-1} and 4 μg mL^{-1}.

3.5.3 Choice of the extraction solvent

Eutectic solvents (ESs) were selected as extraction materials for their desirable properties such as low cost of raw materials, low vapor pressure (compared to conventional organic solvents) and easy preparation[225]. Moreover, the possibility to easily vary their composition allows to overcome some limits of conventional solvents which are normally characterized by a low chemical tunability. From previous studies[221,226], we selected two types of ESs, which have demonstrated good extraction performances for the analysis of the aerial parts of fiber-type *Cannabis sativa* L.. Table 2 reports several properties of the ESs used in this study.

Table 2. Properties of the eutectic solvents adopted in this study.

ID	HBA[a]	Molecular weight (g mol^{-1})[b]	Commercially available	HBD[c]	Molecular weight (g mol^{-1})[b]	Commercially available	Molar ratio	Water Solubility (wt%)[d]
N16	$[N_{1\ 1\ 16\ (2OH)}^{+}][Br^{-}]$	394.482	no	Thymol	150.22	yes	1 : 2	2.41
ML	Menthol	156.26[c]	yes	Linalool	154.25	yes	1 : 1	0.63

Further information about the characterization and properties of the ESs are reported in Section III.3.3 and III.3.4. The first solvent (N16) is formed by a $[Ch^{+}][Br^{-}]$-modified salts as HBA and thymol as HBD, at 1:2 molar ratio. The HBA was synthetized by the authors, and it is characterized by a long alkyl chain with 16 carbon atoms as one of the substituents of the ammonium group. The second mixture (ML) is a natural eutectic solvent formed by menthol and linalool at a 1:1 molar ratio. Apart from the different chemical structure of the components forming the two ESs, they also distinguish for the different hydrophobicity, higher for the natural ESs. The hydrophobicity was calculated by Karl Fischer titration, measuring the water content after preparation and after mixing the solvent in water (as previously reported in Section III.3.3 and III.3.4).

3.5.4 Application of the extraction method on different hemp products

An ultrasound-assisted dispersive solid-liquid microextraction (UA-DSLME) method using ESs was used for the analysis of cannabinoids in the three different hemp products. This method was selected as an alternative of conventional extraction approaches for the simplicity and speed of the procedure while also reducing the amount of solvent to improve the enrichment of analytes in the final extract. The UA-DSLME was optimized in the previous work (Section III.3.3) for the extraction of polar and less polar compounds from the aerial part (leaves and stems) of the plant collected before flowering. The optimized UA-DSLME was then tested on hemp inflorescences and CBD oil to evaluate the applicability and versatility of the method on samples with different features. Compared to leaves and stems, inflorescences are characterized by an oily texture because of the high content of resins which are produced by glandular trichomes, mainly present in female flowers[174]. The presence of these resins made the sample extremely hydrophobic, preventing the plant to enter completely in contact with the aqueous solution, used in the UA-DSLME method. During the extraction, the KBr aqueous solution acts as co-solvent, favoring the transfer of the analytes from the sample to the ES phase. For this

reason, the inflorescences were moistened with few microliters of EtOH 100% before adding 2 mL of KBr 30% w/w aqueous solution and 100 μL of ES. Moreover, the amount of sample to extract (100 mg for the aerial parts) was reduced to 20 mg because of the high content of cannabinoids which saturated the signal of the HPLC-PDA system. For the same reason, once collected, the ES rich phase was diluted with 4 mL of EtOH 100%, instead of 500 μL of MeOH 70%. In the case of CBD oil, only one centrifugation step was necessary to isolate the ES rich phase which was then diluted with 200 μL of EtOH 100%, prior to injection in the HPLC system, because of the lower content in marker analytes. In the case of the inflorescences and CBD oil, the final extracts were diluted in EtOH which presents a lower toxicity compared to MeOH. Regarding the aerial parts, MeOH was used to avoid the back-extraction of chlorophylls, which is more abundant in the herbaceous parts of the plants. When the UA-DSLME was performed with ML for the analysis of CBD oil, it was not possible to separate the ML phase from the oil, after the centrifugation step. Contrary to N16, ML is more hydrophobic and easily solubilized in the oil phase. For this reason, the extraction was performed only with the $[Ch^+][Br^-]$-based ES.

With the above mentioned few modifications (see Figure 2 for details), the developed UA-DSLME method resulted to be a versatile and robust approach for the analysis of hemp samples with different physicochemical properties.

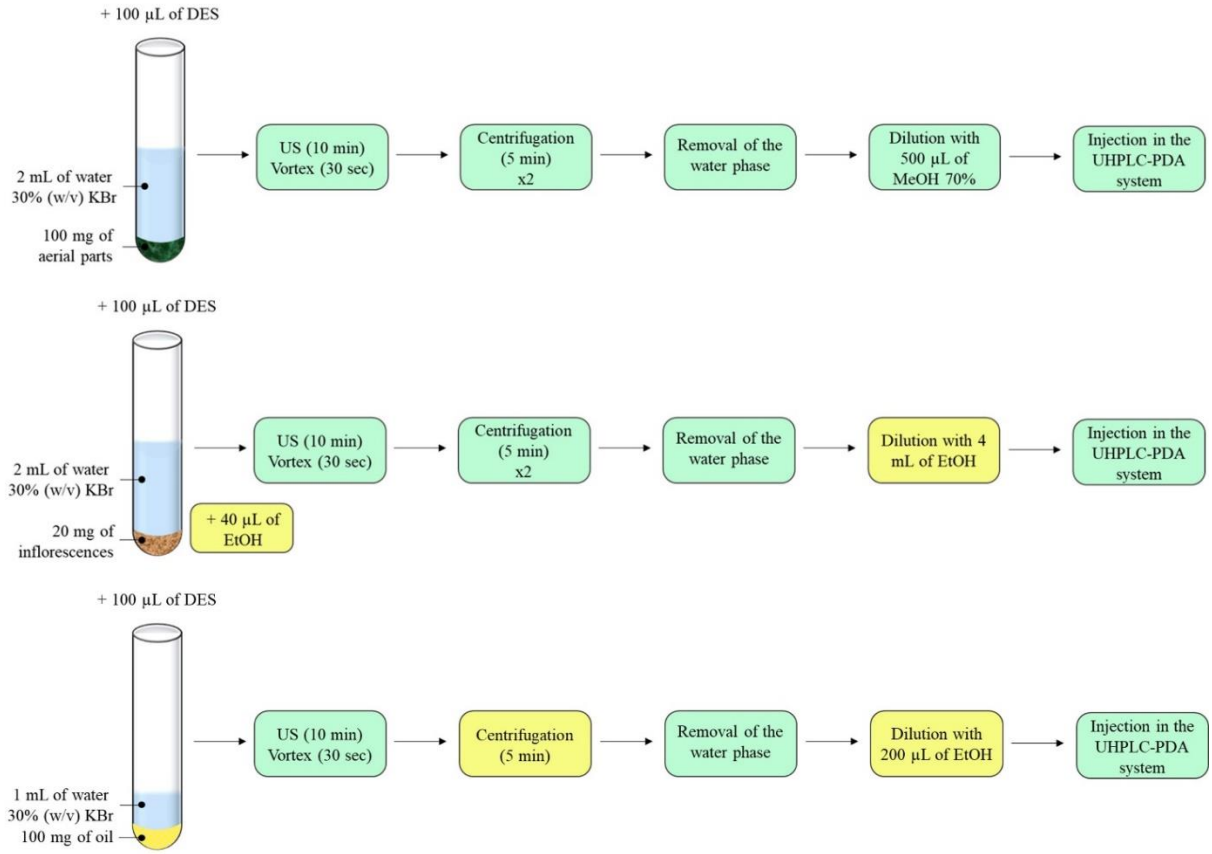

Figure 2. Ultrasound-assisted dispersive solid-liquid microextraction method optimized for the analysis of different hemp products (aerial parts, inflorescences, and CBD oil). The differences between the procedures are highlighted in yellow.

The chromatographic profiles obtained at 254 nm, for the three hemp products, are shown in Figure 3. As reported in our previous study[226], N16 ES allowed to increase the extraction of the more polar flavonoid compounds while maintaining a similar extraction efficiency of cannabinoids compared to the reference ML hydrophobic solvent. As for the inflorescences, the extraction of both the acidic and neutral forms of CBD was improved with N16 solvent. The hydrophobic properties of $[Ch^+][Br^-]$-based HESs, together with hydrophilic domains (hydroxyl group and charge on the ammonium group) seem to facilitate the interaction with both polar and less polar compounds.

Apart from the extraction performance of the ESs, their compatibility with reverse phase liquid chromatography was also investigated since chromatographic techniques are fundamental for the analysis and study of plant metabolome to separate and identify the analytes of interest. The single components of the ESs (menthol, linalool, N16 and thymol) were injected to verify that the signal of the solvent (if present) did not interfere with the one of the target analytes. Only thymol, which features an aromatic ring in its structure, absorbed at the

wavelengths of analysis, however its signal did not interfere the signal of the analytes, as shown in the chromatograms reported in Figure 3. Because of the high concentration of thymol, blank injections of MeOH 100% were regularly repeated within the analysis of the extracts to detect potential carryover.

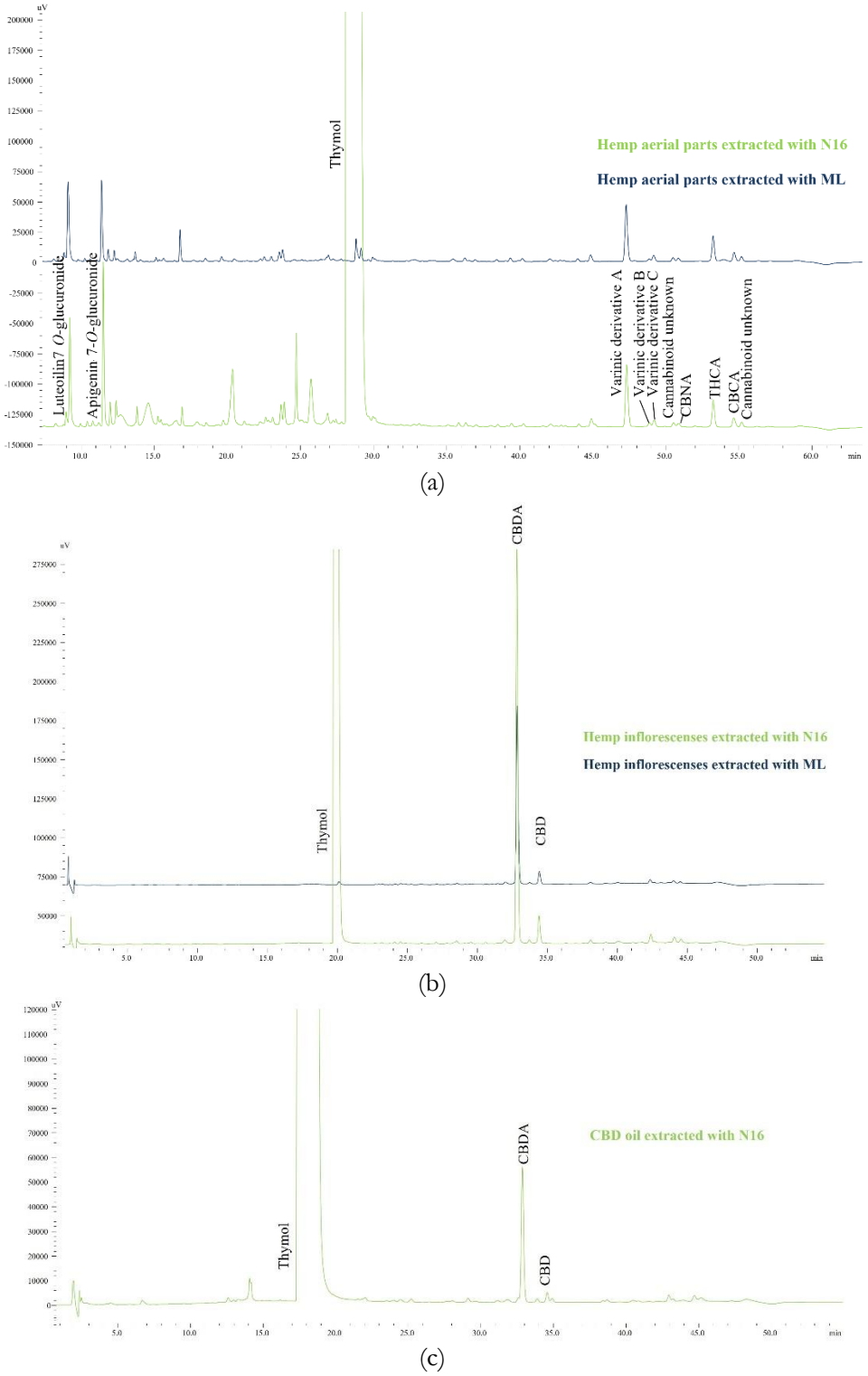

Figure 3. Chromatographic profiles at 254 nm, obtained after the UA-DSLME coupled to UHPLC-PDA of (a) hemp aerial parts (b) hemp inflorescences and (c) CBD oil. For name abbreviation, see Table 1.

3.5.5 Evaluation of the matrix effect

Matrix effect is known to affect the efficiency of chromatographic separation and the extraction efficiency of marker analytes, especially in the analysis of complex matrices [227,228]. Considering the complexity of the hemp samples under study, the contribution of matrix effect in the analysis of cannabinoids, was evaluated in the validation of the UA-DSLME approach developed. To reduce matrix effect during calibration, different strategies are available, among the main: (1) standard addition, (2) isotope labeled internal standard, and (3) matrix-matched calibration. The first approach is used when a blank matrix is not available, however in the case of analytes at high concentration (e.g. CBDA in the inflorescences) high amount of standard are necessary to build the calibration curve. The use of stable isotope labeled internal standards (SIL-ISs) is considered a valid approach to overcome ME, but the main disadvantages is the high cost and stability of SIL-ISs during sample preparation (deuterium can be exchanged with hydrogen) [227].To develop an affordable and easy applicable validation method, matrix-matched calibration was selected. In this case, the marker analytes are spiked to a blank sample and a linear calibration curve is built. The main disadvantage when studying specialized metabolites in plants is to find a matrix exactly similar to the sample and free of the analytes under study. To overcome this problem, an exhaustive extraction of the marker analytes was performed on the aerial parts and inflorescences of the plant, in order to obtain a matrix with similar characteristics to the real samples, avoiding the use of artificial matrices (made to simulate the authentic matrices in terms of composition, salts content, analyte solubility…), which can be tedious and challenging to prepare.

CBD oil is normally prepared by mixing CBD (usually in form of extract or inflorescences) with a carrier oil [229]. According to the label of the CBD oil used in this study, the hemp extract rich of CBDA and CBD was solubilized in fractionated coconut oil. While in the case of aerial parts and inflorescences, the exhausted blank matrix was employed for the validation of the method, pure coconut oil was used for CBD oil. The comparison of the chromatographic profile between the blank and the real samples is shown in Figure 4.

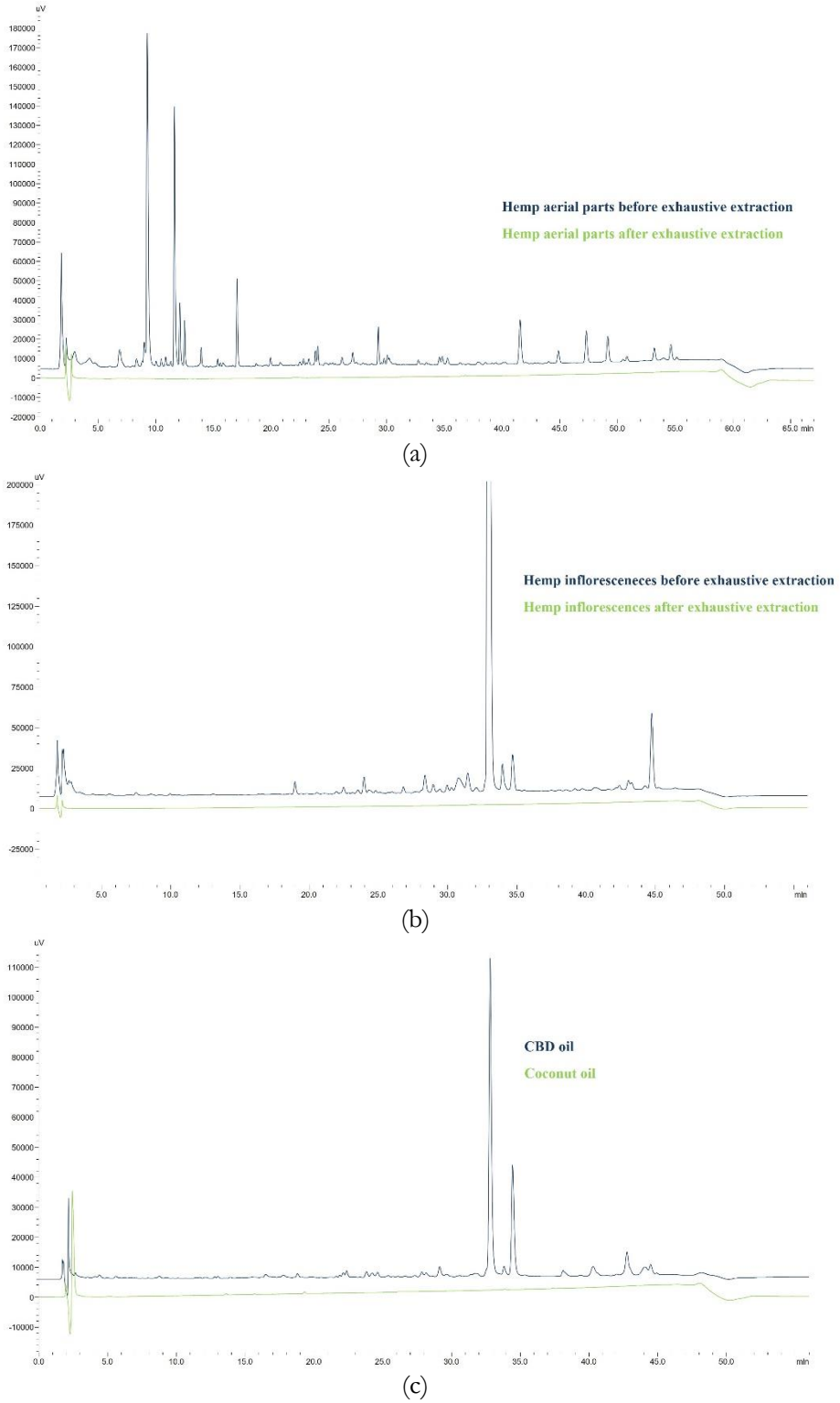

Figure 4. Comparison of the chromatographic profile at 254 nm of the (a) aerial parts, (b) inflorescences and (c) CBD oil, before and after an exhaustive extraction of the marker compounds.

For each sample, increasing concentrations (n=4) of CBDA (for aerial parts, where only cannabinoid acids were present) and CBDA and CBD (inflorescences and oil) were spiked to the blank matrix in order to build a calibration curve. The following ranges were used: 1.5 – 6 μg mL^{-1} for CBDA in the aerial parts, 0.8 – 4 μg mL^{-1} for CBDA and CBD in the inflorescences, and

0.25 – 4 μg mL^{-1} for CBDA and 2 – 6 μg mL^{-1} for CBD in the oil. The same calibration curve was built without the sample (blank), adding the standard mixture in water. For both the approaches, after the addition of the standard mix, the UA-DSLME with the two ESs (ML and N16) was performed.

The matrix effect (ME) of the three hemp extracts was calculated as the slope of the calibration curve built on the blank matrix (k_1) versus the one without the sample (k) using the following equation [230]:

$$ME = \left(1 - \frac{k_1}{k}\right) \times 100$$

Table 3 reports the ME value for the aerial parts, inflorescences and CBD oil after performing the UADSLME with ML and N16. The ME ranged from 26.56 % to 83.27% with higher values for the oil. These results highlighted the important contribution of the matrix effect that could not be overlooked for all the tested samples. For this reason, the calibration curves obtained in the blank matrix were used to measure the analytical performances of the method.

Table 3. Linear equations and matrix effect (ME) under different conditions for aerial parts, inflorescences and CBD oil after performing the UA-DSLME.

Compound name	Without matrix y = kx + b	Blank matrix y = k_1x + b	ME (%)
Aerial parts			
	Eutectic solvent ML		
CBDA	y = 12892x + 21655	y = 9809x + 10670	23.9
	Eutectic solvent N16		
CBDA	y = 27909x + 64828	y = 7740x + 19854	72.3
Inflorescences			
	Eutectic solvent ML		
CBDA	y = 6687x – 643	y = 4308x + 1345	35.6
CBD	y = 655x – 466	y = 482x – 315	26.6
	Eutectic solvent N16		
CBDA	y = 6953x - 557	y = 2962x + 1509	57.4
CBD	y = 751x – 851	y = 385x – 35	48.7
CBD oil			
	Eutectic solvent N16		
CBDA	y = 64438x + 4044	y = 29651x + 1909	54.0
CBD	y = 5671x – -463	y = 949x + 262	83.3

3.5.6 Analytical performance of the UA-DSLME method

As described in the previous section, the method was validated using a matrix-matched calibration, performing the entire UA-DSLME-HPLC-PDA method on blank matrices. CBDA and CBD were used as reference standards for the validation and quantification of cannabinoid acids and neutral, respectively, due to the similar physicochemical features. The neutral form usually presents two UV absorbtion maxima at 210 and 270 nm, while the acid form three UV absorbtion maxima at 220, 270 and 305 nm. Table 4 reports several quality analytical figures of merit of the method, the linearity range, the calibration sensitivity (evaluated as the calibration slope), determination coefficient (R^2), limit of quantification (LOQ), accuracy, enrichment factor (EF) and intra-day RSD. The λ selected for quantification of both CBDA and CBD was 270 nm. The LOQs were estimated as S/N of 10 and experimentally verified by injecting the standard compound at the predicted concentration. LOQ values ranged from 0.1 μg mL^{-1} and 1 μg mL^{-1}, depending on the matrix and solvent employed. The intra-day repeatability of the method was evaluated in terms of RSD (%) after performing three independent experiments within the same day. The intra-day RSD values were lower than 10%, showing a good precision of the method. The EF was calculated at 2 μg·mL^{-1} concentration of the standards mix and varied between 2 and 20. The accuracy of the method was calculated by testing the capacity of the matrix-matched calibration curves to predict a specific concentration in the real samples. The values ranged from 82% to 118%, showing a good accuracy of the developed method.

Table 4. Analytical performance of the overall UA-DSLME method for the determination of cannabinoids using ESs.

Compound	Working range ($\mu g \cdot mL^{-1}$)	(Slope ± SD[a]) 10^{-3}	R^2 [b]	$S_{y/x}$ [c] %	LOQ[d] ($\mu g \cdot mL^{-1}$)	EF[e]	Accuracy[f]	RSD[g]
Aerial parts								
Eutectic solvent ML								
CBDA	1.5 - 6	9.9	0.992	5.93	1	5	108	4.59
Eutectic solvent N16								
CBDA	1.5 - 6	7.7	0.995	5.21	0.6	6	116	2.43
Inflorescences								
Eutectic solvent ML								
CBDA	0.8 - 4	4.6	0.998	3.35	0.3	4	99	5.71
CBD	0.8 - 4	0.5	0.999	0.07	0.5	20	82	3.38
Eutectic solvent N16								
CBDA	0.8 - 4	3.4	0.992	7.84	0.3	5	92	1.96
CBD	0.8 - 4	0.4	0.992	6.88	0.5	20	91	4.69
Oil								
Eutectic solvent N16								
CBDA	0.25 - 4	36.1	0.993	8.96	0.1	3	118	5.26
CBD	2 - 6	1.0	0.998	2.67	1	2	104	8.21

[a] Standard deviation of the slope, [b] Determination coefficient, [c] Standard deviation of the residuals in percent (or error of the estimate), [d] Limit of quantification, were estimated as S/N of 10 and experimentally verified,[e] Enrichment factor, calculated on a standard concentration of 2 $\mu g \cdot mL^{-1}$, [f] Accuracy, calculated on a standard concentration of 3 $\mu g \cdot mL^{-1}$ for oil and inflorescences and 5 $\mu g \cdot mL^{-1}$ for aerial parts, [g] Intra-day relative standard deviation (n=3)

Figure 5 shows the quantification data, expressed as mg of cannabinoids in mL of extract of aerial parts, inflorescences, and CBD oil. The data were obtained performing the UA-DSLME method with both ML and N16 solvent. As already observed in the comparison of the chromatographic profile, N16 improved the enrichment of cannabinoids from the inflorescences (0.714 mg mL^{-1} for CBDA and 0.357 mg mL^{-1} for CBD with N16 *versus* 0.224 mg mL^{-1} for CBDA and 0.174 mg mL^{-1} for CBD with ML) while no relevant difference between the two solvent was found in the extraction of cannabinoids from the aerial parts. Because of the impossibility to perform the extraction of CBD oil with ML, quantification results were obtained only for N16. These results highlighted that the characteristics of the samples under study highly affected the overall analytical method, in terms of sample preparation and analytical performance. Even in the case of inflorescences and aerial parts samples, where the physicochemical differences are less evident (compared to CBD oil), the extraction performance of cannabinoids varied according to the solvent used.

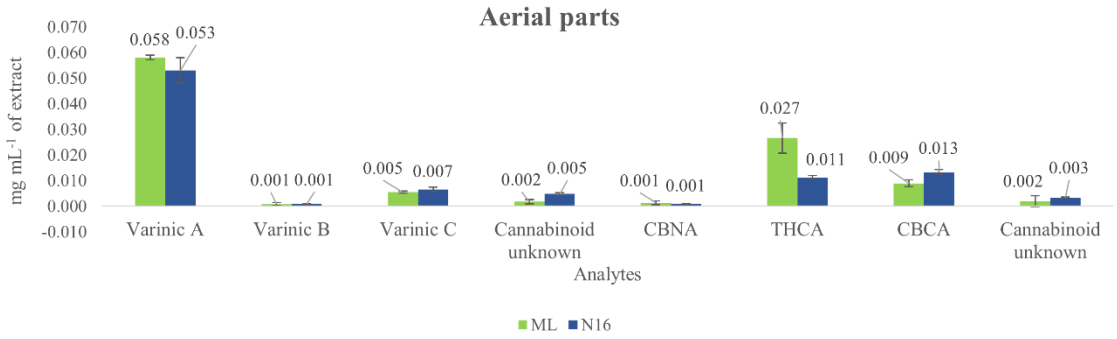

(a)

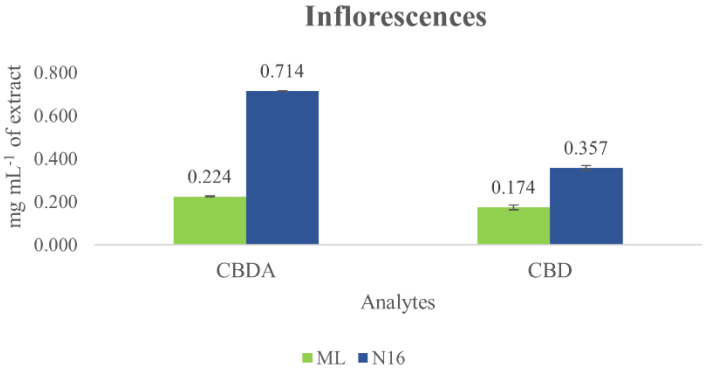

(b)

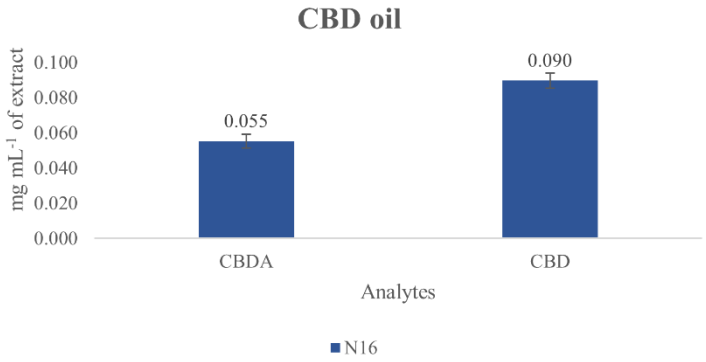

(c)

Figure 5. Quantification data for cannabinoids, expressed as mg of compound in 1 mL of extract, obtained after performing the UA-DSLME with ML and N16 solvents (n=3).

3.5.7 Comparison with other extraction methods

When developing new extraction methods, it is fundamental to compare the procedure and the analytical performance with reference methods reported in literature. Table 5 provides several examples of extraction methods developed for the analysis of cannabinoids in the aerial parts, inflorescences of *C. sativa* L. and CBD oil, together with the methods reported in this study. Organic solvents, such as EtOH or MeOH, are normally employed for the extraction of

cannabinoids, independently from the matrix under study. Hydrophilic DESs have also been successfully applied for the analysis of cannabinoids in hemp leaves. In the case of CBD oil, the most common approach is the dilution of the oil before the injection into the analytical platform. The direct injection of oil samples in the LC system can lead to some problems, depending on the viscosity and complexity of the carrier oil used to prepare CBD oil. The dilution of the sample can help to solve this drawback, but it can affect the enrichment of marker analytes and the limit of detection of the method. For most of the methods reported, external calibration is used for quantification. As shown by this study, matrix effect highly influences the response of marker compounds and it should be taken into consideration during the validation of the method.

Table 5. Analytical methods adopted for the determination of cannabinoids in different hemp products.

Sample (g)	Analytes	Sample treatment	Extraction material (mL)	Analytical platform	Quantitative method	LOD[a] of CBD	Ref
Aerial parts (no flowers)							
Leaves and stems (0.1)	8 cannabinoids	UA-DSLME	ESs (0.1)	UHPLC-PDA	Matrix-matched calibration	0.3-0.1 $\mu g \cdot mL^{-1}$	This work
Leaves and stems (0.1)	12 cannabinoids	Solid-liquid extraction	MeOH (15)	UHPLC-PDA-MS	External calibration	/	204
Leaves and stem barks (0.4)	14 cannabinoids	Solid-liquid extraction	MeOH (20)	HPLC-UV-MS	External calibration	0.0004-0.004 $\mu g \cdot mL^{-1}$	175
Leaves (0.2)	CBD	Solid-liquid extraction	Hydrophilic DESs[b] (5)	HPLC-UV	External calibration	/	56
Inflorescences							
Fiber-type cannabis (0.02)	CBDA, CBD	UA-DSLME	ESs (0.1)	HPLC-PDA	Matrix-matched calibration	0.4 $\mu g \cdot mL^{-1}$	This work
Fiber-type cannabis(0.25)	4 cannabinoids	Solid-liquid extraction (DM[c], UAE[d], MAE[e], SFE[f])	EtOH (10)	HPLC-PDA-MS/MS	External calibration	0.7 $\mu g \cdot mL^{-1}$	231
Fiber-type cannabis (0.05)	5 cannabinoids	Solid-liquid extraction	MeOH (5)	HPLC-UV	External calibration	/	232
Fiber-type cannabis (0.4)	CBDA, CBD	Solid-liquid extraction (DM, UAE, MAE)	EtOH (20)	UPLC-PDA	External calibration	0.07 $\mu g \cdot mL^{-1}$	192
Oil							
MCT[g] from coconut oil (0.1)	CBDA, CBD	UA-DSLME	ESs (0.1)	HPLC-PDA	Matrix-matched calibration	1 $\mu g \cdot mL^{-1}$	This work
Different carrier oil (/)	CBD, THC	Dilution	MeOH/water (/)	HPLC-PDA	External calibration	0.25 $\mu g \cdot mL^{-1}$	233
Different carrier oil (0.01)	11 cannabinoids	Dilution	Isopropanol /MeOH (0.8)	HPLC-PDA	External calibration	/	234
Hemp leaves oil extract (0.1)	CBDA, CBD	Liquid liquid extraction	ACN (0.5) H_2O (5)	HPLC-PDA	Matrix-matched calibration	1.94 $\mu L \cdot mL^{-1}$	235

[a] Limit of detection, [b] HBA: Choline chloride, betaine, HBD: D-sorbitol, urea, oxalic acid, benzoic acid, citric acid, ethyl tartrate, zinc chloride, lactic acid, glycerol, salicylic acid, succinic acid, mannitol, acetamide, [c] Dynamic maceration, [d] Ultrasound-assisted extraction, [e] Microwave-assisted extraction, [f] Supercritical fluid extraction, [g] Medium chain triglycerides

3.5.8 Measurement of greenness of the method using AGREEprep, BAGI and SPMS metrics

Several green metrics have been developed in recent years to "measure" objectively the greenness of analytical procedures. Every metrics consider different aspects of the analytical method and it is important to select the most suitable metric according to the procedure employed and the information that the user want to obtain[16]. In this study, sample preparation step was the fundamental and most critical part of the overall method. In fact, the complexity of the matrices under study required a sample pre-treatment before the analysis in the HPLC-PDA system. Sample preparation is known to have a significant impact on the sustainability of the overall analysis process as they often require the use of disposable materials, energy-consuming equipment and instrumentation, and extraction methods that employ harmful solvents. The UA-DSLME method developed aimed to improve several of the listed aspects, anyway sample preparation was still necessary. AGREEprep metric is the modified version of AGREE tool and was developed to measure the impact of sample preparation [21]. For this reason, AGREEprep was selected to compare the greenness of sample preparation methods used in this study. Figure 6 shows the comparison of the pictograms obtained for the UA-DSLME on the aerial parts, inflorescences and CBD oil, using N16 and ML solvents and the one obtained for the reference MeOH extractions (see Chapter II). The energy consumption was measured with a Zhurui PR10 power meter plug (Zhurui, China). The overall outcome gives by the metric goes from 0 to 1, where 1 means that the criteria of green sample preparation (GSP)[15] are completely fulfilled. As shown in Figure 6, the UA-DSLME approaches have similar scores (around 0.5), meaning that the principles of GSP are partially satisfied. Low values are attributed to *ex situ* sample preparation (criterion 1), due to the impossibility to integrate this step with sampling. Moreover, the developed UA-DSLME is a manual procedure with no degree of automation (criterion 7). In fact, specific and customized tools would be necessary to fully-automated this method. The use of HPLC is also considered a negative aspect due to the high consumption of energy and solvent (criterion 9). On the other hand, the use of a low volume (100 μL) of natural solvents is positively considered by the metric. The few modifications applied for the UA-DSLME on inflorescences allowed to obtain slight improvements to the greenness, due to the low sample amount required (20 mg) and the replacement of MeOH with EtOH (lower number of pictograms in the material safety data sheet) in the final dilution. Regarding CBD oil, only one centrifugation step was

necessary to separate the sample from the ES rich phase, simplifying and reducing the number of sample preparation steps to perform. In general, the use of N16 ES slightly reduced the greenness of the method, due to the synthetic process necessary to obtain the [Ch^+][Br^-]-modified salt. However, as previously discussed, N16 can improve the extraction of some marker analytes, thanks to its peculiar structure, justifying its application. In this regard, several authors have highlighted that in the development of analytical methods, the greenness of a methodology should not be at the expense of its functionality[22,236]. For all the three hemp samples, the use of UA-DSLME improved the final score of the method, compared to the reference one. Regarding the aerial parts and the inflorescences, the main drawbacks of the reference method are the use of quite high volume (15 mL) of MeOH and the need to purify the extract by SPE, making tedious and time-consuming the entire process. The low score obtained for the MeOH extraction of CBD oil is due to the high energy consumption necessary to freeze the oil and separate the MeOH layer. Moreover, this approach has a low sample throughput, because each sample require 1 hour of freezing before being analyzed.

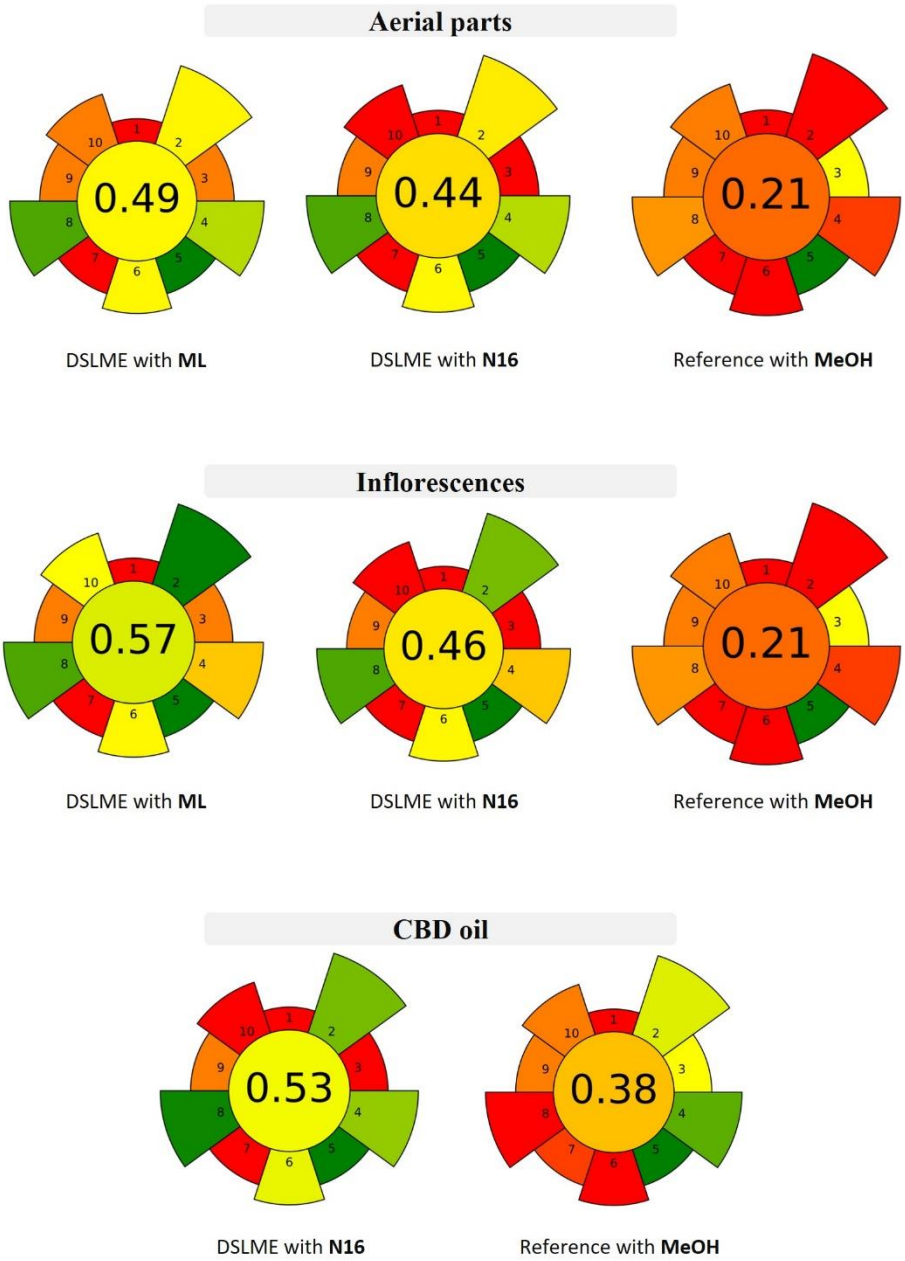

Figure 6. Pictograms obtained with AGREEprep[21] for the UA-DSLME and reference methods using ML, N16 and MeOH solvents for the analysis of the aerial parts, inflorescences and CBD oil. Criterion considered by the metric: 1. Sample preparation placement, 2. Hazardous material, 3. Sustainability and renewability of materials, 4. Waste, 5. Size economy of the sample, 6. Sample throughput, 7. Integration and automation, 8. Energy consumption, 9. Post-sample preparation configuration for analysis, 10. Operator's safety.

More recently, other metrics, namely Blue Applicability Grade Index (BAGI)[237] and Sample Preparation Metric of Sustainability (SPMS)[238] have also been introduced. The first focuses on measuring of the productivity and practical efficiency of the method, a parameter already introduced by Novak *et al.* with the concept of White Analytical Chemistry[22]. The second aims to exclusively evaluate, in term of sustainability, the sample preparation step, without considering the sampling and the instrumental technique, parameters normally covered by other

metrics. As for AGREEprep, the two metrics were applied to the UA-DSLME method on the aerial parts, inflorescences and CBD oil, using N16 and ML solvents and to the MeOH reference extractions. The pictograms are reported in Figure 7 and 8.

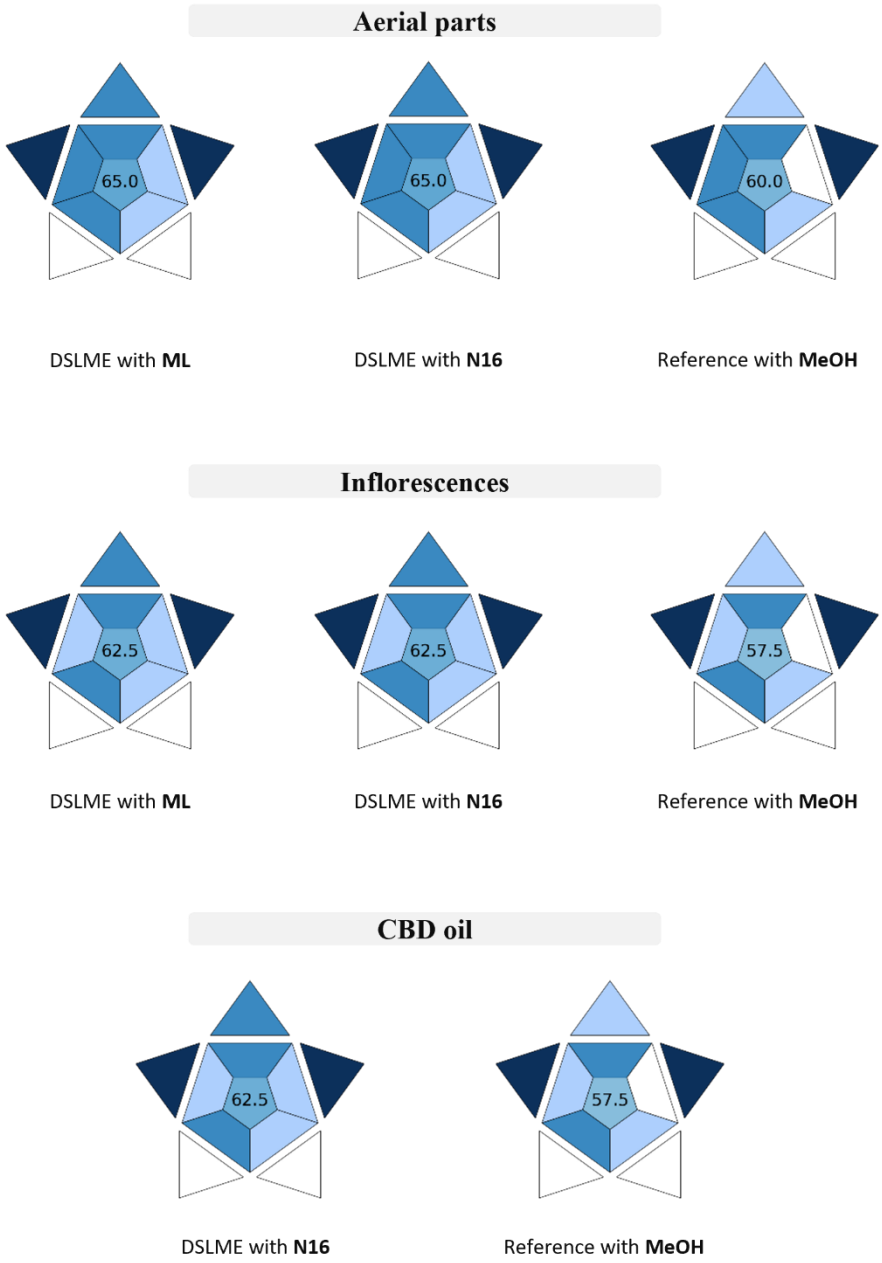

Figure 7. Pictograms obtained with BAGI metric[237], for the UA-DSLME and reference methods using ML, N16 and MeOH solvents for the analysis of the aerial parts, inflorescences, and CBD oil. Criterion considered by the metric: 1. The type of analysis, 2. The number of analytes that are simultaneously determined, 3. The analytical technique and required analytical instrumentation, 4. The number of samples that can be simultaneously treated, 5. The sample preparation, 6. The number of samples that can be analyzed per hour, 7. The type of reagents and materials used in the analytical method, 8. The requirement for preconcentration, 9. The automation degree, 10. The amount of sample.

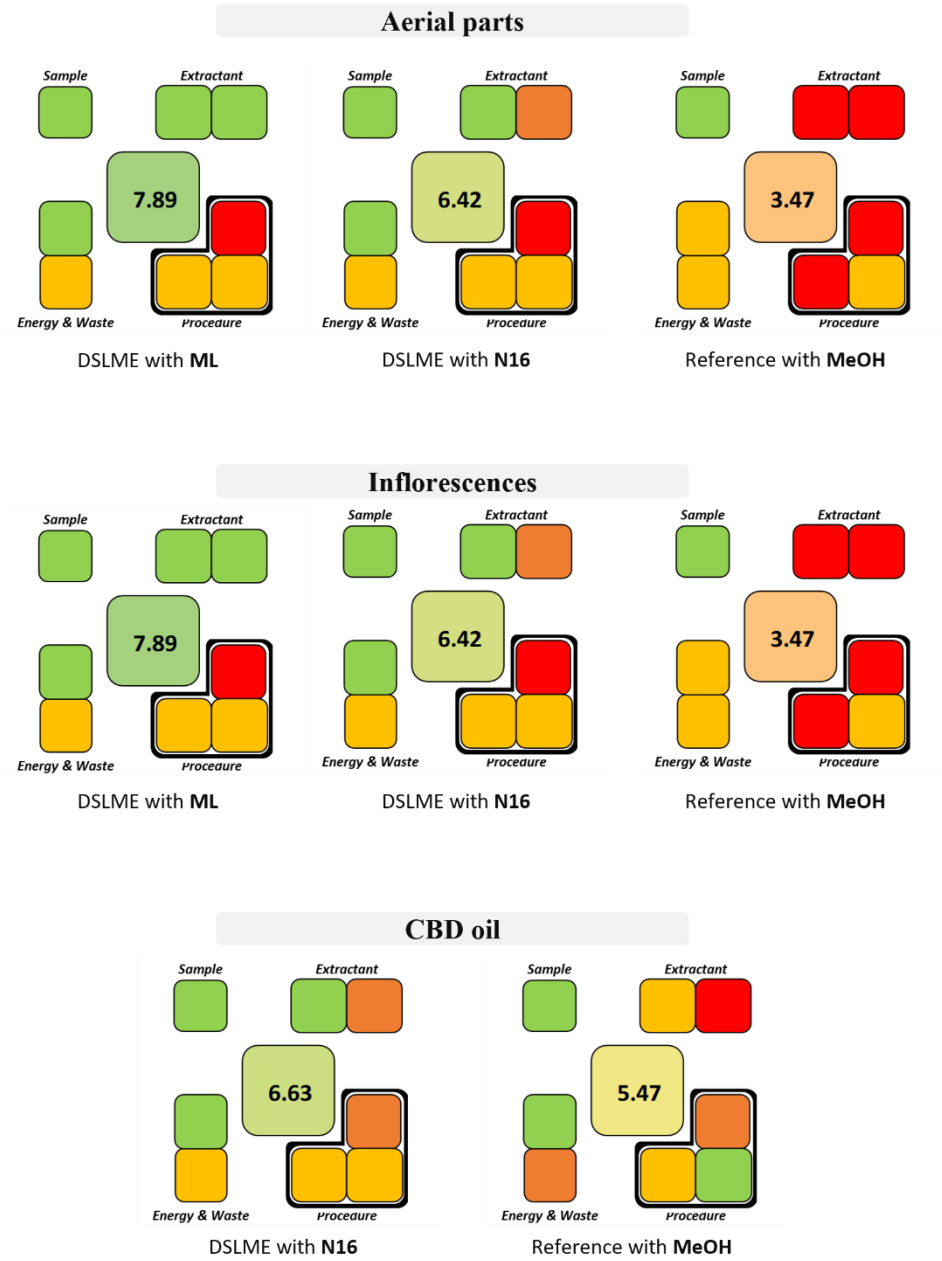

Figure 8. Pictograms obtained with SPMS metric[238], for the UA-DSLME and reference methods using ML, N16 and MeOH solvents for the analysis of the aerial parts, inflorescences, and CBD oil. Criterion considered by the metric: 1. Sample amount, 2. Amount of extractant, 3. Nature of extractant, 4. Number of steps, 5. Extraction time, 6. Additional steps after extraction, 7. Samples throughput, 8. Dispersion/stir, 9. Separation, 10. Temperature, 11. Waste, 12. Reusable.

Table 6 reports the final scores and the color code obtained for each method by the three metric tools. In terms of greenness, a similar ranking was obtained by AGREEprep and SPMS, where the UA-DSLME method with natural ESs was classified with the highest score. The methods developed in this study, mainly differ for the sample preparation step, while the sampling and the instrumental part are similar. Indeed, the use of a chromatographic technique reduces the "absolute" greenness of the developed methods when evaluated with AGREEprep

(about 50% of the maximum score in contrast to 65-80% obtained with SPMS). Moreover, it can be observed that no difference can be seen for the UA-DSLME methods applied to solid samples (aerial parts and inflorescences) with the SPMS metric, showing that the improvements due to further miniaturization and the replacement of MeOH by EtOH are not recognized. The classification given by BAGI was less effective to distinguish between the different methods, because the criteria considered by this metric are more focused on the productivity (e.g multi-element analysis, degree of automation) and less on the greenness of the method (e.g nature of the extractant, operator safety). For instance, the extraction of compounds from different chemical classes (i.e flavonoids and cannabinoids) in the aerial parts, was positively evaluated by BAGI. Because the aim of this study was to improve the sustainability of a method applicable for the determination of phytochemicals in different hemp matrices, AGREEprep and SPMS gave a better understanding of the strengths and weaknesses of the developed approaches. Because several green metrics have been proposed so far, depending on the application, it is important to select the best tool to obtain feedback in line with the scope of the analysis.

Table 6. Total scores of the analytical methods used in this study, obtained by AGREEprep, BAGI and SPMS metrics.

Method	Sample	Extraction material	AGREEPrep[a]	BAGI[b]	SPMS[c]
Developed methods					
UA-DSLME	Aerial parts	ML	0.49	65	7.89
		N16	0.44	65	6.42
UA-DSLME	Inflorescences	ML	0.57	62.5	7.89
		N16	0.46	62.5	6.42
UA-DSLME	Oil	N16	0.53	62.5	6.63
Reference methods					
SLE	Aerial parts	MeOH	0.21	60	3.47
SLE	Inflorescences	MeOH	0.21	57.5	3.47
SLE	Oil	MeOH	0.38	57.5	5.47

[a] Global score: from 1 if the criteria is completely fulfilled to 0 if not fulfilled, color code: from green (completely fulfilled) to red (not fulfilled)[21], [b] Global score: from 100 if the criteria is completely fulfilled to 25 if not fulfilled, color code: dark blue for high, blue for medium, light blue for low, and white for no compliance with the set criteria[237], [c] Global score: from 10 if the criteria is completely fulfilled to 1 if not fulfilled, color code: green for successful, yellow for acceptable, orange for tolerable, and red for inadequate[238].

The determination of the chemical composition of established and emerging hemp products is of utmost importance for regulatory authorities, to guarantee the efficacy and safety in the use of these products. The main challenges of these analyses are related to the complex phytochemical profile of *Cannabis sativa* L. and the diversification of hemp products, that also includes forms of cannabis available on the illicit drug market.

Metal-organic frameworks in matrix solid-phase dispersion for the extraction of phytochemicals from *Cannabis sativa L.* aerial parts

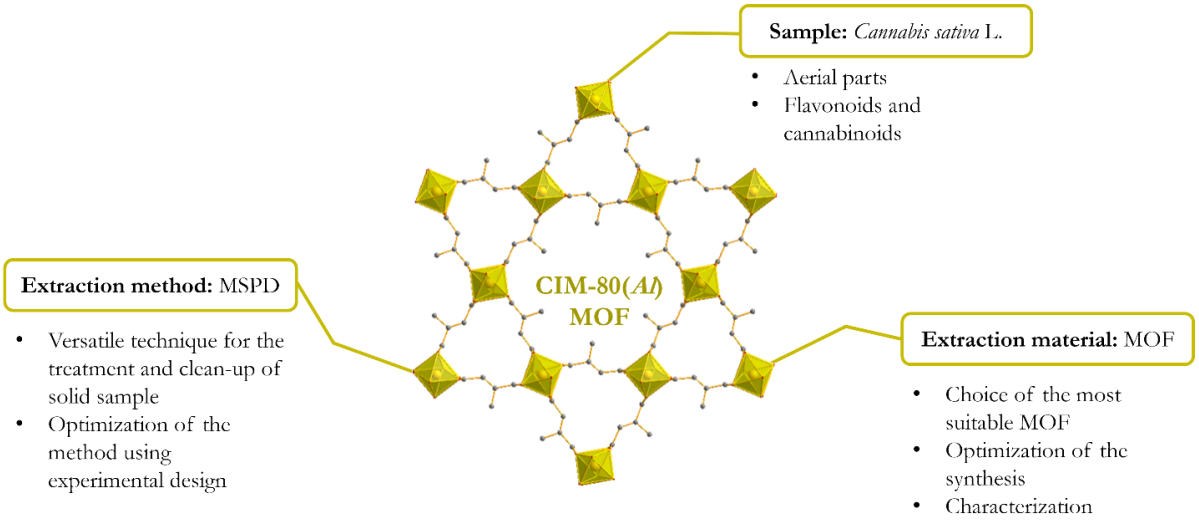

3.6 Metal-organic frameworks in matrix solid-phase dispersion for the extraction of phytochemicals from *Cannabis sativa* L. aerial parts

This Thesis has mainly investigated the extraction performances of liquid phases for the detection of phytochemicals in plant matrices. In fact, due to the complexity of plant samples (most of the matrices are solid), liquid phases are normally preferred since they easily interact with the analytes of interest thanks to solvation properties. However, sorbent-based extraction approaches have also attracted much attention due to the possibility of taking advantage of material science technologies to prepare smart and task-specific solid materials[11,197]. As described in the introduction, a number of solid sorbents have been used as extraction phase in analytical methods. Metal-organic frameworks (MOFs) are a class of crystalline materials composed of metal ions connected by organic ligands through coordination bonds. These materials are characterized by the presence of accessible cages, tunnels and modifiable pores, and exhibit the highest known surface areas. Due to their impressive features, together with their versatility, MOFs have gained significant attention in different scientific field, including sample preparation. In this field, MOFs are employed as sorbents in different procedures, including solid-phase extraction and different modes of solid-phase microextraction[86,239]. However, few data are available regarding the capacity of MOF to extract phytochemicals from plants. In this study, we proposed the use of MOF as sorbent in matrix solid phase dispersion (MSPD) to extract non-volatile phytochemicals from *Cannabis sativa* L. This technique consists in the direct mechanical blending of the sample (usually a solid) with a solid sorbent, which allows to clean-up and homogenize the matrix[240]. *Cannabis sativa* L. aerial parts were used as sample since this matrix has been largely investigated in previous studies of this Thesis and the phytochemical composition was already known.

3.6.1 Comparing extraction performances of different sorbent in matrix solid-phase dispersion

In order to evaluate the extraction capacity and behavior of MOFs for this specific application, CIM-80(*Al*) MOF performance was compared with other sorbents, following the experimental conditions previously reported in literature for MSPD procedures with plant samples, with slight modifications[89,241–243].

C18 were selected as conventional sorbent usually employed in MSPD, while chitosan is a natural biopolymer that has been successfully exploited in sorbent-based microextraction method. Several MOFs were kindly provided by the MAT4LL research group at the Universidad de La Laguna (Tenerife, Spain) and after a preliminary screening (data not shown) CIM-80(*Al*) MOF was selected. This MOF was synthetized for the first time by MAT4LL research group, and it presents several advantages such as stability in water at different pH values, working temperature range from RT to 350 °C, and low cytotoxicity[244].

MSPD preliminary tests were performed on *Cannabis sativa* L. aerial parts and the analytes under study included luteolin 7-*O*-glucuronide, apigenin 7-*O*-glucuronide as more abundant compounds for flavonoids, and six cannabinoids compounds (three varinic cannabinoid acid derivatives, cannabinolic acid, tetrahydrocannabinolic acid and cannabichromenic acid). More information on phytochemical characterization of the sample are reported in Section III.3.2

Figure 1 includes the peak areas obtained with the different sorbents, using MPSD method. Under not-optimized conditions, 20 mg of sample were grinded with 20 mg of sorbent for 2 minutes. The mixture was then transferred in a glass tube with 1 mL of MeOH 85% and vortexed for 2 minutes. To separate the solid part to the liquid phase, the mixture was passed through a filter paper, using an empty SPE cartridge, previously activated with 250 μL of MeOH 85%. The extract was further filtrated with PVDF filters before the analysis by HPLC-PDA. A "control sample" (no MSPD) was also performed, where the plant was directly extracted with 1 mL of MeOH 85%, avoiding the grinding step with the sorbent. In this way, the real contribution of the sorbent (considering that a solid-liquid extraction with an organic solvent is necessary to desorb the analytes after the extraction) was studied. In fact, it can be observed that the peak area obtained with C18 and chitosan were lower than the extraction without sorbent. This may be explained by the fact that the desorption step was not effective to remove the target analytes that remained bounded to the sorbent. However, CIM-80(*Al*) presented higher peak area for flavonoid fraction, while for cannabinoids the difference is less marked. Taking into account these

preliminary results, a careful optimization of every step of the extraction was carried out to further enhance the extraction performance of this MOF.

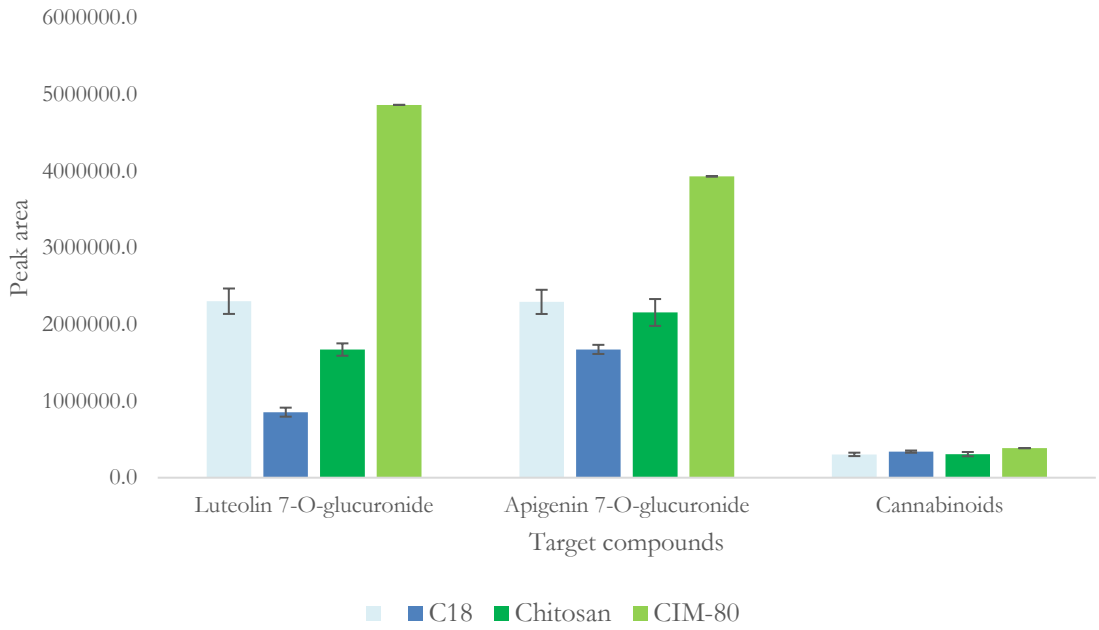

Figure 1. Preliminary screening of the extraction performance (evaluated as peak area) of the MSPD, using different sorbents. The preliminary experimental conditions for the MSPD were 20 mg of sample, 20 mg of sorbent, 2 minutes of grinding, desorption with 1 mL of MeOH 85%, filtration with paper filter in a SPE cartridge. No MSPD refers to the peak area obtained without adding the sorbent material, cannabinoids value refers to the peak area mean of the single cannabinoid compounds.

3.6.2 Optimization of the synthesis of CIM-80(*Al*) MOF

The synthesis of CIM-80(*Al*) MOF was based on Rocìo-Bautista *et al.*[244], with slight modification. Briefly, a mixture of mesaconic acid (1 mmol; 260 mg) and $Al(NO_3)_3 \cdot 9H_2O$ (1 mmol; 750 mg) was put in 30 mL of deionized water containing 0.5 mmol of urea (60 mg), under constant stirring for 20 min. Then, the clear solution is transferred to a Teflon lined stainless steel autoclave and kept at 150 °C for 24 h. Afterwards, the autoclave is cooled down to room temperature, and the obtained white product is isolated by filtration, washed three times with water and EtOH for activation, and air dried at 100 °C for 24 h. Based on the study presented by Figueroa-Quintero *et al.*[245], the molar ratio of urea and mesaconic acid (0.5:1) was modified, while maintaining constant the quantity of aluminum nitrate and deionized water. According to the study, by modifying the acid-base ratio it is possible to achieve high synthesis yields and materials with high crystallinity and accessible porosity. As shown in Figure 2, the optimal molar ratio between urea and mesaconic acid

was 3:2, allowing to obtain 50% of yield. The optimized synthesis procedure employed during this study is schematized in Figure 3.

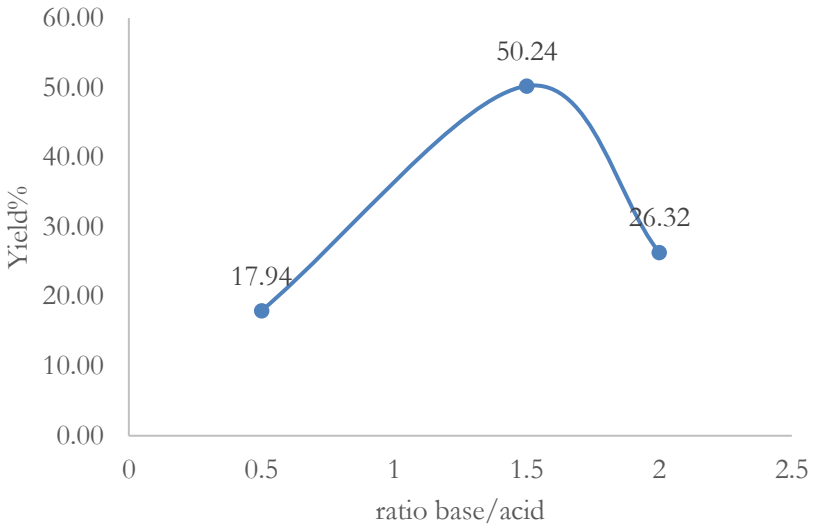

Figure 2. Reaction yield% of CIM-80(*Al*) MOF, modifying molar ratio of urea and mesaconic acid

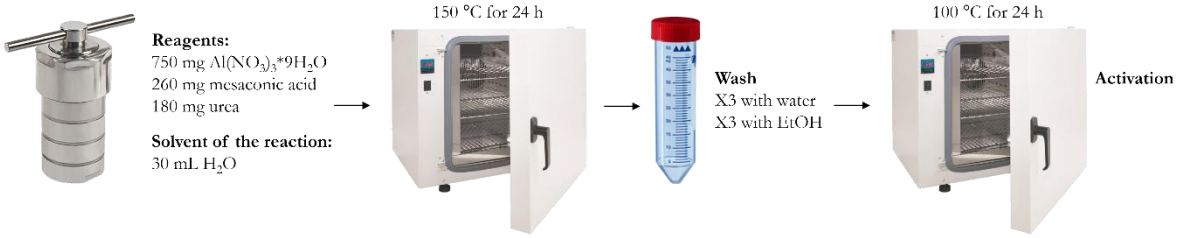

Figure 3. Scheme of optimized synthesis procedure for CIM-80(*Al*) MOF

3.6.3 Optimization of the extraction method

Before proceeding with the design of experiments for the optimization of the extraction method, some variables (filtration step and desorption solvent) were considered individually to reduce the number of factors to optimize in the following step.

Filtration step

To separate the solid part (sorbent + sample), a SPE-like procedure is usually employed in MSPD applications. In our case, simple paper filters were used to mechanically separate the two phases. Before the injection in HPLC-PDA system, a further filtration with PVDF filters was also included to prevent column-clogging and increment of back pressure. Filtration is a critical step of sample preparation because it can also retain the analytes of interest, decreasing their recovery. To ensure that no significant analytes lost occurred, the extraction was performed:

(i) without any filtration step, (ii) only with paper filtration, and (iii) only with PVDF filtration. The results were evaluated as peak area and represented in Figure 4.

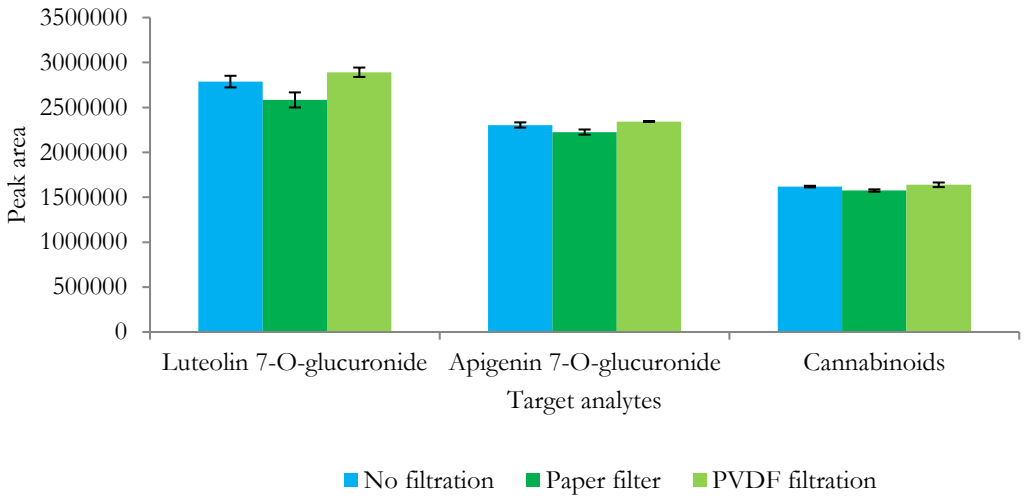

Figure 4. Comparison of peak area when no filtration, filtration with paper filter and PVDF filter is employed.

Although no relevant difference was observed between the three approaches, a slight decrease of peak area occurred when paper filtration was employed. For this reason, this step was replaced with centrifugation (2 minutes × 2200 g), which allowed a fast separation without consuming disposable materials. The extract was then passed through PVDF syringe filter.

Desorption solvent

When using solid sorbent, the desorption step is of utmost importance. In fact, the material can be very effective in the extraction, but if the desorption of the target analytes is not fulfilled, the extraction efficiency is compromised. MOFs are known to have enormous surface area and porosity; however, desorption can be challenging because of the formation of strong interactions. In this study, various organic solvents (normally employed for the extraction of flavonoids and cannabinoids) were tested, including methanol, ethanol, acetonitrile, and acetone, each prepared with 15% water content. From previous studies on the same matrix (Section III.3.2) this percentage of water is known to facilitate the extraction of the more polar flavonoids, without compromising the cannabinoid fraction. Figure 5 showed the comparison between the different solvents, performing MSPD method with CIM-80(*Al*).

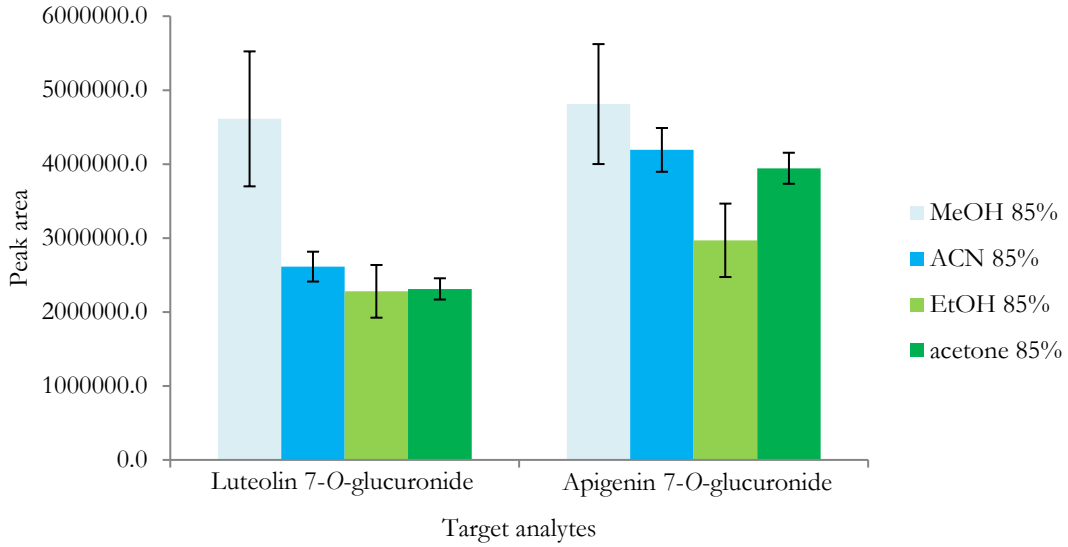

(a)

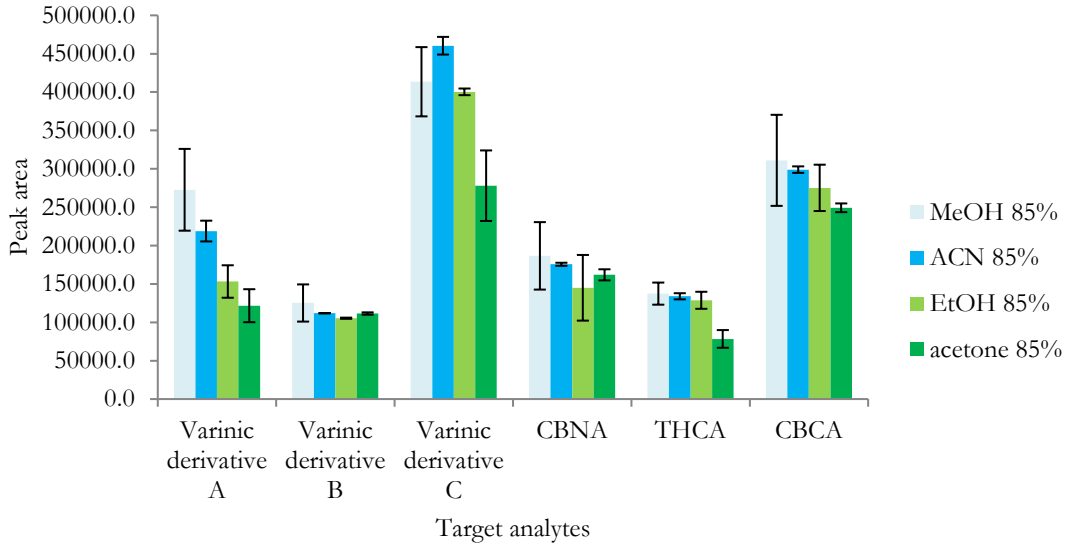

(b)

Figure 5. Comparison of different organic solvents for the desorption of (i) flavonoids and (ii) cannabinoids.

Methanol showed the best desorption capacity for flavonoid compounds. For cannabinoids, the difference between the solvents was less evident, however methanol and acetonitrile seemed to slight increase the peak area of the target analytes. In order to have good recovery for both class of compounds, MeOH was selected as desorption solvent for further optimization.

Screening factorial design

Once the filtration step and desorption solvents conditions were optimized, a screening test was carried out to determine which of the selected parameters (amount of sorbent, vortex time, volume of desorption solvent) significantly affected the extraction. For this test, the amount of sample was set to 20 mg (to reduce the consumption of material) the time of grinding to 2 minutes and the time of centrifugation to 2 minutes, since these timings provided a good homogenization and a fast phase separation. A full two-level factorial design (2^n, with n = 3 variables) was used, which comprises eight experiments combining the minimum and maximum values considered for each factor. Moreover, three replicates of the central point (intermediate value for each variable) were carried out, in order to monitor the reproducibility of the method. For the amount of MOF, the low and high limits were set at 10 and 40 mg, respectively. Regarding the vortex time, a minimum value of 1 minutes and a maximum value of 5 minutes was set, while the desorption volume ranged from 0.5 to 2 mL. These experimental values were selected with the aim of avoiding time- and energy-consuming steps, guaranteeing the use of low amounts of sample and reagents. Figure 6 reports the results obtained in the screening.

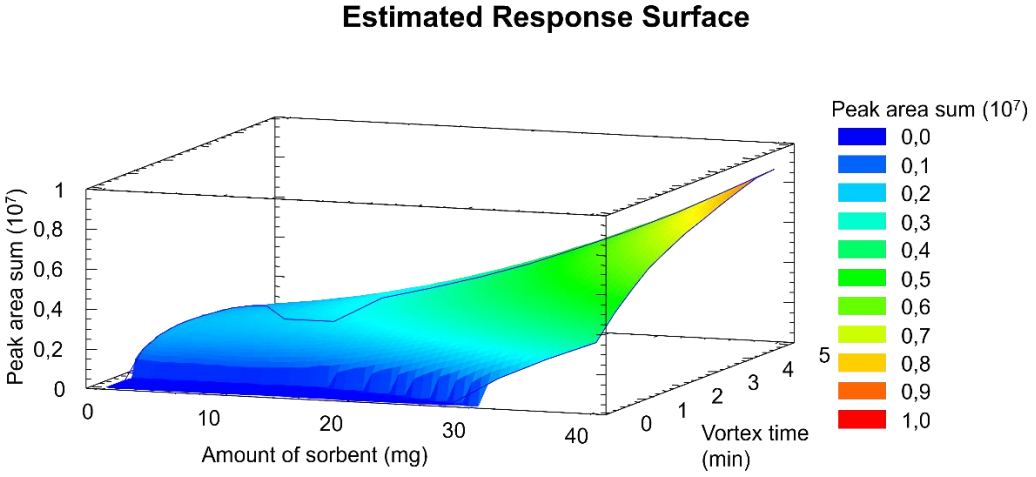

Figure 6. Results obtained in the screening of the main variables represented as estimated response surface for peak area sum of all target analytes.

Because all the compounds showed a similar trend, the response surface was obtained by considering the sum of the peak area for all target analytes. It can be observed that the maximum enhancement of the signal was obtained when 40 mg of sorbent, 4 minutes of vortex and 0.5 mL of desorption solvent were employed. These results showed that the extraction

efficiency was positively affected by the amount of sorbent, demonstrating its fundamental contribution. Moreover, a longer desorption step allowed to increase the release of the target analytes from the sorbent, also when a small volume was used. Taking into account these results, the optimum conditions for the MSPD method for the extraction of the flavonoids and cannabinoids were the following: 20 mg of sample, 40 mg of CIM-80(*Al*), 0.5 mL of MeOH 85% for desorption, 2 minutes of vortex and centrifuge. Figure 7 reports the optimized MSPD method.

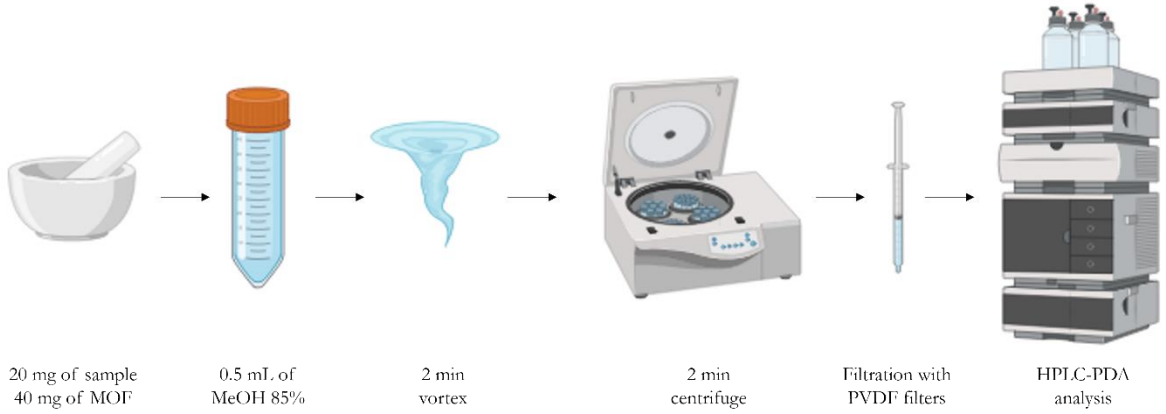

Figure 7. Scheme of the optimized MSPD extraction procedure with CIM-80(*Al*) MOF.

Evaluation of the biological activity of *Cannabis sativa* L. aerial parts: antioxidant activity and inhibition against enzyme involved in skin aging

This paragraph is reproduced from a published article
(Mastellone *et al.*, Plants 11, 2022, 419)

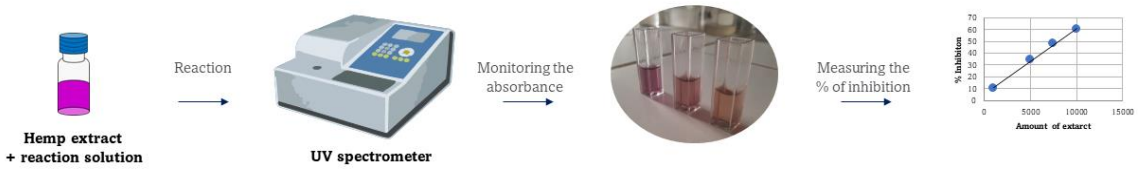

3.7 Evaluation of the biological activity of *Cannabis sativa* L. aerial parts: antioxidant activity and inhibition against enzymes involved in skin aging

3.7.1 Evaluation of the antioxidant activity

After the characterization and quantification of the main chemicals *Cannabis* samples, *in vitro* colorimetric assays, measuring the scavenging of $DPPH^{\bullet}$ and $ABTS^{+\bullet}$ radicals, were carried out to investigate the potential antioxidant activity of this matrices. The screening was carried out on the aerial parts of the plant, because of its richer phytocomplex, mainly composed of flavonoids and cannabinoids. The antioxidant power of flavonoids and phenolic compounds is well-documented, and it is closely linked to their chemical structures, able to reduce free-radical formation and to scavenge free radicals[246]. On the other hand, because of the growing interest in cannabis-derived products, recent studies have been focused on the biological activity of non-psychotomimetic cannabinoids[247–249], including the antioxidant one[250,251]. As for flavonoids, the antioxidant property is mainly related to the presence of phenolic groups easily oxidized to quinoid forms and of unsaturated bonds found in non-olivetolic fragments of some cannabinoid molecules[252].

Since the quantitation results (supported by statistical analysis, Section III.3.2) showed that the chemical pattern of the aerial parts is mainly affected by the drying conditions, the colorimetric assays were performed on two different pools of samples, oven-drying (OD) and freeze-drying (FD), composed by a mixture of the oven-dried and freeze-dried samples, respectively. Moreover, a comparison between the activity of methanolic and acetone extracts was carried out, the first being richer in flavonoids and the second in cannabinoids. Each assay was done in triplicate and the results are summarized in Figure 1.

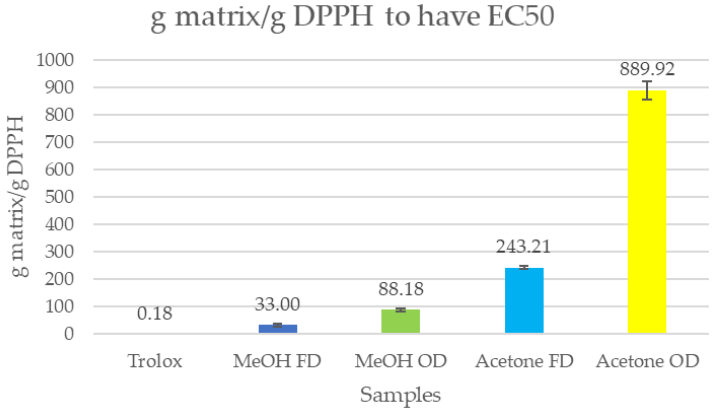

(a)

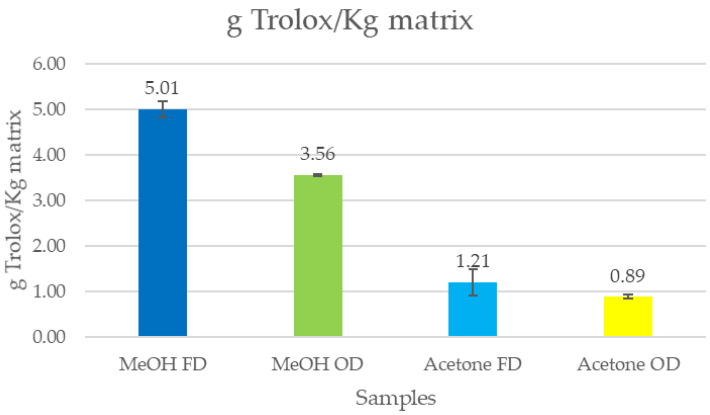

(b)

Figure 1. Results of the DPPH• and ABTS•+ colorimetric assays: (a) g of hemp matrix to obtain 50% of inhibition per 1 g of radical; and (b) g equivalent of (±)–6-hydroxy-2,5,7,8-tetramethylchromane-2-carboxylic acid (Trolox) that correspond to 1 kg of hemp matrix.

To build up the DPPH• inhibition curve to extrapolate the EC_{50} (concentration to inhibit 50% of DPPH), a range of concentrations of each extract (OD MeOH, OD acetone, FD MeOH, and FD acetone) was chosen to obtain a linear response (see Figure 2). For the $ABTS^{+\bullet}$ assay, the concentration of the extracts had to fit the Trolox response curve (absorbance as a function of concentration). Figure 1a reports the EC_{50} value for DPPH• radicals, and Figure 1b the g equivalent of Trolox for $ABTS^{+\bullet}$. For the DPPH assay, in which Trolox was used as control, the MeOH extract, both the FD and OD, presented a lower value of EC_{50} compared to the acetone one. The higher antioxidant capacity of the methanolic extract may be related to the presence of flavonoids, which are well-known for their antioxidant activity. The antioxidant activity of the samples seemed to also be affected, to a lesser extent, by the sample treatment. In particular, the FD samples, richer in bioactive compounds, exhibited a lower value of EC_{50}. Regarding the scavenging of ABTS, a similar behavior was observed, confirming the higher antioxidant power of the FD MeOH extract.

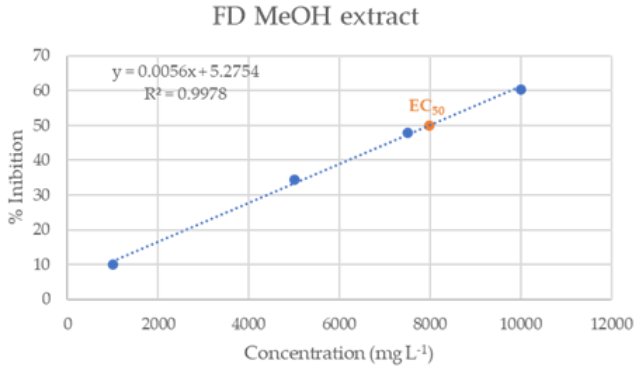

(a)

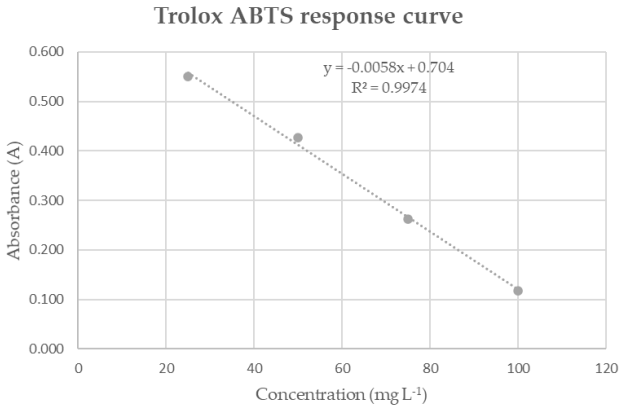

(b)

Figure 2. Representative response curve of FD MeOH extract (a) and Trolox (b), used to measure the scavenging effect on DPPH• and ABTS+•radicals, respectively.

Offline Combination of Antioxidant Assays with HPLC-UV Analysis

To further investigate the contribution of the main components of the extract on the total antioxidant power of the cannabis extracts, an HPLC-PDA analysis was coupled to the *in vitro* colorimetric assays. Methanolic and acetone FD extracts were screened because they have shown to better preserve the chemical composition of the plant. The chromatographic profile was compared before and after the reaction with DPPH• and $ABTS^{+\bullet}$ (see Figure 3) and the % of reduction of the most representative peaks was indicative of the interactions with the radicals and of their scavenging ability. The results are reported in Table 1. The $ABTS^{+\bullet}$ offline analysis was carried out on a different chromatographic column (RP Amide) because the peak of $ABTS^{+\bullet}$ radicals coeluted with some of the target analytes.

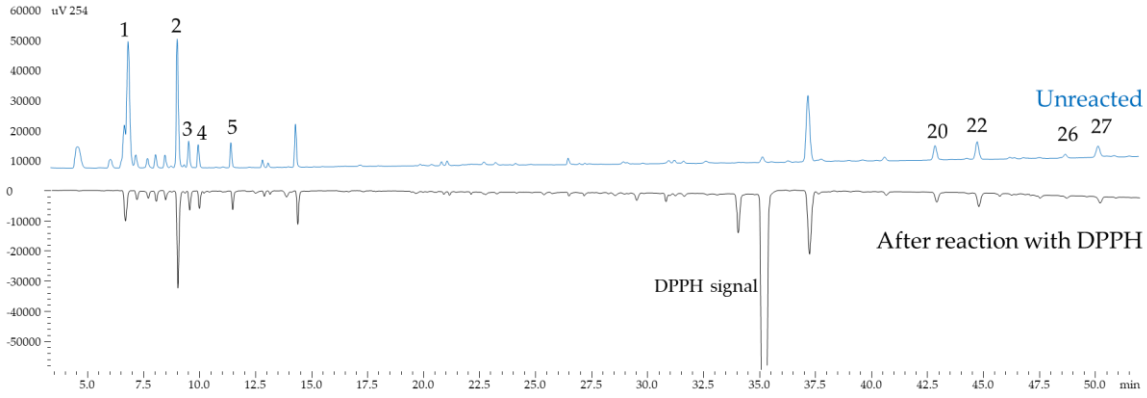

(a)

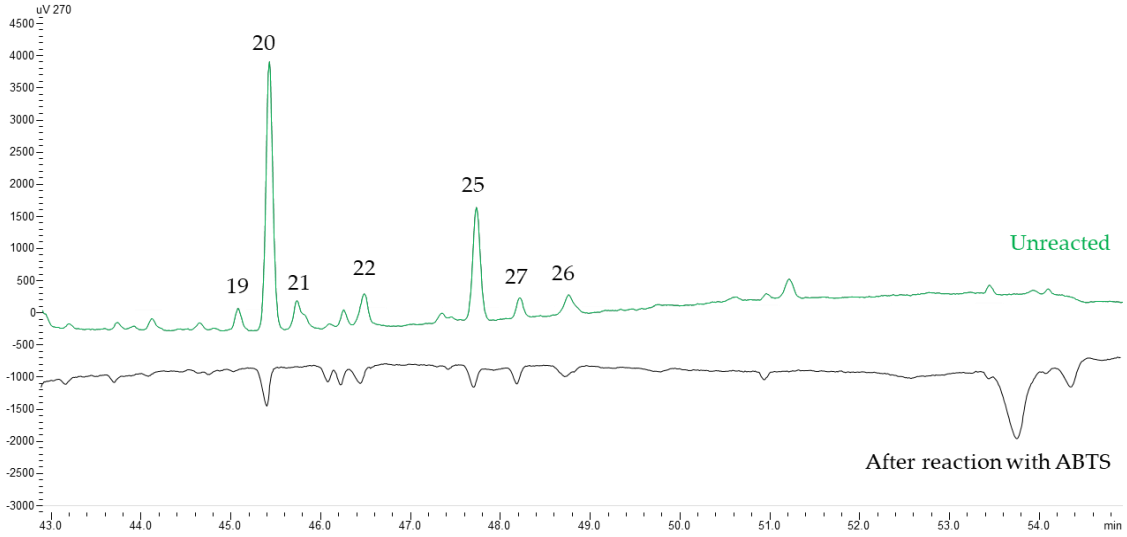

(b)

Figure 3. Representative chromatogram of (a) FD MeOH hemp profile before and after the reaction with DPPH$^{\bullet}$ radicals on C18 column and(b) acetone hemp profile before and after the reaction with $ABTS^{+\bullet}$ on RP-Amide column.

Among the flavonoids, luteolin 7-*O*-glucuronide presented the highest interaction with both radicals (peak area reduction >95%), which is probably related to its abundance and to the presence of an additional free hydroxylic group, compared to the other compounds of the same class. According to literature, the ortho position of the two OH groups on the benzene ring facilitates radical delocalization by resonance, justifying the major scavenging activity of this compound[253]. Cannabinoids showed a clear percentage reduction in the acetone extract, where flavonoids were not present, confirming that, although to a lower extent, they contributed to the total antioxidant power of the plant. Literature data report that in some cases cannabinoid acids may present a lower antioxidant activity compared to the neutral form

because of the hydrogen-bonding formation between the OH and COOH groups, which may decrease the transport ability of electrons[252]. However, the main cannabinoids found in the extracts were in an acid form and seemed to have a similar antioxidant activity as DPPH• radicals. A higher contribution of varinic derivative A and THCA to the total antioxidant activity was observed in the $ABTS^{+\bullet}$ offline analysis.

Table 1. Percentage of peak area reduction (±SD), after the reaction with DPPH• and $ABTS^{+\bullet}$ radicals, for MeOH and acetone extracts

Compounds	% Peak Reduction			
	DPPH•		$ABTS^{+\bullet}$	
	MeOH	Acetone	MeOH	acetone
Luteolin 7-*O*-glucuronide	>95(±0.09)	/	>95(±0.05)	/
Apigenin 7-*O*-glucuronide	19.6(±2.73)	/	18.3(±1.13)	/
Diosmetin glycoside A	24.7(±2.31)	/	37.4(±2.24)	/
Diosmetin glycoside B	22.3(±0.15)	/	/	/
Acacetin glycoside A	25.7(±0.54)	/	89.2(±3.04)	/
Varinic derivative A	27.9(±1.44)	40(±5.65)	/	76.5(±5.89)
Varinic derivative C	19.2(±1.38)	31(±2.28)	/	36(±4.94)
THCA	22.5(±3.77)	42.4(±1.11)	/	72.7(±5.73)
CBCA	42.1(±0.09)	52.1(±0.21)	/	35.3(±6.11)

3.7.2 Evaluation of the inhibitory activity against tyrosinase and elastase enzymes

The chemical characterization and the previous *in vitro* antioxidant assays had demonstrated that the most promising hemp extracts were obtained from FD samples because of the higher content in active compounds (Section III.3.2). For this reason, preliminary *in vitro* inhibitory activities against tyrosinase and elastase were tested on the pool composed by the mixture of the FD samples. Mushroom tyrosinase and elastase from porcine pancreas were used for these preliminary screenings of tyrosinase and elastase inhibition activities[254]. Again, the activity of the acetone extract (mainly characterized by non-psychotomimetic cannabinoids) was compared to the methanolic one, which presented a richer profile with both flavonoids and non-psychotomimetic cannabinoids. Figures 4a and 4b show elastase and tyrosinase reaction progress curves in the absence of any potential inhibitor (i.e., negative control, blue line), in the presence of the investigated extracts (green and red line), and in the presence of ursolic acid and kojic acid, which are elastase and tyrosinase reference inhibitors, respectively (i.e., positive control).

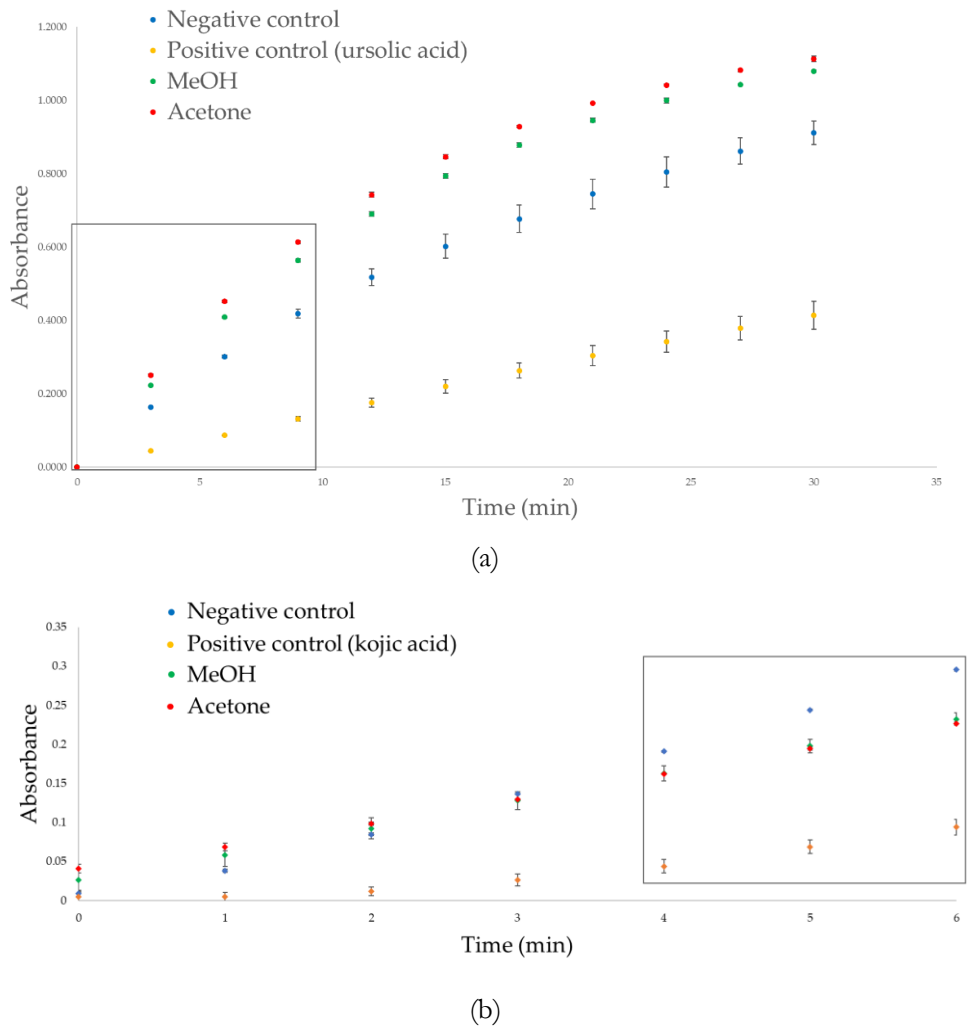

Figure 4. Reaction progress curve for (a) elastase inhibitory activity and (b) tyrosinase inhibitory activity of negative control, ursolic acid and kojic acid (0.2 mg mL^{-1}), MeOH hemp extract, and acetone hemp extract (50 mg mL^{-1}). The linearity region is indicated by the black rectangle.

Both the MeOH and acetone extracts, tested at 50 mg mL^{-1}, showed only slight activity against the selected enzymes. In particular, no inhibition was observed of elastase activity. The addition of both extracts to the reaction mix seemed to slightly increase the reaction initial velocities, but further experiments are needed to evaluate the presence of potential elastase activators within the investigated extracts[255]. As regards the tyrosinase inhibitory activity, in agreement with literature data[251,256] both extracts mildly inhibited mushroom tyrosinase activity, suggesting that, although to a minor extent, both flavonoids (higher in the methanolic one) and non-psychotomimetic cannabinoids (higher in the acetone one) could negatively affect tyrosinase activity. Percentages of tyrosinase inhibition of 33.17% ± 2.04% and 38.46% ± 1.36% were observed for the methanol and acetone extracts, respectively, when tested at a concentration of 50 mg mL^{-1}. The percentage of enzymatic inhibition was measured after six

minutes of incubation to remain under the linearity range of the reaction progress curve, which provides more accurate results[254]. These results were compared to those of kojic acids, which displayed a significantly higher activity (EC_{50} = 0.17 ± 0.015 mg mL^{-1}), indicating that the inhibition of the tyrosinase activity of hemp extracts is minimal.

Chapter IV
CONCLUSIONS

Conclusions

In this Doctoral Thesis, green sample preparation principles were applied to develop different analytical methods for the determination of non-volatile phytochemicals in plant matrices. The studies focused on different agri-food by-products produced in large amount in our territory, aiming to develop more sustainable strategies, from the exploitation of the natural source to its chemical treatment. Among the new extraction phases available, ILs, DESs and MOFs were employed for the sample preparation of complex samples in order to investigate their advantages and limits. In general, the studies presented demonstrated that is possible to improve the extraction approaches (fundamental for the characterization and exploitation of plants), by selecting the most suitable materials and techniques, without affecting the analytical performances of the overall method.

Apart from the chemical characterization, it is fundamental to take into account also the bioactivity and bioavailability of the compounds of interest. In fact, the use of plants as source of phytochemicals depends not only on their content but also on their activity. For this reason, the chemical characterization of every matrix was coupled with preliminary *in vitro* screenings to study their biological properties.

An overview of the main conclusions derived from this Doctoral Thesis is presented below depending on the sample, technique and the material employed as extraction phase.

Section III.1: *Vitis vinifera* L.

- A microwave-assisted solid-liquid extraction (MA-SLE) method was successfully developed for the determination of phenolic compounds from *Vitis vinifera* L. leaves. The method was optimized by using an experimental design and only requires an aqueous solution of the $C_{16}C_4$Im-Br IL-based surfactant in a low concentration, due to its low CMC in the MA-SLE procedure, followed by filtration and direct injection of the extract in the HPLC system. The method resulted in being more effective, simpler, and eco-friendlier in comparison with a more conventional ultrasound-assisted SLE (UA-SLE) method, particularly due to the absence of organic solvent or cleanup steps in the whole procedure. As an additional feature, the aqueous extractant medium avoids co-extraction of chlorophylls and other non-polar interfering compounds from the leaves. Moreover, the method also presented greener features compared to other strategies reported in the

literature dealing with the use of ILs or MA methods for the analysis of plant materials. The proposed methodology was used to determine and compare the phenolic composition of Italian and Canarian grapevine leaves varieties. The results showed that the distribution of the phenolic markers follows a similar pattern in all the cultivars, with quercetin glucuronide and quercetin being the most and least abundant compounds in the samples, respectively. In general, the Canarian varieties exhibited slightly higher total phenolic content, in comparison with the Italian cultivars and other varieties reported in the literature. Considering the previous studies on the potential of grapevine leaves as a source of antioxidant compounds, these results emphasize that these by-products are a source of nutraceutical compounds independently of the variety and geographic origin.

- The quali-quantitative comparison of polyphenol content in different *Vitis vinifera* L. green pruning residues before and after *in vitro* digestion revealed that these compounds are highly stable under the tested conditions and the phenolic compounds are more abundant in the bioaccessible phase than in the excreted fraction. This study demonstrated that these matrices have some potential as sustainable source of active ingredients for nutraceutical purposes. Further investigations should be directed to evaluate the impact of intestinal absorption and the influence of intestinal microbiota on these phytochemicals.

Section IV.2: *Corylus avellana* L.

- The primary aim of this study was to investigate whether natural deep eutectic solvents (NADESs) could be a suitable sample preparation technique for the characterization of polyphenols in hazelnut skin by-products. Different choline-based and betaine-based solvents were prepared and tested. The results proved that these NADESs had the capacity to extract all the compounds of interest with similar performances to the hydroalcoholic extraction method. Moreover, the method was simplified, and the volume of extraction solvent reduced. Overall, the use of these natural solvents should be considered as a green alternative analytical approach for the valorization of hazelnut by-products.
- After demonstrating the applicability of NADESs for the extraction of polyphenol from hazelnut skin, the *in vitro* scavenging activity of NADES-based extracts and the contribute

of these extraction solvents to the total antioxidant activity of the hazelnut extracts, was investigated. Different responses were obtained using $DPPH^{\bullet}$ and $ABTS^{\bullet+}$ tests: in the first experiment, a higher variability of scavenging activity between the NADES-based extracts were observed. Moreover, the neat solvent demonstrated no contribution to the total antioxidant activity. In the case of $ABTS^{\bullet+}$ radical, all the tested extracts showed a similar inhibition and a slight contribution of the NADESs to the antioxidant power of the extracts. This finding could be justified by the different structure of the two radicals which interact in a different way with the extracts.

Section IV.2: *Cannabis sativa* L.

- The non-volatile fractions of fiber-type *Cannabis sativa* L. aerial parts (collected before flowering) were carefully characterized by UHPLC-UV-ESI-MS/MS using an optimized method of extraction. The method of drying, fundamental for storing the plant material, plays a fundamental role in preserving the chemical composition of the plant, especially for thermolabile compounds. The variation in the chemical patterns among the investigated growth stages is less marked and only the content of cannabinoids presented a slight increase at the stage closer to flowering. These results suggested that fiber-type *Cannabis sativa* L. aerial parts can be considered a valuable natural ingredient, considering that their chemical composition seems to be independent of the growth stage of harvesting, provided that they are collected before the flowering stage.
- An innovative dispersive solid liquid microextraction using natural eutectic solvents as extraction phase was proposed for the extraction of phytochemicals from fiber-type hemp matrices. In order to obtain optimal performance in term of sustainability but also efficiency, the dispersive solid-liquid microextraction (DSLME) method was optimized and validated, demonstrating to be faster, greener and easier to apply compared to a conventional SLE with MeOH, with comparable results in terms of extraction performances. The majority of the investigated ESs demonstrated to be more selective for cannabinoids compared to flavonoids enabling to efficiently extract this class of compounds directly from plant materials without using organic solvents. The tunability, stability, easy preparation, low cost and green features of the tested solvents make them good candidates not only for analytical application but also for industrial purposes, where

easy to handle processes are required. Further advances may be directed to study the interaction of these eutectic solvents with other bioactive compounds with similar chemical characteristics to cannabinoids, together with modifications of ES components to change the solvent selectivity.

- The chemical structure of choline was used as model to synthesize a new class of hydrophobic HBAs. Six different hydrophobic $[Ch^+][Br^-]$ derivatives were synthesized by increasing the length of alkyl chain substituents while maintaining the hydroxyl functional group. The $[Ch^+][Br^-]$-modified salts were mixed with thymol to obtain HESs, which were then characterized in terms of hydrophobicity, viscosity and solvation properties. To test their applicability in extraction studies, $[Ch^+][Br^-]$-based HESs were employed as solvents in a DSLME method for the analysis of *Cannabis sativa* L. plant, characterized by a unique phytocomplex that includes compounds with different polarity. In this regard, the hydrophobic features of $[Ch^+][Br^-]$-based HESs, together with hydrophilic domains (hydroxyl group and charge on the ammonium group) in their structure, facilitated the interaction with both polar and less polar compounds. In general, the lower viscosity of the $[Ch^+][Br^-]$-based HESs, compared to eutectic mixtures based on conventional hydrophobic HBAs, promoted the extraction of flavonoids and cannabinoids. Moreover, the extraction of flavonoids appeared to be enhanced by $[Ch^+][Br^-]$-based HESs with lower hydrogen bond basicity. Among the $[Ch^+][Br^-]$-based DESs tested, the HES comprised of the $[N_{1\,1\,16\,(2OH)}^+][Br^-]$ salt demonstrated higher extraction capacity, due to its low viscosity and peculiar solvation properties. Due to the promising extraction performances of the $[Ch^+][Br^-]$-based HESs for compounds of varying polarity in *C. sativa*, future advances will be directed to the application and validation of the DSLME method to different *C. sativa* samples.
- A simple ultrasound-assisted dispersive solid-liquid microextraction method was developed, using two different types of eutectic solvents, one prepared with a $[Ch^+][Br^-]$-modified salts as HBA and one based on natural compounds. The UA-DSLME method was tested for the analysis of cannabinoids in three different hemp products: the aerial parts of *Cannabis sativa* L. collected before flowering, the inflorescences of the plant and the CBD oil, and it resulted to be easily adaptable to matrices with different physicochemical properties. The validation of the procedure showed that the matrix effect

played a fundamental role in the extraction efficiency of the marker analytes for the three samples, therefore a matrix-matched calibration was employed to evaluate the analytical performance of the methodology. The ES formed by the $[Ch^+][Br^-]$-modified salt showed better extraction performance for all the hemp products tested, but slightly lower sustainability (a synthetic reaction is necessary) compared to the natural ES. These results highlighted the importance to balance and consider both these aspects (greenness and functionality) in the development of analytical methods, to obtain truly innovative, efficient, and reliable methodologies.

- The potential of CIM-80(*Al*) MOF as sorbent in MSPD, for the pre-treatment of *Cannabis sativa* L. samples before LC analysis, has been investigated. The methodology was carefully optimized in all its steps, using experimental design to allows for multiple input factors to be manipulated. CIM-80(Al) MOF showed a good applicability for MSPD procedure for the extraction of flavonoids and cannabinoids from *C. sativa*. However, a more in-depth investigation is necessary to fully understand the interaction between this material and the target analytes. Moreover, quantitation data are fundamental to prove the applicability of this methodology as analytical method for quality control.
- The leaves and stems of the plant proved to be a valuable source of specialized metabolites (chiefly flavonoids and non-psychotomimentic cannabinoids) and their antioxidant activity was evaluated by colorimetric *in vitro* assays ($DPPH^•$ and $ABTS^{+•}$). Flavonoids presented the major influence on the antioxidant activity, but cannabinoids also showed a contribution to the total antioxidant power of the hemp extracts. The *in vitro* inhibitory activity against tyrosinase and elastase was also tested on methanolic and acetone extracts. No inhibition was perceived against elastase activity and a slight inhibition of the tyrosinase enzyme was observed for both of the extracts at high concentrations. In this sense, further studies on the biological activity of these extracts are necessary to confirm and support the preliminary results obtained with *in vitro* assays and to evaluate potential toxic effects at the tested concentrations. In particular, the isolation of enriched fractions of the more active compounds and further tests on cellular and animal models may provide a significant contribution for safe and future applications of hemp extracts.

Appendix

Appendix

Solvatochromic dye methods

The choice of dyes employed in calculating Kamlet-Taft solvent parameters are based on a previous approach[215]. Equations 1-4 were used to determine the (E_{NR}) values and Kamlet-Taft solvent parameters:

$$E_{NR}\,(\text{kcal/mol}) = 28591 \,/\, \Lambda_{max}\,(\text{nm}) \quad (1)$$

$$a = (19.9657 - 1.0241\pi^* - \upsilon_{NR}) \,/\, 1.6078 \quad (2)$$

$$\beta = (1.035\,\upsilon_{DENA} + 2.64 - \upsilon_{4\text{-}NA}) \,/\, 2.80 \quad (3)$$

$$\pi^* = 0.314\,(27.52 - \upsilon_{DENA}) \quad (4)$$

$$\text{where } \upsilon = 1 \,/\, (\Lambda_{max} \times 10^{-4})$$

Abraham solvation parameter model

To relate chromatographic retention of analytes to individual solute-solvent interactions, the Abraham solvation parameter model (equation 5) was employed.

$$Log\,k = c + eE + sS + aA + bB + lL \quad (5)$$

In equation 5, *k* represents the retention factor of each probe molecule calculated using the dead time and the retention time of each chromatographic column. The solute descriptors (*E, S, A, B,* and *L*) are specific to analytes and represent the excess molar refraction, dipolarity/polarizability, hydrogen bond acidity, hydrogen bond basicity, and gas-hexadecane partition coefficient at 298 K, respectively. The system constants (*e*, *s*, *a*, *b*, and *l*) represent specific solvation interactions of the DES stationary phase, where *e* measures n-π and π-π interactions, *s* the dipolarity/polarizability, *a* the hydrogen bond basicity, *b* the hydrogen bond acidity, and *l* provides a measure of dispersive-type interactions.

NMR Spectra

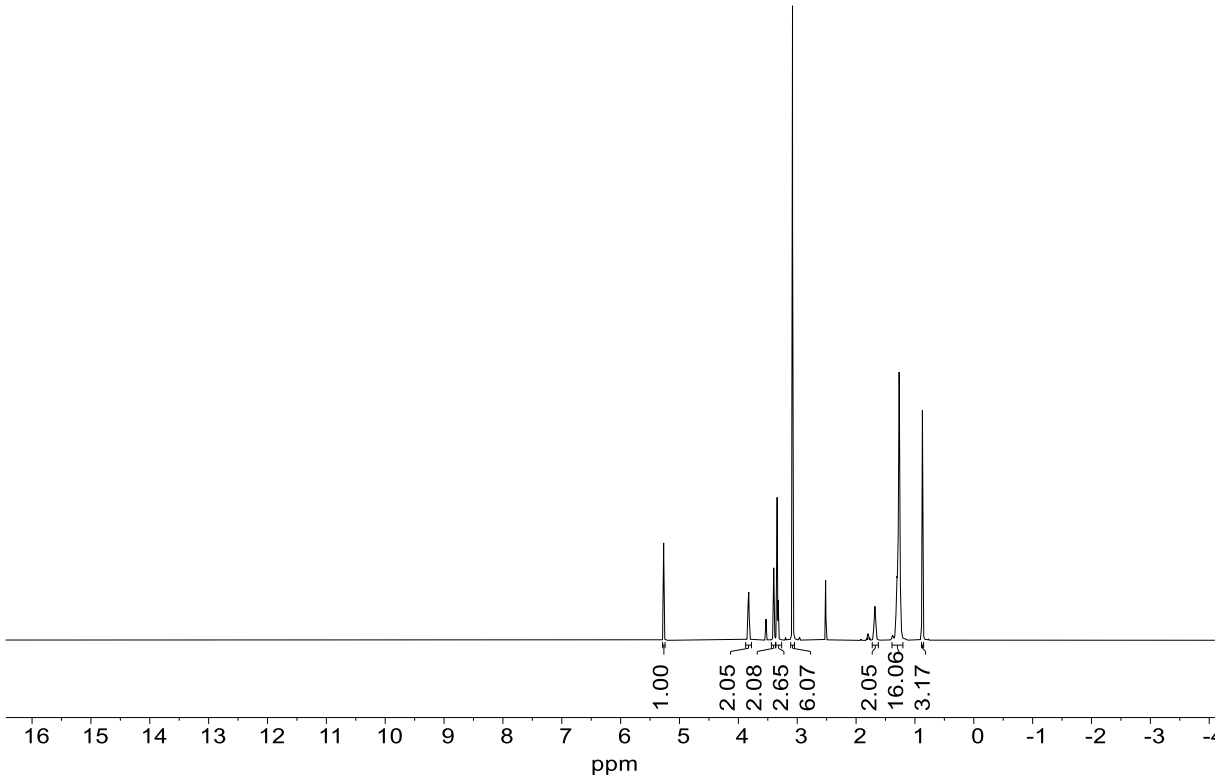

Figure 1. ^{1}H NMR of [N $_{1\,1\,10\,(2OH)}^{+}$][Br^{-}]

^{1}H NMR (600 MHz, DMSO) δ 5.27 (t, *J* = 5.0 Hz, 1H), 3.83 (tdd, *J* = 7.0, 4.9, 2.5 Hz, 2H), 3.44 – 3.36 (m, 2H), 3.37 – 3.26 (m, 3H), 3.08 (s, 6H), 1.73 – 1.62 (m, 2H), 1.29 (d, *J* = 21.6 Hz, 16H), 0.87 (td, *J* = 7.0, 2.5 Hz, 3H).

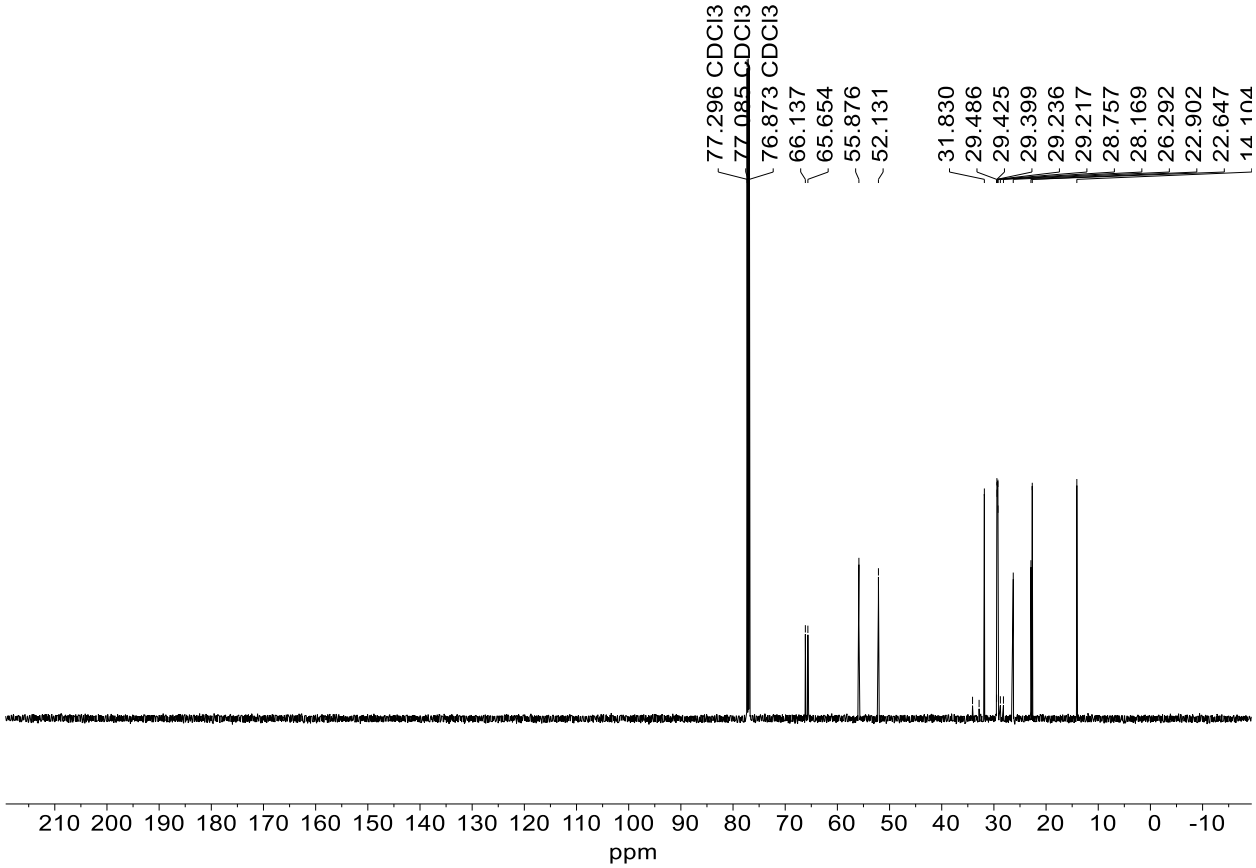

Figure 2. ^{13}C NMR of $[N_{1\,1\,10\,(2OH)}^{+}][Br^{-}]$

^{13}C NMR (151 MHz, $CDCl_3$) δ 66.14, 65.65, 55.88, 52.13, 31.83, 29.43, 29.40, 29.24, 29.22, 28.76, 26.29, 22.90, 22.65, 14.10.

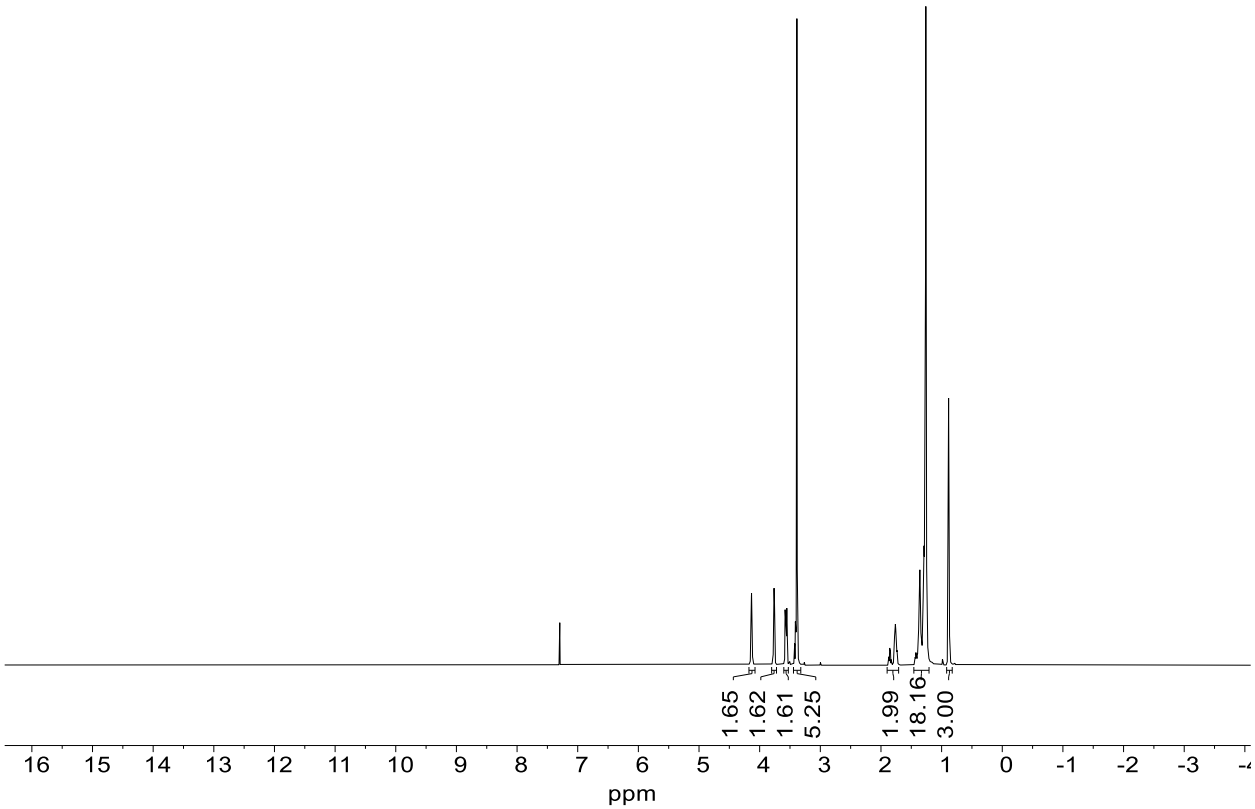

Figure 3. ^{1}H NMR of [N $_{1\,1\,12\,(2OH)}^{+}$][Br^{-}]

^{1}H NMR (600 MHz, $CDCl_3$) δ 4.18 – 4.08 (m, 2H), 3.80 – 3.72 (m, 2H), 3.60 – 3.53 (m, 2H), 3.39 (s, 5H), 1.90 – 1.71 (m, 2H), 1.46 – 1.21 (m, 18H), 0.88 (t, J = 7.0 Hz, 3H).

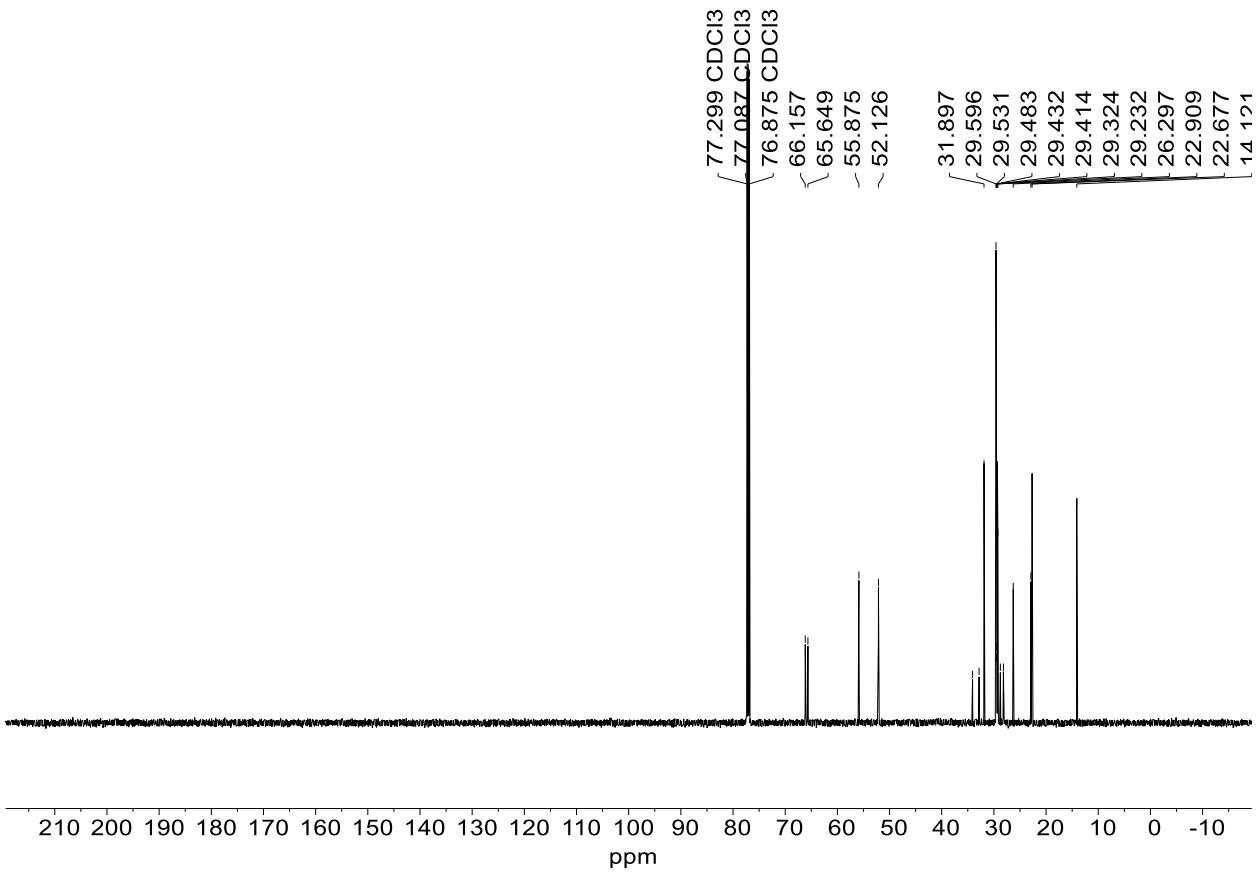

Figure 4. ^{13}C NMR of $[N_{1\,1\,12\,(2OH)}^{+}][Br^{-}]$

^{13}C NMR (151 MHz, $CDCl_3$) δ 66.16, 65.65, 55.88, 52.13, 34.09, 32.84, 31.90, 29.60, 29.53, 29.48, 29.43, 29.41, 29.32, 29.23, 28.76, 28.17, 26.30, 22.91, 22.68, 14.12.

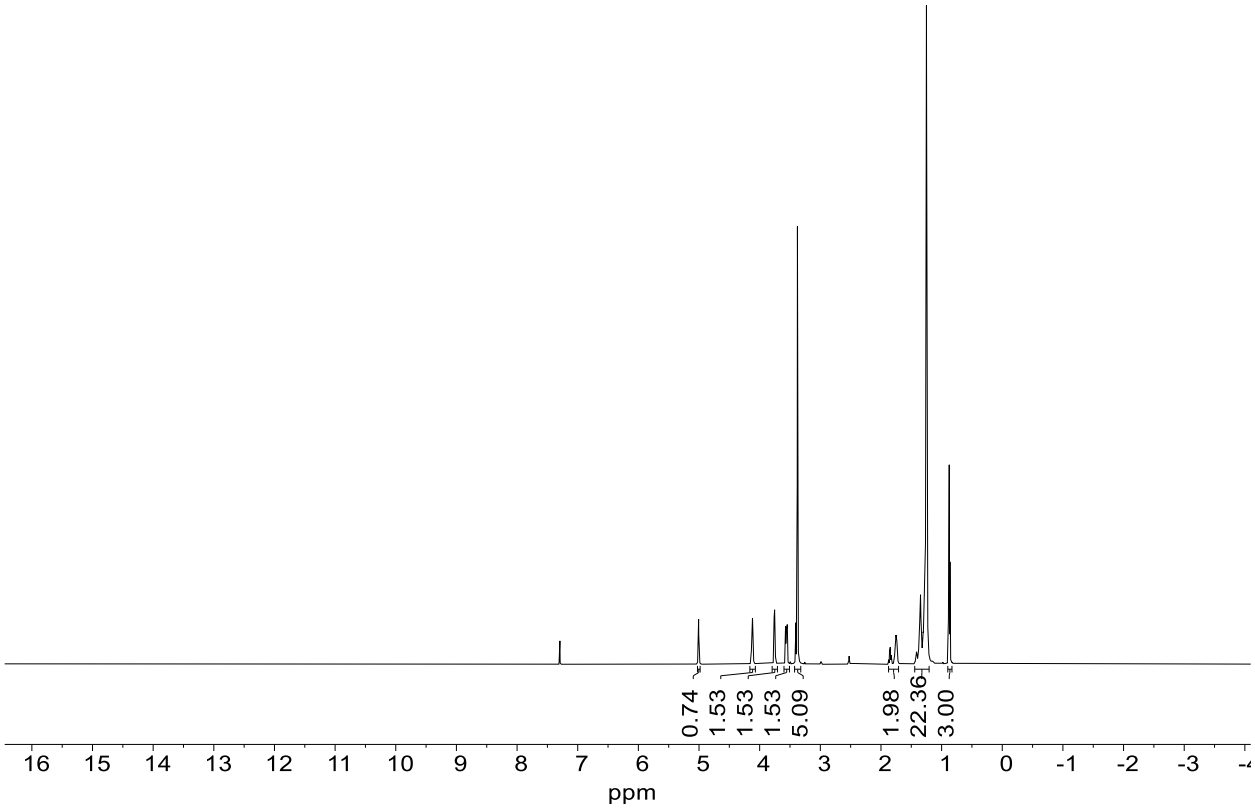

Figure 5. ^{1}H NMR of [N $_{1\ 1\ 14\ (2OH)}^{+}$][Br^{-}]

^{1}H NMR (600 MHz, $CDCl_3$) δ 5.01 (t, *J* = 5.5 Hz, 1H), 4.12 (q, *J* = 5.0 Hz, 2H), 3.79 – 3.71 (m, 2H), 3.60 – 3.51 (m, 2H), 3.38 (s, 5H), 1.87 – 1.71 (m, 2H), 1.44 – 1.21 (m, 22H), 0.87 (t, *J* = 7.0 Hz, 3H).

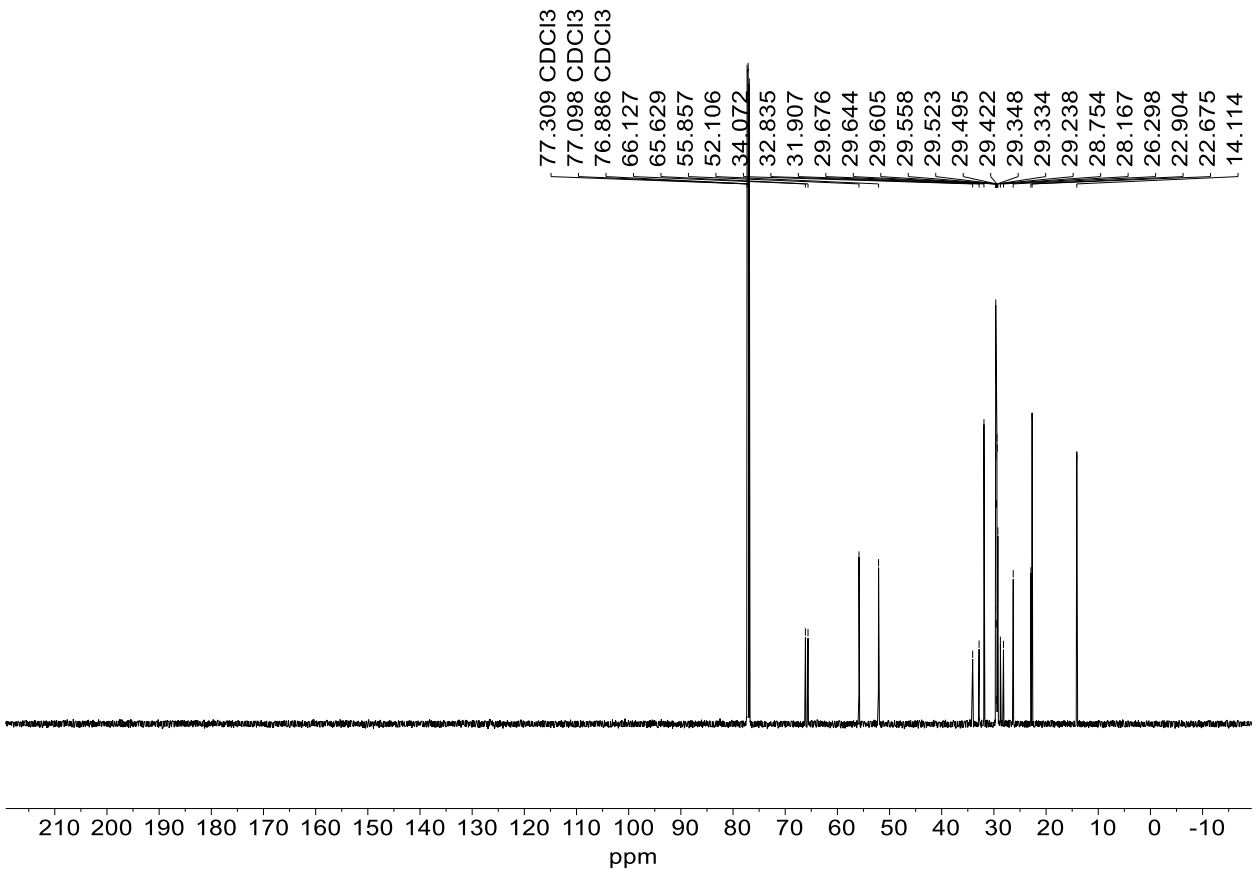

Figure 6. ^{13}C NMR of $[N_{1\,1\,14\,(2OH)}{}^{+}][Br^{-}]$

^{13}C NMR (151 MHz, $CDCl_3$) δ 66.13, 65.63, 55.86, 52.11, 34.07, 32.84, 31.91, 29.68, 29.64, 29.60, 29.52, 29.50, 29.42, 29.35, 29.33, 29.24, 28.75, 28.17, 26.30, 22.90, 22.67, 14.11.

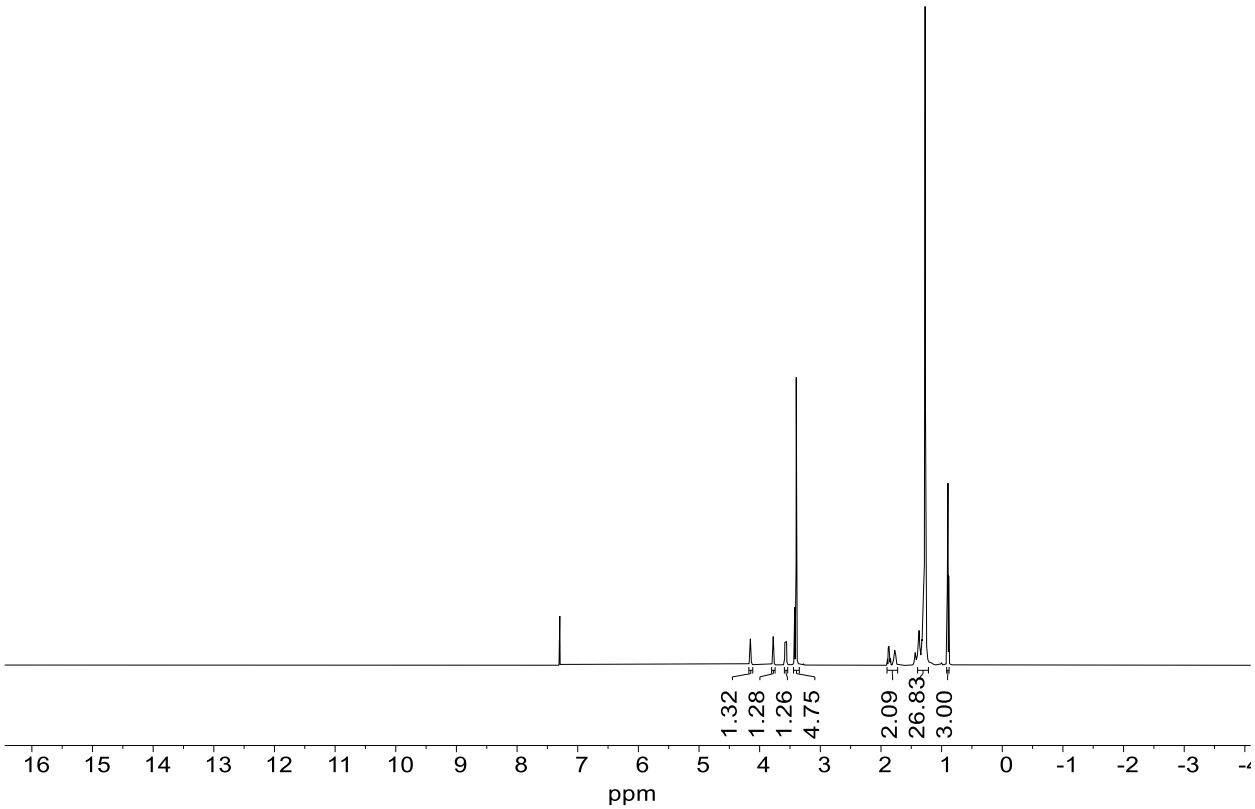

Figure 7. ^{1}H NMR of [N $_{1\,1\,16\,(2OH)}^{+}$][Br^{-}]

^{1}H NMR (600 MHz, $CDCl_3$) δ 4.18 – 4.11 (m, 1H), 3.80 – 3.75 (m, 1H), 3.59 – 3.54 (m, 1H), 3.41 (d, J = 15.0 Hz, 5H), 1.90 – 1.72 (m, 2H), 1.40 – 1.22 (m, 27H), 0.90 (t, J = 7.0 Hz, 3H).

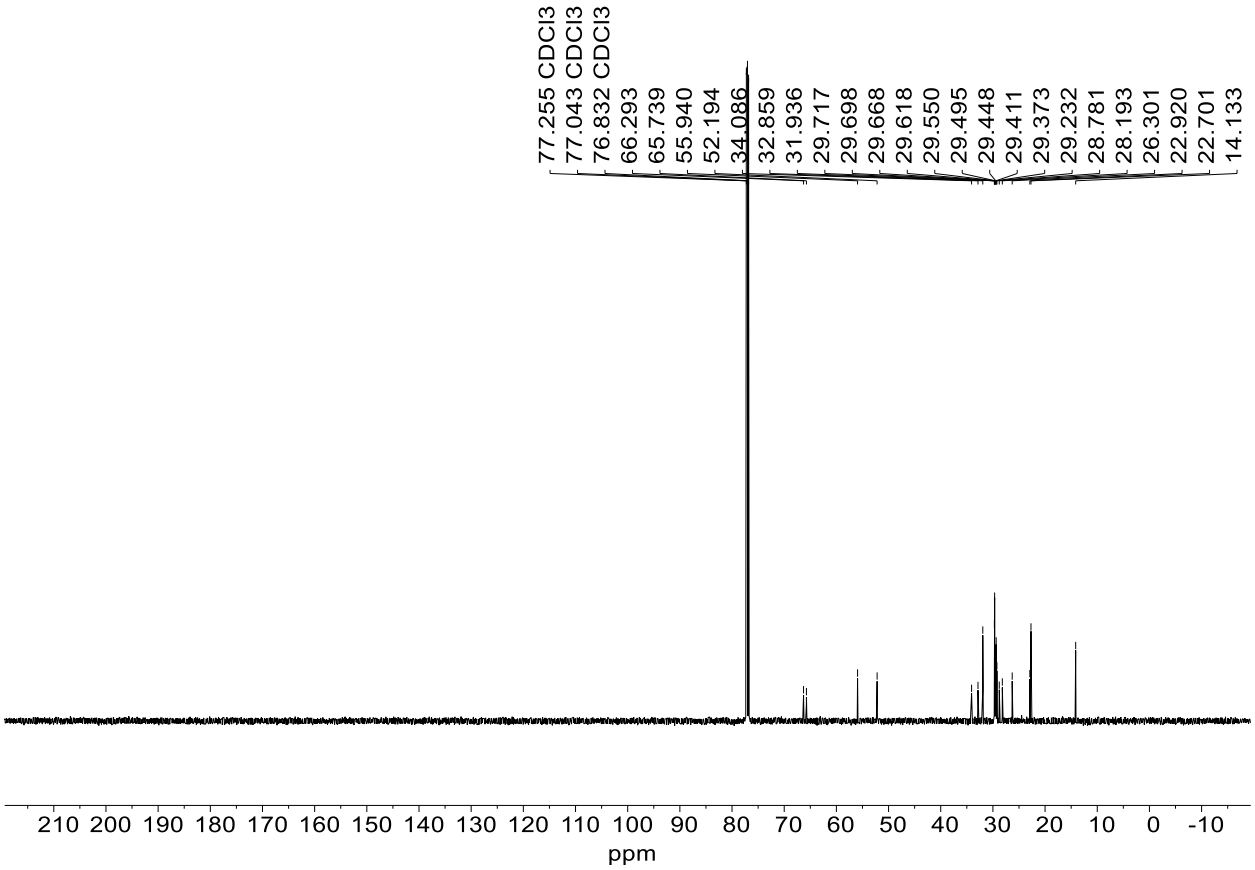

Figure 8. ^{13}C NMR of $[N_{1\,1\,16\,(2OH)}^{+}][Br^{-}]$

^{13}C NMR (151 MHz, $CDCl_3$) δ 66.29, 65.74, 55.94, 52.19, 34.09, 32.86, 31.94, 29.72, 29.70, 29.67, 29.62, 29.55, 29.49, 29.45, 29.41, 29.37, 29.23, 28.78, 28.19, 26.30, 22.92, 22.70, 14.13.

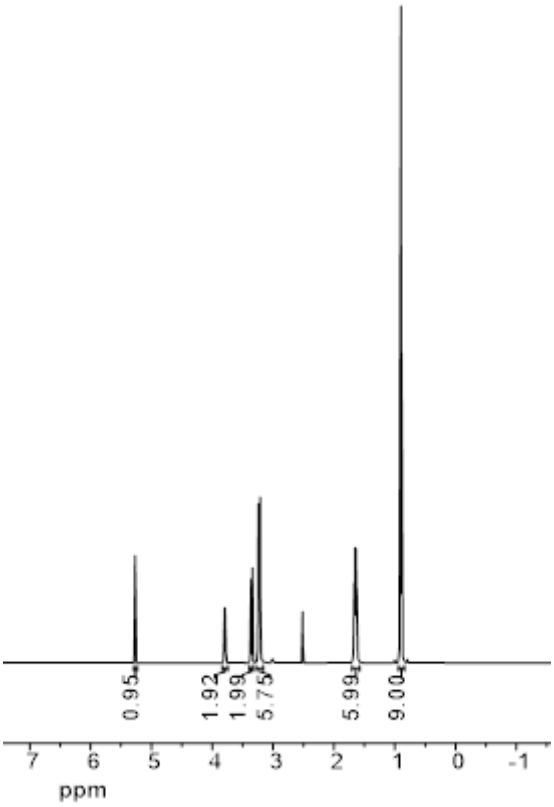

Figure 9. ^{1}H NMR of [$N_{3\,3\,3\,(2OH)}^{+}$][Br^{-}]

^{1}H NMR (600 MHz, DMSO) δ 5.27 (t, *J* = 5.2 Hz, 1H), 3.79 (q, *J* = 4.9 Hz, 2H), 3.36 (dd, *J* = 6.1, 4.2 Hz, 2H), 3.28 – 3.16 (m, 6H), 1.70 – 1.58 (m, 6H), 0.90 (t, *J* = 7.3 Hz, 9H).

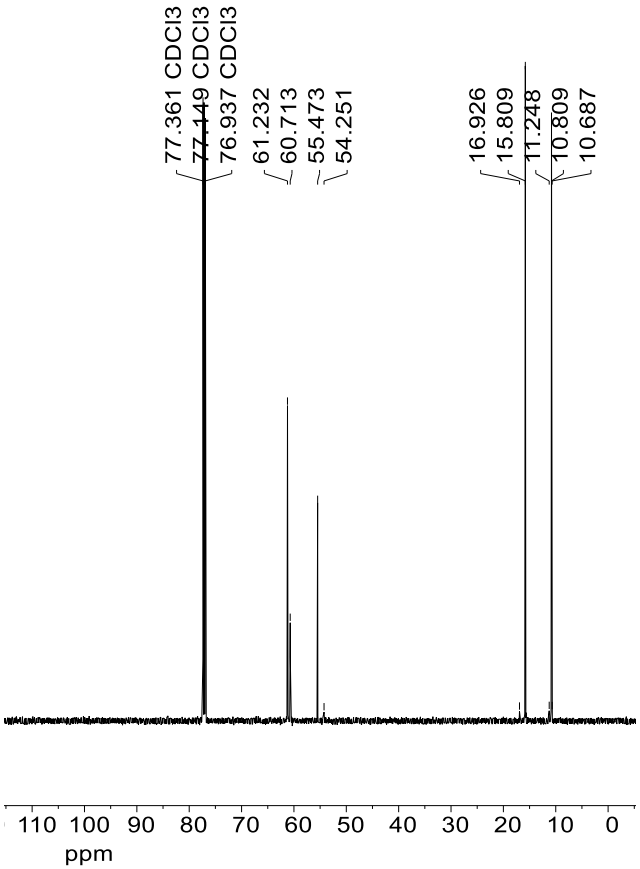

Figure 10. ^{13}C NMR of $[N_{3\,3\,3\,(2OH)}^{+}][Br^{-}]$

^{13}C NMR (151 MHz, $CDCl_3$) δ 61.23, 60.71, 55.47, 15.81, 10.81.

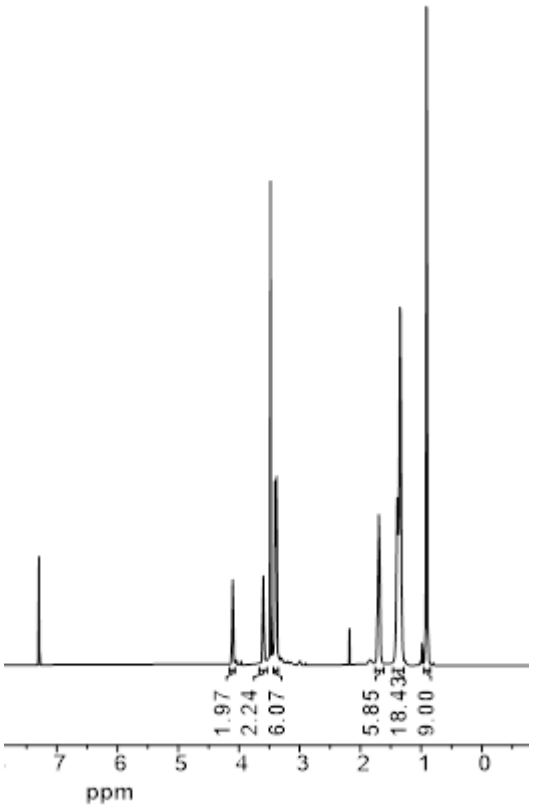

Figure 11. ^{1}H NMR of [$N_{6\,6\,6\,(2OH)}^{+}$][Br^{-}]

^{1}H NMR (600 MHz, $CDCl_3$) δ 4.11 (t, *J* = 4.6 Hz, 2H), 3.66 – 3.54 (m, 2H), 3.43 – 3.35 (m, 6H), 1.76 – 1.61 (m, 6H), 1.46 – 1.28 (m, 18H), 0.95 – 0.85 (m, 9H).

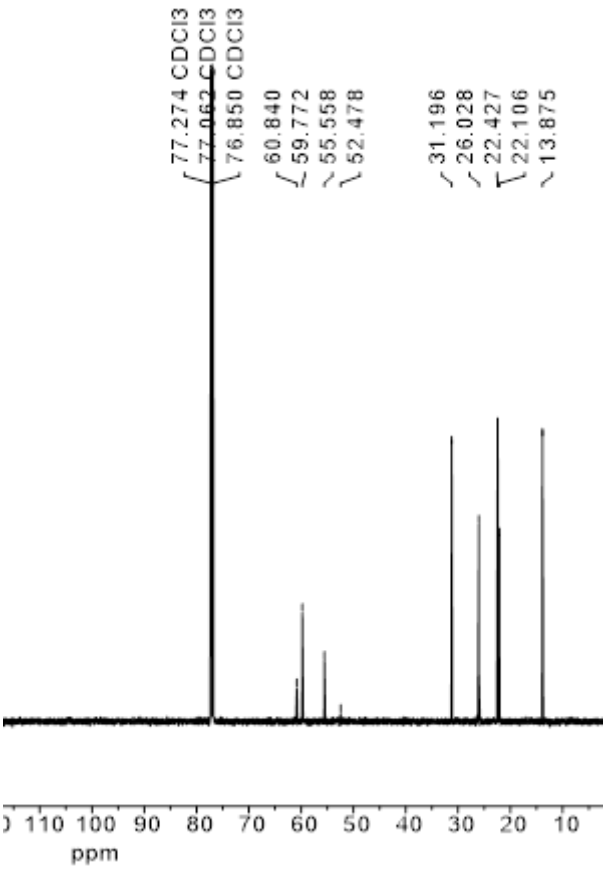

Figure 12. ^{13}C NMR of $[N_{6\,6\,6\,(2OH)}^{+}][Br^{-}]$

^{13}C NMR (151 MHz, $CDCl_3$) δ 60.84, 59.77, 55.56, 31.20, 26.03, 22.43, 22.11, 13.88.

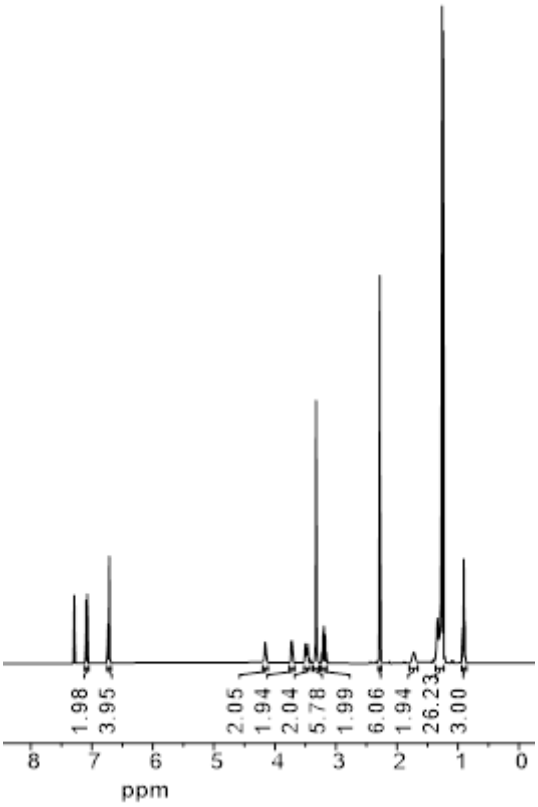

Figure 13. ^{1}H NMR of [N $_{1\,1\,10\,(2OH)}^{+}$][Br^{-}] : 2 Thymol HES

^{1}H NMR (400 MHz, $CDCl_3$) δ 7.09 (d, *J* = 7.6 Hz, 2H), 6.75 – 6.68 (m, 4H), 4.16 (t, *J* = 4.7 Hz, 2H), 3.76 – 3.68 (m, 2H), 3.52 – 3.42 (m, 2H), 3.32 (s, 6H), 3.19 (p, *J* = 6.9 Hz, 2H), 2.28 (s, 6H), 1.80 – 1.66 (m, 2H), 1.37 – 1.23 (m, 26H), 0.91 (t, *J* = 6.9 Hz, 3H).

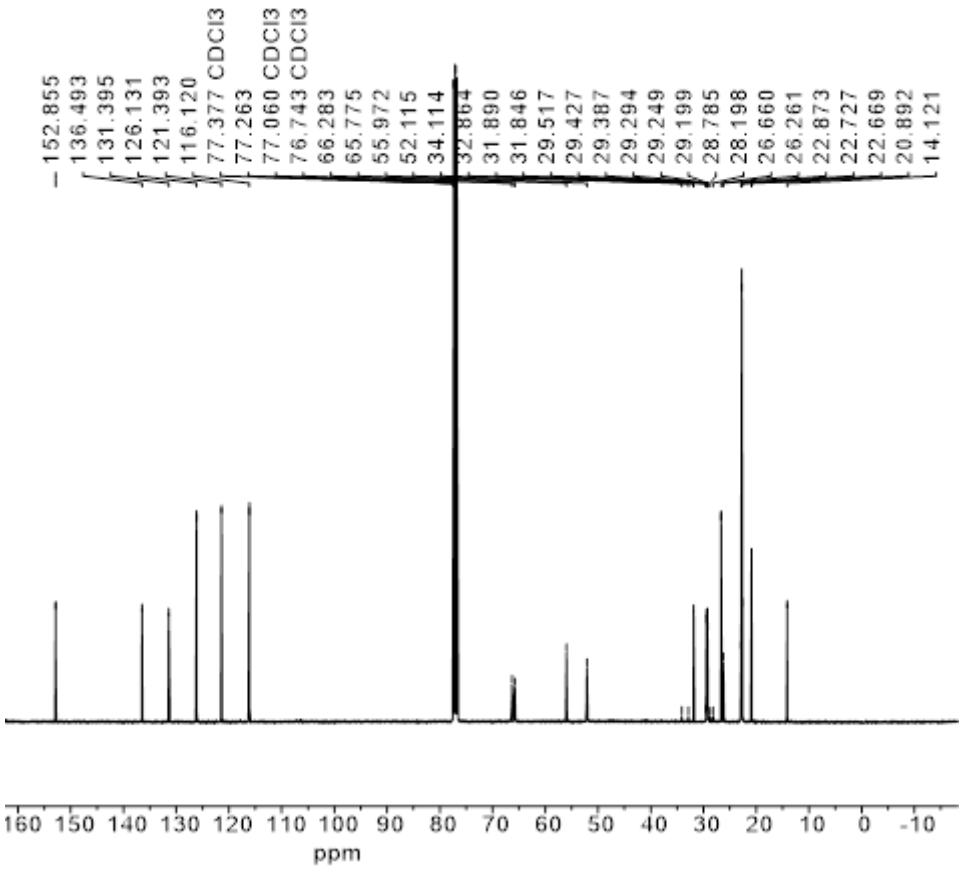

Figure 14. ^{13}C NMR of $[N_{1\,1\,10\,(2OH)}^{+}][Br^{-}]$: 2 Thymol HDES

^{13}C NMR (101 MHz, $CDCl_3$) δ 152.86, 136.49, 131.39, 126.13, 121.39, 116.12, 77.26, 66.28, 65.78, 55.97, 52.11, 31.85, 29.43, 29.39, 29.25, 29.20, 26.66, 26.26, 22.87, 22.73, 22.67, 20.89, 14.12.

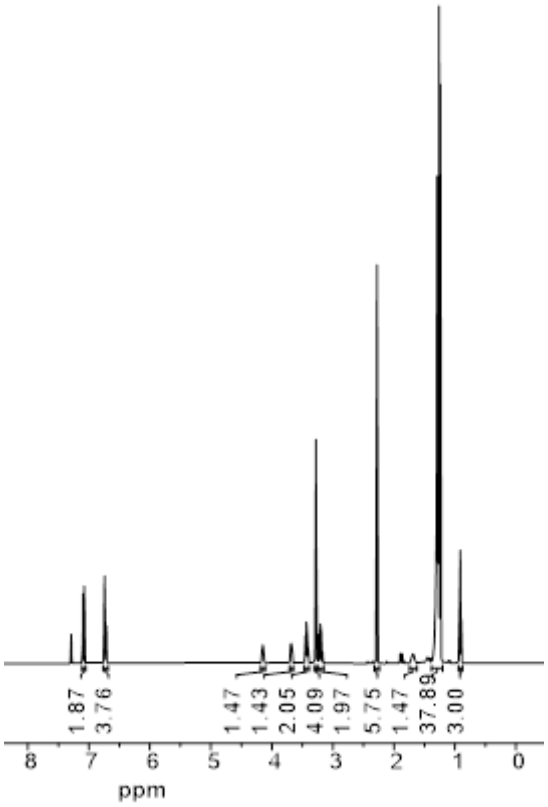

Figure 15. ^{1}H NMR of [N $_{1\,1\,16\,(2OH)}^{+}$][Br] : 2 Thymol HES

^{1}H NMR (400 MHz, $CDCl_3$) δ 7.09 (d, *J* = 7.7 Hz, 2H), 6.77 – 6.69 (m, 4H), 4.18 – 4.11 (m, 1H), 3.71 – 3.65 (m, 1H), 3.47 – 3.39 (m, 2H), 3.28 (s, 4H), 3.20 (h, *J* = 6.9 Hz, 2H), 2.28 (s, 6H), 1.69 (dq, *J* = 10.0, 5.5 Hz, 1H), 1.38 – 1.20 (m, 38H), 0.94 – 0.88 (m, 3H).

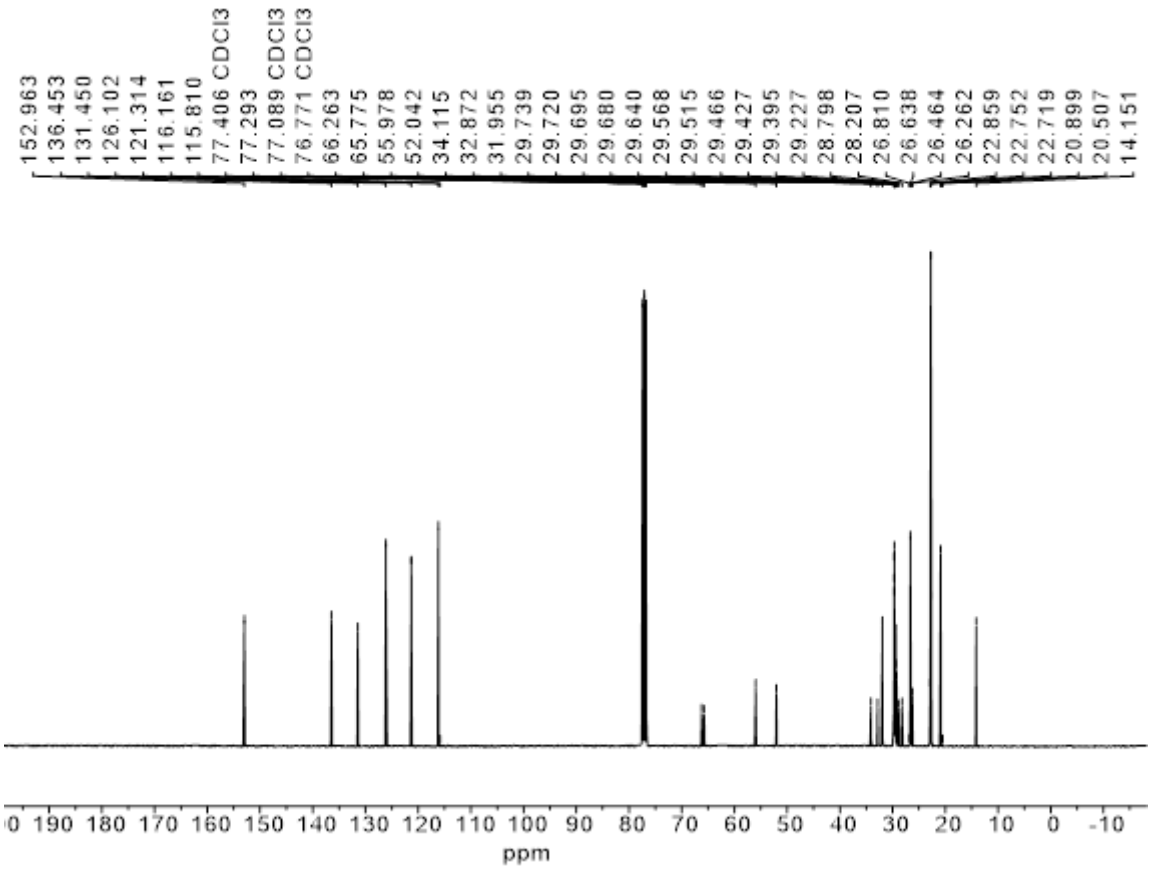

Figure 16. ^{13}C NMR of $[N_{1\,1\,16\,(2OH)}^{+}][Br^{-}]$: 2 Thymol HES

^{13}C NMR (101 MHz, $CDCl_3$) δ 152.96, 136.45, 131.45, 126.10, 121.31, 116.16, 77.29, 66.26, 65.78, 55.98, 52.04, 34.12, 32.87, 31.95, 29.74, 29.72, 29.69, 29.68, 29.64, 29.57, 29.52, 29.47, 29.43, 29.39, 29.23, 28.80, 28.21, 26.64, 26.26, 22.86, 22.75, 22.72, 20.90, 14.15.

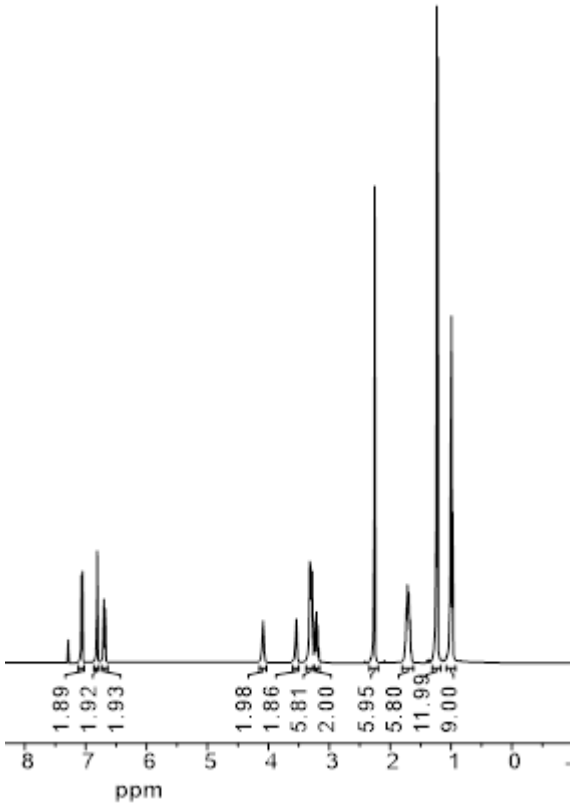

Figure 17. ^{1}H NMR of [N $_{3\,3\,3\,(2OH)}^{+}$][Br^{-}] : 2 Thymol HES

^{1}H NMR (400 MHz, $CDCl_3$) δ 7.06 (d, *J* = 7.7 Hz, 2H), 6.81 (d, *J* = 1.7 Hz, 2H), 6.69 (dd, *J* = 7.8, 1.8 Hz, 2H), 4.15 – 4.03 (m, 2H), 3.60 – 3.50 (m, 2H), 3.38 – 3.26 (m, 6H), 3.20 (h, *J* = 6.9 Hz, 2H), 2.25 (s, 6H), 1.80 – 1.62 (m, 6H), 1.23 (d, *J* = 7.0 Hz, 12H), 0.99 (t, *J* = 7.2 Hz, 9H).

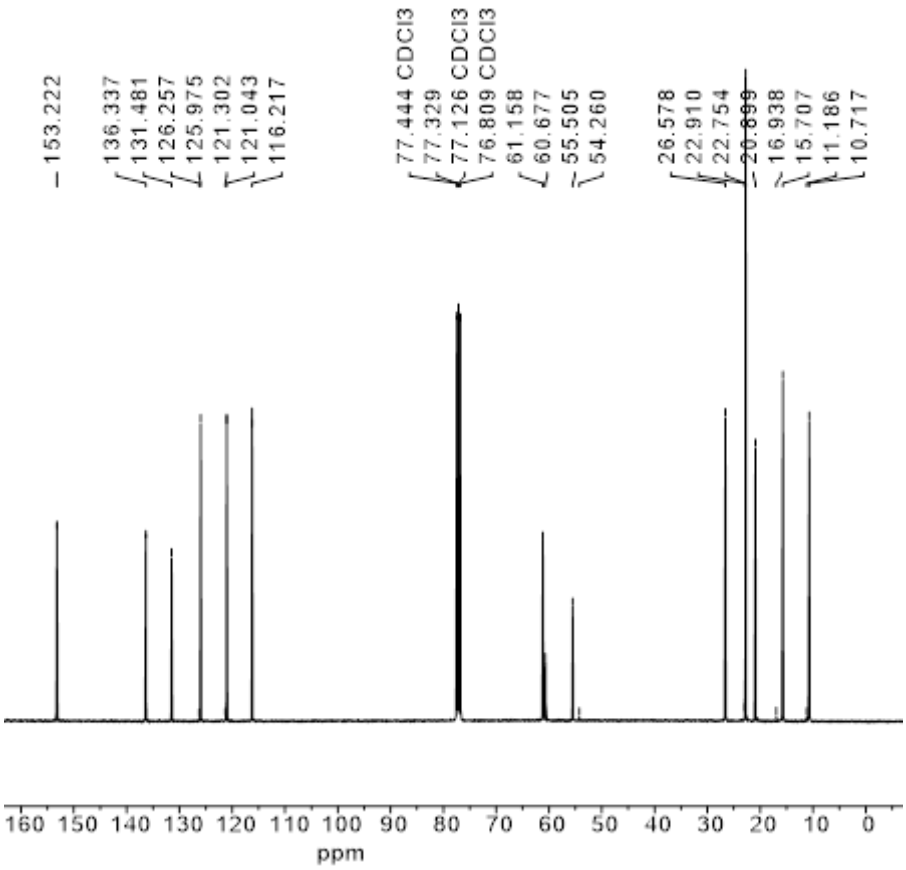

Figure 18. ^{13}C NMR of $[N_{3\,3\,3\,(2OH)}^{+}][Br^{-}]$: 2 Thymol HES

^{13}C NMR (101 MHz, $CDCl_3$) δ 153.22, 136.34, 131.48, 125.97, 121.04, 116.22, 61.16, 60.68, 55.50, 26.58, 22.75, 20.90, 15.71, 10.72.

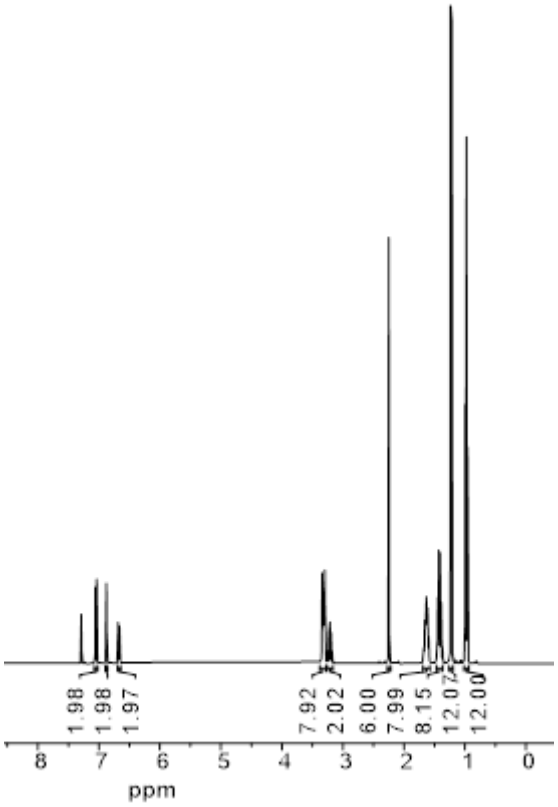

Figure 19. ^{1}H NMR of [N_{4444}^{+}][Br] : 2 Thymol HES

^{1}H NMR (400 MHz, $CDCl_3$) δ 7.05 (d, *J* = 7.7 Hz, 2H), 6.88 (dd, *J* = 1.7, 0.8 Hz, 2H), 6.69 – 6.64 (m, 2H), 3.38 – 3.28 (m, 8H), 3.21 (p, *J* = 7.0 Hz, 2H), 2.25 (s, 6H), 1.63 (dq, *J* = 11.9, 7.6 Hz, 8H), 1.42 (h, *J* = 7.4 Hz, 8H), 1.22 (d, *J* = 6.9 Hz, 12H), 0.98 (t, *J* = 7.3 Hz, 12H).

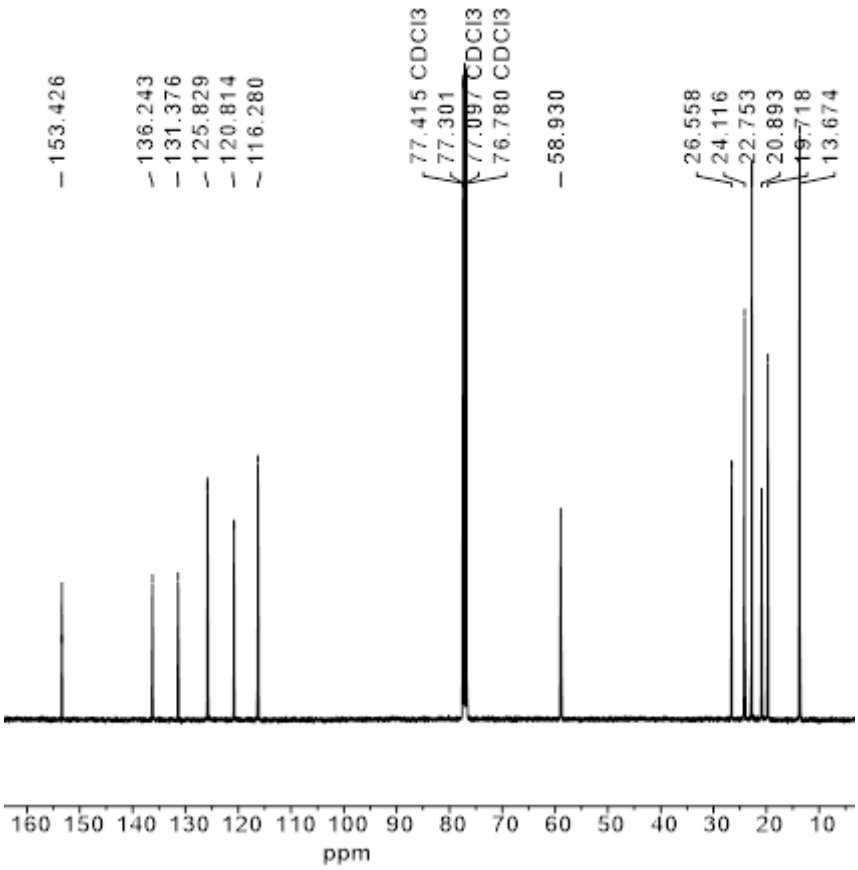

Figure 20. ^{13}C NMR of $[N_{4444}^{+}][Br^{-}]$: 2 Thymol HES

^{13}C NMR (101 MHz, $CDCl_3$) δ 153.43, 136.24, 131.38, 125.83, 120.81, 116.28, 77.30, 58.93, 26.56, 24.12, 22.75, 20.89, 19.72, 13.67.

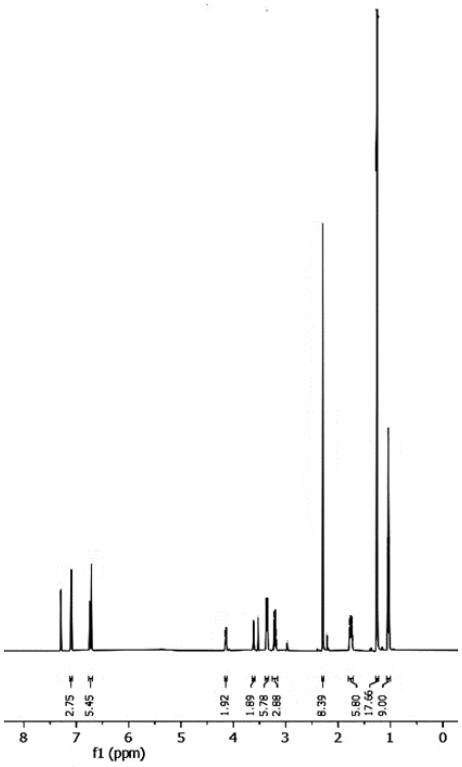

Figure 21. ^{1}H NMR of [$N_{3\,3\,3\,(2OH)}^{+}$][Br^{-}] : 2 Thymol HES before extraction in KBr 30% aqueous solution

^{1}H NMR (400 MHz, $CDCl_3$) δ 7.06 (d, *J* = 7.7 Hz, 3H), 6.81 (d, *J* = 1.7 Hz, 6H), 4.15 – 4.03 (m, 2H), 3.60 – 3.50 (m, 2H), 3.38 – 3.26 (m, 6H), 3.20 (h, *J* = 6.9 Hz, 3H), 2.25 (s, 9H), 1.80 – 1.62 (m, 6H), 1.23 (d, *J* = 7.0 Hz, 18H), 0.98 (t, *J* = 7.2 Hz, 9H).

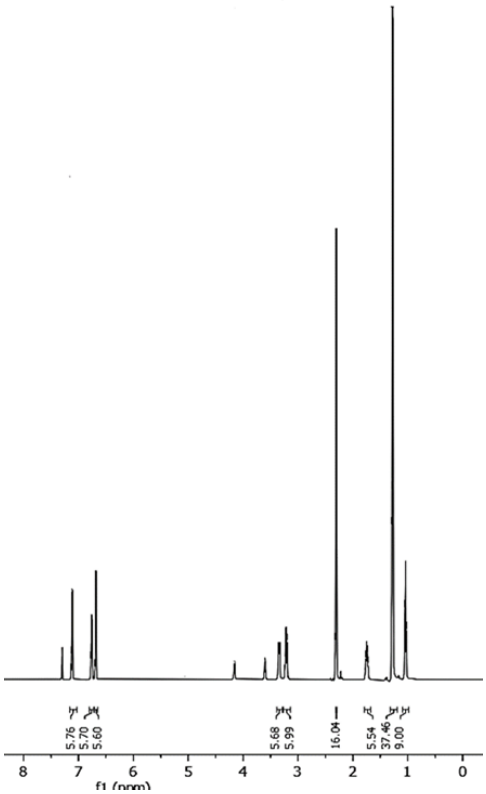

Figure 22. ^{1}H NMR of [N $_{3\,3\,3\,(2OH)}^{+}$][Br^{-}] : 2 Thymol HES after extraction in KBr 30% aqueous solution

^{1}H NMR (400 MHz, $CDCl_3$) δ 7.10 (d, *J* = 7.7 Hz, 6H), 6.80 (d, *J* = 1.7 Hz, 6H), 6.67– 6.54 (m, 2H), 3.40 (m, 6H), 3.33 (h, *J* = 6.9 Hz, 6H), 2.30 (s, 16H), 1.79 – 1.65 (m, 6H), 1.34 (d, *J* = 7.0 Hz, 37H), 0.99 (t, *J* = 7.2 Hz, 9H).

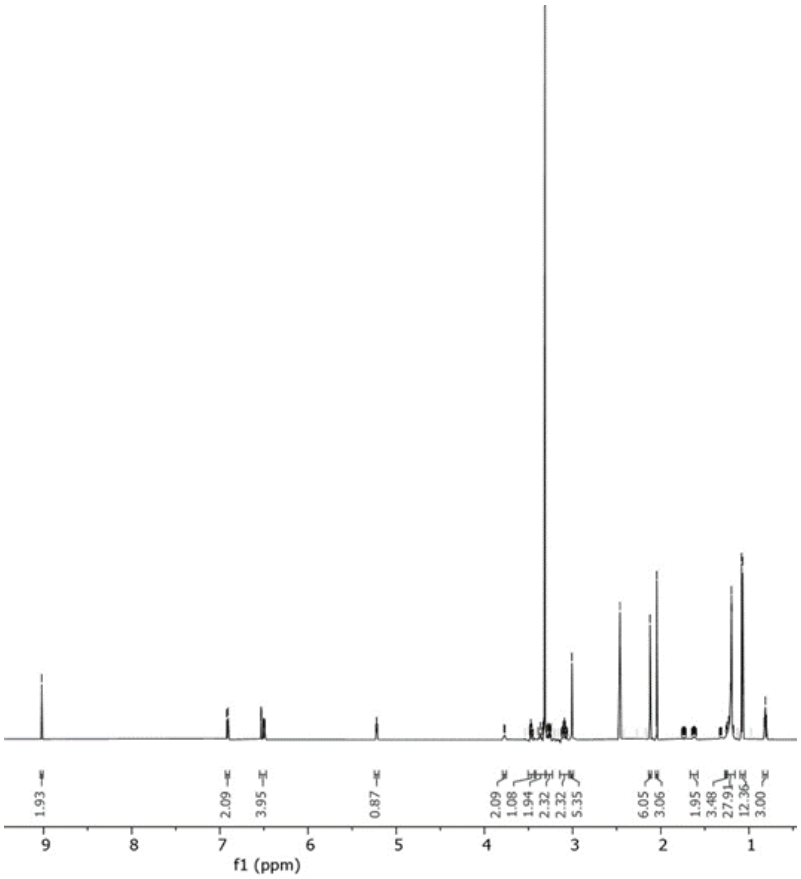

Figure 23. ^{1}H NMR of [N $_{1\,1\,16\,(2OH)}^{+}$][Br] : 2 Thymol HES before extraction in KBr 30% aqueous solution

^{1}H NMR (600 MHz, DMSO- d_6) δ 9.02 (s, 2H), 6.91 (d, J = 7.7 Hz, 2H), 6.55 – 6.48 (m, 4H), 5.22 (t, J = 4.9 Hz, 1H), 3.77 (d, J = 5.1 Hz, 2H), 3.50 – 3.43 (m, 1H), 3.42 – 3.31 (m, 2H), 3.30 – 3.23 (m, 2H), 3.09 (p, J = 6.9 Hz, 2H), 3.01 (s, 5H), 2.12 (s, 6H), 2.05 (s, 3H), 1.62 (dq, J = 15.0, 7.7 Hz, 2H), 1.26 (s, 3H), 1.20 (t, J = 3.1 Hz, 28H), 1.08 (d, J = 6.9 Hz, 12H), 0.81 (td, J = 7.1, 0.9 Hz, 3H).

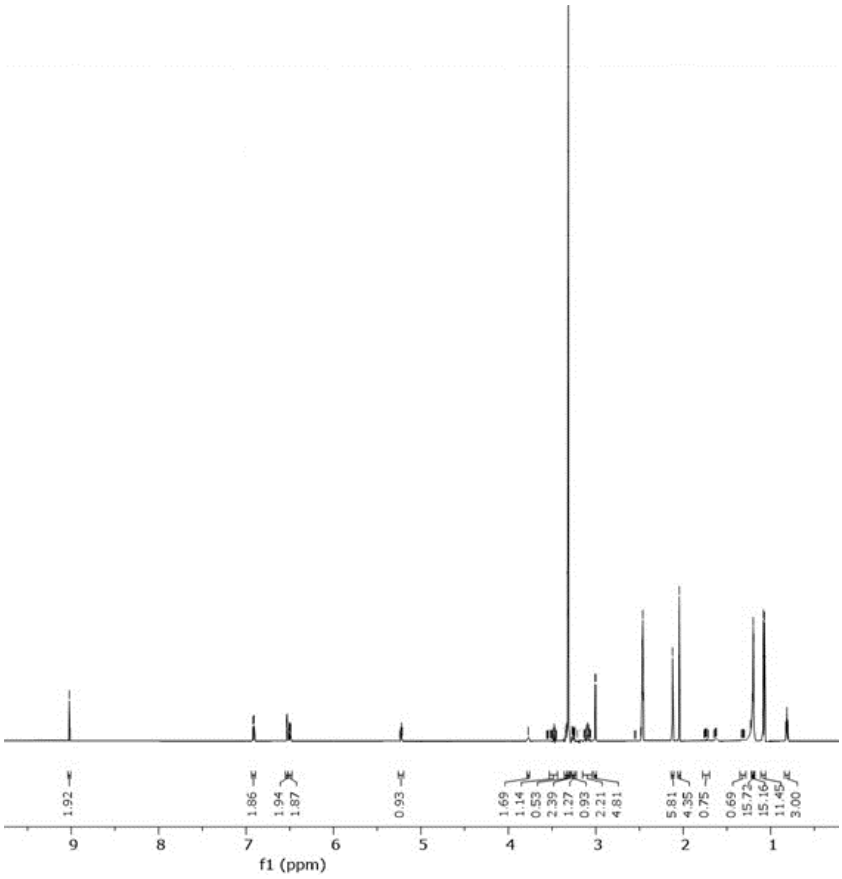

Figure 24. ^{1}H NMR of $[N_{1\,1\,16\,(2OH)}^{+}][Br^{-}]$: 2 Thymol HES after extraction in KBr 30% aqueous solution

^{1}H NMR (600 MHz, DMSO- d_6) δ 9.02 (s, 2H), 6.91 (d, J = 7.7 Hz, 2H), 6.53 (dd, J = 1.7, 0.8 Hz, 2H), 6.52 – 6.48 (m, 2H), 5.22 (t, J = 5.0 Hz, 1H), 3.77 (s, 2H), 3.53 – 3.44 (m, 1H), 3.34 (d, J = 3.3 Hz, 1H), 3.32 (s, 2H), 3.26 (s, 1H), 3.25 (dd, J = 16.5, 4.0 Hz, 1H), 3.09 (dq, J = 14.0, 7.0 Hz, 2H), 3.01 (s, 5H), 2.12 (s, 6H), 2.05 (s, 4H), 1.74 (dt, J = 14.5, 6.8 Hz, 1H), 1.32 (q, J = 7.5 Hz, 1H), 1.21 (s, 16H), 1.20 (d, J = 1.3 Hz, 15H), 1.08 (d, J = 6.9 Hz, 11H), 0.84 – 0.79 (m, 3H).

References

1. Chemat, F. *et al.* Green extraction of natural products. Origins, current status, and future challenges. *TrAC Trends Anal. Chem.* **118**, 248–263 (2019).

2. Li, Y. & Chemat, F. *Plant Based "Green Chemistry 2.0"*. (Springer Singapore, 2019).

3. European Commission. Circular economy action plan. https://ec.europa.eu/environment/circular-economy/pdf/new_circular_economy_action_plan.pdf (2020).

4. Pintać, D. *et al.* Investigation of the chemical composition and biological activity of edible grapevine (*Vitis vinifera* L.) leaf varieties. *Food Chem.* **286**, 686–695 (2019).

5. Teixeira, A. *et al.* Natural Bioactive Compounds from Winery By-Products as Health Promoters: A Review. *Int. J. Mol. Sci.* **15**, 15638–15678 (2014).

6. Tacchini, M. *et al.* Chemical characterisation, antioxidant and antimicrobial screening for the revaluation of wine supply chain by-products oriented to circular economy. *Plant Biosyst. - An Int. J. Deal. with all Asp. Plant Biol.* **153**, 809–816 (2019).

7. Galanakis, C. M. *Handbook of grape processing by-products : sustainable solutions*. (Academic Press, 2017).

8. Maciel, E. V. S., de Toffoli, A. L., Neto, E. S., Nazario, C. E. D. & Lanças, F. M. New materials in sample preparation: Recent advances and future trends. *TrAC - Trends Anal. Chem.* **119**, (2019).

9. Cvjetko Bubalo, M., Vidović, S., Radojčić Redovniković, I. & Jokić, S. New perspective in extraction of plant biologically active compounds by green solvents. *Food Bioprod. Process.* **109**, 52–73 (2018).

10. Chemat, F. *et al.* Ultrasound assisted extraction of food and natural products. Mechanisms, techniques, combinations, protocols and applications. A review. *Ultrason. Sonochem.* **34**, 540–560 (2017).

11. Pacheco-Fernández, I. *et al.* Biopolymers in sorbent-based microextraction methods. *TrAC Trends Anal. Chem.* **125**, 115839 (2020).

12. Anastas & Warner. *Green Chemistry:Theory and Practice*. (Oxford University Press, 1998).

13. Armenta, S., Garrigues, S. & de la Guardia, M. Green Analytical Chemistry. *TrAC Trends Anal. Chem. Anal. Chem.* **27**, 497–511 (2008).

14. Gałuszka, A., Migaszewski, Z. & Namieśnik, J. The 12 principles of green analytical chemistry and the SIGNIFICANCE mnemonic of green analytical practices. *TrAC Trends Anal. Chem.* **50**, 78–84 (2013).

15. López-Lorente, Á. I. *et al.* The ten principles of green sample preparation. *TrAC Trends Anal. Chem.* **148**, 116530 (2022).

16. Sajid, M. & Płotka-Wasylka, J. Green analytical chemistry metrics: A review. *Talanta* **238**, 123046 (2022).

17. Mohamed, D. & Fouad, M. M. Application of NEMI, Analytical Eco-Scale and GAPI tools for greenness assessment of three developed chromatographic methods for quantification of sulfadiazine and trimethoprim in bovine meat and chicken muscles: Comparison to greenness profile of reporte. *Microchem. J.* **157**, 104873 (2020).

18. Płotka-Wasylka, J. A new tool for the evaluation of the analytical procedure: Green Analytical Procedure Index. *Talanta* **181**, 204–209 (2018).

19. Gałuszka, A., Migaszewski, Z. M., Konieczka, P. & Namieśnik, J. Analytical Eco-Scale for assessing the greenness of analytical procedures. *TrAC Trends Anal. Chem.* **37**, 61–72 (2012).

20. Pena-Pereira, F., Wojnowski, W. & Tobiszewski, M. AGREE—Analytical GREEnness Metric Approach and Software. *Anal. Chem.* **92**, 10076–10082 (2020).

21. Wojnowski, W., Tobiszewski, M., Pena-Pereira, F. & Psillakis, E. AGREEprep – Analytical greenness metric for sample preparation. *TrAC Trends Anal. Chem.* **149**, 116553 (2022).

22. Nowak, P. M., Wietecha-Posłuszny, R. & Pawliszyn, J. White Analytical Chemistry: An approach to reconcile the principles of Green Analytical Chemistry and functionality. *TrAC Trends Anal. Chem.* **138**, 116223 (2021).

23. Mushtaq, M. Y., Choi, Y. H., Verpoorte, R. & Wilson, E. G. Extraction for metabolomics: Access to the metabolome. *Phytochem. Anal.* **25**, 291–306 (2014).

24. Brandt, A., Gräsvik, J., Hallett, J. P. & Welton, T. Deconstruction of lignocellulosic biomass with ionic liquids. *Green Chem.* **15**, 550–583 (2013).

25. Clark, K. D., Emaus, M. N., Varona, M., Bowers, A. N. & Anderson, J. L. Ionic liquids: solvents and sorbents in sample preparation. *J. Sep. Sci.* **41**, 209–235 (2018).

26. Lanari, D., Marcotullio, M. C. & Neri, A. A design of experiment approach for ionic liquid-based extraction of toxic components-minimized essential oil from *Myristica fragrans* houtt. *Molecules* **23**, (2018).

27. Mastellone, G., Pacheco-Fernández, I., Rubiolo, P., Pino, V. & Cagliero, C. Sustainable Micro-Scale Extraction of Bioactive Phenolic Compounds from *Vitis vinifera* Leaves with Ionic Liquid-Based Surfactants. *Molecules* **25**, (2020).

28. Moučková, K., Pacheco-Fernández, I., Ayala, J. H., Bajerová, P. & Pino, V. Evaluation of structurally different ionic liquid-based surfactants in a green microwave-assisted extraction for the flavonoids profile determination of *Mangifera* sp. and *Passiflora* sp. leaves from canary Islands. *Molecules* **25**, 1–17 (2020).

29. Liang, Q., Zhang, J., Su, X., Meng, Q. & Dou, J. Extraction and separation of eight ginsenosides from flower buds of *Panax ginseng* using aqueous ionic liquid-based ultrasonic-assisted extraction coupled with an aqueous biphasic system. *Molecules* **24**, 1–12 (2019).

30. Zhang, R. *et al.* Determination of pyrethroid residues in herbal tea using temperature-controlled ionic liquid dispersive liquid-liquid microextraction by high performance liquid chromatography. *Sci. Rep.* **10**, 1–8 (2020).

31. Trujillo-Rodríguez, M. J. *et al.* Advances of Ionic Liquids in Analytical Chemistry. *Anal. Chem.* **91**, 505–531 (2019).

32. Li, Q. *et al.* Ultrasonic-assisted extraction of sinomenine from *Sinomenium acutum* using magnetic ionic liquids coupled with further purification by reversed micellar extraction. *Process Biochem.* **58**, 282–288 (2017).

33. Nie, L. R., Song, H., Yohannes, A., Liang, S. & Yao, S. Extraction in cholinium-based magnetic ionic liquid aqueous two-phase system for the determination of berberine hydrochloride in: Rhizoma coptidis. *RSC Adv.* **8**, 25201–25209 (2018).

34. Marengo, A. *et al.* Development of an innovative and sustainable one-step method for rapid plant DNA isolation for targeted PCR using magnetic ionic liquids. *Plant Methods* **15**, 1–11 (2019).

35. Gutiérrez-Serpa, A., Napolitano-Tabares, P. I., Šulc, J., Pacheco-Fernández, I. & Pino, V. Role of ionic liquids in composites in analytical sample preparation. *Separations* **7**, 1–32 (2020).

36. Kaya, M., Merdivan, M., Tashakkori, P., Erdem, P. & Anderson, J. L. Analysis of Echinacea flower volatile constituents by HS-SPME-GC/MS using laboratory-prepared and commercial SPME fibers. *J. Essent. Oil Res.* **31**, 91–98 (2019).

37. Liu, X., Jing, X. & Li, G. A process to acquire essential oil by distillation concatenated liquid-liquid extraction and flavonoids by solid-liquid extraction simultaneously from *Helichrysum arenarium* (L.) Moench inflorescences under ionic liquid-microwave mediated. *Sep. Purif. Technol.* **209**, 164–174 (2019).

38. Li, C. *et al.* Separation of the main flavonoids and essential oil from seabuckthorn leaves by ultrasonic/microwave-assisted simultaneous distillation extraction. *R. Soc.*

Open Sci. **5**, 7 (2018).

39. Hou, K. *et al.* Aqueous enzymatic pretreatment ionic liquid–lithium salt based microwave–assisted extraction of essential oil and procyanidins from pinecones of Pinus koraiensis. *J. Clean. Prod.* **236**, 117581 (2019).

40. Kou, X. *et al.* Simultaneous extraction of hydrophobic and hydrophilic bioactive compounds from ginger (*Zingiber officinale* Roscoe). *Food Chem.* **257**, 223–229 (2018).

41. Wang, T., Wang, Q., Li, P. & Yang, H. Temperature-responsive ionic liquids to set up a method for the simultaneous extraction and: In situ preconcentration of hydrophilic and lipophilic compounds from medicinal plant matrices. *Green Chem.* **21**, 4133–4142 (2019).

42. Xiao, J., Chen, G. & Li, N. Ionic liquid solutions as a green tool for the extraction and isolation of natural products. *Molecules* **23**, 1765 (2018).

43. Zhang, C., Cagliero, C., Pierson, S. A. & Anderson, J. L. Rapid and sensitive analysis of polychlorinated biphenyls and acrylamide in food samples using ionic liquid-based in situ dispersive liquid-liquid microextraction coupled to headspace gas chromatography. *J. Chromatogr. A* **1481**, 1–11 (2017).

44. Hulsbosch, J., De Vos, D. E., Binnemans, K. & Ameloot, R. Biobased Ionic Liquids: Solvents for a Green Processing Industry? *ACS Sustain. Chem. Eng.* **4**, 2917–2931 (2016).

45. Wang, Z. *et al.* Novel bio-renewable matrinium-based ionic liquids derived from Chinese herb medicine: Synthesis, physicochemical properties and biological activity. *J. Mol. Liq.* **296**, (2019).

46. Farooq, M. Q., Abbasi, N. M. & Anderson, J. L. Deep eutectic solvents in separations: Methods of preparation, polarity, and applications in extractions and capillary electrochromatography. *J. Chromatogr. A* **1633**, 461613 (2020).

47. Yao, X. H. *et al.* Preparation and determination of phenolic compounds from *Pyrola incarnata* Fisch. with a green polyols based-deep eutectic solvent. *Sep. Purif. Technol.* **149**, 116–123 (2015).

48. Duan, L., Dou, L. L., Guo, L., Li, P. & Liu, E. H. Comprehensive Evaluation of Deep Eutectic Solvents in Extraction of Bioactive Natural Products. *ACS Sustain. Chem. Eng.* **4**, 2405–2411 (2016).

49. Huang, J. *et al.* Ionic deep eutectic solvents for the extraction and separation of natural products. *J. Chromatogr. A* **1598**, 1–19 (2019).

50. Fu, N. *et al.* Environmentally friendly and non-polluting solvent pretreatment of palm samples for polyphenol analysis using choline chloride deep eutectic solvents. *J. Chromatogr. A* **1492**, 1–11 (2017).

51. Zhuang, B., Dou, L. L., Li, P. & Liu, E. H. Deep eutectic solvents as green media for extraction of flavonoid glycosides and aglycones from *Platycladi Cacumen*. *J. Pharm. Biomed. Anal.* **134**, 214–219 (2017).

52. Choi, Y. H. *et al.* Are natural deep eutectic solvents the missing link in understanding cellular metabolism and physiology? *Plant Physiol.* **156**, 1701–1705 (2011).

53. Oomen, W. W. *et al.* Natural Deep Eutectic Solvent Extraction of Flavonoids of Scutellaria baicalensis as a Replacement for Conventional Organic Solvents. *Molecules* **25**, 1–11 (2020).

54. Fan, X. H. *et al.* A simple and efficient sample preparation for taxanes in Taxus chinensis needles with natural menthol-based aqueous deep eutectic solvent. *J. Sep. Sci.* **43**, 1339–1347 (2020).

55. Křížek, T. *et al.* Menthol-based hydrophobic deep eutectic solvents: Towards greener and efficient extraction of phytocannabinoids. *J. Clean. Prod.* **193**, 391–396 (2018).

56. Cai, C. *et al.* Green extraction of cannabidiol from industrial hemp (*Cannabis sativa* L.) using deep eutectic solvents coupled with further enrichment and recovery by macroporous resin. *J. Mol. Liq.* **287**, 110957 (2019).

57. Sang, J. *et al.* Deep eutectic solvent-based extraction coupled with green two-dimensional HPLC-DAD-ESI-MS/MS for the determination of anthocyanins from: *Lycium ruthenicum* Murr. fruit. *Anal. Methods* **10**, 1247–1257 (2018).

58. Ruesgas-Ramón, M., Figueroa-Espinoza, M. C. & Durand, E. Application of Deep Eutectic Solvents (DES) for Phenolic Compounds Extraction: Overview, Challenges, and Opportunities. *J. Agric. Food Chem.* **65**, 3591–3601 (2017).

59. Cao, J., Yang, M., Cao, F., Wang, J. & Su, E. Well-Designed Hydrophobic Deep Eutectic Solvents As Green and Efficient Media for the Extraction of Artemisinin from *Artemisia annua* Leaves. *ACS Sustain. Chem. Eng.* **5**, 3270–3278 (2017).

60. Bajkacz, S. *et al.* Highly efficient extraction procedures based on natural deep eutectic solvents or ionic liquids for determination of 20-hydroxyecdysone in spinach. *Molecules* **25**, 1–14 (2020).

61. Nie, J. *et al.* Microwave-assisted deep eutectic solvent extraction coupled with headspace solid-phase microextraction followed by GC-MS for the analysis of volatile compounds from tobacco. *Anal. Methods* **9**, 856–863 (2017).

62. Jeong, K. M. *et al.* One-step sample preparation for convenient examination of volatile monoterpenes and phenolic compounds in peppermint leaves using deep eutectic solvents. *Food Chem.* **251**, 69–76 (2018).

63. Barbieri, J. B. *et al.* Deep eutectic solvents applied in the extraction and stabilization of rosemary (*Rosmarinus officinalis* L.) phenolic compounds. *Ind. Crops Prod.* **144**, 112049 (2020).

64. Mafra, G. *et al.* Returning to nature for the design of sorptive phases in solid-phase microextraction. *Separations* **7**, 1–22 (2020).

65. Wu, W. *et al.* Determination of caffeoylquinic acid derivatives in *Azolla imbricata* by chitosan-based matrix solid-phase dispersion coupled with HPLC–PDA. *J. Pharm. Biomed. Anal.* **163**, 197–203 (2019).

66. Shu, H. *et al.* Hybrid-type carbon microcoil-chitosan composite for selective extraction of aristolochic acid I from Aristolochiaceae medicinal plants. *J. Chromatogr. A* **1561**, 13–19 (2018).

67. Li, Z., Lu, S., Jin, J. & Wang, T. Preparation of a new cellulose magnetic molecularly imprinted polymer micro-spheres to extract and analyze the indole-3-acetic acid in plant tissues. *J. Chromatogr. B Anal. Technol. Biomed. Life Sci.* **1092**, 343–349 (2018).

68. Zeng, Q. *et al.* Development of Graphene Oxide Functionalized Cotton Fiber Based Solid Phase Extraction Combined with Liquid Chromatography-Fluorescence Detection for Determination of Trace Auxins in Plant Samples. *Chromatographia* **81**, 861–869 (2018).

69. Markus, A., Gbadamosi, A. O., Yusuff, A. S., Agi, A. & Oseh, J. Magnetite-sporopollenin/graphene oxide as new preconcentration adsorbent for removal of polar organophosphorus pesticides in vegetables. *Environ. Sci. Pollut. Res.* **25**, 35130–35142 (2018).

70. Jiang, L. *et al.* New vortex-synchronized matrix solid-phase dispersion method for simultaneous determination of four anthraquinones in Cassiae semen. *Molecules* **24**, 6–13 (2019).

71. Li, M. *et al.* Solid phase extraction of carbamate pesticides with banana peel derived hierarchical porous carbon prior to high performance liquid chromatography. *Anal. Methods* **9**, 593–599 (2017).

72. Ren, K., Zhang, W., Cao, S., Wang, G. & Zhou, Z. Carbon-based Fe_3O_4 nanocomposites derived from waste pomelo peels for magnetic solid-phase extraction of 11 triazole fungicides in fruit samples. *Nanomaterials* **8**, 302 (2018).

73. Öztürk Er, E., Maltepe, E. & Bakirdere, S. A novel analytical method for the determination of cadmium in sorrel and rocket plants at ultratrace levels: Magnetic chitosan hydrogels based solid phase microextraction-slotted quartz tube-flame atomic absorption spectrophotometry. *Microchem. J.* **143**, 393–399 (2018).

74. Wang, C. *et al.* Preparation of ionic liquid-mediated imprinted monolith for selective capture and purification of corilagin. *J. Chromatogr. B Anal. Technol. Biomed. Life Sci.* **1041–1042**, 98–103 (2017).

75. Han, Y., Yang, C., Zhou, Y., Han, D. & Yan, H. Ionic Liquid-Hybrid Molecularly Imprinted Material-Filter Solid-Phase Extraction Coupled with HPLC for Determination of 6-Benzyladenine and 4-Chlorophenoxyacetic Acid in Bean Sprouts. *J. Agric. Food Chem.* **65**, 1750–1757 (2017).

76. Turiel, E. & Martín-Esteban, A. Molecularly imprinted polymers-based microextraction techniques. *TrAC - Trends Anal. Chem.* **118**, 574–586 (2019).

77. Zhang, Q. *et al.* Preparation and application of molecularly imprinted polymer solid-phase microextraction fiber for the selective analysis of auxins in tobacco. *J. Sep. Sci.* **42**, 2687–2695 (2019).

78. Luo, Z. *et al.* Molecularly imprinted polymer solid-phase microextraction coupled with ultra high performance liquid chromatography and tandem mass spectrometry for rapid analysis of pyrrolizidine alkaloids in herbal medicine. *J. Sep. Sci.* **42**, 3352–3362 (2019).

79. Arabi, M. *et al.* Strategies of molecular imprinting-based solid-phase extraction prior to chromatographic analysis. *TrAC - Trends Anal. Chem.* **128**, 115923 (2020).

80. Li, X., Dai, Y. & Row, K. H. Preparation of two-dimensional magnetic molecularly imprinted polymers based on boron nitride and a deep eutectic solvent for the selective recognition of flavonoids. *Analyst* **144**, 1777–1788 (2019).

81. Sun, G. *et al.* "Two-dimensional" molecularly imprinted solid-phase extraction

coupled with crystallization and high performance liquid chromatography for fast semi-preparative purification of tannins from pomegranate husk extract. *J. Chromatogr. A* **1505**, 35–42 (2017).

82. Xiao, D., Lu, T., Zeng, R. & Bi, Y. Preparation and highlighted applications of magnetic microparticles and nanoparticles : a review on recent advances. *Microchim. Acta* **183**, 2655–2675 (2016).

83. Abujaber, F., Bernardo, F. J. G. & Martín-doimeadios, R. C. R. Talanta Magnetic cellulose nanoparticles as sorbents for stir bar-sorptive dispersive microextraction of polychlorinated biphenyls in juice samples. **201**, 266–270 (2019).

84. Chen, J. *et al.* Fabrication of a high selectivity magnetic solid phase extraction adsorbent based on β-cyclodextrin and application for recognition of plant growth regulators. *J. Chromatogr. A* **1547**, 1–13 (2018).

85. Zhang, Q. *et al.* Amino-terminated supramolecular cucurbit [6] uril pseudorotaxane complexes immobilized on magnetite@silica nanoparticles: A highly efficient sorbent for salvianolic acids. *Talanta* **195**, 354–365 (2019).

86. Gutiérrez-Serpa, A., Pacheco-Fernández, I., Pasán, J. & Pino, V. Metal–organic frameworks as key materials for solid-phase microextraction devices—a review. *Separations* **6**, 47 (2019).

87. Abdelhameed, R. M., Abdel-Gawad, H., Taha, M. & Hegazi, B. Separation of bioactive chamazulene from chamomile extract using metal-organic framework. *J. Pharm. Biomed. Anal.* **146**, 126–134 (2017).

88. Cui, Y. Y., Yang, C. X., Yang, X. D. & Yan, X. P. Zeolitic imidazolate framework-8 for selective extraction of a highly active anti-oxidant flavonoid from *Caragana Jubata*. *J. Chromatogr. A* **1544**, 8–15 (2018).

89. Zhang, R. *et al.* Metal–organic framework assisted matrix solid-phase dispersion microextraction of saponins using response surface methodology. *Electrophoresis* **41**,

1354–1363 (2020).

90. Bahrani, S. *et al.* MOF-5(Zn)-Fe_2O_4 nanocomposite based magnetic solid-phase microextraction followed by HPLC-UV for efficient enrichment of colchicine in root of colchicium extracts and plasma samples. *J. Chromatogr. B Anal. Technol. Biomed. Life Sci.* **1067**, 45–52 (2017).

91. Durmus, Z., Zengin Kurt, B., Gazioğlu, I., Sevgi, E. & Kizilarslan Hancer, C. Spectrofluorimetric Determination of Aflatoxin B1 in Winter Herbal Teas via Magnetic Solid Phase Extraction Method by using Metal–Organic Framework (MOF) Hybrid Structures Anchored with Magnetic Nanoparticles. *Appl. Organomet. Chem.* **34**, 2–11 (2020).

92. Moradi, Z., Alipanahpour Dil, E. & Asfaram, A. Dispersive micro-solid phase extraction based on Fe_3O_4@SiO_2@Ti-MOF as a magnetic nanocomposite sorbent for the trace analysis of caffeic acid in the medical extracts of plants and water samples prior to HPLC-UV analysis. *Analyst* **144**, 4351–4361 (2019).

93. Zhou, Y. *et al.* Magnetic nanoparticles speed up mechanochemical solid phase extraction with enhanced enrichment capability for organochlorines in plants. *Anal. Chim. Acta* **1066**, 49–57 (2019).

94. Ghiasvand, A., Koonani, S., Yazdankhah, F. & Farhadi, S. A comparison study on a sulfonated graphene-polyaniline nanocomposite coated fiber for analysis of nicotine in solid samples through the traditional and vacuum-assisted HS-SPME. *J. Pharm. Biomed. Anal.* **149**, 271–277 (2018).

95. Su, Y. *et al.* Zr-MOF modified cotton fiber for pipette tip solid-phase extraction of four phenoxy herbicides in complex samples. *Ecotoxicol. Environ. Saf.* **201**, 110764 (2020).

96. Pang, X. *et al.* Monolithic Column Prepared with UiO-66-2COOH MOF as Monomer for Enrichment and Purification of Ursolic Acid in Plants by Online

Solid-Phase Extraction. *Chromatographia* **83**, 1121–1131 (2020).

97. Pang, X. *et al.* A metal organic framework polymer monolithic column as a novel adsorbent for on-line solid phase extraction and determination of ursolic acid in Chinese herbal medicine. *J. Chromatogr. B Anal. Technol. Biomed. Life Sci.* **1125**, (2019).

98. Zhang, M., Liu, H., Han, Y., Bai, L. & Yan, H. On-line enrichment and determination of aristolochic acid in medicinal plants using a MOF-based composite monolith as adsorbent. *J. Chromatogr. B Anal. Technol. Biomed. Life Sci.* **1159**, (2020).

99. Pacheco-Fernández, I., Rentero, M., Ayala, J. H., Pasán, J. & Pino, V. Green solid-phase microextraction fiber coating based on the metal-organic framework CIM-80(Al): Analytical performance evaluation in direct immersion and headspace using gas chromatography and mass spectrometry for the analysis of water, urine and brewed. *Anal. Chim. Acta* **1133**, 137–149 (2020).

100. Zhu, Y. *et al.* Graphene and graphene oxide: Synthesis, properties, and applications. *Adv. Mater.* **22**, 3906–3924 (2010).

101. Zhang, H. *et al.* An ionic liquid functionalized graphene adsorbent with multiple adsorption mechanisms for pipette-tip solid-phase extraction of auxins in soybean sprouts. *Food Chem.* **265**, 290–297 (2018).

102. Akamine, L. A., Vargas Medina, D. A. & Lanças, F. M. Magnetic solid-phase extraction of gingerols in ginger containing products. *Talanta* **222**, 121683 (2021).

103. Jiang, D. *et al.* Multiwalled carbon nanotube for one-step cleanup of 21 mycotoxins in corn and wheat prior to ultraperformance liquid chromatography–tandem mass spectrometry analysis. *Toxins (Basel).* **10**, 1–17 (2018).

104. Song, S. *et al.* Determination of Six Paraben Residues in Fresh-cut Vegetables Using QuEChERS with Multi-walled Carbon Nanotubes and High-Performance Liquid Chromatography–Tandem Mass Spectrometry. *Food Anal. Methods* **10**, 3972–3979 (2017).

105. Jiang, K. *et al.* Iron (II, III) oxide/multi-walled carbon nanotube composite as solid-phase extraction sorbent followed by ultra-high performance liquid chromatography tandem mass spectrometry for simultaneous determination of zearalenone and type A trichothecenes in Salv. *J. Chromatogr. A* **1482**, 1–10 (2017).

106. Liu, H., Lin, T. & Li, Q. A magnetic multi-walled carbon nanotube preparative method for analyzing asymmetric carbon, phosphorus and sulfur atoms of chiral pesticide residues in Chinese herbals by chiral liquid chromatography-quadrupole/linear ion trap mass spectrometry determinat. *J. Chromatogr. B Anal. Technol. Biomed. Life Sci.* **1148**, 122152 (2020).

107. Ling, X., Zou, L. & Chen, Z. Polymeric monolith column composited with multiwalled carbon nanotubes-β-cyclodextrin for the selective extraction of psoralen and isopsoralen. *J. Sep. Sci.* **40**, 3718–3724 (2017).

108. Chen, T. & Xu, H. In vivo investigation of pesticide residues in garlic using solid phase microextraction-gas chromatography-mass spectrometry. *Anal. Chim. Acta* **1090**, 72–81 (2019).

109. Křížek, T. *et al.* Menthol-based hydrophobic deep eutectic solvents: Towards greener and efficient extraction of phytocannabinoids. *J. Clean. Prod.* **193**, 391–396 (2018).

110. Acquadro, S. *et al.* Grapevine Green Pruning Residues as a Promising and Sustainable Source of Bioactive Phenolic Compounds. *Molecules* **25**, 464 (2020).

111. Pacheco-Fernández, I., Pino, V., Lorenzo-Morales, J., Ayala, J. H. & Afonso, A. M. Salt-induced ionic liquid-based microextraction using a low cytotoxic guanidinium ionic liquid and liquid chromatography with fluorescence detection to determine monohydroxylated polycyclic aromatic hydrocarbons in urine. *Anal. Bioanal. Chem.* **410**, 4701–4713 (2018).

112. Baltazar, Q. Q., Chandawalla, J., Sawyer, K. & Anderson, J. L. Interfacial and

micellar properties of imidazolium-based monocationic and dicationic ionic liquids. *Colloids Surfaces A Physicochem. Eng. Asp.* **302**, 150–156 (2007).

113. Dupont, D., Renders, E. & Binnemans, K. Alkylsulfuric acid ionic liquids: a promising class of strongly acidic room-temperature ionic liquids. *Chem. Commun.* **52**, 4640–4643 (2016).

114. Costa, A. J. L. *et al.* Density, Thermal Expansion and Viscosity of Cholinium-Derived Ionic Liquids. *ChemPhysChem* **13**, 1902–1909 (2012).

115. Acquadro, S. *et al. Punica granatum* Leaf Ethanolic Extract and Ellagic Acid as Inhibitors of Zika Virus Infection. *Planta Med.* **86**, 1363–1374 (2020).

116. Król, A., Amarowicz, R. & Weidner, S. Changes in the composition of phenolic compounds and antioxidant properties of grapevine roots and leaves (*Vitis vinifera* L.) under continuous of long-term drought stress. *Acta Physiol. Plant.* **36**, 1491–1499 (2014).

117. Zheng, Z.-P., Tan, H.-Y., Chen, J. & Wang, M. Characterization of tyrosinase inhibitors in the twigs of *Cudrania tricuspidata* and their structure–activity relationship study. *Fitoterapia* **84**, 242–247 (2013).

118. Joseph Bieth, Bernard Spiess, C. G. W. The synthesis and analytical use of a highly sensitive and convenient substrate of elastase. *Biochem. Med.* **11**, 350–357 (1974).

119. Dresch, R. R. *et al.* Potential use of secondary products of the agri-food industry for topical formulations and comparative analysis of antioxidant activity of grape leaf polyphenols. *Nat. Prod. Res.* **32**, 486–492 (2018).

120. Monagas, M., Hernández-Ledesma, B., Gómez-Cordovés, C. & Bartolomé, B. Commercial dietary ingredients from *Vitis vinifera* L. leaves and grape skins: Antioxidant and chemical characterization. *J. Agric. Food Chem.* **54**, 319–327 (2006).

121. Pacheco-Fernández, I., Pino, V., Ayala, J. H. & Afonso, A. M. Guanidinium ionic

liquid-based surfactants as low cytotoxic extractants: Analytical performance in an in-situ dispersive liquid–liquid microextraction method for determining personal care products. *J. Chromatogr. A* **1559**, 102–111 (2018).

122. Song, Y., Li, Q. & Li, Y. Self-aggregation and antimicrobial activity of alkylguanidium salts. *Colloids Surfaces A Physicochem. Eng. Asp.* **393**, 11–16 (2012).

123. Germán-Hernández, M., Pino, V., Anderson, J. L. & Afonso, A. M. Use of ionic liquid aggregates of 1-hexadecyl-3-butyl imidazolium bromide in a focused-microwave assisted extraction method followed by high-performance liquid chromatography with ultraviolet and fluorescence detection to determine the 15+1 EU priority PA. *Talanta* **85**, 1199–1206 (2011).

124. Tao, Y., Zhang, Z. & Sun, D. W. Kinetic modeling of ultrasound-assisted extraction of phenolic compounds from grape marc: Influence of acoustic energy density and temperature. *Ultrason. Sonochem.* **21**, 1461–1469 (2014).

125. Li, X. J. *et al.* Application of ionic liquid-based surfactants in the microwave-assisted extraction for the determination of four main phloroglucinols from Dryopteris fragrans. *J. Sep. Sci.* **35**, 3600–3608 (2012).

126. Yuan, Y., Wang, Y., Xu, R., Huang, M. & Zeng, H. Application of ionic liquids in the microwave-assisted extraction of podophyllotoxin from Chinese herbal medicine. *Analyst* **136**, 2294–2305 (2011).

127. Ferreira, S. L. C., dos Santos, W. N. ., Quintella, C. M., Neto, B. B. & Bosque-Sendra, J. M. Doehlert matrix: a chemometric tool for analytical chemistry—review. *Talanta* **63**, 1061–1067 (2004).

128. Tradit, A. J. *et al.* Proper Actions. *Lect. Notes Math.* **1902**, 121–130 (2007).

129. Loizzo, M. R. *et al.* Comparative analysis of chemical composition, antioxidant and anti-proliferative activities of Italian *Vitis vinifera* by-products for a sustainable agro-industry. *Food Chem. Toxicol.* **127**, 127–134 (2019).

130. Alara, O. R., Abdurahman, N. H., Ukaegbu, C. I. & Azhari, N. H. *Vernonia cinerea* leaves as the source of phenolic compounds, antioxidants, and anti-diabetic activity using microwave-assisted extraction technique. *Ind. Crops Prod.* **122**, 533–544 (2018).

131. Wang, Z. *et al.* Microwave-assisted ionic liquid homogeneous liquid-liquid microextraction coupled with high performance liquid chromatography for the determination of anthraquinones in *Rheum palmatum* L. *J. Pharm. Biomed. Anal.* **125**, 178–185 (2016).

132. Barrera Vázquez, M. F. *et al.* Comparisons between conventional, ultrasound-assisted and microwave-assisted methods for extraction of anthraquinones from *Heterophyllaea pustulata* Hook f. (Rubiaceae). *Ultrason. Sonochem.* **21**, 478–484 (2014).

133. Cardoso-Ugarte, G. A., Sosa-Morales, M. E., Ballard, T., Liceaga, A. & San Martín-González, M. F. Microwave-assisted extraction of betalains from red beet (*Beta vulgaris*). *LWT - Food Sci. Technol.* **59**, 276–282 (2014).

134. Yunchang Fan 1,* , Zeyu Niu 2, Chen Xu 1, L. Y. 1 and T. Y. Protic Ionic Liquids as Efficient Solvents in Microwave-Assisted Extraction of Rhein and Emodin from *Rheum palmatum* L. *Molecules* **24**, 2770 (2019).

135. Gao, M. Z. *et al.* A green and integrated strategy for enhanced phenolic compounds extraction from mulberry (*Morus alba* L.) leaves by deep eutectic solvent. *Microchem. J.* **154**, 104598 (2020).

136. Sik, B., Hanczné, E. L., Kapcsándi, V. & Ajtony, Z. Conventional and nonconventional extraction techniques for optimal extraction processes of rosmarinic acid from six Lamiaceae plants as determined by HPLC-DAD measurement. *J. Pharm. Biomed. Anal.* **184**, 113173 (2020).

137. Ye, Z. Y., Li, Z. G., Wei, D. & Lee, M. R. Microwave-assisted extraction/dispersive liquid-liquid microextraction coupled with DSI-GC-IT/MS for analysis of essential oil from three species of cardamom. *Chromatographia* **77**, 347–358 (2014).

138. Zhong, Q., Su, P., Zhang, Y., Wang, R. & Yang, Y. In-situ ionic liquid-based microwave-assisted dispersive liquid-liquid microextraction of triazine herbicides. *Microchim. Acta* **178**, 341–347 (2012).

139. Chu, C. *et al.* Microwave-assisted ionic liquid-based micelle extraction combined with trace-fluorinated carbon nanotubes in dispersive micro-solid-phase extraction to determine three sesquiterpenes in roots of *Curcuma wenyujin*. *Phytochem. Anal.* **30**, 700–709 (2019).

140. Absalan, G., Akhond, M. & Sheikhian, L. Extraction and high performance liquid chromatographic determination of 3-indole butyric acid in pea plants by using imidazolium-based ionic liquids as extractant. *Talanta* **77**, 407–411 (2008).

141. Wang, Y. *et al.* Matrix solid-phase dispersion coupled with magnetic ionic liquid dispersive liquid-liquid microextraction for the determination of triazine herbicides in oilseeds. *Anal. Chim. Acta* **888**, 67–74 (2015).

142. Du, F. Y., Xiao, X. H., Luo, X. J. & Li, G. K. Application of ionic liquids in the microwave-assisted extraction of polyphenolic compounds from medicinal plants. *Talanta* **78**, 1177–1184 (2009).

143. Ma, W. *et al.* Application of ionic liquids based microwave-assisted extraction of three alkaloids N-nornuciferine, O-nornuciferine, and nuciferine from lotus leaf. *Talanta* **80**, 1292–1297 (2010).

144. Wang, X. *et al.* Microwave-assisted ionic liquid microextraction combined with high performance liquid chromatography for the determination of naphthoquinones from *Arnebia euchroma* (Royle) Johnst. *J. Liq. Chromatogr. Relat. Technol.* **42**, 638–647 (2019).

145. Zeng, H., Wang, Y., Kong, J., Nie, C. & Yuan, Y. Ionic liquid-based microwave-assisted extraction of rutin from Chinese medicinal plants. *Talanta* **83**, 582–590 (2010).

146. Armenta, S., Garrigues, S., Esteve-Turrillas, F. A. & de la Guardia, M. Green extraction techniques in green analytical chemistry. *TrAC - Trends Anal. Chem.* **116**, 248–253 (2019).

147. Ferrer-Gallego, R., Hernández-Hierro, J. M., Rivas-Gonzalo, J. C. & Escribano-Bailón, M. T. Influence of climatic conditions on the phenolic composition of *Vitis vinifera* L. cv. Graciano. *Anal. Chim. Acta* **732**, 73–77 (2012).

148. HASELGROVE, L. *et al.* Canopy microclimate and berry composition: The effect of bunch exposure on the phenolic composition of *Vitis vinifera* L cv. Shiraz grape berries. *Aust. J. Grape Wine Res.* **6**, 141–149 (2000).

149. Spayd, S. E., Tarara, J. M., Mee, D. L. & Ferguson, J. C. Separation of light and temp on Merlot. *Am. J. Enol. Vitic.* **3**, 171–182 (2002).

150. José M. Lorenzo, Mario Estévez, Francisco J. Barba, Rohit Thirumdas, Daniel Franco, P. E. S. M. Polyphenols: Bioaccessibility and bioavailability of bioactive components. in *Innovative Thermal and Non-Thermal Processing, Bioaccessibility and Bioavailability of Nutrients and Bioactive Compounds,* ***12,*** 309–332 (2019).

151. Katalinic, V. et al. Phenolic profile, antioxidant capacity, and antimicrobial activity of leaf extracts from six *Vitis vinifera* L. Varieties. *Int. J. Food Prop.* **16**, 45–60 (2013).

152. Brodkorb, A. et al. INFOGEST static in vitro simulation of gastrointestinal food digestion. *Nat. Protoc.* **14**, 991–1014 (2019).

153. Eran Nagar, E., Okun, Z. & Shpigelman, A. Digestive fate of polyphenols: updated view of the influence of chemical structure and the presence of cell wall material. *Curr. Opin. Food Sci.* **31**, 38–46 (2020).

154. Eran Nagar, E., Okun, Z. & Shpigelman, A. In vitro bioaccessibility of polyphenolic compounds: The effect of dissolved oxygen and bile. *Food Chem.* **404**, 134490 (2023).

155. Alexandru, L. *et al.* Efficient green extraction of polyphenols from post-harvested

agro-industry vegetal sources in Piedmont. *Comptes Rendus Chim.* **17**, 212–217 (2014).

156. Bottone, A. *et al.* Plant Specialized Metabolites in Hazelnut (*Corylus avellan*a) Kernel and Byproducts : An Update on Chemistry , Biological Activity , and Analytical Aspects 1 Authors. **85**, 840–855 (2019).

157. Del Rio, D., Calani, L., Dall'Asta, M. & Brighenti, F. Polyphenolic Composition of Hazelnut Skin. *J. Agric. Food Chem.* **59**, 9935–9941 (2011).

158. Slatnar, A., Mikulic-Petkovsek, M., Stampar, F., Veberic, R. & Solar, A. HPLC-MSn identification and quantification of phenolic compounds in hazelnut kernels, oil and bagasse pellets. *Food Res. Int.* **64**, 783–789 (2014).

159. Shataer, D. *et al.* Chemical Composition of the Hazelnut Kernel (*Corylus avellana* L.) and Its Anti-inflammatory, Antimicrobial, and Antioxidant Activities. *J. Agric. Food Chem.* **69**, 4111–4119 (2021).

160. Balik, H. I. Bioactive Compounds and Fatty Acid Composition of New Turkish Hazelnut Cultivars. *Int. J. Fruit Sci.* **21**, 106–114 (2021).

161. Taş, N. G. & Gökmen, V. Phenolic compounds in natural and roasted nuts and their skins: a brief review. *Curr. Opin. Food Sci.* **14**, 103–109 (2017).

162. Piccinelli, A. L. *et al.* HRMS Profile of a Hazelnut Skin Proanthocyanidin-rich Fraction with Antioxidant and Anti- *Candida albicans* Activities. *J. Agric. Food Chem.* **64**, 585–595 (2016).

163. Lainas, K., Alasalvar, C. & Bolling, B. W. Effects of roasting on proanthocyanidin contents of Turkish Tombul hazelnut and its skin. *J. Funct. Foods* **23**, 647–653 (2016).

164. Fanali, C. *et al.* Choline Chloride–Lactic Acid-Based NADES As an Extraction Medium in a Response Surface Methodology-Optimized Method for the Extraction of Phenolic Compounds from Hazelnut Skin. *Molecules* **26**, 2652 (2021).

165. Bener, M. *et al.* Microwave-assisted extraction of antioxidant compounds from by-

products of Turkish hazelnut (*Corylus avellana* L.) using natural deep eutectic solvents: Modeling, optimization and phenolic characterization. *Food Chem.* **385**, 132633 (2022).

166. Mazzeo, L. *et al.* Equilibrium and fixed-bed kinetics study on hazelnut skin polyphenols extraction using choline chloride –lactic acid-based NADES and water as solvents. *Sep. Purif. Technol.* **327**, 124896 (2023).

167. Turck, D. *et al.* Safety of betaine as a novel food pursuant to Regulation (EU) 2015/2283. *EFSA J.* **17**, (2019).

168. Dai, Y., Witkamp, G.-J., Verpoorte, R. & Choi, Y. H. Tailoring properties of natural deep eutectic solvents with water to facilitate their applications. *Food Chem.* **187**, 14–19 (2015).

169. Rehman, M. *et al.* Evaluation of hemp (*Cannabis sativa* L.) as an industrial crop: a review. *Environ. Sci. Pollut. Res.* **28**, 52832–52843 (2021).

170. Fike, J. Industrial Hemp: Renewed Opportunities for an Ancient Crop. *CRC. Crit. Rev. Plant Sci.* **35**, 406–424 (2016).

171. Brighenti, V. *et al.* Emerging challenges in the extraction, analysis and bioanalysis of cannabidiol and related compounds. *J. Pharm. Biomed. Anal.* **192**, 113633 (2021).

172. Pellati, F. *et al.* New Methods for the Comprehensive Analysis of Bioactive Compounds in *Cannabis sativa* L. (hemp). *Molecules* **23**, 2639 (2018).

173. Izzo, L. *et al.* Analysis of Phenolic Compounds in Commercial. *Molecules* **25**, 1–12 (2020).

174. Pavlovic, R. *et al.* Phytochemical and Ecological Analysis of Two Varieties of Hemp (*Cannabis sativa* L.) Grown in a Mountain Environment of Italian Alps. *Front. Plant Sci.* **10**, 1–20 (2019).

175. Jin, D., Dai, K., Xie, Z. & Chen, J. Secondary Metabolites Profiled in Cannabis

Inflorescences, Leaves, Stem Barks, and Roots for Medicinal Purposes. *Sci. Rep.* **10**, 1–14 (2020).

176. Cirrincione, M. *et al.* Discriminating different *Cannabis sativa* L. chemotypes using attenuated total reflectance - infrared (ATR-FTIR) spectroscopy: A proof of concept. *J. Pharm. Biomed. Anal.* **204**, 114270 (2021).

177. Micalizzi, G. *et al. Cannabis Sativa* L.: a comprehensive review on the analytical methodologies for cannabinoids and terpenes characterization. *J. Chromatogr. A* **1637**, (2021).

178. UNITED NATIONS OFFICE ON DRUGS AND CRIME. *Recommended Methods for the Identification and Analysis of Cannabis and Cannabis Products*. (2022).

179. Pellati, F. *et al.* New methods for the comprehensive analysis of bioactive compounds in *Cannabis sativa* L. (hemp). *Molecules* **23**, (2018).

180. Izzo, L. *et al.* Analysis of Phenolic Compounds in Commercial. *Molecules* **25**, 1–12 (2020).

181. Ferrante, C. *et al.* Multiple pharmacognostic characterization on hemp commercial cultivars: Focus on inflorescence water extract activity. *Food Chem. Toxicol.* **125**, 452–461 (2019).

182. Gunjević, V. *et al.* Selective recovery of terpenes, polyphenols and cannabinoids from *Cannabis sativa* L. inflorescences under microwaves. *Ind. Crops Prod.* **162**, 113247 (2021).

183. Ferrer, I. Analyses of cannabinoids in hemp oils by LC/Q-TOF-MS. *Compr. Anal. Chem.* **90**, 415–452 (2020).

184. Ingallina, C. *et al. Cannabis sativa* L. inflorescences from monoecious cultivars grown in central Italy: An untargeted chemical characterization from early flowering to ripening. *Molecules* **25**, 1908 (2020).

185. Pollastro, F., Minassi, A. & Fresu, L. G. Cannabis Phenolics and their Bioactivities. *Curr. Med. Chem.* **25**, 1160–1185 (2017).

186. Sumner, L. W. *et al.* Proposed minimum reporting standards for chemical analysis Working Group (CAWG) Metabolomics Standards Initiative (MSI). *Metabolomics* **3**, 211–221 (2007).

187. Andre, C. M., Hausman, J.-F. & Guerriero, G. *Cannabis sativa*: The Plant of the Thousand and One Molecules. *Front. Plant Sci.* **7**, 1–17 (2016).

188. Flores-Sanchez, I. J. & Verpoorte, R. Secondary metabolism in cannabis. *Phytochem. Rev.* **7**, 615–639 (2008).

189. Berman, P. *et al.* A new ESI-LC/MS approach for comprehensive metabolic profiling of phytocannabinoids in Cannabis. *Sci. Rep.* **8**, 14280 (2018).

190. Wang, M. *et al.* Decarboxylation Study of Acidic Cannabinoids: A Novel Approach Using Ultra-High-Performance Supercritical Fluid Chromatography/Photodiode Array-Mass Spectrometry. *Cannabis Cannabinoid Res.* **1**, 262–271 (2016).

191. Giacometti, J., Žauhar, G. & Žuvić, M. Optimization of ultrasonic-assisted extraction of major phenolic compounds from olive leaves (*Olea europaea* L.) using response surface methodology. *Foods* **7**, 1–14 (2018).

192. Tzimas, P. S., Petrakis, E. A., Halabalaki, M. & Skaltsounis, L. A. Effective determination of the principal non-psychoactive cannabinoids in fiber-type *Cannabis sativa* L. by UPLC-PDA following a comprehensive design and optimization of extraction methodology. *Anal. Chim. Acta* **1150**, 338200 (2021).

193. Qamar, S., Torres, Y. J. M., Parekh, H. S. & Robert Falconer, J. Extraction of medicinal cannabinoids through supercritical carbon dioxide technologies: A review. *J. Chromatogr. B Anal. Technol. Biomed. Life Sci.* **1167**, 122581 (2021).

194. Richins, R. D., Rodriguez-Uribe, L., Lowe, K., Ferral, R. & O'Connell, M. A.

Accumulation of bioactive metabolites in cultivated medical Cannabis. *PLoS One* **13**, 1–20 (2018).

195. Tremlová, B. *et al.* Influence of technological maturity on the secondary metabolites of hemp concentrate (*Cannabis sativa* L.). *Foods* **10**, 1418 (2021).

196. Jimenez-Garcia, S. N. *et al.* Changes in the content of phenolic compounds and biological activity in traditional Mexican herbal infusions with different drying methods. *Molecules* **25**, 1601 (2020).

197. Mastellone, G., Marengo, A., Sgorbini, B., Rubiolo, P. & Cagliero, C. New phases for analytical scale extraction from plants: Current and future trends. *TrAC Trends Anal. Chem.* **141**, 116288 (2021).

198. Toma, M., Vinatoru, M., Paniwnyk, L. & Mason, T. . Investigation of the effects of ultrasound on vegetal tissues during solvent extraction. *Ultrason. Sonochem.* **8**, 137–142 (2001).

199. Swatloski, R. P., Spear, S. K., Holbrey, J. D. & Rogers, R. D. Dissolution of cellose with ionic liquids. *J. Am. Chem. Soc.* **124**, 4974–4975 (2002).

200. Kumari, P., Pillai, V. V. S. & Benedetto, A. Mechanisms of action of ionic liquids on living cells: the state of the art. *Biophys. Rev.* **12**, 1187–1215 (2020).

201. Zhang, H. *et al.* Study on the Dissolution Mechanism of Cellulose by ChCl-Based Deep Eutectic Solvents. *Materials (Basel).* **13**, 278 (2020).

202. Cao, J. & Su, E. Hydrophobic deep eutectic solvents: the new generation of green solvents for diversified and colorful applications in green chemistry. *J. Clean. Prod.* **314**, 127965 (2021).

203. Florindo, C., Lima, F., Branco, L. C. & Marrucho, I. M. Hydrophobic Deep Eutectic Solvents: A Circular Approach to Purify Water Contaminated with Ciprofloxacin. *ACS Sustain. Chem. Eng.* **7**, 14739–14746 (2019).

204. Mastellone, G. *et al.* Characterization and Biological Activity of Fiber-Type *Cannabis sativa* L. Aerial Parts at Different Growth Stages. *Plants* **11**, 419 (2022).

205. Cicaloni, V., Salvini, L., Vitalini, S. & Garzoli, S. Chemical Profiling and Characterization of Different Cultivars of *Cannabis sativa* L. Inflorescences by SPME-GC-MS and UPLC-MS. *Separations* **9**, (2022).

206. Ahmad, S. M., Gonçalves, O. C., Oliveira, M. N., Neng, N. R. & Nogueira, J. M. F. Application of Microextraction-Based Techniques for Screening-Controlled Drugs in Forensic Context—A Review. *Molecules* **26**, 2168 (2021).

207. Birk, L., Santos, S. O., Eller, S., Merib, J. O. & Oliveira, T. F. Determinations of new psychoactive substances in biological matrices with focus on microextraction techniques: a review of fundamentals and state-of-the-art extraction methods. *Forensic Toxicol.* **39**, 350–367 (2021).

208. Morisue Sartore, D., Costa, J. L., Lanças, F. M. & Santos-Neto, Á. J. Packed in-tube SPME–LC–MS/MS for fast and straightforward analysis of cannabinoids and metabolites in human urine. *Electrophoresis* **43**, 1–12 (2022).

209. Tomai, P. *et al.* Dispersive liquid-liquid microextraction, an effective tool for the determination of synthetic cannabinoids in oral fluid by liquid chromatography–tandem mass spectrometry. *J. Pharm. Anal.* **11**, 292–298 (2021).

210. Jin, D., Henry, P., Shan, J. & Chen, J. Identification of Chemotypic Markers in Three Chemotype Categories of Cannabis Using Secondary Metabolites Profiled in Inflorescences, Leaves, Stem Bark, and Roots. *Front. Plant Sci.* **12**, 1–16 (2021).

211. Abbott, A. P., Capper, G., Davies, D. L., Rasheed, R. K. & Tambyrajah, V. Novel solvent properties of choline chloride/urea mixtures. *Chem. Commun.* **1**,70–71 (2003).

212. Migliorati, V., Sessa, F. & D'Angelo, P. Deep eutectic solvents: A structural point of view on the role of the cation. *Chem. Phys. Lett.* **737**, 100001 (2019).

213. Zainal-Abidin, M. H., Hayyan, M. & Wong, W. F. Hydrophobic deep eutectic solvents: Current progress and future directions. *J. Ind. Eng. Chem.* **97**, 142–162 (2021).

214. Van Osch, D. J. G. P., Dietz, C. H. J. T., Warrag, S. E. E. & Kroon, M. C. The Curious Case of Hydrophobic Deep Eutectic Solvents: A Story on the Discovery, Design, and Applications. *ACS Sustain. Chem. Eng.* **8**, 10591-10612, (2020).

215. Abbasi, N. M., Farooq, M. Q. & Anderson, J. L. Investigating the Variation in Solvation Interactions of Choline Chloride-Based Deep Eutectic Solvents Formed Using Different Hydrogen Bond Donors. *ACS Sustain. Chem. Eng.* **9**, 11970–11980 (2021).

216. Abbasi, N. M., Farooq, M. Q. & Anderson, J. L. Modulating solvation interactions of deep eutectic solvents formed by ammonium salts and carboxylic acids through varying the molar ratio of hydrogen bond donor and acceptor. *J. Chromatogr. A* **1643**, 462011 (2021).

217. Endo, S., Pfennigsdorff, A. & Goss, K.-U. Salting-Out Effect in Aqueous NaCl Solutions: Trends with Size and Polarity of Solute Molecules. *Environ. Sci. Technol.* **46**, 1496–1503 (2012).

218. Tighrine, A., Amir, Y., Alfaro, P., Mamou, M. & Nerín, C. Simultaneous extraction and analysis of preservatives and artificial sweeteners in juices by salting out liquid-liquid extraction method prior to ultra-high performance liquid chromatography. *Food Chem.* **277**, 586–594 (2019).

219. Gezahegn, T., Tegegne, B., Zewge, F. & Chandravanshi, B. S. Salting-out assisted liquid–liquid extraction for the determination of ciprofloxacin residues in water samples by high performance liquid chromatography–diode array detector. *BMC Chem.* **13**, 28 (2019).

220. Hammad, S. F., Abdallah, I. A., Bedair, A. & Mansour, F. R. Salting-out induced

liquid–liquid microextraction for alogliptin benzoate determination in human plasma by HPLC/UV. *BMC Chem.* **15**, 2 (2021).

221. Mastellone, G., Marengo, A., Sgorbini, B., Rubiolo, P. & Cagliero, C. Development of a dispersive solid-liquid microextraction method using natural eutectic solvents for a greener extraction of phytochemicals from fiber-type *Cannabis* sp. *Ind. Crops Prod.* **187**, 115476 (2022).

222. Dai, Y., Rozema, E., Verpoorte, R. & Choi, Y. H. Application of natural deep eutectic solvents to the extraction of anthocyanins from *Catharanthus roseus* with high extractability and stability replacing conventional organic solvents. *J. Chromatogr. A* **1434**, 50–56 (2016).

223. Fan, C., Liu, Y., Sebbah, T. & Cao, X. A Theoretical Study on Terpene-Based Natural Deep Eutectic Solvent: Relationship between Viscosity and Hydrogen-Bonding Interactions. *Glob. Challenges* **5**, 2000103 (2021).

224. Contreras, R., Lodeiro, L., Rozas-Castro, N. & Ormazábal-Toledo, R. On the role of water in the hydrogen bond network in DESs: an ab initio molecular dynamics and quantum mechanical study on the urea–betaine system. *Phys. Chem. Chem. Phys.* **23**, 1994–2004 (2021).

225. Farooq, M. Q., Abbasi, N. M. & Anderson, J. L. Deep eutectic solvents in separations: Methods of preparation, polarity, and applications in extractions and capillary electrochromatography. *J. Chromatogr. A* **1633**, 461613 (2020).

226. Mastellone, G., Abbasi, N. M., Cagliero, C. & Anderson, J. L. New Class of Tunable Choline Bromide-Based Hydrophobic Deep Eutectic Solvents for the Extraction of Bioactive Compounds of Varying Polarity from a Plant Matrix. *ACS Sustain. Chem. Eng.* **11**, 6665–6675 (2023).

227. Nasiri, A. *et al.* Overview, consequences, and strategies for overcoming matrix effects in LC-MS analysis: A critical review. *Analyst* **146**, 6049–6063 (2021).

228. Fu, Y. *et al.* Representative matrices for use in matrix-matched calibration in gas chromatography-mass spectrometry for the analysis of pesticide residues in different types of food-medicine plants. *J. Food Compos. Anal.* **111**, 104617 (2022).

229. Baratta, F. *et al.* Development of Standard Operating Protocols for the Optimization of Cannabis-Based Formulations for Medical Purposes. *Front. Pharmacol.* **10**, 1–10 (2019).

230. Zhang, J. *et al.* pH-responsive switchable deep eutectic solvents to mediate pretreatment method for trace analysis of triazole fungicides in peel wastes. *Food Chem.* **411**, 135486 (2023).

231. Brighenti, V., Pellati, F., Steinbach, M., Maran, D. & Benvenuti, S. Development of a new extraction technique and HPLC method for the analysis of non-psychoactive cannabinoids in fibre-type *Cannabis sativa* L. (hemp). *J. Pharm. Biomed. Anal.* **143**, 228–236 (2017).

232. Dei Cas, M. *et al.* The Italian panorama of cannabis light preparation: Determination of cannabinoids by LC-UV. *Forensic Sci. Int.* **307**, 110113 (2020).

233. Miller, O. S., Elder, E. J., Jones, K. J. & Gidal, B. E. Analysis of cannabidiol (CBD) and THC in nonprescription consumer products: Implications for patients and practitioners. *Epilepsy Behav.* **127**, 108514 (2022).

234. Shimadzu. The Determination of CBD and General Cannabinoid Content in Hemp Oils Using HPLC with UV Detection. https://www.shimadzu.com/an/literature/hplc/sil220001.html (2018).

235. Madej, K., Kózka, G., Winiarski, M. & Piekoszewski, W. A Simple, Fast, and Green Oil Sample Preparation Method for Determination of Cannabidioloic Acid and Cannabidiol by HPLC-DAD. *Separations* **7**, 60 (2020).

236. Bechis, G. *et al.* Assessing the environmental and overall performance of gas chromatographic analyses. Development of a comprehensive evaluation framework

and application to routine chiral analyses of fragrances as a case study. *Sustain. Chem. Pharm.* **35**, 101217 (2023).

237. Manousi, N., Wojnowski, W., Płotka-Wasylka, J. & Samanidou, V. Blue applicability grade index (BAGI) and software: a new tool for the evaluation of method practicality. *Green Chem.* **25**, 7598–7604 (2023).

238. González-Martín, R., Gutiérrez-Serpa, A., Pino, V. & Sajid, M. A tool to assess analytical sample preparation procedures: Sample preparation metric of sustainability. *J. Chromatogr. A* **1707**, 464291 (2023).

239. Rocío-Bautista, P., Taima-Mancera, I., Pasán, J. & Pino, V. Metal-organic frameworks in green analytical chemistry. *Separations* **6**, 1–21 (2019).

240. Barker, S. A. Matrix solid-phase dispersion. *J. Chromatogr. A* **885**, 115–127 (2000).

241. Santos Barreto, A. *et al.* Characterization and application of a lanthanide-based metal–organic framework in the development and validation of a matrix solid-phase dispersion procedure for pesticide extraction on peppers (*Capsicum annuum* L.) with gas chromatography–mass spectrometr. *J. Sep. Sci.* **41**, 1593–1599 (2018).

242. de Jesus, J. R., Wanderley, K. A., Alves Júnior, S. & Navickiene, S. Evaluation of a novel metal–organic framework as an adsorbent for the extraction of multiclass pesticides from coconut palm (*Cocos nucifera* L.): An analytical approach using matrix solid-phase dispersion and liquid chromatography. *J. Sep. Sci.* **40**, 3327–3334 (2017).

243. dos Anjos de Jesus, R., Santos, L. F. S., Navickiene, S. & de Mesquita, M. E. Evaluation of Metal-Organic Framework as Low-Cost Adsorbent Material in the Determination of Pesticide Residues in Soursop Exotic Fruit (*Annona muricata*) by Liquid Chromatography. *Food Anal. Methods* **8**, 446–451 (2015).

244. Rocío-Bautista, P. *et al.* A green metal–organic framework to monitor water contaminants. *RSC Adv.* **8**, 31304–31310 (2018).

245. Figueroa-Quintero, L., Ramos-Fernandez, E. V. & Narciso, J. Synthesis and Characterization of the Metal–Organic Framework CIM-80 for Organic Compounds Adsorption. *Materials (Basel).* **15**, 5326 (2022).

246. Pietta, P. G. Flavonoids as antioxidants. *J. Nat. Prod.* **63**, 1035–1042 (2000).

247. Tóth, K. F., Ádám, D., Bíró, T. & Oláh, A. Cannabinoid signaling in the skin: Therapeutic potential of the 'cannabinoid' system. *Molecules* **24**, 1–56 (2019).

248. Zamberletti, E., Rubino, T. & Parolaro, D. Therapeutic potential of cannabidivarin for epilepsy and autism spectrum disorder. *Pharmacol. Ther.* **226**, 107878 (2021).

249. Baswan, S. M. *et al.* Therapeutic potential of cannabidiol (CBD) for skin health and disorders. *Clin. Cosmet. Investig. Dermatol.* **13**, 927–942 (2020).

250. Guo, T. T. *et al.* Bioactive spirans and other constituents from the leaves of *Cannabis sativa* f. sativa. *J. Asian Nat. Prod. Res.* **19**, 793–802 (2017).

251. Manosroi, A. *et al.* Pharmaceutical and cosmeceutical biological activities of hemp (*Cannabis sativa* L var. *sativa*) leaf and seed extracts. *Chiang Mai J. Sci.* **46**, 180–195 (2019).

252. Dawidowicz, A. L., Olszowy-Tomczyk, M. & Typek, R. CBG, CBD, Δ^9-THC, CBN, CBGA, CBDA and Δ^9-THCA as antioxidant agents and their intervention abilities in antioxidant action. *Fitoterapia* **152**, 104915 (2021).

253. Moussa, M. A. A.-M. and Z. Antioxidant Activity: The Presence and Impact of Hydroxyl Groups in Small Molecules of Natural and Synthetic Origin. *IntechOpen* 13 (2016).

254. Capetti, F. *et al.* Citral-Containing Essential Oils as Potential Tyrosinase Inhibitors: A Bio-Guided Fractionation Approach. *Plants* **10**, 969 (2021).

255. Sadeghi-Kaji, S., Shareghi, B., Saboury, A. A. & Farhadian, S. Spermine as a porcine pancreatic elastase activator: spectroscopic and molecular simulation studies. *J.*

Biomol. Struct. Dyn. **38**, 78–88 (2020).

256. Corni, G., Brighenti, V., Pellati, F. & Morlock, G. E. Effect-directed analysis of bioactive compounds in *Cannabis sativa* L. by high-performance thin-layer chromatography. *J. Chromatogr. A* **1629**, 461511 (2020).

Abbreviations

$[Ch^+][Br^-]$	Choline bromide
$[Ch^+][Cl^-]$	Choline chloride
μ-dSPE	Miniaturized version of dispersive SPE
^{13}C NMR	Carbon nuclear magnetic resonance spectroscopy
^{1}H-NMR	Proton nuclear magnetic resonance spectroscopy
4-NA	4-nitroaniline dye
ABS	Aqueous biphasic system
$ABTS^{+\bullet}$	2,2'-azinobis (3-ethylbenzothiazoline-6-sulfonic acid) diammonium salt
ACN	Acetonitrile
AGREE	Analytical GREEnness Metric Approach
AGREEprep	Analytical GREEnness Metric for sample preparation
ANOVA	Analysis of variance
ATR	Attenuated total reflectance
BAGI	Blue Applicability Grade Index
Bet	Betaine
Bio-IL	Bio-renewable IL
BSTFA	*N,O*-bis(trimetilsilil)trifluoroacetamide
C_{10}Gu-Cl	Decylguanidinium chloride
$C_{16}C_4$Im-Br	1-hexadecyl-3-butyl imidazolium bromide
CA	Caftaric acid
CAR	Carboxen
CBCA	Cannabichromenic acid
CBD	Cannabidiol
CBDA	Cannabidiolic acid
CBDVA	Cannabivarinic acid
CBGA	Cannabigerolic acid
CBNA	Cannabinolic acid
CD	Cyclodextrin
$CDCl_3$	Deuterated chloroform
CMC	Critical micelle concentration
CNT	Carbon nanotube
COF	Covalent-organic framework
DES	Deep eutectic solvent
DI	Direct immersion
DL	Desolvation line
DLLME	Dispersive liquid-liquid microextraction
DMSO	Dimethyl sulfoxide
DMSO-d_6	Dimethyl sulfoxide-d_6
$DPPH^{\bullet}$	1,1-diphenyl-2-picrylhydrazyl
DSC	Differential scanning calorimetry
DSLME	Dispersive solid-liquid microextraction
dSPE	Dispersive SPE
DVB	Divinylbenzene
EC_{50}	Half-maximal concentration that halved the substance/enzyme activity
E_F	Enrichment factor
ESI	Electrospray ionization

ES	Eutectic solvent
EtOH	Ethanol
FD	Freeze-drying
FTIR	Fourier transform infrared spectroscopy
GAC	Green Analytical Chemistry
GAPI	Green Analytical Procedure Index
GC	Gas chromatography
Gly	Glycerol
GO	Graphene oxide
GPR	Green pruning residue
GSP	Green Sample Preparation
HBA	Hydrogen bond acceptor
HBD	Hydrogen bond donor
HC	Hierarchical clustering
HES	Hydrophobic ES
HS	Headspace
IL	Ionic liquid
IL-HIM	IL-hybrid molecularly imprinted material
IL-MHDE	IL-mediated microwave-assisted hydro distillation liquid-liquid extraction
IL-UMASDE	IL-based ultrasound/microwave-assisted simultaneous distillation extraction
IN	Bioaccessible fraction after digestion
$K_2S_2O_8$	Potassium persulfate
KBr	Potassium bromide
LA	Lactic acid
LB	Listán Blanco grapevine variety
LC	Liquid chromatography
Lev	Levulinic acid
LLE	Liquid-liquid extraction
LN	Listán Negro grapevine variety
LOD	Limit of detection
LOQ	Limit of quantification
MA	Moscatel Alejandría grapevine variety
MAE	Microwave assisted extraction
MCE	Mechanochemical extraction
MCT	Medium chain triglycerides
ME	Matrix effect
MeOH	Methanol
MIL	Magnetic ionic liquid
MIP	Molecular imprinted polymer
ML	Malvasía Lanzarote grapevine variety
MNP	Magnetic nanoparticle
MOF	Metal organic framework
MS	Mass spectrometry
MS/MS	Tandem mass spectrometry
MSPD	Matrix solid phase dispersion
m-SPE	Magnetic solid phase extraction
MW	Microwave
MWCNT	Multiwalled carbon nanotube

N,N-DENA	*N,N*-diethyl-4-nitroaniline dye
NADES	Natural deep eutectic solvent
NEMI	National Environmental Methods Index
NM	Negra Moll grapevine variety
NMR	Nuclear magnetic resonance
NR	Nile red dye
OD	Oven-drying
OUT	Extracted fraction after digestion
PANI	Polyaniline
PCA	Principal component analysis
PCB	Polychlorobiphenyl
PDA	Photo-diode array detector
PDMS	Polydimethylsiloxane
PIL	Polymeric ionic liquid
PPy	Polypyrrole
PSA	Primary-secondary amine
PVC	Polyvinyl chloride
PVDF	Polyvinylidene fluoride
QU	Quercetin
QuEChERS	Quick, Easy, Cheap, Effective, Rugged, and Safe
QUGlucos	Quercetin-3-*O*-glucoside
QUGlucur	Querceting-3-*O*-glucuronide
R^2	Determination coefficient
rGO	Reduced graphene oxide
RP	Reverse phase
RSD	Relative standard deviation
RT	Room temperature
RU	Rutin
S/N	Signal to noise ratio
SD	Standard deviation
SIL-IS	Stable isotope labeled internal standard
SLE	Solid-liquid extraction
SPE	Solid phase extraction
SPME	Solid phase microextraction
SPMS	Sample Preparation Metric of Sustainability
$S_{y/x}$	Standard deviation of the residuals or error of the estimate
T	Tintilla grapevine variety
TEG	Triethylene glycol
ToF	Time of flight
TRIL	Temperature-responsive hydrophobic ionic liquid
UAE	Ultrasound-assisted extraction
UCTS	Upper critical solution temperature
UHPLC	Ultra-high performance liquid chromatography
US	Ultrasound
UV−vis	Ultra-violet visible
WAC	White Analytical Chemistry
Δ^9-THC	Delta^9-Tetrahydrocannabinol
Δ^9-THCA	Delta^9-Tetrahydrocannabinolic acid

Δ^9-THCVA	Delta9-tetrahydrocannabivarinic acid
λ_{max}	Maximum wavelength of adsorption

For the abbreviations of the [Ch^+][Br^-]-modified salts and hydrophobic NADESs, refer to Table 2 in Chapter II (Experimental) and Table 1 of Section III.3.3, respectively.